2022

Development of the novel isoxazolo[3,4-d]pyridazinone scaffold, which positively modulates the metabotropic glutamate receptor subtypes 2 and 4

Christina Ann Gates
University of Montana - Missoula

Development of the novel isoxazolo[3,4-d]pyridazinone scaffold, which positively modulates the metabotropic glutamate receptor subtypes 2 and 4

By

Christina Ann Gates

Bachelor of Science, Chemistry, University of Montana

Dissertation

Presented in partial fulfillment of the requirements
for the degree of

Doctor of Philosophy in Medicinal Chemistry

The University of Montana
Missoula, MT

January 2022

Approved by:

Scott Whittenburg,
Graduate School Dean

Dr. Nicholas Natale, Chair
Department of Biomedical and Pharmaceutical Sciences

Dr. Christopher Palmer
Department of Chemistry and Biochemistry

Dr. Keith Parker
Department of Biomedical and Pharmaceutical Sciences

Dr. Elizabeth Putnam
Department of Biomedical and Pharmaceutical Sciences

Dr. Monica Serban
Department of Biomedical and Pharmaceutical Sciences

Gates, Christina, PhD, January 2022 Medicinal Chemistry

Development of the novel isoxazolo[3,4-d]pyridazinone scaffold, which positively modulates the metabotropic glutamate receptor subtypes 2 and 4

Chairperson: Dr. Nicholas R. Natale

The seven transmembrane (7TM) superfamily, also known as G-protein coupled receptors (GPCR), are one of the largest superfamilies in the human genome. With approximately 30% of marketed drugs targeting the GPCRs, these proteins are among the most successful as therapeutic targets. Within the GPCR receptor family there is a subgroup called the metabotropic glutamate receptors (mGluR). Compounds that target mGluRs are important for the treatment of a variety of central nervous system (CNS) disorders, as well as cancer. The $mGluR_2$ subtype is a target for treatment of anxiety and schizophrenia. Activation of $mGluR_4$ helps to ease the symptoms of Parkinson's disease and may even slow progress of the disease. Additionally, both of these receptors have been implicated in the treatment of variety of cancers such as giloma, medulloblastoma, or colorectal carcinoma, presenting another target to overcome these diseases. Selectively targeting the mGluRs are difficult due to the high sequence similarities. This difficulty can be overcome by targeting the allosteric site, which is located in the 7TM.Our isoxazolo[3,4-d]pyridazinones compounds were tested and found to have selective activity at mGluR 2 and 4. This selectivity, along with other tests, imply binding may not be at the venus flytrap domain (where glutamate binds), but rather at the allosteric site as positive allosteric modulators (PAMs). Further modifications of our compounds will be developed to optimize selectivity and activity, based on structural drug design and modeling at the allosteric site.

Table of Contents

Chapter 3: 3-(1,3-Diphenylpropan-2-yl)-4-methyl-6- phenylisoxazolo[3,4-d]pyridazin-7(6H)- one

Chapter 4: The lateral metalation of isoxazolo[3,4-d]pyridazinones: selective positive modulators of metabotropic Glutamate Receptors

Chapter 5: Future Directions: Asymmetric synthesis, metabolism, and the blood brain barrier

List of Figures

List of Tables

List of Schemes

List of Charts

Introduction: Selectively targeting mGluRs with Isoxazolo[3,4-d]Pyridazinones

To selectively target a small molecule to a receptor. The first steps for developing the 3,4-ds was to better understand the metabotropic glutamate receptors (mGluR) 3D structural components and the super family they belong to. Followed by modeling and synthetic strategy development.

mGluR super family-G-protein coupled receptors

G-protein coupled receptors (GPCR) are one of the largest superfamilies in the human genome.[1] With approximately 30% of marketed drugs targeting GPCRs, they are among the most successful therapeutic targets. GPCRs share a common seven transmembrane (7TM) architecture linked by three extracellular (ECL) and three intracellular (ICL) loops that interact with G-proteins and modulate production of cAMP through the enzyme adenylyl cyclase. This starts a signal cascade.[2] **(Intro-Figure 1)**

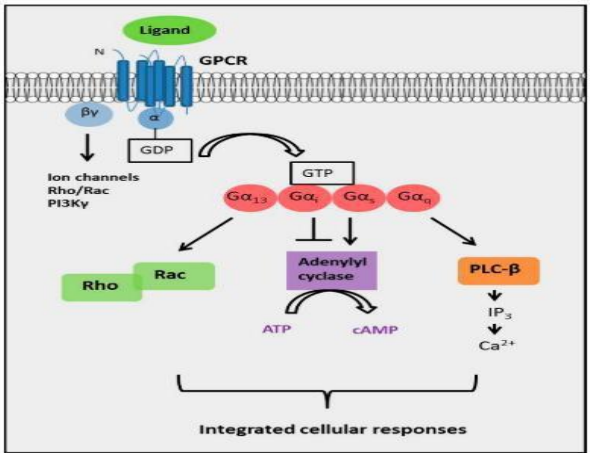

Intro-Figure 1: General signal cascade for GPCRs [1]

These receptors are responsible for modulating several signaling processes involved in behavior, blood pressure regulation, cognition, immune response, mood, smell, and taste. There are currently six known sub-classes within the GPCRs: A-F. Each class is separated based on structural similarities and functional characteristics. Each has had varied success as drug targets, as well as degree of molecular level knowledge about them. [2,3,4,5] The focus of the

this dissertation will be on developing synthetic routes that produce small molecules selectively targeting the Class C mGluRs.

mGluRs

The mGluRs are members of the class C of GPCRs. These receptors are located on both post and pre-synaptic neurons and are involved with signal regulation. The class is further broken down into 3 subgroups: 1, 2, and 3 by sequence homology. Subgroup 1 has excitatory receptors, $mGluR_1$ and $mGluR_5$. Subgroup 2, ($mGluR_{2-3}$) and Subgroup 3 ($mGluR_{4,\ 6-8}$) are inhibitory. [6] This work will focus on developing small molecules targeting inhibitory receptors $mGluR_2$ and $mGluR_4$. Compounds that target mGluRs are important for the treatment of a variety of central nervous system (CNS) disorders, as well as cancer.[7,8,9,10,11] The $mGluR_2$ is a target for treatment of anxiety and schizophrenia. Activation of $mGluR_4$ helps to ease the symptoms of Parkinson's disease and may even slow progress of the disease. [7,8,12,13,14] Additionally, both of these receptors have been implicated in the treatment of variety of cancers such as glioma, medulloblastoma, or colorectal carcinoma, presenting another target to overcome these diseases.

Structurally mGluRs have a rather unique venus flytrap domain (VFD) for its orthosteric site which is responsible for binding to glutamate, a cysteine rich linker that connects the VFD to the 7TM which spans the membrane and interacts with the G-protein, this is also where the allosteric site is located. (**Intro-Figure 2**). mGluR receptors can achieve the signaling cascade by either signaling on their own or more frequently they form homodimers or heterodimers with other mGluRs. A curious note is that only one needs to have bound glutamate but both can be active.[15,16,17]

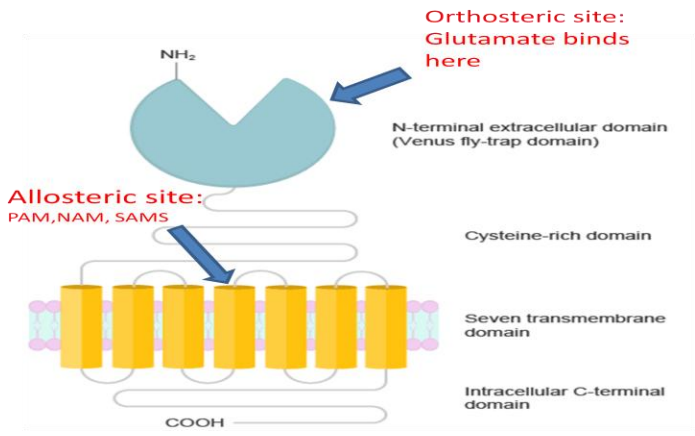

Intro-Figure 2: mGluRs are structural comprised of a the orthosteric site venus flytrap domain , the 7TM which contains the allosteric site and cysteine rich linker between the two.

Once glutamate binds at the VFD a large amount of structural movement must occur for the signal cascade to start. Even though the allosteric sites in mGluRs are less conserved structurally between the different subgroups there are however regions that are conserved in all the mGluRs, called the hinge, ionic lock, and water bridge regions. (**Intro-Figure 3**) Together they help control and promote the 7TM movement. Once glutamate binds, the VFD closes and interacts with the cysteine rich linker which then causes movement of the 7TM. In particular, TM6 swings out 14Å to allow for the G-protein to bind. This swing is facilitated by the hinge region, which contains a crucial residues phenylalanine and tryptophan that act as a strut to help in moving and holding open TM6. The ionic lock and water bridge regions are areas that must be disrupted before the movement of TM6 can occur. These regions are also key areas for small molecule allosteric modulators to interact with and help to stabilize different conformational states of the receptor and therefore its activity. [18,19,20,15, 21,22]

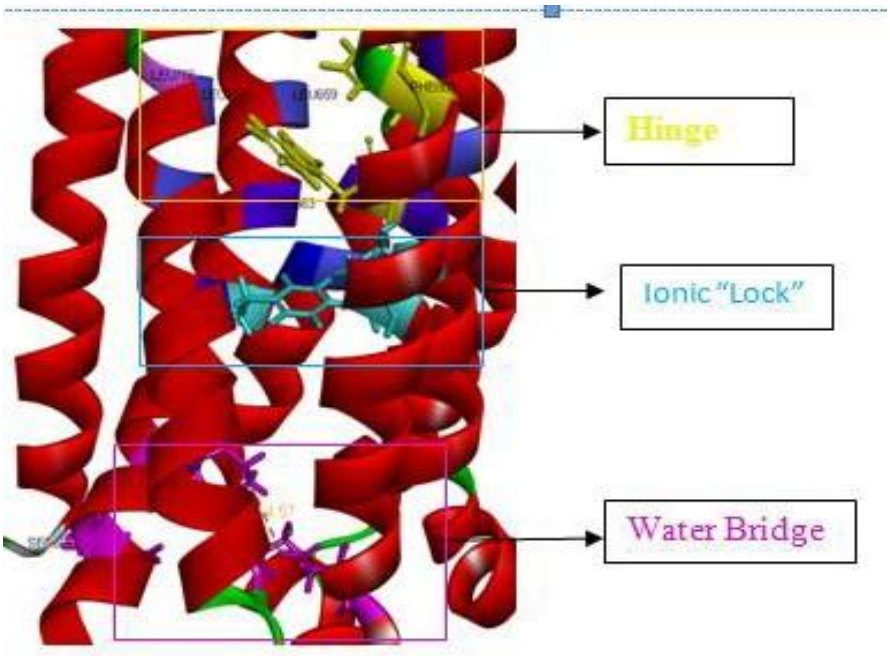

Intro-Figure 3: Homology model of $mGluR_4$ with the hinge, ionic "lock", and "water-bridge

The structural features of the allosteric site were further elucidated and confirmed with recent x-ray crystal structures of the 7TM of $mGluR_1$[18] and mGluR $\frac{23}{5}$ and a cryo-EM structure for $mGluR_4$.[24] These crystal and cyro-EM structures available allow for more accurate modeling of small molecules and help guide synthetic efforts to make small molecules that selectively target these mGluRs. Developing synthetic strategies to effectively synthesize this molecule is another step in the development process.

Synthetic strategies

Developing a molecule that can selectively target the mGluRs is a challenging test due to their high sequence homology at both the orthosteric VFD as well as structural similarities with other GPCRs. Targeting the allosteric sites become more favorable to achieve selective activity within the mGluRs as well as avoiding interaction at other GPCRs. While the allosteric site still has high conservation between the subgroups it does have certain residues and specific structural

shapes that can be exploited. Being able to develop molecules to achieve this is synthetically challenging. There have been small molecules that have been developed that have successfully targeted the mGluRs. Much of this focus, however, has been with subgroup 1, $mGluR_1$ and $mGluR_5$. These molecules still help us to further understand the residues necessary for interaction to achieve allosteric modulation at these particular mGluRs as well an overall understanding of the allosteric site, but does not extensively help with understanding molecular binding necessary for other subgroups. Using the crystal structures and cryo-EM structure homology models can be generated for the other subgroups. We developed a homology model for $mGlu_2$ and $mGluR_4$. These along with regions and residues of interest, and scaffold development will be discussed in more detail in Ch. 2 and 4. The modeling provides structural insights for the development of small molecules.

Isoxazoles have been used not only as synthons in organic chemistry but included in many scaffolds for drug development and current drugs on the market. Our isoxazolo[3,4-d]pyridazinone molecules exploit the residues and structural shape differences to achieve selective interaction within $mGlu_2$ and $mGluR_4$. The first series and part of the second series of compound were developed using hydrazone chemistry to incorporate different functionalized rings and provide conformational constraint to hold the molecule in position to interact with the necessary residues to achieve selectivity as well as activity. For the remainder of the second series of compounds, further modifications of the scaffold were explored to exploit and access more regions of the allosteric site and connecting cysteine rich linker region based on structural drug design and modeling. Synthetically these modifications were achieved through lateral metalation and electrophillic quenching. This particular synthetic method allows for development of highly functionalized molecule as well as developments of a chiral center in a

regio and chiral specific manner. By using this method a variety of synthetic analogs can be produced and used to explore the mGluR allosteric binding pocket additionally possibly lead to molecule that has additional therapeutic activity.

It is important to note while the application of lateral metalation to the isoxazolo[3,4-d]pyridazinones is unique it is a synthetically diverse tool. The lateral metalation and electrophillic quenching was first introduced by Micetich and Chin [24] in 1960 and then further developed over the decades. Notables Beak and Meyers[25] looked at the stereo and region control that could be achieved though the complexing the metal via the isoxazole in complex-induced proximity effect (CIPE) rather than a standard electron-metal interaction. Being able to have a synthetic pathway that allows for more diverse functionalization provides more ready access to a variety of scaffold from a common intermediate. An overview of the scope and use of lateral metalation is discussed in Ch. 1 and our efforts to synthesis selective isoxazolo[3,4-d]pyridazinones to target the mGluRs are discussed in Ch. 4.

References

(1) Benovic, J. L. G-Protein-Coupled Receptors Signal Victory. *Cell* **2012**, *151* (6), 1148–1150 DOI: 10.1016/J.CELL.2012.11.015.

(2) Weis, W. I.; Kobilka, B. K. The Molecular Basis of G Protein–Coupled Receptor Activation. *Annu. Rev. Biochem.* **2018**, *87*, 897 DOI: 10.1146/ANNUREV-BIOCHEM-060614-033910.

(3) Lynch, J.; Wang, J. G Protein-Coupled Receptor Signaling in Stem Cells and Cancer. *Int. J. Mol. Sci.* **2016**, *17* (5), 707 DOI: 10.3390/ijms17050707.

(4) Ferreira, L. G.; Lamba, D.; Consiglio, N.; Delle, R.; Dharmendra, I.; Yadav, K.; Kang, S.; Choi, S.; Basith, S.; Cui, M.; Macalino, S. J. Y.; Park, J.; Clavio, N. A. B. Exploring G Protein-Coupled Receptors (GPCRs) Ligand Space via Cheminformatics Approaches: Impact on Rational Drug Design. *Front. Pharmacol. | www.frontiersin.org* **2018**, *1*, 128 DOI: 10.3389/fphar.2018.00128.

(5) Rajagopal, S.; Shenoy, S. K. GPCR Desensitization: Acute and Prolonged Phases. *Cell. Signal.* **2017**, 1–8 DOI: 10.1016/j.cellsig.2017.01.024.

(6) Bai, M. Dimerization of G-Protein-Coupled Receptors: Roles in Signal Transduction. *Cell. Signal.* **2004**, *16* (2), 175–186 DOI: 10.1016/S0898-6568(03)00128-1.

(7) Conn, P. J.; Christopoulos, A.; Lindsley, C. W. Allosteric Modulators of GPCRs: A Novel Approach for the Treatment of CNS Disorders. *Nat. Rev. drug Discov.* **2010**, *8* (1), 41–54 DOI: 10.1038/nrd2760.Allosteric.

(8) Conn, P. J.; Lindsley, C. W.; Meiler, J.; Niswender, C. M. Opportunities and Challenges in the Discovery of Allosteric Modulators of GPCRs for Treating CNS Disorders. *Nat. Rev. Drug Discov.* **2014**, *13* (9), 692–708 DOI: 10.1038/nrd4308.

(9) Engers, J. L.; Rodriguez, A. L.; Konkol, L. C.; Morrison, R. D.; Thompson, A. D.; Byers, F. W.; Blobaum, A. L.; Chang, S.; Venable, D. F.; Loch, M. T.; Niswender, C. M.; Daniels, J. S.; Jones, C. K.; Conn, P. J.; Lindsley, C. W.; Emmitte, K. A. Discovery of a Selective and CNS Penetrant Negative Allosteric Modulator of Metabotropic Glutamate Receptor Subtype 3 with Antidepressant and Anxiolytic Activity in Rodents. *J. Med. Chem.* **2015**, *58* (18) DOI: 10.1021/acs.jmedchem.5b01005.

(10) Volpi, C.; Fallarino, F.; Mondanelli, G.; Macchiarulo, A.; Grohmann, U. Opportunities and Challenges in Drug Discovery Targeting Metabotropic Glutamate Receptor 4. *Expert Opinion on Drug Discovery*. Taylor and Francis Ltd May 4, 2018, pp 411–423.

(11) Crupi, R.; Impellizzeri, D.; Cuzzocrea, S. Role of Metabotropic Glutamate Receptors in Neurological Disorders. *Frontiers in Molecular Neuroscience*. Frontiers Media S.A. February 12, 2019.

(12) Conn, P. J.; Lindsley, C. W.; Meiler, J.; Niswender, C. M. Opportunities and Challenges in the Discovery of Allosteric Modulators of GPCRs for Treating CNS Disorders. *Nature*

Reviews Drug Discovery. Nature Publishing Group 2014, pp 692–708.

(13) De Filippis, B.; Lyon, L.; Taylor, A.; Lane, T.; Burnet, P. W. J.; Harrison, P. J.; Bannerman, D. M. The Role of Group II Metabotropic Glutamate Receptors in Cognition and Anxiety: Comparative Studies in GRM2-/-, GRM3-/- and GRM2/3-/- Knockout Mice. *Neuropharmacology* **2015**, *89*, 19–32 DOI: 10.1016/j.neuropharm.2014.08.010.

(14) Niswender, C. M.; Conn, P. J. Metabotropic Glutamate Receptors: Physiology, Pharmacology, and Disease. *Annu Rev Pharmacol Toxicol* **2010**, *50* (1), 295–322 DOI: 10.1146/annurev.pharmtox.011008.145533.

(15) Koehl, A.; Hu, H.; Feng, D.; Sun, B.; Zhang, Y.; Robertson, M. J.; Chu, M.; Kobilka, S.; Steyaert, J.; Tarrasch, J.; Dutta, S.; Fonseca, R.; Weis, W. I.; Mathiesen, J. M.; Skiniotis, G.; Kobilka, B. K. Structural Insights into the Activation of Metabotropic Glutamate Receptors. *Nature* **2019** DOI: 10.1038/s41586-019-0881-4.

(16) Levitz, J.; Habrian, C.; Bharill, S.; Fu, Z.; Vafabakhsh, R.; Isacoff, E. Y. Mechanism of Assembly and Cooperativity of Homomeric and Heteromeric Metabotropic Glutamate Receptors. *Neuron* **2016**, *92* (1), 143–159 DOI: 10.1016/j.neuron.2016.08.036.

(17) Rondard, P.; Pin, J. P. Dynamics and Modulation of Metabotropic Glutamate Receptors. *Curr. Opin. Pharmacol.* **2015**, *20*, 95–106 DOI: 10.1016/j.coph.2014.12.001.

(18) Harpsøe, K.; Isberg, V.; Tehan, B. G.; Weiss, D.; Arsova, A.; Marshall, F. H.; Bräuner-Osborne, H.; Gloriam, D. E. Selective Negative Allosteric Modulation Of Metabotropic Glutamate Receptors - A Structural Perspective of Ligands and Mutants. *Sci. Rep.* **2015**, *5* (January), 13869 DOI: 10.1038/srep13869.

(19) Hilger, D.; Masureel, M.; Kobilka, B. K. Structure and Dynamics of GPCR Signaling Complexes. *Nat. Struct. Mol. Biol.* **2018**, *25* (1) DOI: 10.1038/s41594-017-0011-7.

(20) Xue, L.; Rovira, X.; Scholler, P.; Zhao, H.; Liu, J.; Pin, J.-P.; Rondard, P. Major Ligand-Induced Rearrangement of the Heptahelical Domain Interface in a GPCR Dimer. *Nat. Chem. Biol.* **2014**, *11* (2) DOI: 10.1038/nchembio.1711.

(21) Feng, Z.; Ma, S.; Hu, G.; Xie, X. Allosteric Binding Site and Activation Mechanism of Class C G-Protein Coupled Receptors: Metabotropic Glutamate Receptor Family. *AAPS J.* **2015**, *17* (3), 737–753 DOI: 10.1208/s12248-015-9742-8.

(22) Rovira, X.; Malhaire, F.; Scholler, P.; Rodrigo, J.; Gonzalez-Bulnes, P.; Llebaria, A.; Pin, J.-P. P.; Giraldo, J.; Goudet, C. Overlapping Binding Sites Drive Allosteric Agonism and Positive Cooperativity in Type 4 Metabotropic Glutamate Receptors. *FASEB J.* **2015**, *29* (1), 116–130 DOI: 10.1096/fj.14-257287.

(23) Topiol, S.; Sabio, M. 7TM X-Ray Structures for Class C GPCRs as New Drug-Discovery Tools. 1. MGluR5. *Bioorganic Med. Chem. Lett.* **2016**, *26* (2), 484–494 DOI: 10.1016/j.bmcl.2015.11.087.

(24) Lin, S.; Han, S.; Cai, X.; Tan, Q.; Zhou, K.; Wang, D.; Wang, X.; Du, J.; Yi, C.; Chu, X.; Dai, A.; Zhou, Y.; Chen, Y.; Zhou, Y.; Liu, H.; Liu, J.; Yang, D.; Wang, M.-W.; Zhao, Q.;

Wu, B. Structures of Gi-Bound Metabotropic Glutamate Receptors MGlu2 and MGlu4. *Nat. 2021 5947864* **2021**, *594* (7864), 583–588 DOI: 10.1038/s41586-021-03495-2.

(25) Micetich, R. G.; Chin, C. G. Studies in Isoxazole Chemistry. 111.' The Preparation and Lithiation of 3,5-Disubstituted Isoxazoles. *Can. J. Chem.* **1970**, *48*, 1371.

(26) Beak, P.; Meyers, A. I. Stereo- and Regiocontrol by Complex Induced Proximity Effects: Reactions of Organolithium Compounds. *Acc. Chem. Res.* **1986**, *19* (11), 356–363 DOI: 10.1021/ar00131a005.

Chapter 1: Isoxazole Lateral Metalation, the sequel update of an earlier review. The updated review was invited by the journal *Trends in Organic Chemistry* on 10 August, 2021

Table of contents

Chapter 1: Isoxazole Lateral Metalation, the sequel

Christina A. Gates, Joseph R. Mirzaei and Nicholas R. Natale*
Medicinal Chemistry Graduate Program, Department of Biomedical and Pharmaceutical Sciences, The University of Montana, Missoula MT 59812.

Lateral metalation of heterocycles[1] has proved to be a useful tool over the years, and particularly in the case of elaborating the isoxazole scaffold[2,3,4] Isoxazole have seen useful service as precursors for 1,3-dicarbonyl synthons, a tactic that can be used in the continued pursuit of polyketides, which are the base synthons of many fused ring systems found in flavonones and tetracyclines.[5] The isoxazole ring can be of interest for its intrinsic biological activity), and often serves as an element of conformational constraint.[6,7,8,9,10]

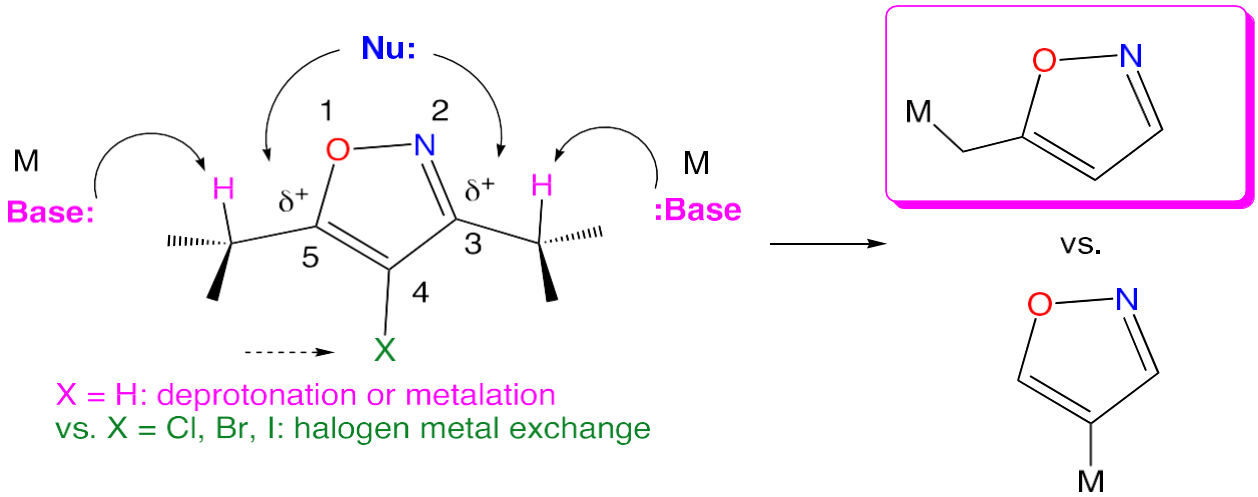

Figure 1-1. Lateral metalation (box) can be a useful tool, but is fraught with potential difficulties in functionally complex examples. When X =H, the isoxazole can be directly ring deprotonated; when X=Halogen, halogen metal exchange leads to a metalated heterocycle. However, nucleophilic attack at the ring, and electron transfer ring opening are also known alternative outcomes.

This account represents an up-date of our 1993 review on the lateral metalation topic,[3] expanded to encompass the important developments in ring metalation and halogen-metal exchange, with brief discussions of the uses of the resulting functionalized products. Other aspects of isoxazole

chemistry have been created in the interim. The literature is reviewed from mid-1992, exceptions are made for earlier work where citations were missed in our earlier account. Articles are included to 2020, except for a few cases where we were aware of articles in press in 2020 and subsequently appeared the next year. Furthermore, we have also included discussion of isoxazole coordination chemistry where it is deemed relevant, again up-dating our own review[4] because of the critical impact of pre-coordination or proximity chelation on the outcome of metalation processes (*vide infra*). Essentially any report which requires and/or postulates the involvement of an isoxazole–metal complex as an intermediate was considered in this present review. Searches were conducted using both metalation and metallation spellings, and we found that substructure searches for the laterally metalated ring (**Figure 1-1**) produced over two thousand hits, including isoxazoles with ring metalation as well as metal ion complexes elsewhere in the molecule. Therefore we have decided to include a depiction of the metal ion complexes in the presence of isoxazoles, where a useful electrophilic quenching or cross coupling is facilitated. This review focuses on isoxazoles and there lateral metalation and coordination of metals. For more examples or to explore lateral metalation of other scaffolds see reviews by Hu[8], Zhang[9], Badenock[10] , and Walunj[11],Ali[12] and Roger[13].

Why Lateral Metalation is necessary

Direct deprotonation of an isoxazole or benzisoxazole alpha to the ring heteroatom usually gives rise to ring fragmentation. The Kemp elimination is the deprotonation of the C-3 of a benzisoxazole (**1**), through the step illustrated in **2**, to give ring opening (**3**).[14] (**Figure 1-2**) The Kemp elimination has been the subject of recent interest wherein computational enzyme design was used to develop an enzyme to catalyze the deprotonation (**Figure 1-3**).[15]

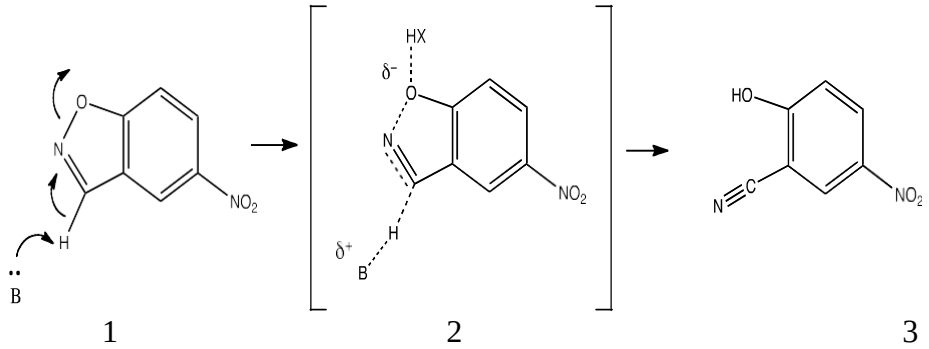

Figure 1-2 The Kemp elimination

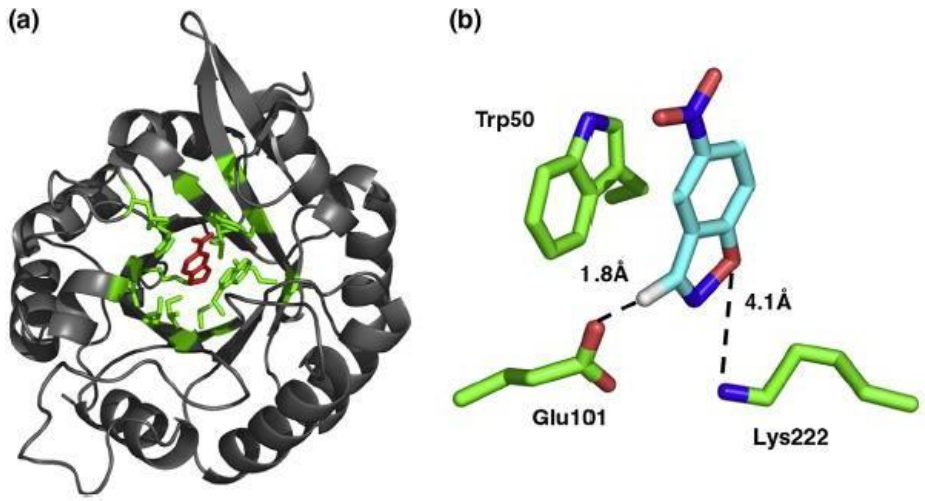

Figure 1-3 (a) Engineered enzyme that promotes the Kemp elimination (b) the amino acids involved in the reaction.

While synthetically the Kemp elimination and ring opening can present some challenges, it does have somed therapeutic applications, such as in the case of Leflunomide, an immunsupressive disease modifying antirheumatic drug (DMARD. The isoxazole of Lefluonimde represents a prodrug that opens to the active drug Teriflunomide via the Kemp elimination. (**Figure 1-4**)

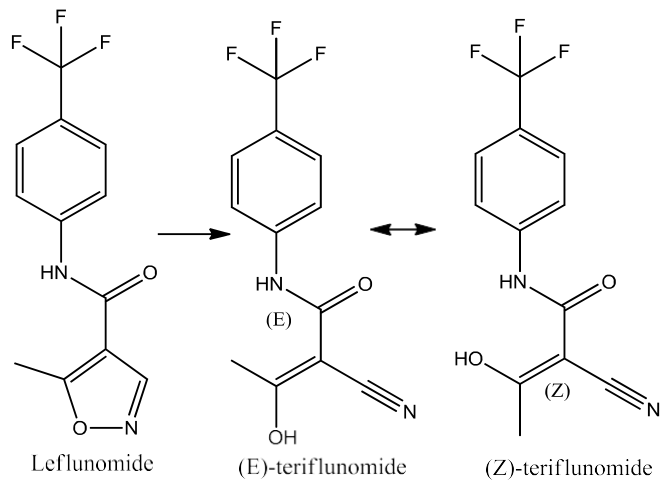

Figure 1-4 Leflunomide Kemp elimination and isoxazole ring opening to active drug Teriflunomide

Synthetically avoiding Kemp elimination ring opening of the isoxazole and being able to have the versatility to be able to add a group to a specific position in the presence of a labile groups or reactive position is has additional synthetic utility. This review will look at the lateral metalation catalized reaction of lithium as well as early and late transition metals. Each metal in lateral metalation provides a different synthetic utility and can vary regio- and stereo- control of the functional groups as well as what synthetic environments are tolerated. This in turn provides access to a wide variety highly functionalized isoxazole in a regio- and stereo- specific manner that can minimized or avoid undesired products. First though it is necessary to briefly discuss how metals are coordinated by isoxazoles and other atoms.

COORDINATION WITH TRANSITION METALS

Our general discussion of interactions will begin with common modes of interaction that have been observed in coordination chemistry. Isoxazole binding modes observed in metal complexes, can generalized to interactions with Lewis Acids (delta+). In the Munsey review, conjugated

amino groups were considered in the coordination chemistry with metals, here generalized to conjugated Lewis bases (LB).(**Chart 1-1**)[16,17].

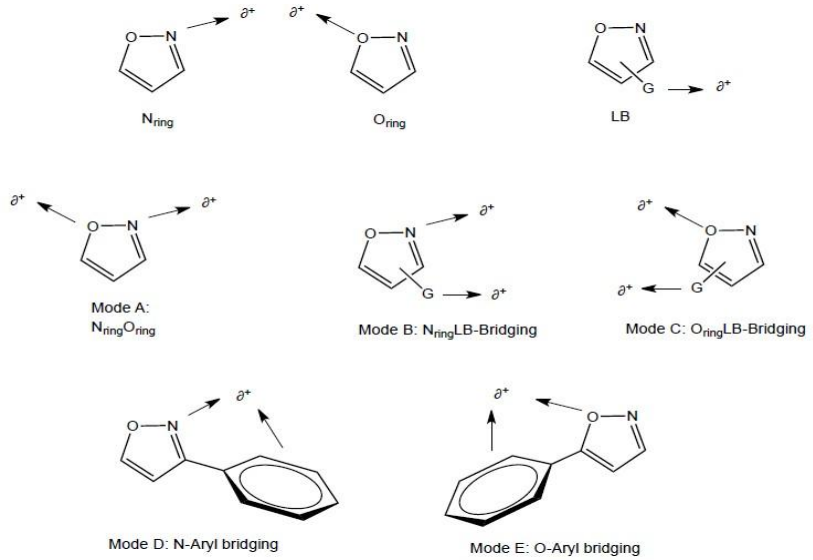

Chart 1-1 General coordination chemistry with metals of isoxazoles

This coordination has been looked at in detail.G. G. Mohamed reported that hexachlorocyclodiphospho(V)azene of sulfamethoxazole, H_2L, reacts with stoichiometric amounts of transition metal salts such as Fe(III), Co(II), Ni(II), Cu(II), Zn(II), and UO_2(II) to afford colored complexes in a moderate to high yield. The complexes are found to have the general formula $[(MX_n)_2(H_2L)(H_2O)_m]$ and H_2L behaves as a neutral bidentate ligand coordinated to the metal ions through enolic sulfonamide OH and isoxazole N atoms. (**Figure 1-5**)

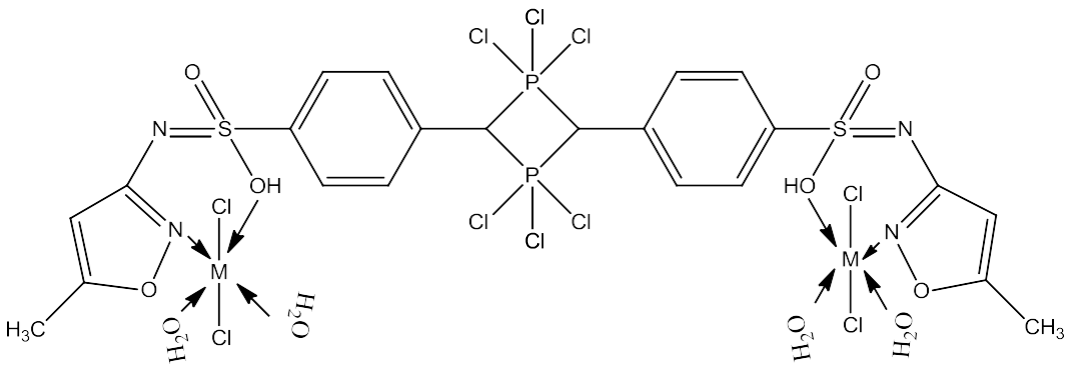

Figure 1-5 -Suggested structures of H2L metal complexes

It is reported that isoxazoles form complexes with various transition metals and behave as monodentate or bidentate ligands,[18] in spite of its low basisity.[19]

In the reduction of isoxazole by $Mo(CO)_5$, isoxazole forms a complex with $Mo(CO)_5$.[20] A similar intermediate with **1** was suggested in the reductive cleavage of isoxazole by samarium ion. [21]

Therefore, the reduction of isoxazoles by DHLAm-Fe(II) might proceed as in **Figure 1-6**

Isoxazole makes a complex with DHLAm-Fe(II) through nitrogen and is subjected to one-electron reduction by DHLAm-Fe(II) to produce intermediate **1** which is transformed simultaneously to **2** by isomerization. One-electron reduction of **2** by DHLAm-Fe(II) then gives b-amnio enone, LAm, and ferrous ion.

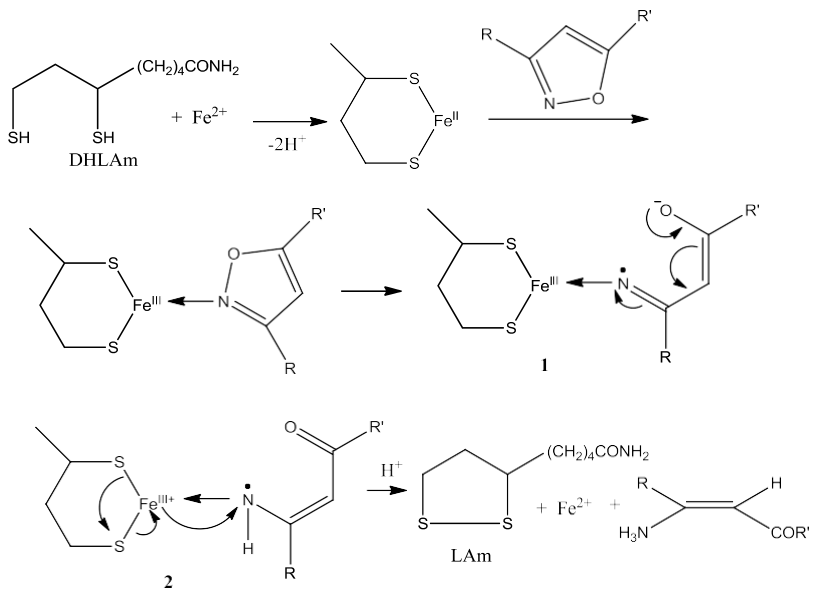

Figure 1-6 DHLAm-Fe(II) mechanism

The metal complexes of Cu(II), Ni(II) and Co(II) with Schiff bases of 3-(2-hydroxy-3-ethoxybenzylideneamino)-5-methyl isoxazole [HEBMI] and 3-(2-hydroxy-5-nitrobenzylidene amino)-5-methyl isoxazole [HNBMI] which were obtained by the condensation of 3-amino-5-methyl isoxazole with substituted salicylaldehydes have been synthesized.(**Figure 1-7**)[22]

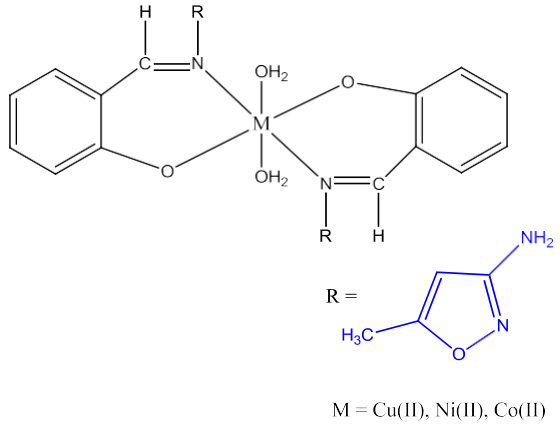

Figure 1-7 metal complex with Schiff bases

Pitteri has studied the reactivity of neutral nitrogen donors in square-planar d^8 metal complexes. They showed that for the reaction, both forward and reverse reactions obey the usual two-term rate law observed in square-planar substitution.

$$[Pt(terpy)Cl]^+ + nu \rightleftharpoons [Pt(terpy)(nu)]^{2+} + Cl^-$$

Figure 1-8 General platinium exchange with nucleophile

(nu = thiazole, oxazole, isoxazole, imidazole, pyrazole and 3,5-dimethylpyrazole) although these nucleophiles are ambidents but they bind to Pt(II) through nitrogen by displacement of chlorine and binding mostly dependent on basisity of nitrogene hetrocycle. (**Figrue 1-8**)[23]

Two new hydrazone chelating ligands, 2-(2-(5-methylisoxazol-3-yl)hydrazono)5,5-dimethylcyclohexane-1,3-dione (HL^1) and 2-(2-(5-tert-butylisoxazol-3-yl)hydrazono)5,5-dimethylcyclohexane-1,3-dione (HL^2), and their nickel(II) and copper(II) coplexes were synthesized using the procedure ofdiazotization, coupling and metallization.(**Scheme 1-1**) [24]

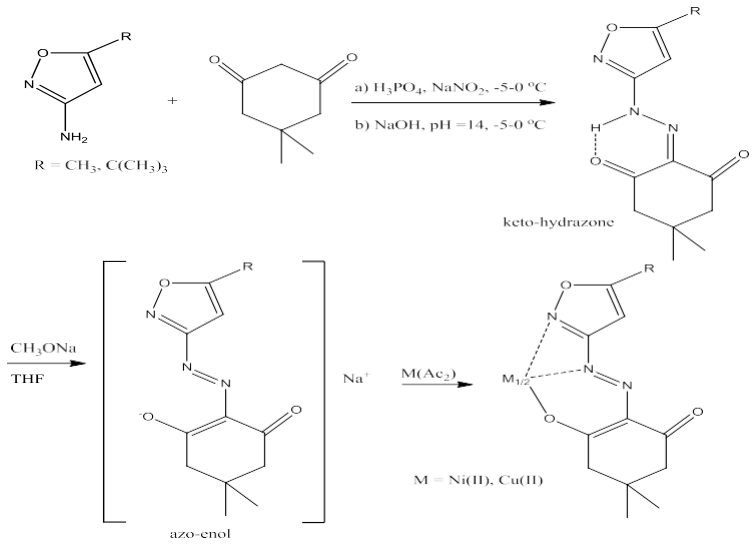

Scheme 1-1 Syntheis of hydrazone chelating ligand via Copper(II) and Nickel(II) complexes)

In an earlier report Chen and co-workers reported the synthesis of the ligand, 2-(2-(5-tert-butylisoxazol-3-yl)hydrazono)-*N*-(2,4-dimethylphenyl)-3-oxobutanamide (HL), and its four binuclear transition metal complexes, $M_2(L)_2(\mu\text{-}OCH_3)_2$ [M = Ni(II), Co(II), Cu(II), Zn(II).(**Figure 1-9**) [25]

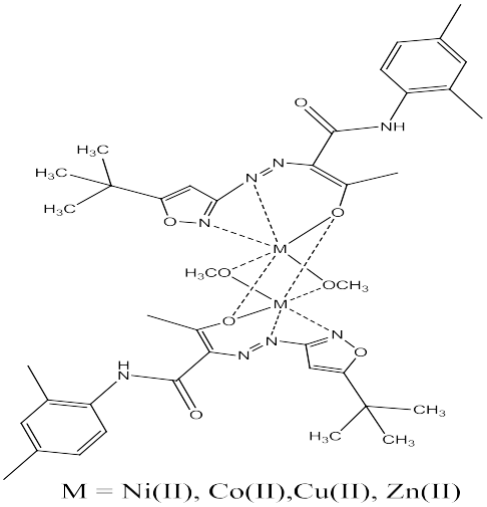

Figure 1-9 HL four binuclear transition metal complexes

Four novel tetrafluoropropanol soluble metal(II) hydrazone complexes [Ni(L)2, Co(L)2, Cu(L)2, and Zn(L)2] were designed and synthesized in good yields through the reaction between metal(II) acetate and hydrazone ligand (5-(2-(5-tert-butylisoxazol-3-yl)hydrazono)-1,3-dimethylpyrimidine-2,4,6-trione, HL) prepared beforehand. They were evaluated as suitable optical recording materials for the recordable blu-ray disc system. Their structures are proposed in (**Figure 1-10**). [26]

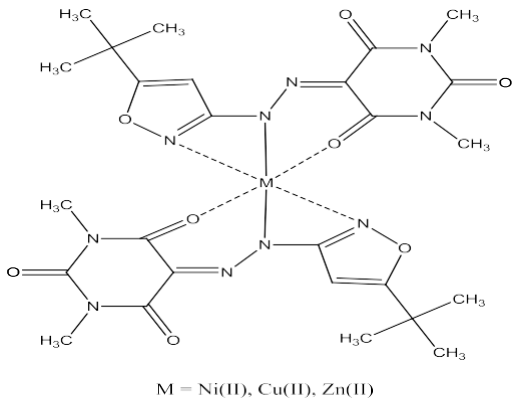

Figure 1-10 further exploration of HL metal complexes with different ligands and metals

Fenga reported the preparation of **2**, 6-bis-(5-ferrocenylisoxazole-3-yl) pyridine **4** and complex of Pd(II) **5** is shown in (**Scheme 1-2**). They achieved synthesis of complex **5** by reaction of 2,6-bis-(5-ferrocenylisoxazol-3-yl)pyridine **4** with $Pd(OAc)_2$ in CH_2Cl_2. Complex **5** was determined by spectroscopic analysis. The ligand is bound to palladium in a tridentate fashion via the three N atoms, forming two five-member chelate rings. They used coupling of iodobenzene with phenylacetylene Sonogashira cross-coupling catalyzed by 1 mol% of complex **5** in the absence of CuI as a co-catalyst. Moreover, adding TBAB (tetrabutylammoniumbromide) to the reaction mixture enhanced the activity of the catalyst.[27]

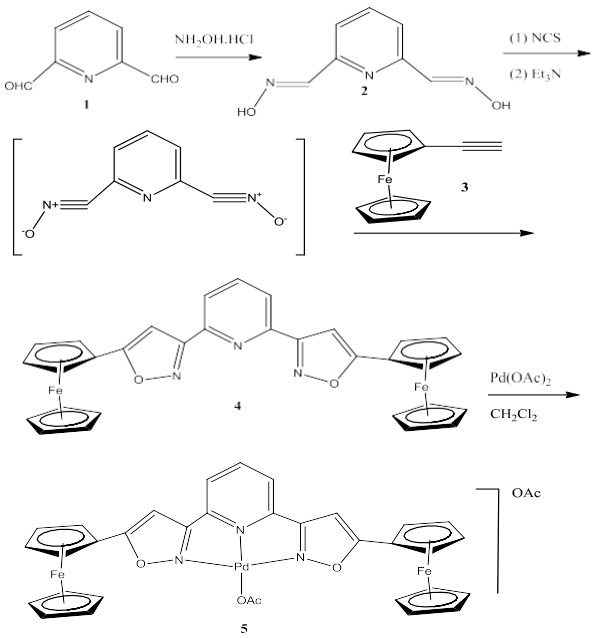

Scheme 1-2, preparation of **2**, 6-bis-(5-ferrocenylisoxazole-3-yl) pyridine **4** and complex of Pd(II) **5** complex of Pd(II) **5**

La Cour and co-workers reported the synthesis Schiff-base complexes of isoxazole and biologically important 3d metal(II) ions (M = Ni, Cu or Zn). The crystal structure have been determined for [*N*,*N*9-bis(3-phenyl-5-sulfanylisoxazol-4-ylmethylene)butane-1,4-diaminato]copper(II), which shows the metal atom is coordinated to two nitrogen and to two sulfur atoms which form a flattened tetrahedron with the dihedral angle between the two N-M-S planes being 48.6(1). (**Figure 1-11**)The physicochemical properties of these complexes have been studied in solution.[28]

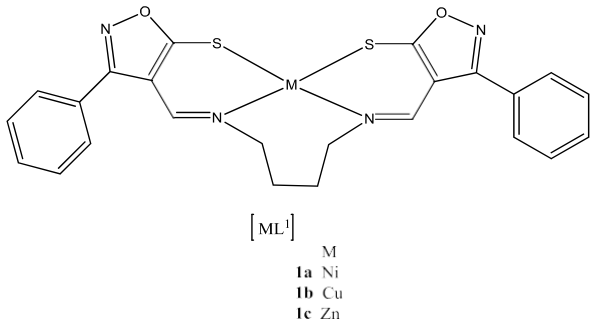

Figure 1-11 metal atom is coordinated to two nitrogen and to two sulfur atoms which form a flattened tetrahedron with the dihedral angle between the two N-M-S planes

Lithium

Lithium is used frequently in synthesis as both an additive and a base. Many of these reagents are commercial available or can be synthesized readily. One such application is in polyketide biomimetic cyclizations which was proposed by Birch[29] as illustrated for citromyetin, and an early demonstration that isoxazoles could be used to assemble polyketide synthons for these biomimetic cyclizations was the report of Tanaka[30] (**scheme 1-3**). The keto-bisisoxazole was regarded as the equivalent of the penta-acetate.

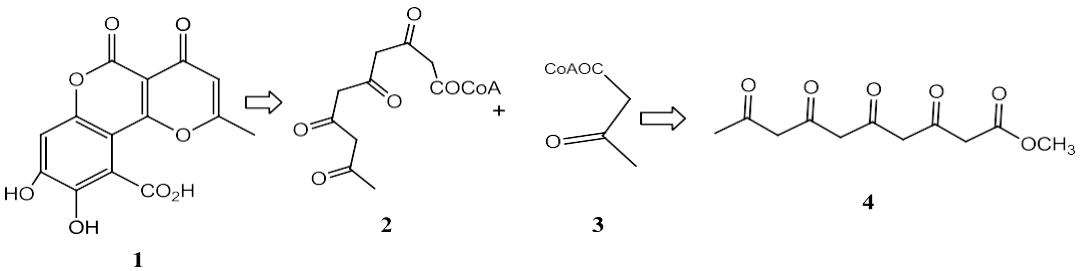

Scheme 1-3 Polyketide synthesis

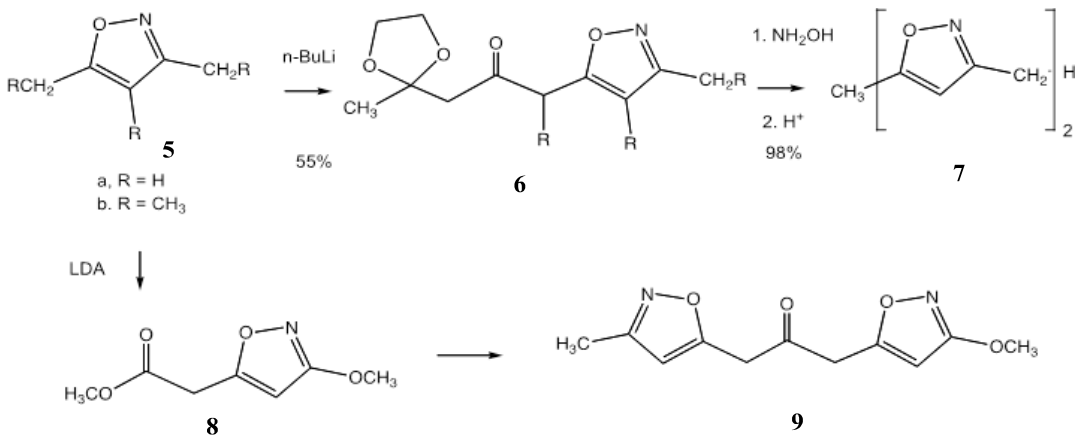

Scheme 1-4 Isoxazole synthons to expand polyketides

The fruition of this hypothesis in the realization of subsequent biomimetic cyclizations was found in the elegant work of Gibreath[31], discussed in detail in our previous review.[4]

The modular nature of polyketides is still a theme of current interest, although the main emphasis for the use of heterocycles as masked synthons for biomimetic synthesis in this arena has moved towards isoxazolines. However, given the potential number of new targets of polyketide origin exemplified in the work of Khosla[32], it is entirely plausible that isoxazole synthons are poised for a renaissance of application. (**Scheme 1-4**)

One example such example was by Bode et al[33] (**Scheme 1-5**) by utilizing C-chloro oximes and cyclic 1-3 diketones through a base promoted cylcocondensation functionalized isoxazoles were achieved this then was converted into polyketides derived polycyclic structures. This synthetic method is direct and allows for the production of highly functionalize isoxazoles by using milder reaction conditions that accommodate a variety of functional groups. While polyketides are a good synthetic precusors so are a number of other functional groups that can be obtained with lateral metalation.

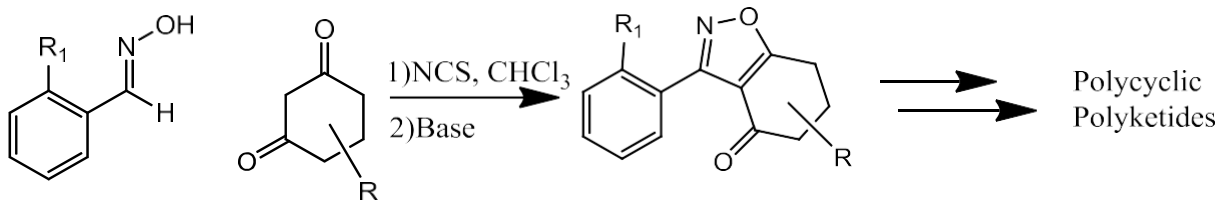

Scheme 1-5 Conituned expansion of polyketide synthesis using isoxazoles as an intermediate

Krogsgaard-Larsen used lateral metalation of the N-nitroso-isoxazole to accomplish a critical acylation in his preparation of conformationally restricted ibotenic acid analogs **(Scheme 1-6)**.[34]

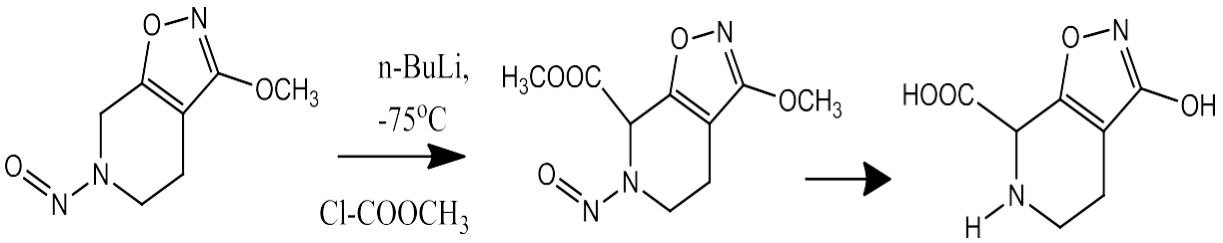

Scheme 1-6 Lateral metalation of N-nitroso-isoxazole to accomplish a critical acylation in the preparation of conformationally restricted ibotenic acid analogs

In an effort to synthesize 2-Me-Tet-AMPA analogues, Vogensen utilized C-4 lithiation of isoxazole **1** and a Michael addition of **1** to amino acrylate **2** afforded **3**. Treatment of **3** with sodium azide and triethyamine hydrochloride gave access to tetrazole **4 (Scheme 1-7)**. [35]

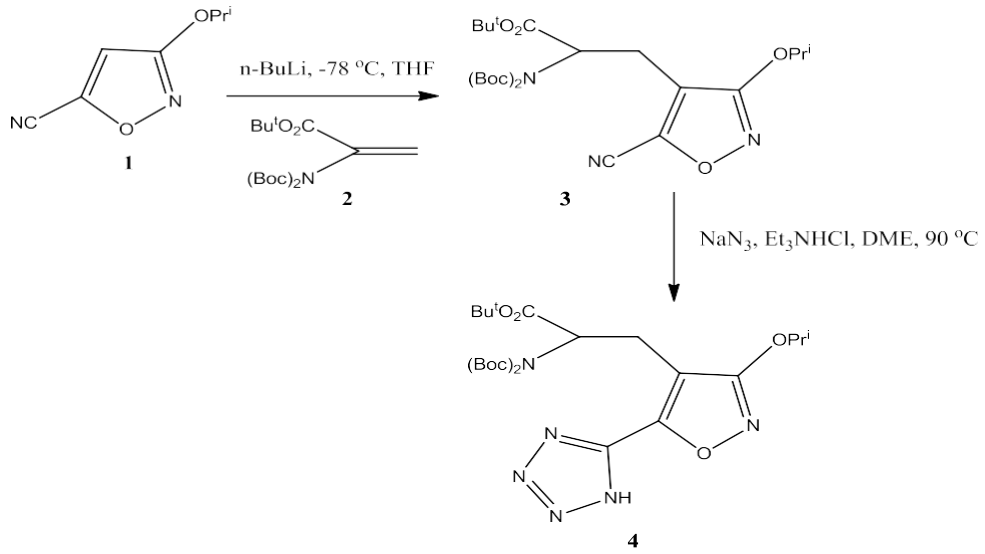

Scheme 1-7 Controlled synthesis of isoxazole substituted with tetrazoles using lateral metalation and sodium azide

Treatment of 3,5-dimethylisoxazole (**1**) with n-butyllithium3a and thereafter with α-bromoethyl tetrahydropyranyl ether afforded isoxazole **2a** in 73% yield, whose exposure to methanolic acid furnished alcohol **2b** in 94 % yield. Jones oxidation of the latter yielded (85%) acid **3a**. Exposure of acids **3a** to oxalyl chloride, vacuum removal of the excess reagent, and slow addition of ether solution of the remaining acid chloride to an ethereal diazomethane solution led to diazo ketone **3b** (67%). Decomposition of diazo ketone **3b** was carried out over dirhodium tetraacetate in methylene chloride solution. Diazo ketone **3b** produced bicyclic ketone **6** (61%), indicative of the outlined reaction mode in (**Scheme 1-8**).This reaction used two different metals the coordinated the metal and stabililed the transition state and addition next to the oxygen. The Rh stabilized and assisted with ring closer to produce the final bicycle ketone products. [36]

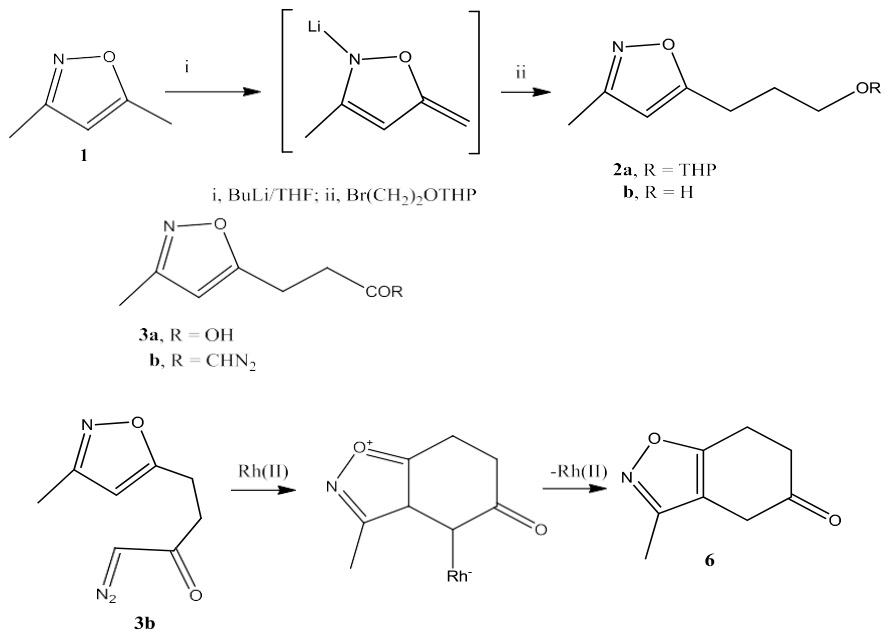

Scheme 1-8 production bicyclic ketone using various metals

To investigate the potential of small, substituted heterocycles to act as glycine agonists, Drummond et al evaluated the similarities between glycine and a series of hydroxy- and amino-substituted pyrazoles and isoxazoles through complementary molecular modeling techniques. By using a "scorecard" approach to determine the overall similarity of projected agonist structures to glycine, novel derivatives was synthesized. The 5-phenyl analogue **3** was synthesized by the method shown in **Scheme 1-9.** The 1:l mixture of *0*- and *N*-methylated isomers **(32** and **33)** were separated by chromatography on silica gel. The *0*-methylated compound **(33)** was converted to the 4- carboxylic acid derivative by metalation at the 4-position followed by quenching with crushed dry ice. The 4-amino group was introduced by a Curtius rearrangement following the method of Poutler and Capson. [37]

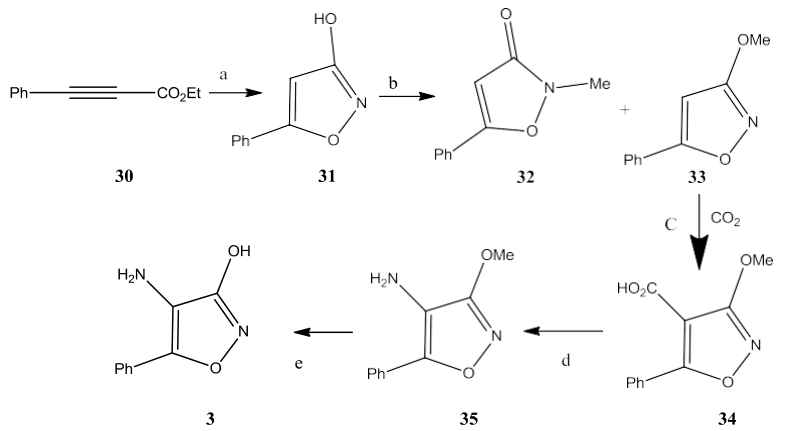

(a) $NH_2OH \cdot HCl$, $NaOH/H_2O$; (b) CH_2N_2, MeOH; (c) (1) *n*-BuLi/THF, -78 °C, (2) CO_2,

(3) H_3O+; (d) (1) DPPA, Et_3N, (2) $TMS(CH_2)_2OH$, (3) *n*-Bu4NF, THF; (e) 31% HBr/HOAc[3]

Scheme 1-9 synthesis of trisubstituted isoxazoles from alkynes

Myers reported a practical, enantioselective synthetic route to a key precursor to the tetracyclineantibiotics. Key steps in the route involve enantioselective addition of divinylzinc to 3-benzyloxy-5-isoxazolecarboxaldehyde and an endo-selective intramolecular furan Diels-Alder cycloaddition reaction. This was able to proceed with a high ee (93%) and in large gram scale quantities. They developed two procedures to transform **2** into the optically enriched (*R*)-allylic alcohol **3**.. The configuration of the product **3** (**Scheme 1-10**) is opposite to that observed in related additions to non-heteroaromatic aldehydes. Which suggests that **2** may bind to the metal complex in bidentate fashion during the addition (thus presenting the enantiotopic π-face of the aldehyde to the nucleophile (**Scheme 1-11**).

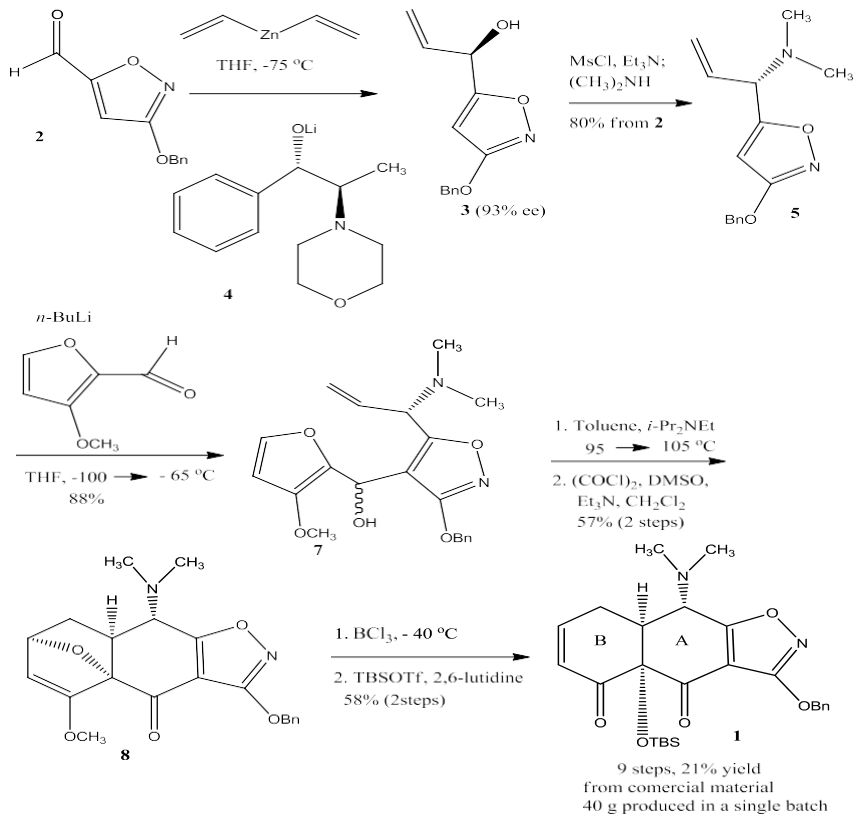

Scheme 1-10 Synthetic route to products with high ee

The reversal in enantioselectivity they observed with a potentially bis-chelate substrate has not been documented in the Oppolzer system so far as they are aware. Dinuclear zinc catalysts apparently do not show such behavior. The lithium cation may prove a key organizational element, as suggested in **Scheme 1-11** and originally proposed by Oppolzer and Radinov. A convergent coupling was achieved by metalation of the isoxazole ring of the (*S*)-allylic amine **5** Detailed analysis of the product mixture shows that cycloaddition occurs from a single π-face of the allylic amine (dienophile) and that the two major products are both endo-diastereomers, stereochemically homologous with the target **1** at the AB juncture (see **Scheme 1-10**). While both of the epimeric substrates **7** undergo endo-selective cycloaddition, the endo/exo ratios are different (6.2:1 for the (*S*)-alcohol, and 1.6:1 for the (*R*)- alcohol), as are the rates of cycloaddition, with the (*S*)-alcohol **7** reacting somewhat more rapidly. The endo selectivityof the

cycloaddition reaction is notable, given that the majority of furan Diels-Alder reactions are exo-selective, reversible processes. Retro-cycloaddition apparently does not occur in the present case.[38]

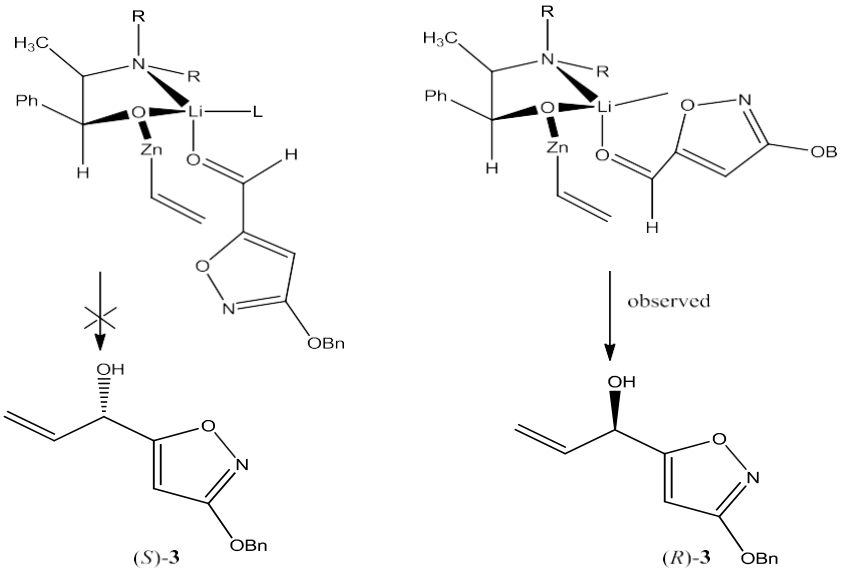

Scheme 1-11 Dinuclear zinc catalysts apparently do not show such behavior. The lithium cation may prove a key organizational element

Masciadri and co-workers reported highly regioselective (> 90%) MOM-protection of 3-hydroxy-5-phenyl-isoxazole followed by elaboration in 4 position via directed ortho-metalation and mild deprotection with cold methanolic HCl provided ready access to a zwitterionic isoxazole derivatives**.(Scheme 1-12)**[39]

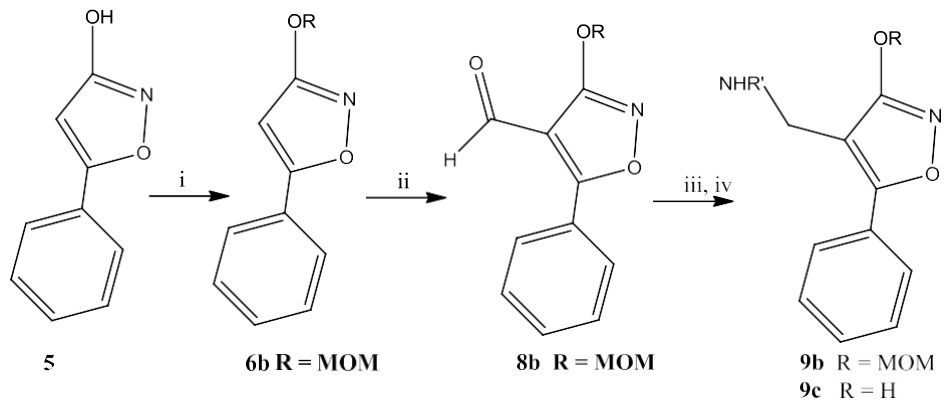

i) Et_3N/methyl sulfoxide, chloromethyl methyl ether, 0 °C/Ar 10 min, r.t. 20 min; ii) *n*-BuLi/THF, -70 °C ; DMF; iii) $R'NH_2$/EtOH, reflux; $NaBH_4$ 0-20 °C; iv) cold MeOH, HCl

Scheme 1-12 directed ortho-metalation and mild deprotection with cold methanolic HCl provided ready access to a zwitterionic isoxazole derivatives

Campana et al were able to successfully obtain an x-crystal structure of potential mGluR selective a dialkylated isoxazolo[3,4-d]pyridazinones selectively at the C-3 position of the isoxazole. This was achieved via lateral metalation of the C-3 position versus the C-10 using LiHMDS as the base and benzyl bromide as the electrophile. (**Scheme 1-13**)[40]

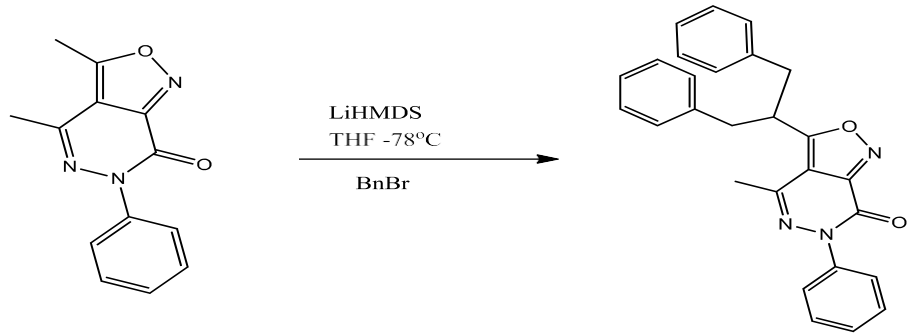

Scheme 1-13 Selective C5 functionalization of dialkylated isoxazolo[3,4-d]pyridazinones

Hulubei et al (**Scheme 1-14)** used lateral metalation on structure 2 to produce a variety of branched and unbranched IDHP analogues. These analogues exhibited inhibitory activity at MDR and had a SAR unique from their activity at the voltage gated calcium channel. With a

unique SAR profile and a versatile synthetic methodology provides a route for creating additional selective compounds. [41]

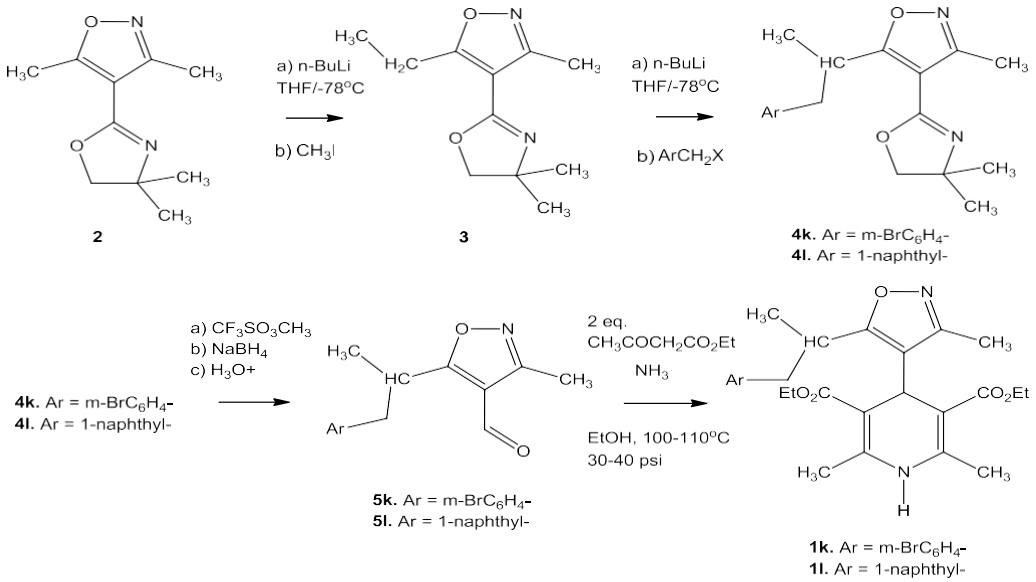

Scheme 1-14 produce a variety of branched and unbranched IDHP analogues

Patel et al developed and tested analogues of AMPA. This was achieved through lateral metalation and electrophillic quenching of the starting AMPA to generate more liphophilic analogues to better access and bind System $_{Xc}$. These compounds were evaluated for activity and SAR insights. Though modeling a pharmacophore model and SAR was developed that illustrated that there was a liphophilic pocket adjacent to the main binding pocket that could contribute the increased activity of the more liphophilic analogues.(**Scheme 1-15**) [42]

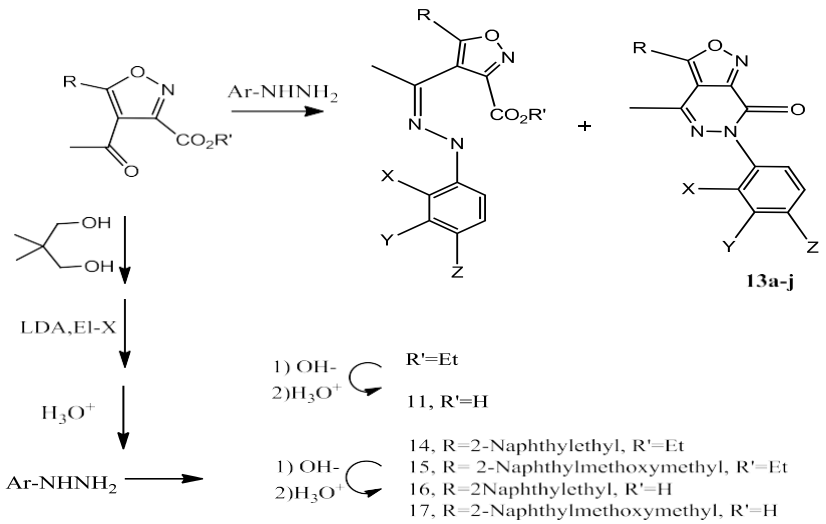

Scheme 1-16 lateral metalation and electrophillic quenching of the starting AMPA to generate more liphophilic analogues

Li et al synthesized and successfully achieved a X-ray crystal structure of a highly functionalized 3-(9'-anthyl)- isoxazolyl sulfonamides for use in exploring binding to the G-4 quadruplex. These compounds were achieved by selective metalation at the C-5 of the isoxazole and generation of a single racemic diasteromers (**Scheme 1-16**). [43]

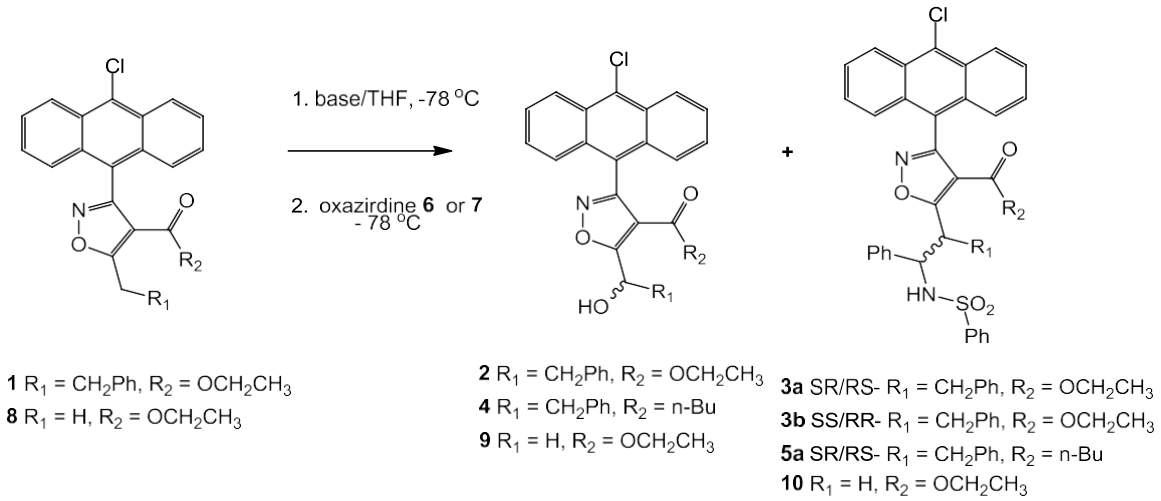

Scheme 1-16 Synthesis highly functionalized 3-(9'-anthyl)- isoxazolyl sulfonamides

Han et al used 3-(10'-halo-9'-anthracenyl)-5-methyl-4-isoxazolcarboxylic acid ethyl esters as a highly versatile and efficient scaffold for lateral metalation at the C-5 of the isoxazole as well as

Suzuki-Fu palladium cross-coupling at the C-10 of the anthracene (**Scheme 1-17**). Being able to perform a selective lateral metalation or Pd coupling in the presence of an aryl halogen and an isoxazole, which has known issues in the presence of low valence metals, provides a versatile reaction route for elaborating the scaffold.[44]

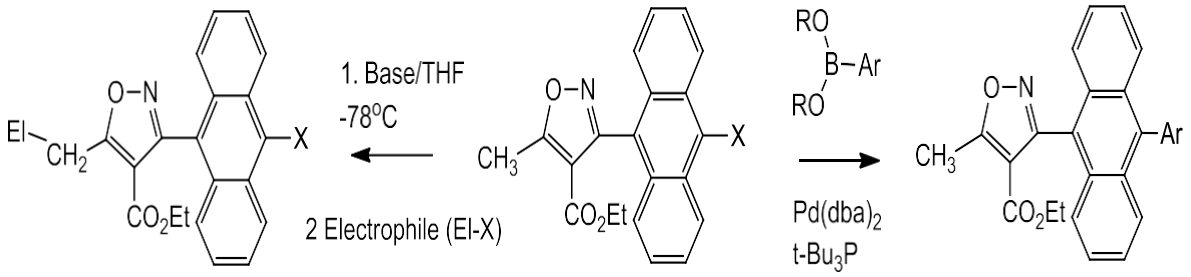

Scheme 1-17 3-(10'-halo-9'-anthracenyl)-5-methyl-4-isoxazolcarboxylic acid ethyl esters as a highly versatile and efficient scaffold for lateral metalation at the C-5 of the isoxazole as well as Suzuki-Fu palladium cross-coupling at the C-10 of the anthracene

Mosher et al used lateral metalation to selectively produce anti-cancer agents through the anion of the 3,5-disubstituted isoxazole-4-carboxylic acid at the C-5 position of the isoxazole followed by nucleophilic aromatic substitution on a 9-chloroacridine.Varying the amount of base and what groups were present on the isoxazole additionally helped to direct to the C-5 position and further the understanding of how different conditions affect the lateral metalation at that position over other potential sites. (**Scheme 1-18**) [45]

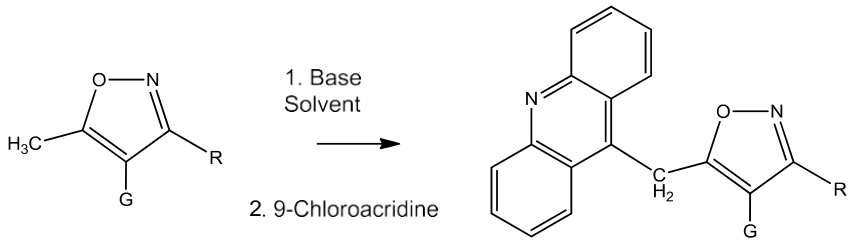

	R	G	Base	Solvent	Yield
a	$-CH_3$	$CON(iPr)_2$	*n*-BuLi,40°	THF	53%
b	$-CH_3$	oxazoline	*n*-BuLi -78°	THF	5.5%
c	$-CH_3$	-COOH	2*n*-BuLi, -78°	THF	–
e	$-CH_3$	-COOEt	*t*-BuLi -78°	THF	–
f	$-CH_3$	-COOEt	*n*-BuLt -78°	THF	see A below
g	-Ph	oxazoline	*n*-BuLi, -78°	THF	12%
h	-Ph	oxazoline	*n*-BuLi, -78°	THF:HMPA 6:1	20%
i	-Ph	oxazoline	*n*-BuLi, -78°	THF:HMPA 3:1	22%
j	-Ph	oxazoline	*n*-BuLi, -78°	TMEDA	–
k	-Ph	oxazoline	*n*-BuLi, -24°	DME	5%

A - the major product (70%) of this reaction was:

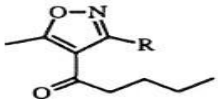

Scheme 1-18 Varying the amount of base and what groups were present on the isoxazole additionally helped to direct to the C-5 position and further the understanding of how different conditions affect the lateral metalation at that position over other potential sites

Zhou et al generated functionalized AMPA analogs through lateral metalation of ethyl-4-acetyl-5-methyl-3-isoxazoyl carboxylates using 5,5-dimethyl-1,3-dioxanyl as a directing group. This synthetic route tolerated a variety of electrophiles and resulted in good to excellent yields (41-81%).[46] **(Scheme 1-19)**

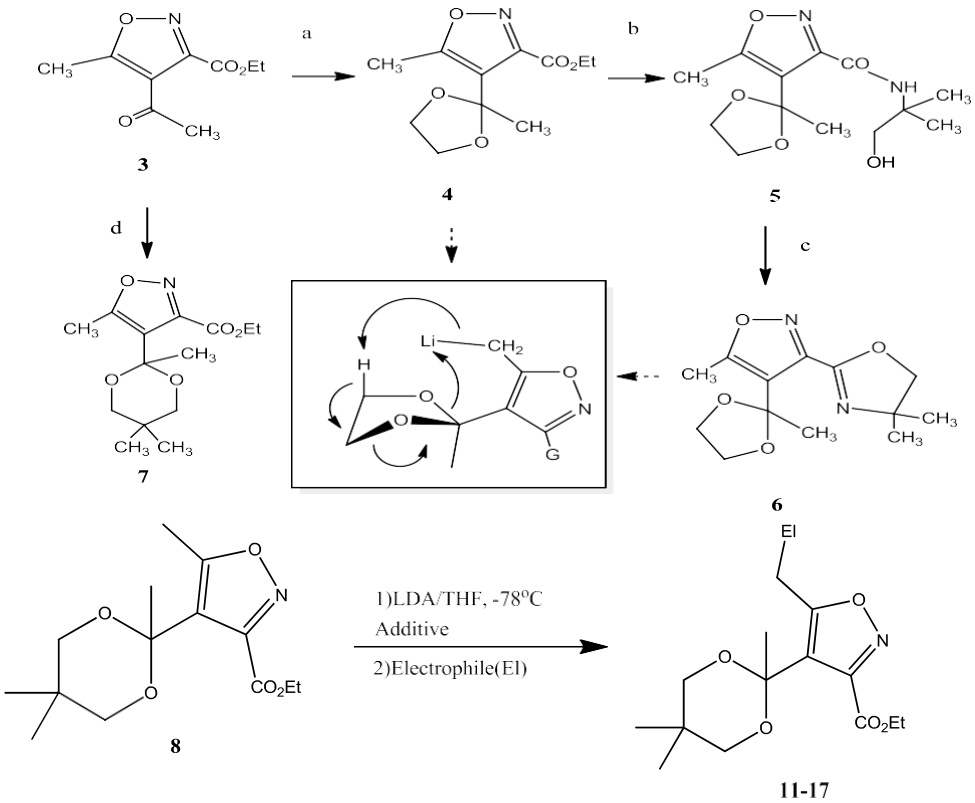

Entry	Electrophile	Product	Yield (%)
1	MeI	8a	81
2	EtBr	8b	65
3	BnBr	8c	64
4	PhCHO	8d	72
5	MeCOMe	8e	68
6	PhNCO	8f	68
7	TMSCl	8g	66
8	Me_3SnCl	8h	42
9	MeSSMe	8i	61

Scheme 1-19 generated functionalized AMPA analogs through lateral metalation of ethyl-4-acetyl-5-methyl-3-isoxazoyl carboxylates using 5,5-dimethyl-1,3-dioxanyl as a directing group

Nelson et al continued with additional developed a novel synthetic route to produce highly functionalized isoxazoles. By using a nucleophilic reaction between haloalkylphthalimides and the isoxazole compounds could be produced the in good yield. This is reaction route provides a controlled access to the carbonyl which can be challenging due to the competing electrophilic

centers at the carbon with the halogen and the imide carbonyl. This was also additionally verified with a crystal structure.(**Scheme 1-20**) [47]

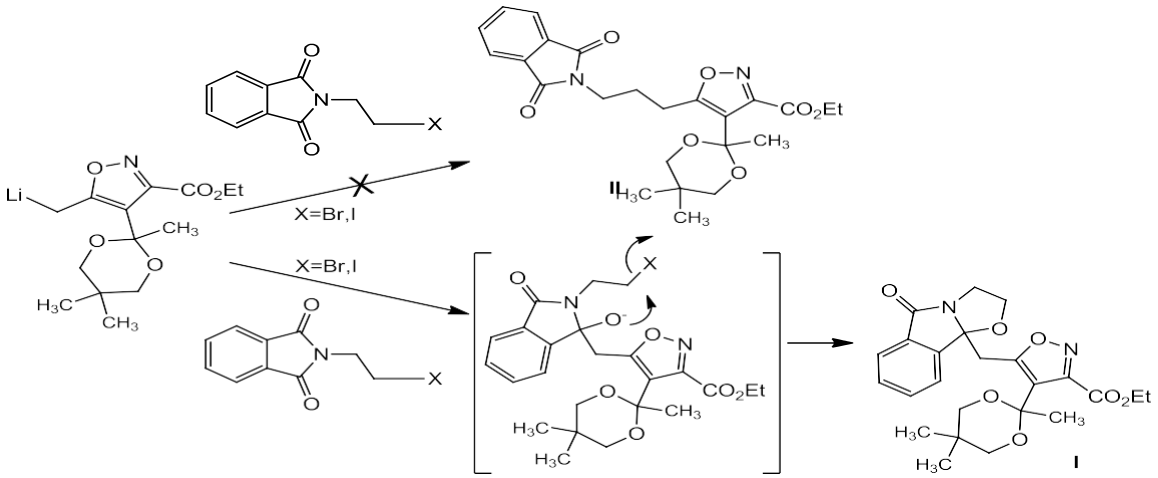

Scheme 1-20 Novel synthetic route to produce highly functionalized isoxazoles. By using a nucleophilic reaction between haloalkylphthalimides and the isoxazole compounds could be produced the in good yield.

Natale et al developed a series of 4-isoxazolyl-1,4-dihydropyridines (IDHP) that have lipophilic side chains at the C-5 position of the isoxazole ring and used to target the calcium channel and evaluate their antagonistic activity. A SAR was developed. The SAR helped to further understand the tolerance of lipophilic groups on IDHPs and potentially what residues would be factors affecting them. A crystal structure was also obtained to further view the 3D shape it takes.(**Scheme 1-21**)[48]

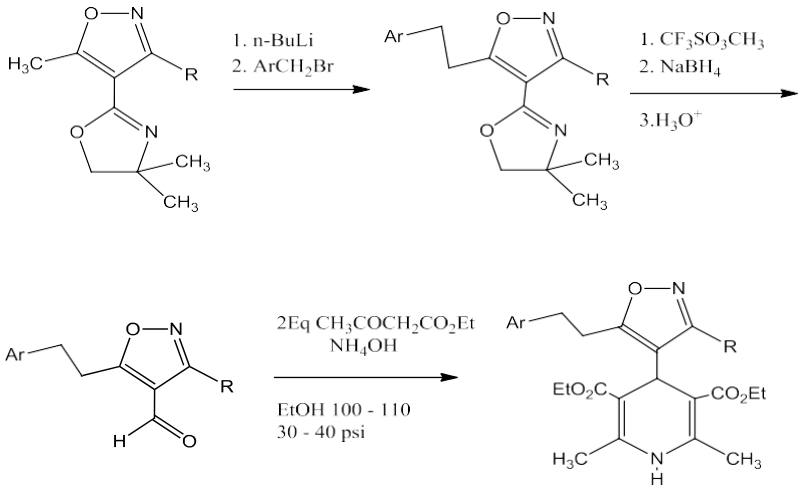

Scheme 1-214-isoxazolyl-1,4-dihydropyridines (IDHP) that have lipophilic side chains at the C-5 position of the isoxazole ring and used to target the calcium channel and evaluate their antagonistic activity

Di Nunno investigated the C-4 verses C-5 position lateral metalation of 3-aryl-isoxazoles, and observed that coordinatively unsaturated alkyl lithium reagents produced ring metalation in competition with LM, while lithium amide bases gave clean LM. This is similar to results previously reported for 3,5-dilakyl isoxazoles, and consistent with Beak's rationale that alkyl lithium reagents produce proximity directed ortho metalation in a kinetic process, while the lithium amides lateral metalation is a thermodynamic deprotonation.(**Scheme 1-22**)[49]

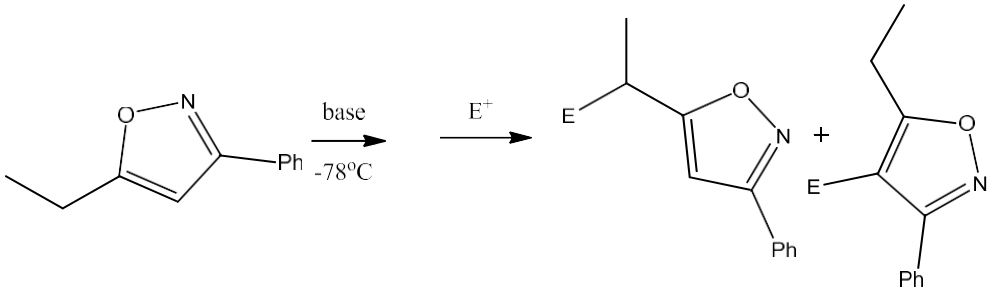

Scheme 1-22 alkyl lithium reagents produce proximity directed ortho metalation in a kinetic process, while the lithium amides lateral metalation is a thermodynamic deprotonation

In pursuit of generating heterocyclic analogues of anthracyclines, Alguacil et al investigated the reactivity of isoxazole-fused furanone **304** with functionalized quinine monoketals, and the corresponding annulated products could be prepared in moderate yields.

The atypical formation of the Michael adduct **307** is explained in terms of nucleophilic attack of the resonance stabilized anion through the oxygen at the 4-position.(**Scheme 1-23**). [50, 51]

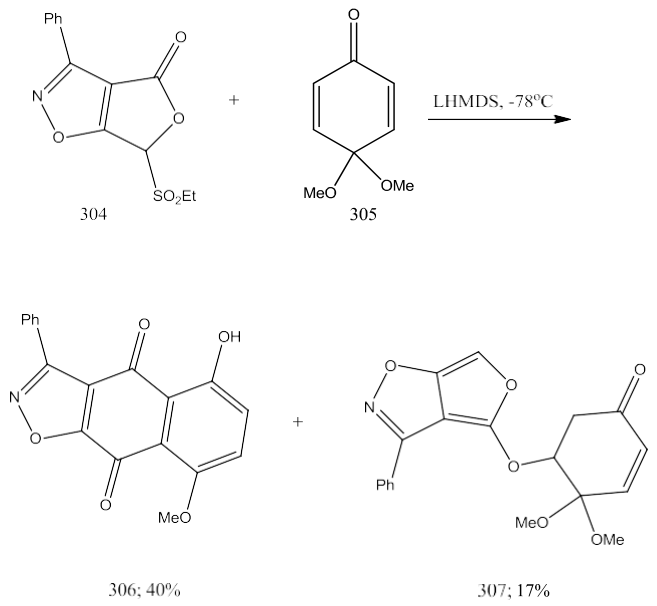

Scheme 1-23 generating heterocyclic analogues of anthracyclines using isoxazole-fused furanone and functionalized quinine monoketals

Epoxide ring opening

In their continuing search for antiviral analogs of Disoxaril, Diana and co-workers utilized the ring opening of oxirane (**Scheme 1-24**)to extend the tether length between key protein coat binding moieties.[52]

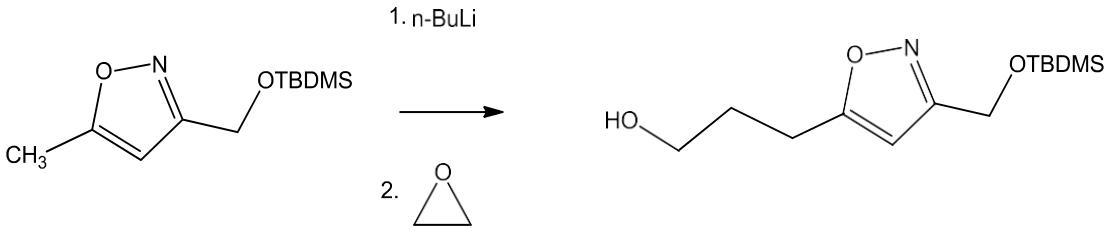

Scheme 1-24 ring opening of oxirane to extend the tether length between key protein coat binding moieties

Diana et al al also synthesizing Disoxaril analogues, by C-5 lateral metalation of isoxazole **1** as outlined in **Scheme 1-25** to obtain (chloropropyl)isoxazole **2**. Treatment of **2** with 3,5-dimethyl-4-hydroxybenzonitrile **3** afforded nitrile **4**. Reaction of **4** with sodium azide provided tetrazole **5**

53

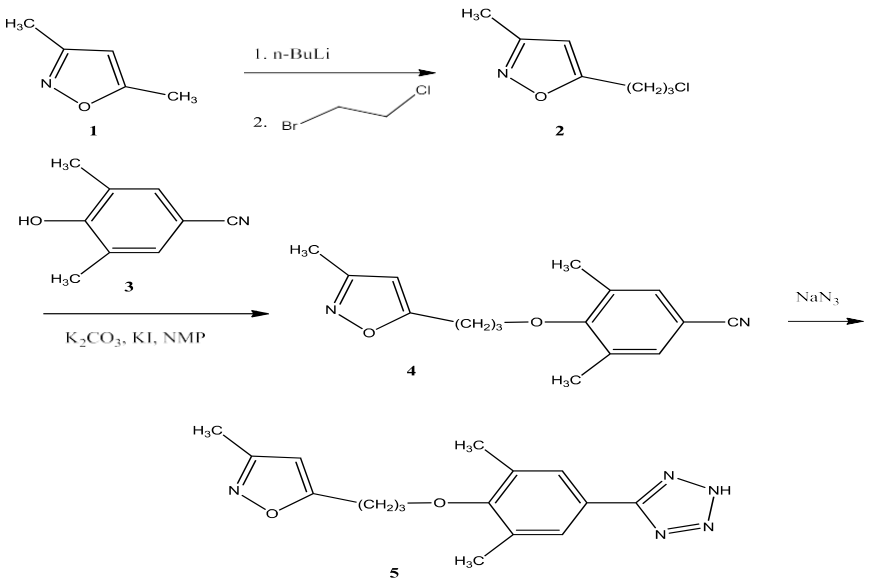

Scheme 1-25 Disoxaril analogues, by C-5 lateral metalation of isoxazoles

Nelson et al looked at the synthetic utility and scope of epoxides for chiral functionalization of isoxazoles. Through bioisostere replacement of 4-aryl with a substituted isoxazole compounds were produced with robust activity at the L-type calcium channel. Lateral metalation selectively generated and anion at the C-5 position which was able to successfully ring open the epoxide

single regioisomer for aliphatic and a mix for those with α,β-unsaturation. Addition of various Lewis acids helped to provide control of regiochemical outcomes with limited success, but there was inversion that occurs at the benzylic carbon, which has potential synthetic utility (**Scheme 1-26**).[54]

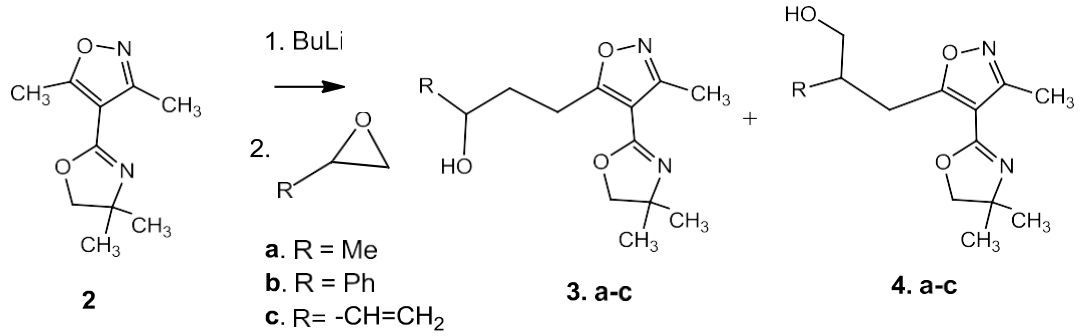

Scheme 1-26 synthetic utility and scope of epoxides for chiral functionalization of isoxazoles

Metal catalysts

β-keto nitrile **2** were prepared form isoxazole **1** in high yield using NaH. In light of the obtained results Dominguez were able to propose only the 4,5-substituted isoxazole, not the 3,4-disubstituted isoxazole, would be able to react with base to directly produce cyanoketone. **Scheme-1-27**. [55]

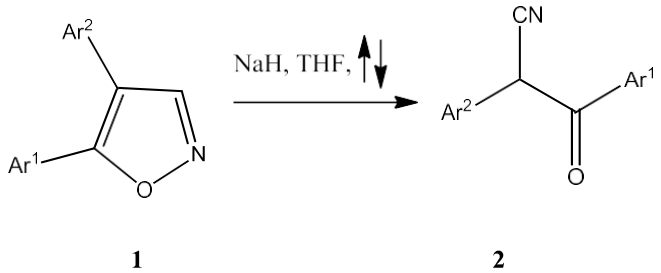

Scheme 1-27 Preparation of cyanoketone products from isoxazoles

Jackowski et al developed a novel regioselective, rapid, and simple method to obtain 3,4,5-trisubstituted isoxazoles in a one pot reaction. This is achieved via a direct synthesis with

aluminum substituted alkynes. The carbon-aluminum bond is able to react with several electrophiles without the need for transmetalations therefore minimizing steps. **(Scheme 1-28)** [56]

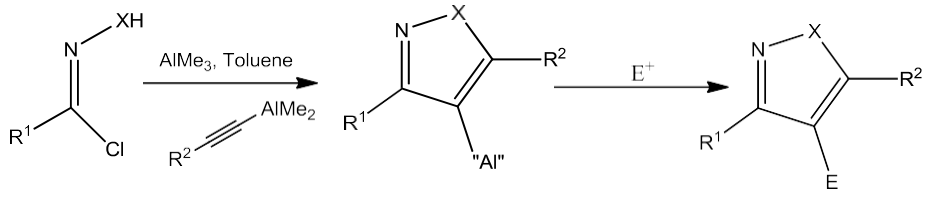

Scheme 1-28 carbon-aluminum bond is able to react with several electrophiles without the need for transmetalations therefore minimizing steps

Buckner utilized isoxazole ring opening methodology as part of a protocol for synthesizing Tipifarnib analogues, which are starting material for development of anti-Chagas drug (**Scheme 1-29**). [57]

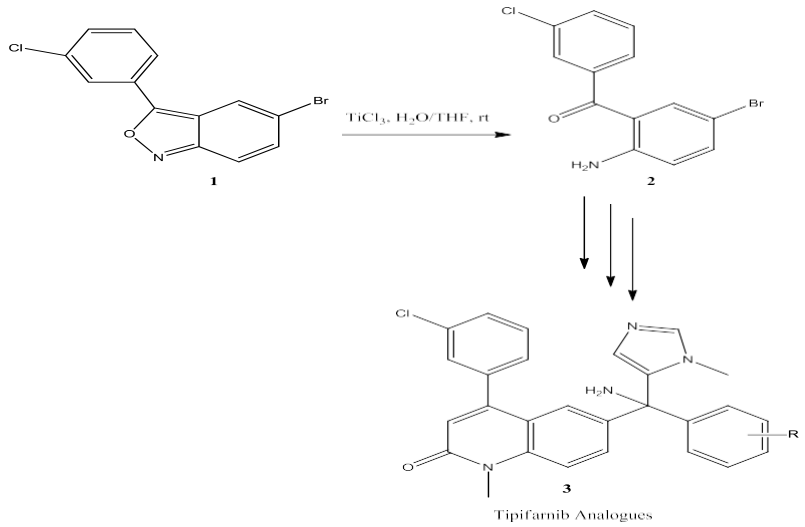

Scheme 1-29 isoxazole ring opening methodology as part of a protocol for synthesizing Tipifarnib analogues, which are starting material for development of anti-Chagas drug

Singh reported an efficient method for synthesis of substituted 2-pyrrolidinones, 2-pyrrolones, and pyrrolidines from enaminones of Baylis-Hilman derivatives of 3-isoxazolecarbaldehydes, **Scheme-1-30** [58]

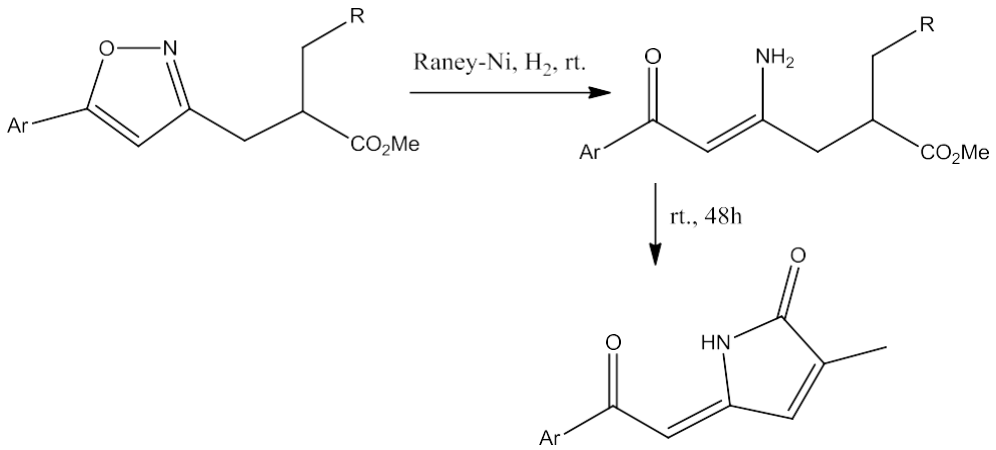

Scheme 1-30 synthesis of substituted 2-pyrrolidinones, 2-pyrrolones, and pyrrolidines from enaminones of Baylis-Hilman derivatives of 3-isoxazolecarbaldehydes

COPPER

The copper catalyzed 1,3- dipolar cycloaddition of nitrile oxides with alkynes can now be performed in a single pot from the precursor aldehyde and gives clean 3,5-regiochemistry in the reaction with terminal alkynes, and it has been argued that this cycloaddition is useful enough to be included in the *Click* category as defined by Sharpless, with the more familiar azide/alkyne 1,3-dipolar cycloaddition. Long[59] considered a concerted reaction, a recent proposal by Volkin[60] suggests that the copper (I) catalyzed version is best explained as a step wise process, and supports their argument with DFT computations. The proposed mechanism explains the observed regiochemistry and rate enhancement, and the postulated intermediates at the C-4 of the isoxozaole, offer several testable hypotheses in terms of copper intermediates, which could be experimentally intercepted and potentially put to good use (**Figure 1-12**).

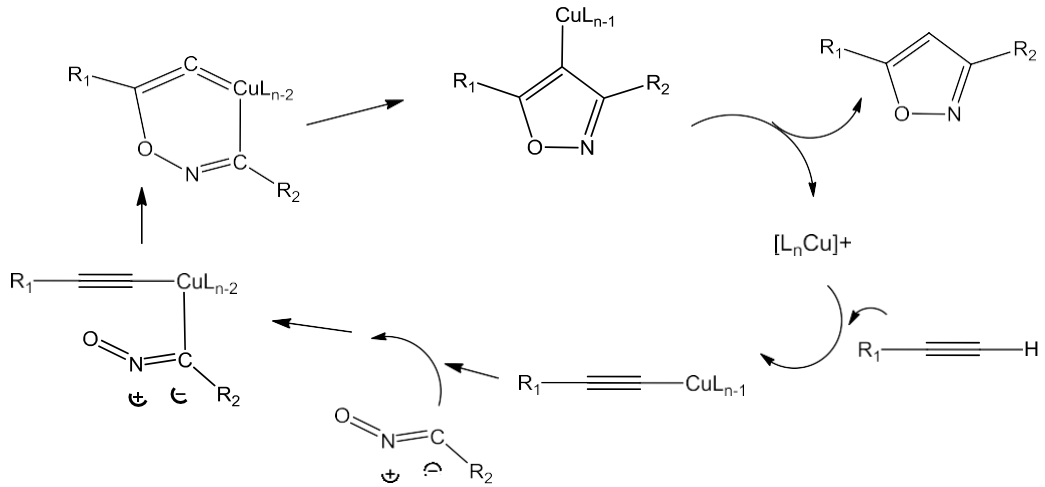

Figure 1-12 Proposed mechanism of one pot reactions of copper catalyzed 1,3-dipolar cycloaddition of nitrile oxides with alkynes.

Ueda et al used $Cu(OTf)_2$ as a catalyst with o-arylmethyl alkynyl oxime ethers giving a trisubstituted 4-arylmehtylisoxazole in good to excellent yields. This reaction proceeds through an alkynyl oxime ether in a sequential intramolecular addition of the oxime oxygen to the alkyne group with subsequent 1,3 migration of the substituted benzyl group. This synthetic route tolerates a variety of functional group while maintaining a good balance between product and side reactions (**Scheme 1-31**). [61]

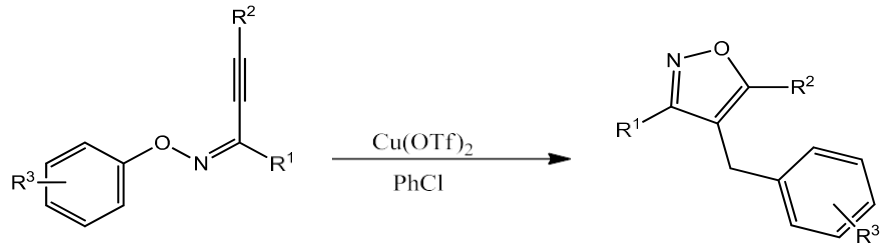

Scheme 1-31 $Cu(OTf)_2$ as a catalyst with o-arylmethyl alkynyl oxime ethers giving a trisubstituted 4-arylmehtylisoxazole

Hansen et al used a one pot synthesis with Cu(I) as a catalyst to obtain 3,5 disubstituted isoxazoles. This was done by generating an nitrile oxide insitu from aldehydes followed by the addition of a terminal acetylene and Cu(I) catalyst and achieved the 3,5-disubstituted product in good yield and regioselectivity. Another plus is most functional groups are tolerated in the reaction and can be performed in aqueous solvents without protecting from oxygen. All reagents are used in stoichiometric amounts to minimize production of by products. This also allows for versatility in the scale the reaction can be run on (**Scheme 1-32**). [60]

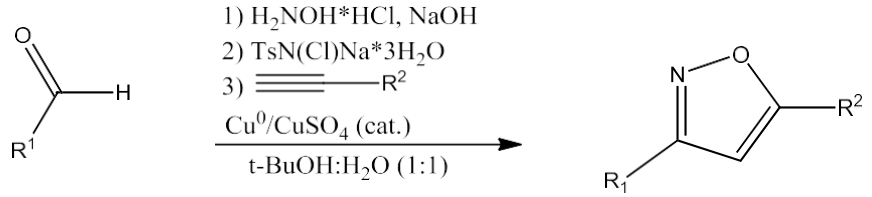

Scheme 1-32 one pot synthesis with Cu(I) as a catalyst to obtain 3,5 disubstituted isoxazoles

Himo et al used DFT studies looking at reactivity and intermediates for Cu(I) catalyzed of azoles and isoxazoles. By using a Cu(I) catalyst the reaction for forming 3,5-disubstituted isoxazoles is accelerated greatly and increased yield while minimizing side products and allowing for more regiospecific control versus uncatalyzed. The process is highly reliable and exhibits an unusually wide scope with respect to both components (**Scheme 1-33**). [62]

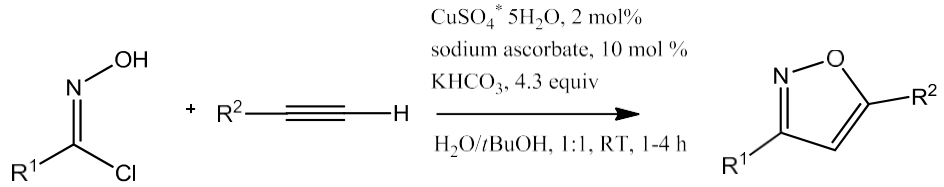

Scheme 1-33 Cu(I) catalyst the reaction for forming 3,5-disubstituted isoxazoles is accelerated greatly and increased yield while minimizing side products and allowing for more regiospecific control versus uncatalyzed

Nelson et al achieved catalytic asymmetric addition of alkyl- and aryl-zinc reagents to an isoxazole aldehyde to generate ACPA analogs targeting GluR2. This proceeds with high enantioselectivity (85-95% ee) by nucleophilic addition of an alkyl or aryl-zinc using the amino catalyst (S)-2-piperidinyl-1,1,2 triphenyl ethanol. A zinc based catalyst was used due to abundance of it, commercial availability and variety of alkyl and aryl substituted zinc or if they could be synthesized in a single step, and the rate of the uncatalyzed (racemic) rxn is most often extremely low to zero(**Scheme 1-34**). [63]

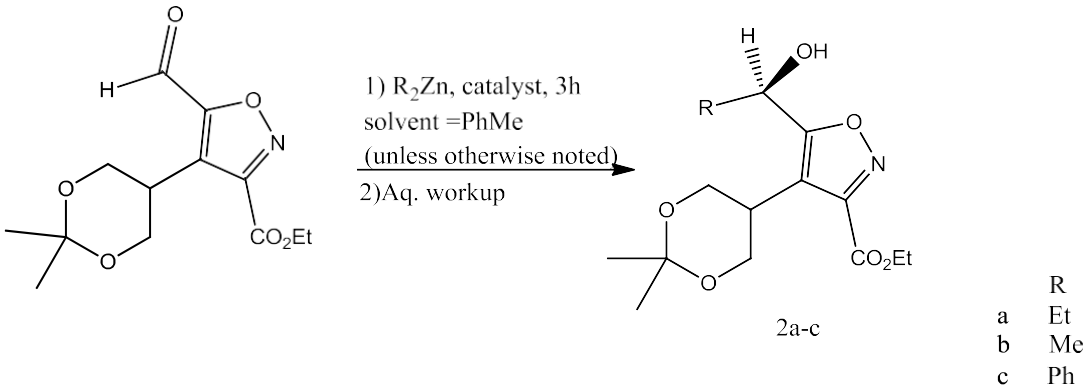

Scheme 1-34 catalytic asymmetric addition of alkyl- and aryl-zinc reagents to an isoxazole aldehyde to generate ACPA analogs targeting GluR2

PALLADATION AND C–H Activation: Cross-Coupling Reactions on Isoxazoles

Palladium mediated cross-couplings have emerged as one of the most robust synthetic methods for carbon-carbon bond formation.**(Figure 1-13)** Even for the well-explored C-4 ring metalation of isoxazoles, the palladium methodology greatly expands the scope of application, especially in terms of functional group diversity that can be tolerated in the process.

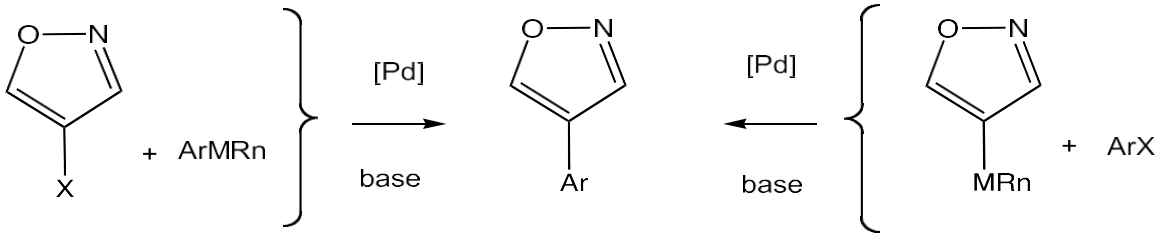

Figure 1-13 General Palladium mediated cross-couplings

It is well established that isoxazoles are susceptible to reductive ring opening therefore there is a concern with direct C-H insertion with low valent metals could possibly lead to cleavage of the O-N bond. Mechanistically, the only critical difference in the catalytic cycle starting from halides could be the transformation of the palladium hydride formed on initial insertion to a better leaving group to produce the critical diaryl palladium intermediate. However, there are at least five ways for C-H insertion to approach that intermediate. The first is electrophilic aromatic substitution on the aryl palladium intermediate. Given the electron deficient nature of the isoxazole as an aromatic entity, this seems unfavorable especially in cases with additional electron withdrawing groups on the heterocycle. The second and third possibilities involve either p,h^1 or p,h^2 initial coordination. The fourth is a Heck-type addition. The final possibility is a direct C-H insertion, which should involve a palladium hydride intermediate, and hence should be facilitated by a Wacker-type cycle, a mechanistic and synthetic detail that might possibly improve many palladium mediated couplings under study. Finally, Alberico et al [64] caution that given different conditions of solvents, base and additives, it is entirely possible that different mechanisms are favored under different sets of conditions. (**Figure 1-14**)

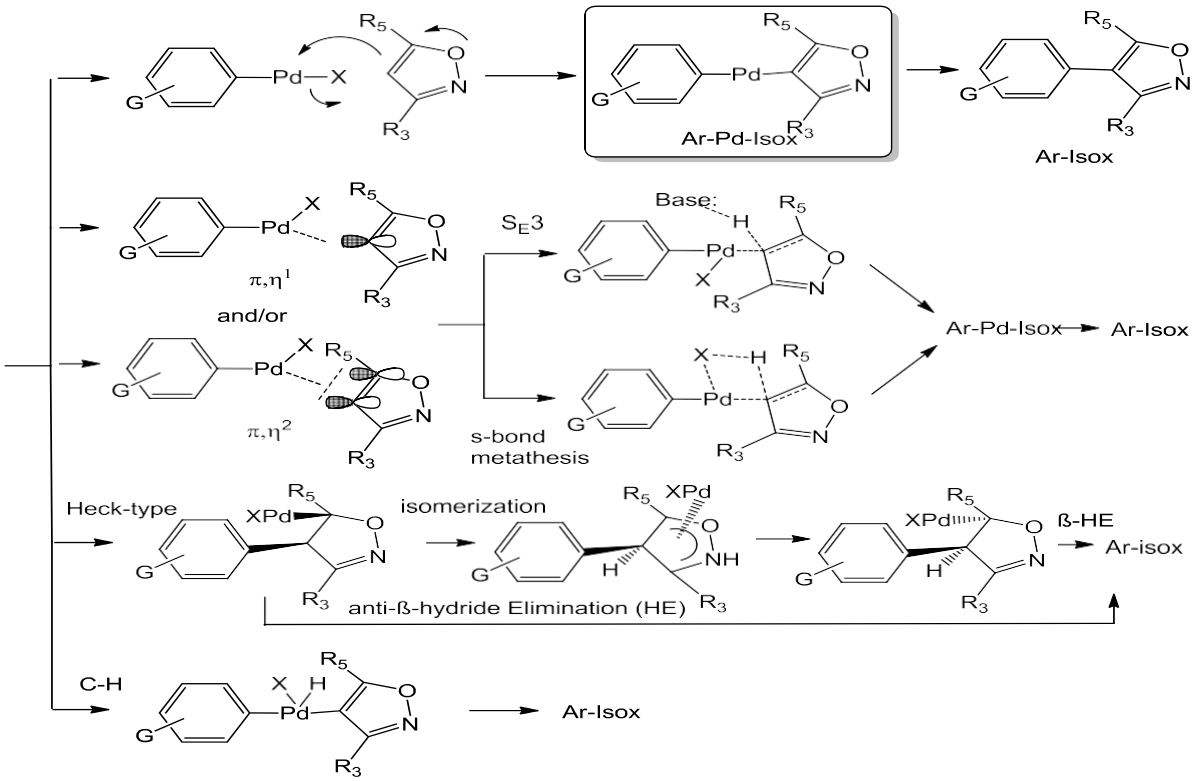

Figure 1-14 different palladium catalyzed reaction of isoxazoles and there outcomes

Whether the cross coupling proceeds from isoxazolyl-tin or boronate, or begins with the isoxazolyl-halide, the mechanism of the reaction proceeds via the critical diaryl palladium metallated intermediate (**Figure 1-15**).

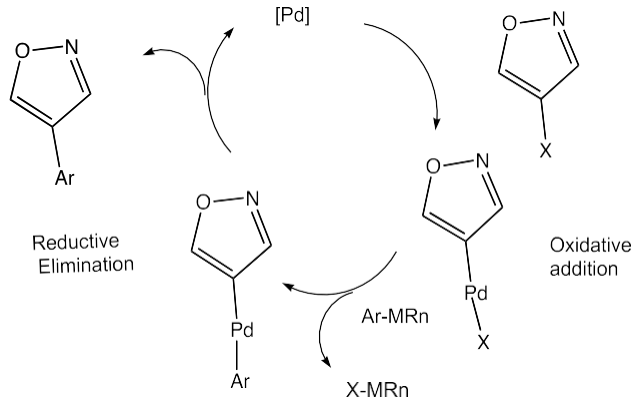

Figure 1-15 General mechanism of Pd catalysis of isoxazoles

Nakamura reported the coupling of an aryl iodide to an isoxazole as a key step in the total synthesis of a liphophilic derivative of the GABA agonist muscimol. (**Scheme 1-35**)

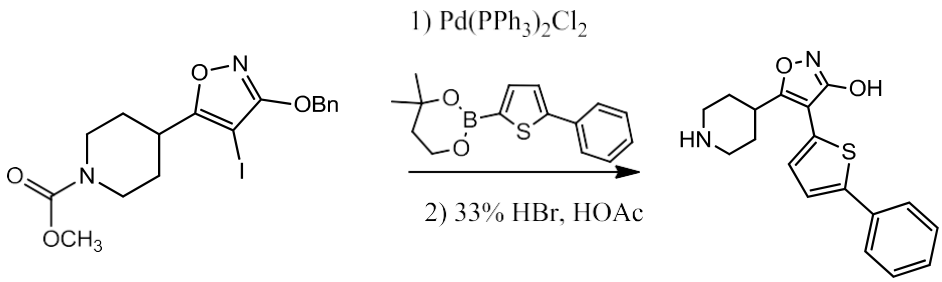

Scheme 1-35 coupling of an aryl iodide to an isoxazole as a key step in the total synthesis of a liphophilic derivative of the GABA agonist muscimol

While an oxidative coupling strategy was first investigated using benzene and catalytic $Pd(OAc)_2$with $Cu(OAc)_2$/oxygen as the oxidant, the authors found that use of almost stoichiometric palladium was required to obtain synthetically useful yields. Hence, an alternative strategy using iodobenzene and base was employed, allowing the use of catalytic amounts of palladium while still obtaining the desired coupled product in low to moderate yields.[65] **Scheme 1-36 and 1-37**

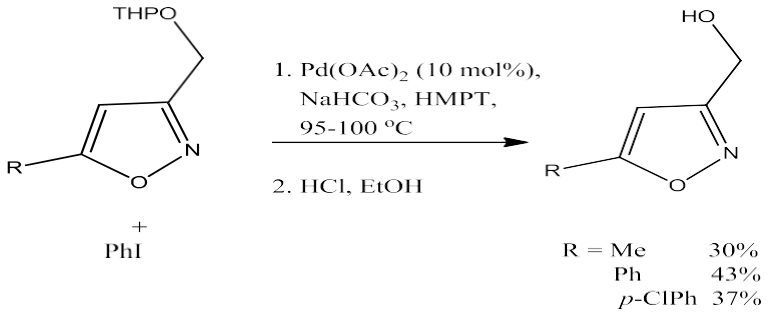

Scheme 1-36 oxidative coupling strategy $Pd(OAc)_2$with $Cu(OAc)_2$/oxygen as the oxidant

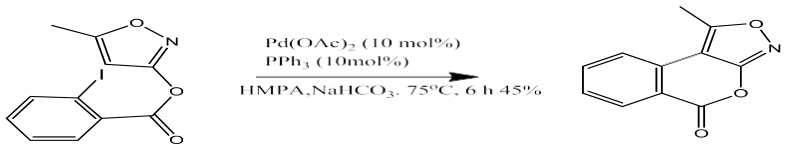

Scheme 1-37 iodobenzene and base was employed

Basolo et al expanded upon Nakamura et by using an intramolecular cyclization of a 3-substiuted isoxazole. They used $Pd(OAc)_2/PPh_3$ HMPA to form a tricyclic compound with a 45% yield. 5-substituted isoxazoles have also been cyclized to give tricylclic compound. (**Scheme 1-38 and 1-39**)

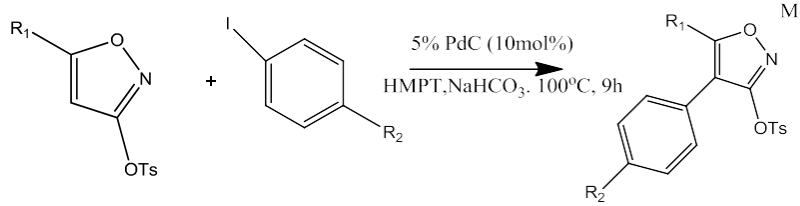

R_1	R2	Yield (%)
Me	H	44
Ph	H	48
Me	Cl	43

Scheme 1-38 intramolecular cyclization of a 3-substiuted isoxazole

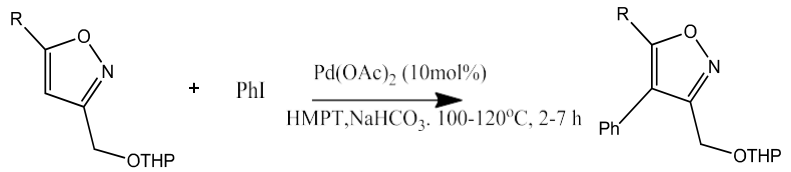

R_1	Yield (%)
Me	30
Ph	43
$4\text{-}ClC_6H_4$	37

Scheme 1-39 intramolecular cyclization of a 5-substiuted isoxazole

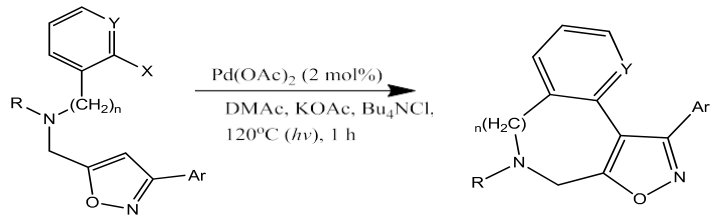

X	Y	n	R	Yield[%]
I	CH	0	CO_2tBu	60
Br	N	0	CO_2tBu	9
I	CH	1	Me	12
Br	CH	2	CO_2tBu	49

Scheme 1-40 cyclization of a tricyclic isoxozoles

Basolo et al additionally used cyclization process led to fused heterocyclic with 9-60% yield with ligand-free $Pd(OAc)_2$ as catalyst with microwave heating. Biomolecular 4-arylation of isoxazoles was also found to be possible but required higher temps and longer reaction times. Coupling iodobenzene or 4-iodotoluene with 3,5 disubstitued isoxazoles resulted in 4-arylated isoxazoles in 30-48% yield. [66](**Scheme 1-40**).

Chiong and Daugulis worked to extended to include aryl chlorides, when 1-chloronaphthalene was used as a coupling partner (**Scheme 1-41**). To facilitate the oxidative addition of 1-chloronaphthalene to palladium, $Pd(OAc)_2$ was associated to the bulky and electron-rich ligand, *n*-butyl-di-1-adamantylphosphine to act as catalyst. The expected product, 3,5-dimethyl-4-naphthalen-1-ylisoxazole, was obtained in 76% yield.[67]

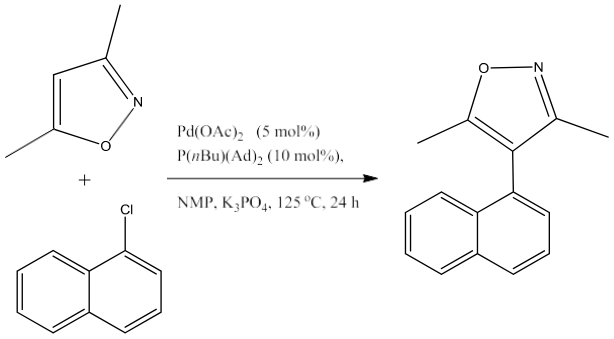

Scheme 1-41 include aryl chlorides, when 1-chloronaphthalene was used as a coupling

Sahoo et al (**Scheme 1-42**) report a palladium catalyzed intramolecular cross dehydrogenative coupling (CDC) that allows for access to the highly π-conjugated benzoindoles[1,2-α] quinoline fused isoxazoles(BQI) scaffolds. Using a Pd and O2 with a base, co-catalyst, and metal oxidant free to generate a variety of substituted benzoindoles[1,2-α] qunoline fused isoxazoles. An interesting note is this synthesis set up allows for C4 functionalization of isoxazoles without the need for a co-catalyst such as AgI. Using deuterium studies and kinetic studies it was found that the C-H activation step was not the rate limiting step and that the carbometalation was the rate

limiting step. Interaction of the Pd interacting with the benzimidazole and shift to the C2 position between the nitrogens of the imidazole followed by a metallotropism-triggered to the active intermediate that leads to the intramolecular C-H bond cleavage concerted metalation deprotonation of the C4 of the isoxazole with the last step of reductive elimination with yields between 61-84%. With the addition of HOPiv the reaction progressed more smoothly. It was also observed that substrates with electron-withdrawing groups reacted slightly slower that ones with electron-donating. BQIs could be further diversified by using Fe powder to cleave the isoxazole O-N bond and generate benzo[4,5]imidizolo[1,2-α] quinolines. These scaffolds have implications/utility, such as in pharmaceutical design, but were previously difficult to synthesis.[68]

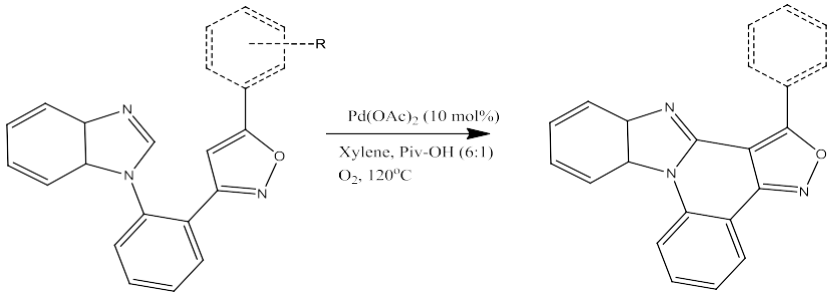

Scheme 1-42 palladium catalyzed intramolecular cross dehydrogenative coupling (CDC) that allows for access to the highly π-conjugated benzoindoles[1,2-α] quinoline fused isoxazoles(BQI) scaffolds

Galenko et al (**Scheme 1-43**) used 4-propargylisoxazole as a synthon intermediate to synthesis new 2,2'-bipyrimindine, symmetrical and unsymmetrical 6,6' binicotinates, and 2,2'-bipyridine-5 carboxylates with yields between 20-90%. These compounds are utilized in the design of metal-organic frameworks (MOFs) which have been used as catalysts but also as fluorescent probes to measure pH and molecular separations to name a few. To achieve symmetrical 2,2'-bipyrimindine compounds a Glasser/Eglinton with $Cu(OAc)_2$ followed by

$Fe(NTf_2)_2/Au(NTf_2)$tBuXPhos was used. While a copper free Sonogashira coupling followed by Fe(II)/Au(I) relay catalyst condition to achieve the unsymmetrical product. These reaction methods present a more general strategy to readily generate a wider variety of diverse symmetrical and unsymmetrical compounds.[69]

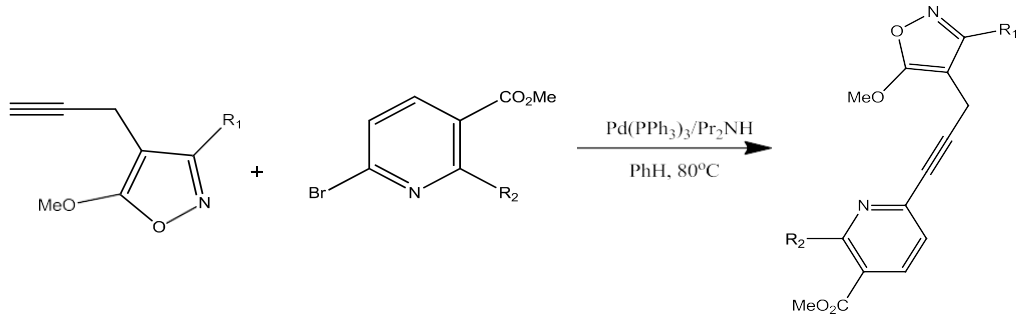

Scheme 1-434-propargylisoxazole as a synthon intermediate to synthesis new 2,2'-bipyrimindine, symmetrical and unsymmetrical 6,6' binicotinates, and 2,2'-bipyridine-5 carboxylates

Shen et al were looking at platinum catalyzed [5 +2] and [4+2] annulations of isoxazoles with heterosubstituted alkynes. This approach allows for synthesis of valuable 1,3-oxazepines and 2,5-dihydropyridines. This exploration also provided information about novel α-oxo and α-imino platinum carbenes and the resulting selectivity switch they can provide for synthesis of diverse intricate scaffolds.(**Scheme 1-44**) [70]

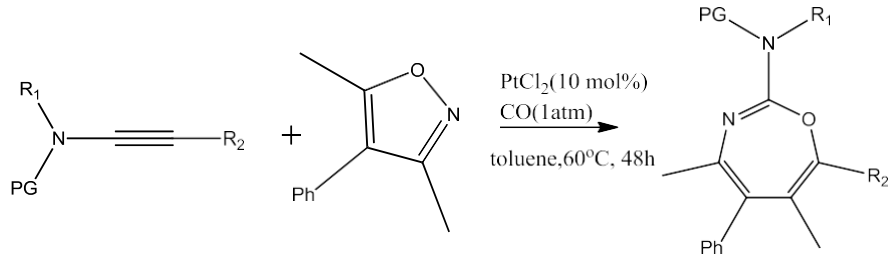

Scheme 1-44 platinum catalyzed [5 +2] and [4+2] annulations of isoxazoles with heterosubstituted alkynes

Frølund et al synthesized a series of 4-aryl-5-(4-piperidyl)3-isozolol $GABA_a$ antagonists. This series of compounds had significantly higher potencies than previously reported 4-PIOL antagonists and standard $GABA_a$ antagonists. Using a Suzuki conditions with $Pd(PPh_3)_2Cl_2$, various aryl boronic acids or ester , and 4-iodo substituted isoxazole to generate the various substituted analogues (**Scheme 1-45**).[71]

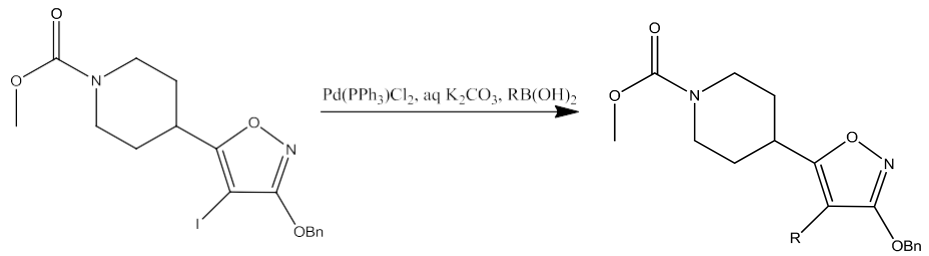

Scheme 1-45 4-aryl-5-(4-piperidyl)3-isozolol $GABA_a$ antagonists. This series of compoundshad significantly higher potencies than previously reported 4-PIOL antagonists and standard$GABA_a$ antagonists

Banerjee et al (**Scheme 1-46**) expanded further explored the higher directing ability of nitrogen versus oxygen in a 3,5-diaryl isoxazole in the relationship to the construction of C-C and C-O bonds. Using $Pd(OAc)_2$ as the catalysts they found that regioselective aroylation and acetoxylation takes place at the ortho-CHs neighboring the nitrogen atom. The substitution at the ortho position occurred via chelated assisted approach rather than the more acidic isoxazole C4 position. [72]

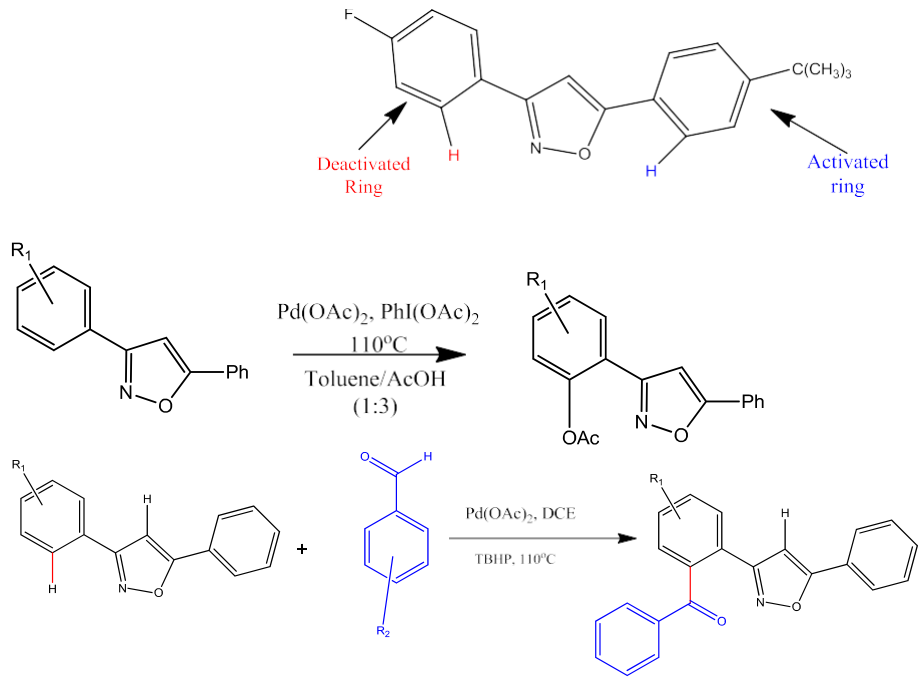

Scheme 1-46 higher directing ability of nitrogen versus oxygen in a 3,5-diaryl isoxazole in the relationship to the construction of C-C and C-O bonds

Fall et al (**Scheme 1-47**) generated 4-arylisoxazoles with a variety of functional groups tolerated using a palladium-catalyzed activation/arylation of 3,5-disubstituted isoxazoles using aryl or heteroaryl bromides. This reaction is attractive since there is no need for preparation of the organometallic derivatives and only HX associated with the base as a by-product. The presented proceed allowed for product formation with electronically and sterically diverse aryl bromides and 3,5-disubstituted isoxazoles at low catalyst loading in ligand-free palladium conditions. They found that though this reaction was able to tolerate a variety of groups were tolerated on the aryl bromide better results were obtained when it was electron-deficient. Examples included acetyl, formyl, fluoro, nitro, trifluoromethyl or nitrile. Other heterocyclic bromides could be cross coupled to the isoxazole, including pyridine, 1- or 2- quinoline, and diazenes. Additionally, isoxazoles with electron-withdrawing groups on the C-3 position to be less reactive and proceeded sluggishly. [73,74]

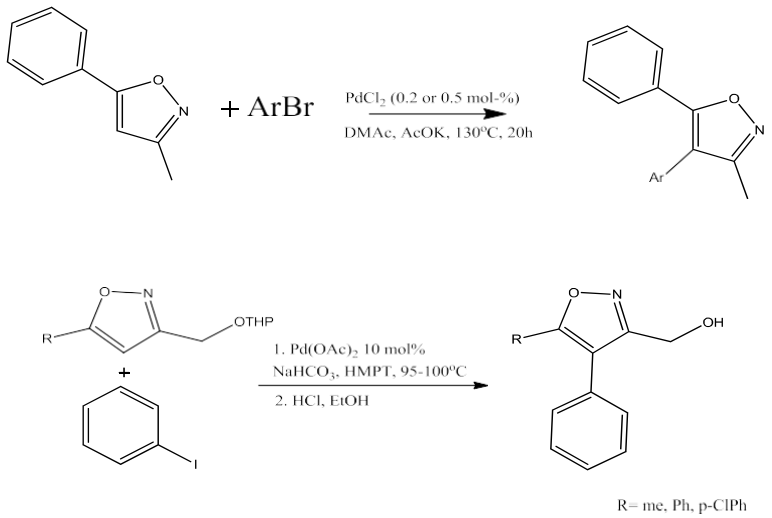

Scheme 1-47 4-arylisoxazoles with a variety of functional groups tolerated using a palladium-catalyzed activation/arylation of 3,5-disubstituted isoxazoles using aryl or heteroaryl bromides

Piller et al reported preparation of polyfunctional arylmagnesium, arylzinc, and benzylic zinc reagents by using magnesium in the presence of LiCl, and subsequent utilizing them Pd catyzed cross-coupling reaction. The presence of LiCl considerably facilitates the insertion of magnesium into various aromatic and heterocyclic bromides. Several functional groups, such as -OBoc, -OTs, -Cl, -F,-CF_3, -OMe, were well tolerated. Five-membered rings incorporating two heteroatoms often require mild conditions for their metalation, since these metalated ring systems often display a tendency to undergo fragmentation reactions. Thus, 4-bromo-3,5-dimethylisoxazole (**3v**) was smoothly converted to the corresponding zinc reagent within 15 min at 25 ^{o}C by treatment with Mg/LiCl/$ZnCl_2$. After a Negishi cross-coupling reaction with 3-bromoanisole, the arylated isoxazole **5x** was isolated in 90% yield (entry 4). (**Scheme 1-48**) [75]

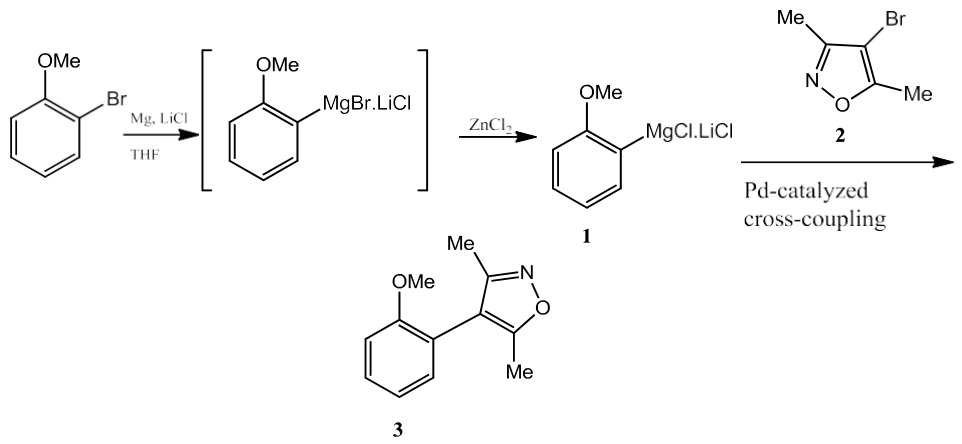

Scheme 1-48 preparation of polyfunctional arylmagnesium, arylzinc, and benzylic zinc reagents by using magnesium in the presence of LiCl, and subsequent utilizing them Pd catyzed cross-coupling reaction

The $Pd(TFA)_2$/SPRIX catalyst system was applied to an alkoxy alkylative desymmetrization reaction initiated by oxypalladation of an alkene, followed by trapping of the Pd-alkyl intermediate by a pendant alkene. [76] This reaction gave high levels of enantioselectivity (up to 97% ee) with 20 mol % Pd. Subsequent reports investigated the use of spiro bis- (isoxazole) **154** [77] and hybrid spiro (isoxazole-isoxazoline) **155** ligands.[78] Although **154** was not as effective as the SPRIX ligand class, hybrid spiro (isoxazole-isoxazoline) ligands 155 were more promising, affording a catalyst with increased reactivity without compromising enantiocontrol (**Scheme 1-49**).

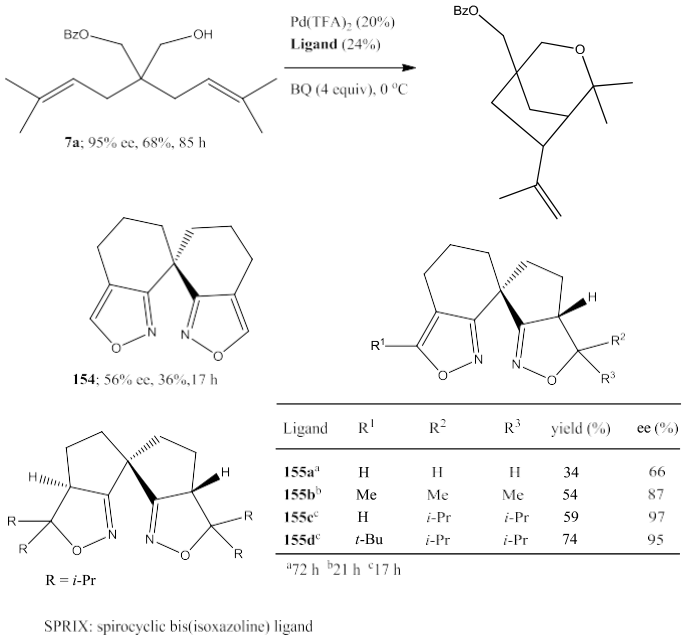

Ligand	R^1	R^2	R^3	yield (%)	ee (%)
155a[a]	H	H	H	34	66
155b[b]	Me	Me	Me	54	87
155c[c]	H	*i*-Pr	*i*-Pr	59	97
155d[c]	*t*-Bu	*i*-Pr	*i*-Pr	74	95

[a]72 h [b]21 h [c]17 h

Scheme 1-49 $Pd(TFA)_2$/SPRIX catalyst system was applied to an alkoxy alkylative desymmetrization reaction initiated by oxypalladation of an alkene, followed by trapping of the Pd-alkyl intermediate by a pendant alkene

The Suzuki–Miyaura Reaction is a commonly employed synthetic strategies for cross coupling functional groups by using Pd and various functionalized boranes.

McDaniel et al used microwave condition with a Suzuki-Miyaura cross-coupling of benzylic bromides to produce a library of structurally diverse compounds as potential System X_c. Up until this work there were few examples of Suzuki cross-couplings at benzylic positions and even fewer of heteroaromatic rings. This protocol gives better access to these scaffolds and provides a useful method synthesis of water sensitive compounds with a commercially available

catalyst.(**Scheme 1-50**)[79]

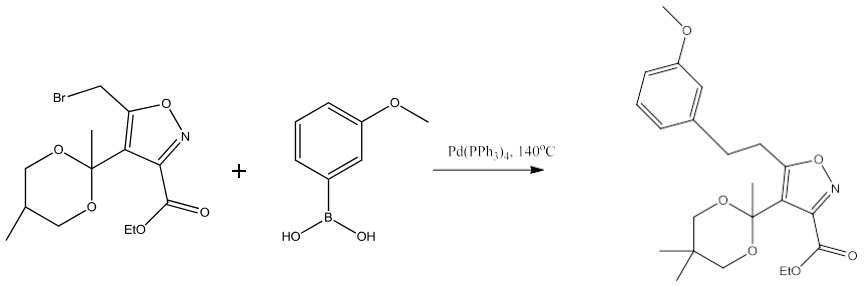

Scheme 1-50 microwave condition with a Suzuki-Miyaura cross-coupling of benzylic bromides

Davies et al used a Suzuki–Miyaura where the organoboranes were not synthesized by a metalation-quenching strategy but directly introduced through cyclization of nitrile oxides **228** and alkynylboronic acid esters. In the cyclization reaction, two regioisomers bearing the boronic acid ester in the 4- or 5- position (**229** or **230**) can be formed. Methods were reported with good control of the regiochemistry in the final product depending on the substituents in the starting material. Subsequent cross-coupling of the isoxazole-4-boronic acid ester gave the products **231** in up to 97% yield; however, only few examples were reported (**Scheme 1-51**).[80]

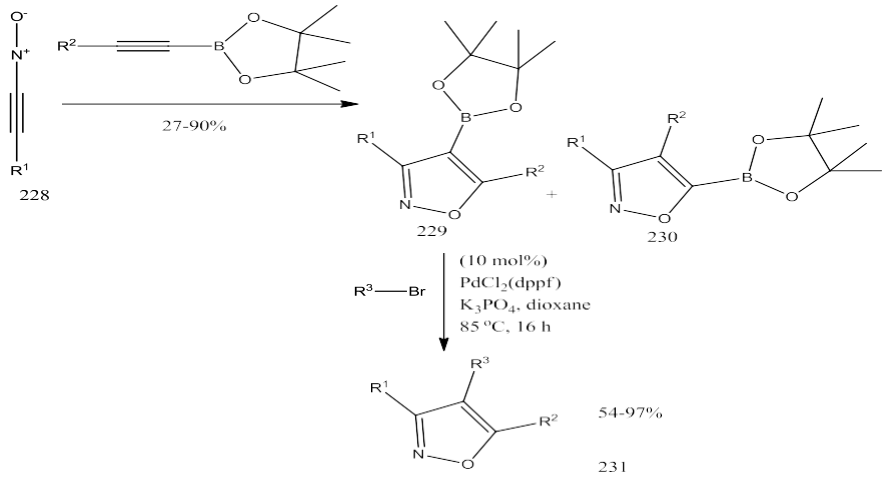

Scheme 1-51 Suzuki–Miyaura with direct cylation of nitrile oxides and alkynylboronic acid esters

Moreover, isoxazolyl 4- and isoxazolyl-5-boronic esters have also been obtained by 1,3-dipolar cycloaddition reactions between alkynyl boronates [80] and nitrile oxides, which can also be generated in situ from the oxime **218** (**Scheme 1-52)** for the synthesis of the bromoisoxazole boronic ester 21**9**, being used in palladium-catalyzed cross-coupling reactions to afford the isoxazole **220**.[81]

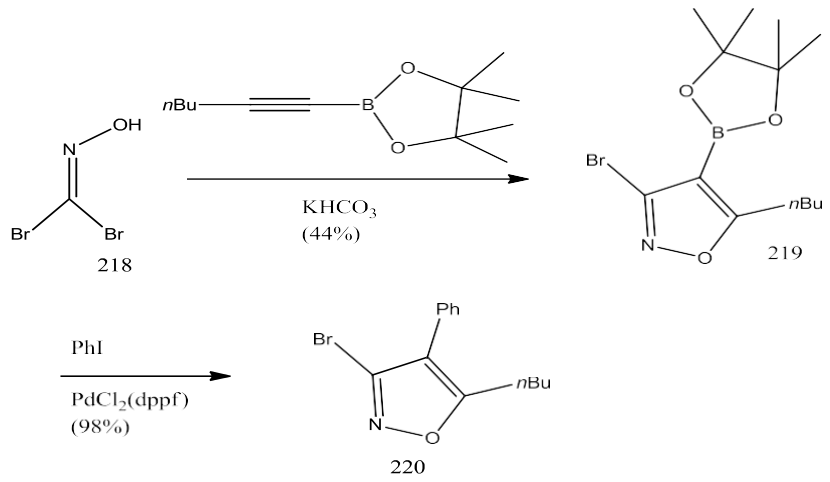

Scheme 1-52 synthesis of the bromoisoxazole boronic ester 21**9**, being used in palladium-catalyzed cross-coupling reactions to afford the isoxazole

Larock reported synthesis of 4-iodoisoxazole products. To demonstrate the value of the generated in this methodology, they carried out a number of reactions utilizing the iodine handle. They reasoned that they could approach the highly potent COX-2 inhibitor 4-(5-methyl-3-phenyl-4-isoxazolyl)benzenesulfonamide (Valdecoxib) (**46**) by a Suzuki-Miyaura cross-coupling of isoxazole **4** with the appropriate boronic acid ester. Using their isoxazole methodology to prepare **4** and a Suzuki-Miyaura coupling with the commercially available

benzenesulfonamide-4-boronic acid pinacol ester, they were able to develop a very efficient route to valdecoxib (**Scheme 1-53**). After several protocols were screened, Suzuki cross-coupling was best accomplished using 5 mol % $PdCl_2$ catalyst, 1.4 equiv of $KHCO_3$ in 4:1 DMF:H_2O at 85 °C for 3 h to provide valdecoxib (**46**).[82]

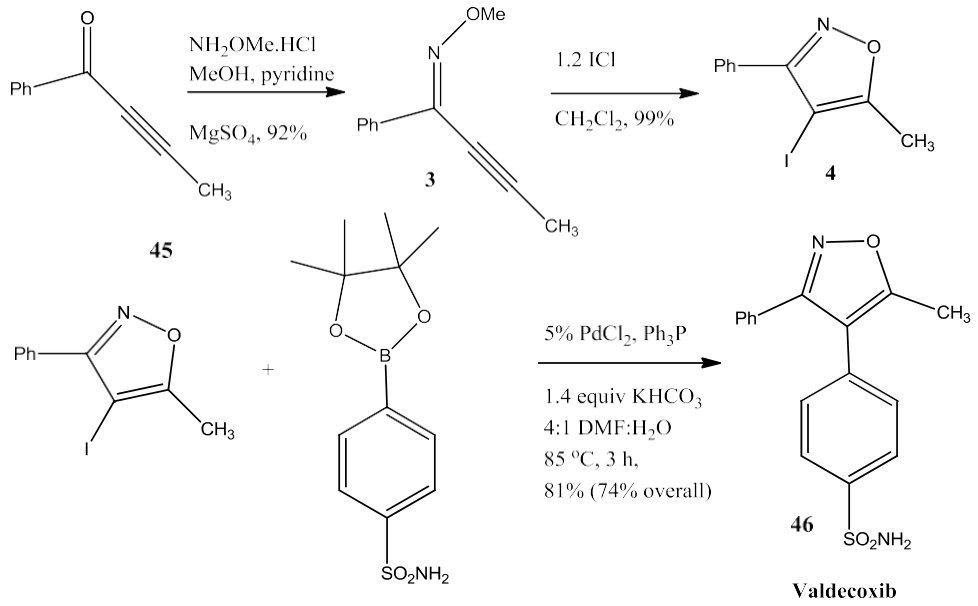

Scheme 1-53 synthesis of 4-iodoisoxazole products

Wada reported switchable synthesis of Valdecoxib (**9**) (**Scheme 1-54**). Valdecoxib is a cyclooxigenase-2 (COX-2) selective inhibitor and was used for a nonsteroidal antiinflammatory drug (NSAID) to treat osteoarthritis, rheumatoid it was accessed from *N*-isopropyloxycarbonyl-*O*-propargylic hydroxylamine **1ae** in two steps; NIS/BF_3.OEt_2-mediated tandem iodocyclization/oxidation process of **1ae** produced isoxazole **3ae** in 96% yield, and subsequent Suzuki-Miyaura cross coupling with commercially available 4-sulphamoylbenzeneboronic acid afforded valdecoxib (**9**) in 54% yield. Their methodology allowed not only the substituent

diversity but also the choice of skeleton, a wide variety of analogs of valdecoxib (**9**) could be provided.[83]

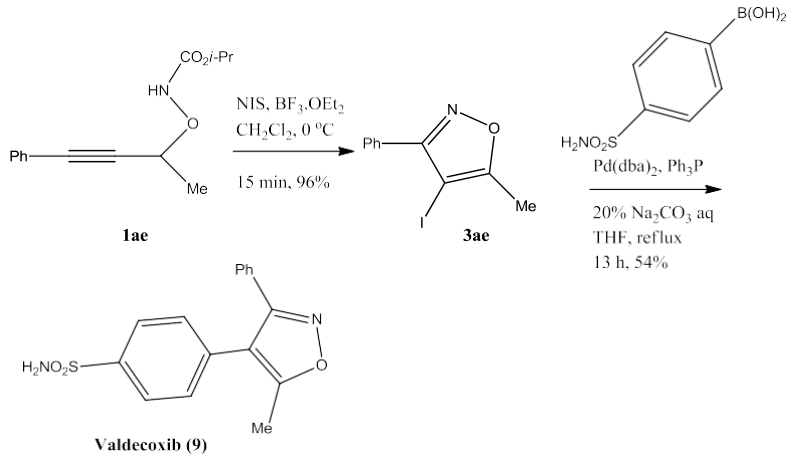

Scheme 1-54 switchable synthesis of Valdecoxib

A number of monoligated Pd–N-heterocyclic carbene (Pd–NHC) complexes have been prepared and show high levels of activity in a variety of Pd-catalyzed cross-coupling reactions as reported by Organ and co-workers. Whereas ortho-substituted biaryls are important substructures of many biologically active compounds and organic materials, the formation of tetra-ortho-substituted biaryls under mild conditions remains a challenge. The need for significantly elevated temperatures is a major drawback for these systems and the development of a catalyst that could affect such conversions at much lower temperatures would be a considerable advancement in the production of sterically congested biaryls.The Suzuki–Miyaura coupling to explore the effect of catalyst bulk on biaryl formation. That phenol formation is base dependent suggests that transmetalation is rate limiting. Additional investigation of hindered aryl chlorides was particularly productive. Chlorides, which are sluggish toward oxidative addition, coupled not

only with higher yields than the corresponding bromides, but the product mixtures were also generally much cleaner. By using **16** at 65°C and the KO*t*Bu/*t*BuOH system, with few exceptions they were able to synthesize a striking array of hindered biaryls from aryl chlorides under very mild reaction conditions.(**Scheme 1-55**)[84]

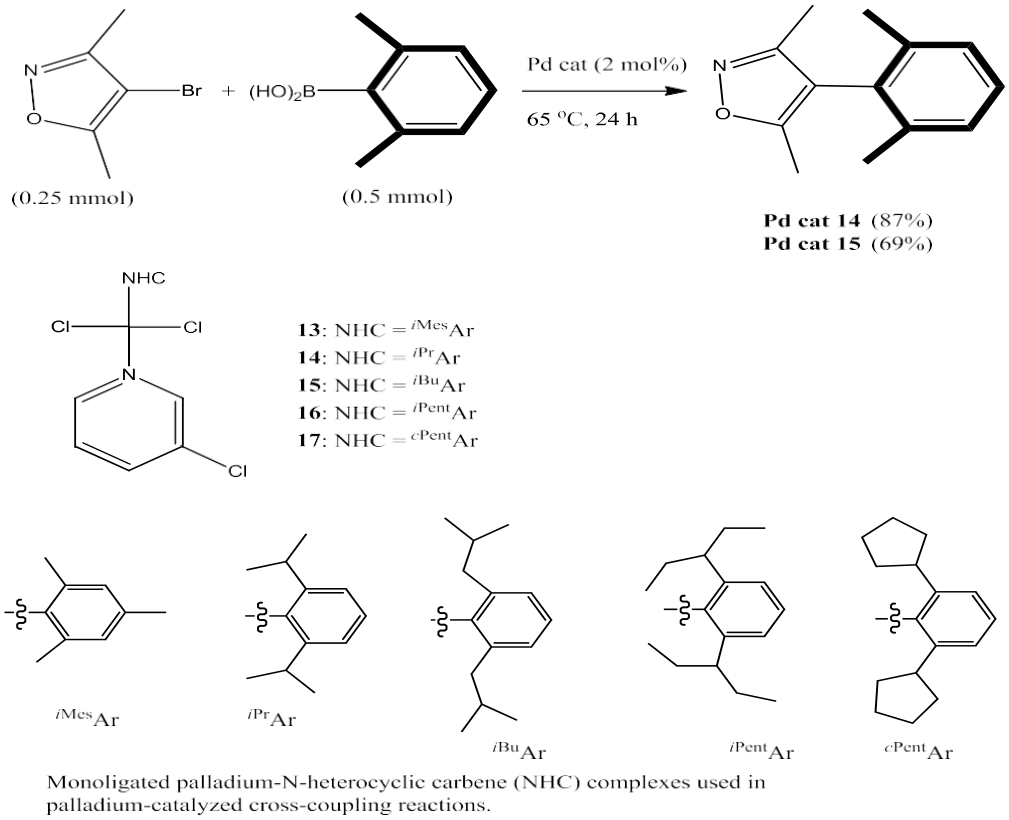

Scheme 1-55 synthesize a striking array of hindered biaryls from aryl chlorides under very mild reaction conditions

Addtionally Organ et al used a Suzuki–Miyaura coupling reaction of N-protected 4-iodopheyl alanine isoxazoles with arylboronic acids, catalyzed by palladium, efficiently produced benzyl-N-(4-bipheyl)-2-(3-methyl-5(E)-2-aryl-1-ethenyl-4-isoxazolyl)-amino-2-oxoethyl) carbamates in

good yields. This process is first of its kind to construct carbon–carbon bond formation having biaryl motif on amino acid linked isoxazole moiety.(**Scheme 1-56**)[85]

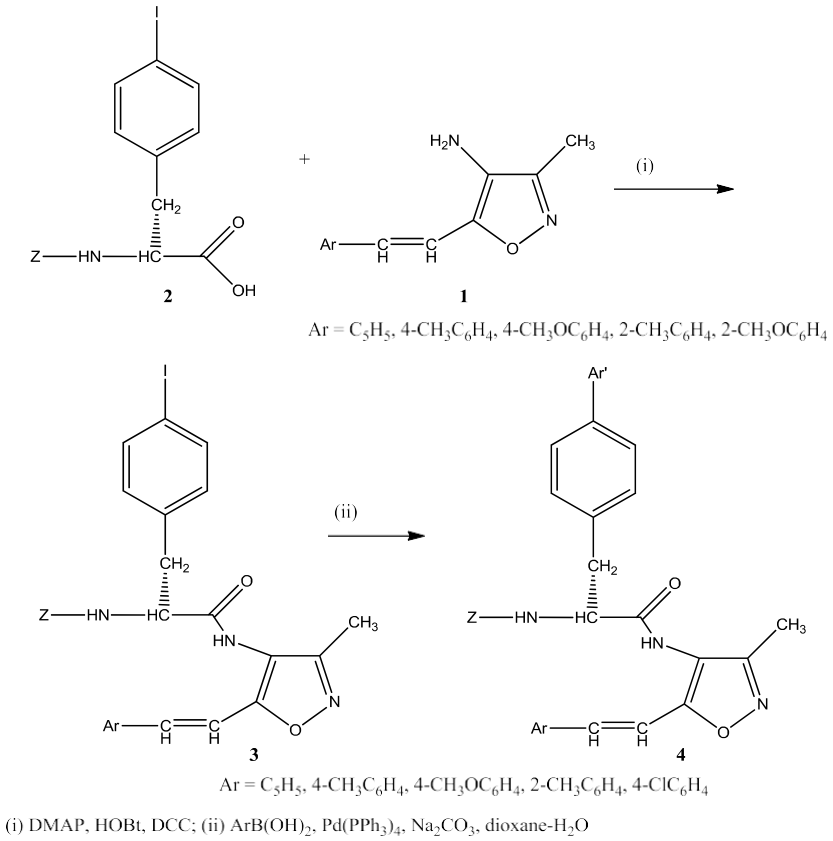

Scheme 1-56 Suzuki–Miyaura coupling reaction of N-protected 4-iodopheyl alanine isoxazoles with arylboronic acids, catalyzed by palladium, efficiently produced benzyl-N-(4-bipheyl)-2-(3-methyl-5(E)-2-aryl-1-ethenyl-4-isoxazolyl)-amino-2-oxoethyl) carbamates

Another way of diversifying isoxazole rings is through Heck, Naghishi or Sonogashira cross-couplings. Waldo and Larock reported that other palladium-catalyzed methodology has also proven useful for further elaboration of iodoisoxazoles. For example, they were able to convert 4-iodo-3,5-diphenylisoxazole (**2**) to the corresponding methyl ester by allowing **2** to react in the presence of catalytic amounts of $Pd(OAc)_2$ plus a ferrocene ligand, carbon monoxide, and methanol to afford methyl ester **47** in a 51% yield (eq 3). Reduction of compound **2** to 3,5-

diphenylisoxazole was an observed minor side product. In addition, we were able to convert 4-iodo-5-methyl-3-phenylisoxazole (**4**) to the corresponding phenethylamide by a similar approach using a modified Heck's procedure. By allowing compound **4** to react in the presence of catalytic amounts of $PdCl_2(PPh_3)_2$, carbon monoxide, and 2-phenethyl amine, we were able to obtain **48** cleanly in good yield (**Scheme 1-57**).[82]

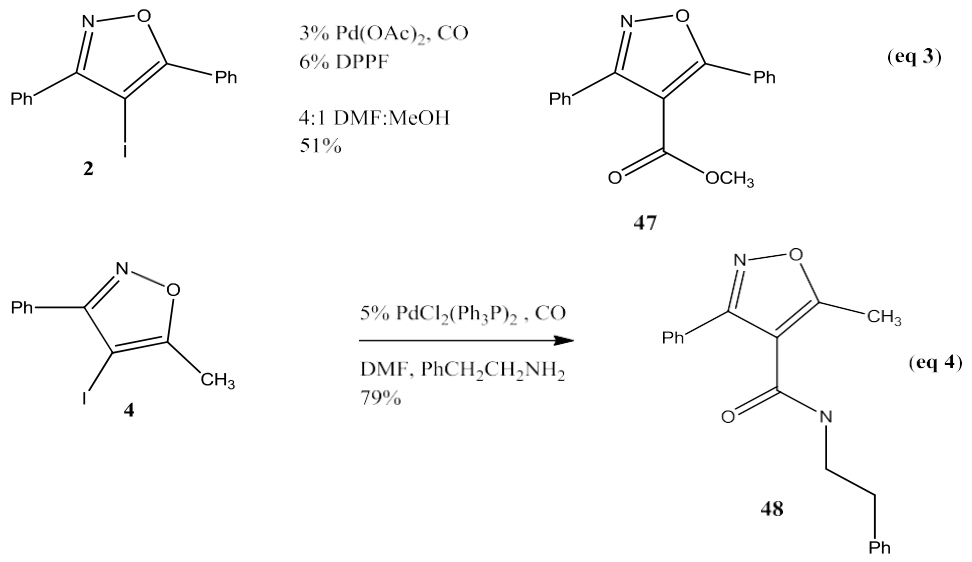

Scheme 1-57 palladium-catalyzed further elaboration of iodoisoxazoles

These molecules could be further modified by using a Heck and Sonogashira cross-couplings on a 4-iodo-5-methyl-3-phenylisoxazole (**4**) (**Scheme 1-58**). Compound **4** reacted under standard Sonogashira conditions in the presence of 1.2 equivalents of phenyl acetylene, alkyne **49** was obtained in a good yield. Also, allowing compound **4** to react under Heck reaction conditions in the presence of *N*-acryloylmorpholine provided the desired *α,β*-unsaturated amide **50** in excellent yield.[82]

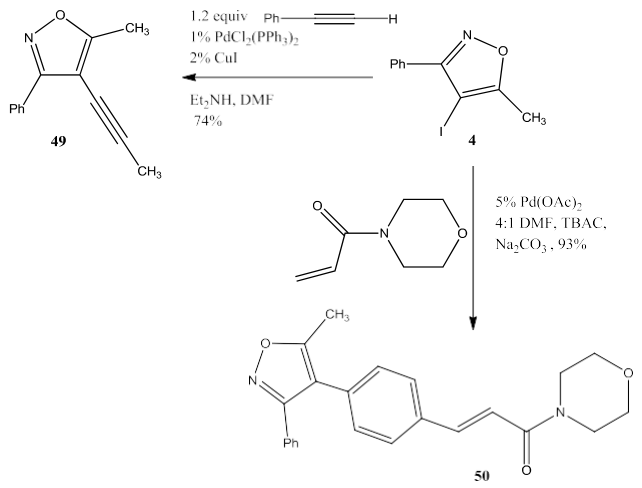

Scheme 1-58 Heck and Sonogashira cross-couplings on a 4-iodo-5-methyl-3-phenylisoxazole

Crossley et al reported the thermally promoted cycloaddition between alkynyliodides and nitrile oxides. The process offers excellent regioselectivity and a broad scope with respect to both the iodoalkynes and chloro-oximes. Further functionalization of the highly decorated iodoisoxazole motifs were achieved via Suzuki cross-coupling. With the halogenated isoxazoles in hand, they looked to demonstrate their functionalization via Suzuki cross-coupling. (**Scheme 1-59**).[86]

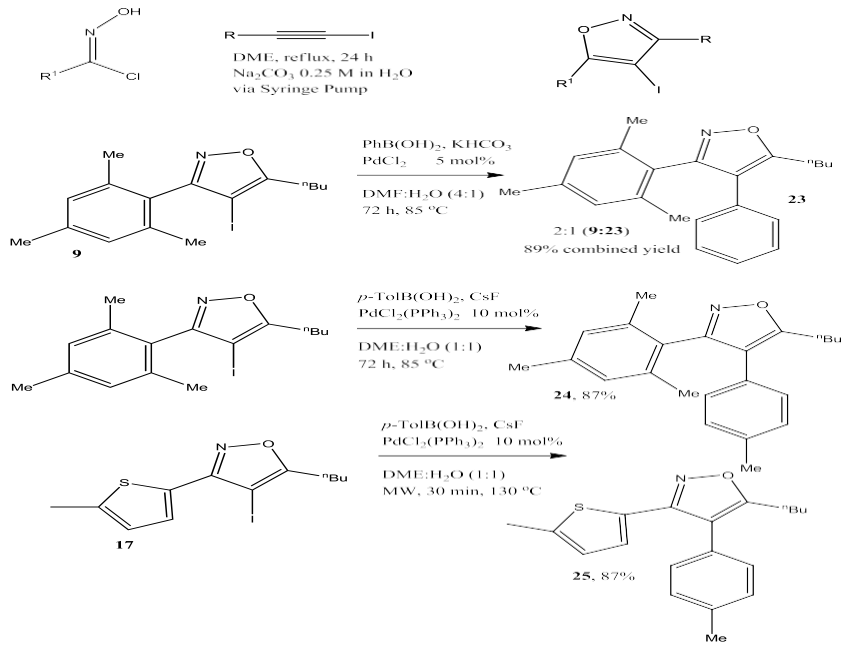

Scheme 1-59 thermally promoted cycloaddition between alkynyliodides and nitrile oxides

<u>C-H insertion</u>

Chu et al (**Scheme 1-60**) developed a method for stoichiometric C-H activation of 3,5-diphenylisoxazoles using $Pd(OAc)_2$ in acetic acid to allow for arylation and alkylations with boronic acids via C-H activation. This reaction proceeds through a stepwise C-H activation/C-C bond forming reaction pathway. The boronic acids with electron-withdrawing groups on the phenyl ring gave better yields than those with donating groups. Two interesting things were found in the palladacycle: the phenyl and the isoxazole rings on the metal center are parallel in space and located in opposite directions in a head-to-tail structure. Second, the π-π interaction between these two aromatic rings appear to play a critical role in reducing Pd-Pd distance.[87]

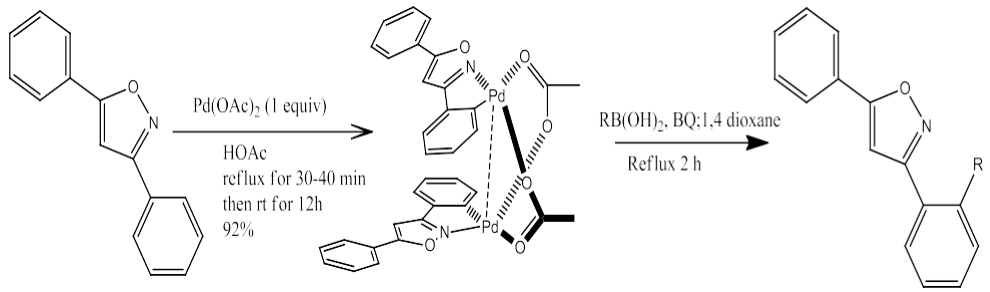

Scheme 1-60 stoichiometric C-H activation of 3,5-diphenylisoxazoles using $Pd(OAc)_2$ in acetic acid to allow for arylation and alkylations with boronic acids via C-H activation

Gao et al (**Scheme 1-61**) used a Rh(III)-catalyst directed oxidizing-directed-group assisted activation to achieve a redox-neutral [4+1] annulations of N-phenoxy amides with α,α-difluoromethylene alkynes to give direct access to Z-configured monofluoroalkenyl dihydrobenozo[d]isoxazole frameworks that have a variety of functional groups. This method helps to avoid the need for prefunctionalization and stoichiometric amounts of external oxidants and with it being regioselective in nature allow for access to a variety of privileged monoheterocyclic rings. To understand the reaction mechanism DFT was implemented and revealed that β-F elimination involving an allene species played a crucial role in determining the reaction out come and Z-configuration. The propargyl fluorination effect is essential in controlling the observed chemoselectivity by fine tuning the β-F elimination process.[88]

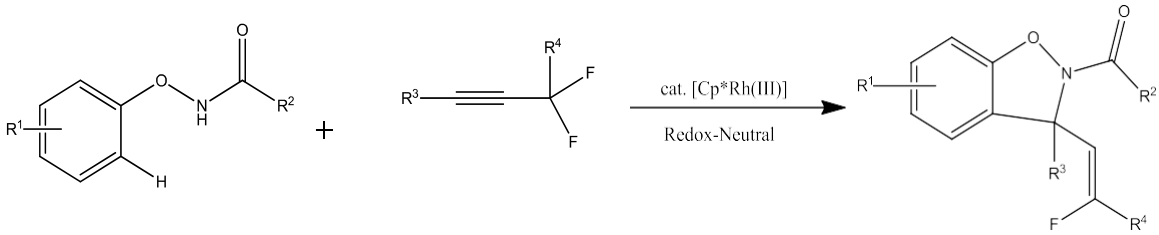

Scheme 1-61 Rh(III)-catalyst directed oxidizing-directed-group assisted activation to achieve a redox-neutral [4+1] annulations of N-phenoxy amides with α,α-difluoromethylene alkynes to give direct access to Z-configured monofluoroalkenyl dihydrobenozo[d]isoxazole

When isoxazole **47** was subjected to the standard Rh(II) cyclization conditions , the resulting rhodium carbenoid preferred to insert into the available CH bond producing **48** in modest yield. These observations suggest that the low basicity of the isoxazole nitrogen lone pair precludes cyclization to the azomethine ylide dipole (**Scheme 1-62**).[89]

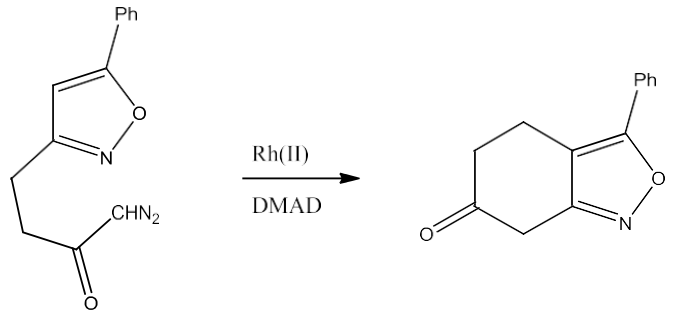

47 **48**

Scheme 1-62 Cylzation of azomethine isoxazole under Rh(II) conditions

Kumar and Kapur looked the selective C-H alkenylation of 3,5-diaryl substituted isoxazoles. Using a cationic rhodium or palladium catalysts they were able to achieve selective functionalization at either the ortho-position the aryl ring that was lateral to the isoxazole nitrogen or to the 4 position directly on the isoxazole ring. It was found that the Rh-catalyst was better at coordinating to the isoxazole nitrogen and resulting in more direct metalation lateral ortho-position on the aryl lateral to the nitrogen. Interestingly if the Pd-product was carried forward to produce a pyrrole via Ruthenium catalyst, the proposed mechanism proceeded through coordination with the isoxazole nitrogen followed by ring opening and subsequent coordinated attack on the olefin to produce the pyrrole. (**Scheme 1-63**) [90]

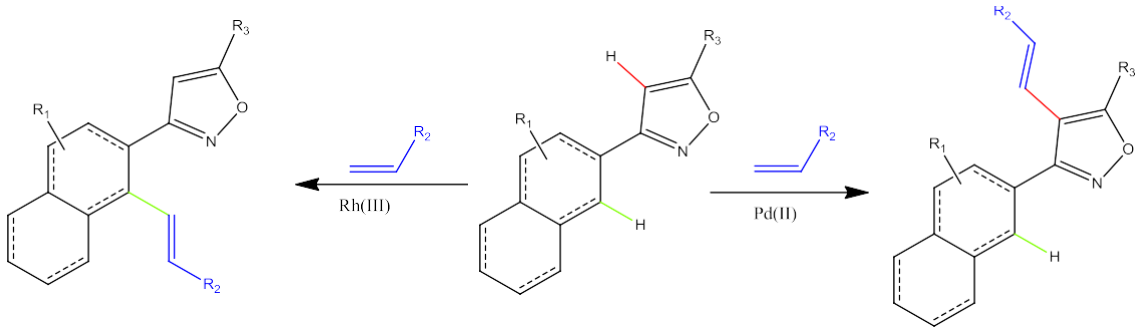

Scheme 1-63 selective C-H alkenylation of 3,5-diaryl substituted isoxazoles

GOLD

Yamamoto has reported $AuBr_3$-catalyzed cyclization of *o*-alkylnitrobenzens **1** (**Scheme 1-64**).This reaction afforded isatogens **2** or anthranils **3**, depending on the nature of R^1.[91]

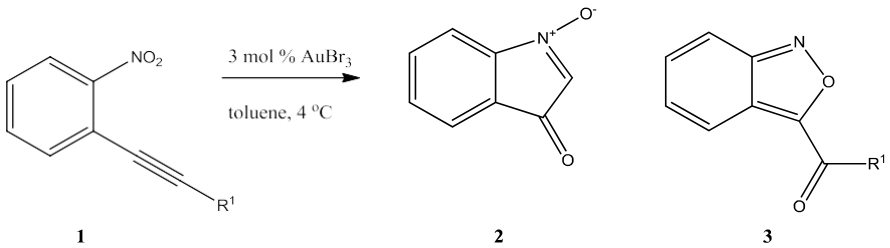

Scheme 1-64 $AuBr_3$-catalyzed cyclization of *o*-alkylnitrobenzens

Sahani et al further developed Au(I) catalyzed for the [4+1] and [2+2+1]/[4+2] annulations of propiolates with substituted and unsubstituted isoxazoles and their reaction mechanism. This reaction proceeded through a seven membered heterocyclic ring intermediate via an initial N-attack of the isoxazole followed by the unusual formation of a 2H-azirine containing intermediate, 6π electrons, then ring expansion. Ogunlana et al further verified and expanded on this reaction mechanism using DFT (**Scheme 1-65**) [92,93]

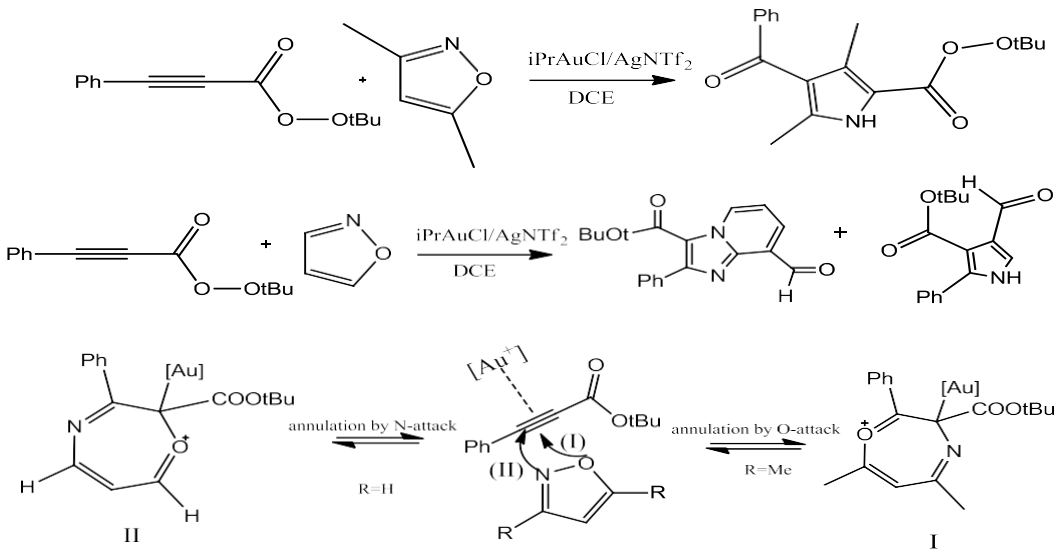

Scheme 1-65 Au(I) catalyzed for the [4+1] and [2+2+1]/[4+2] annulations of propiolates with substituted and unsubstituted isoxazoles and their reaction mechanism

Bimetallics

Lithium examples

In their continuing studies of 3-acetyl-4-hydroxy- pyridones and pyrones (**Scheme 1-66)**, Jones and co-workers required a facile entry into unsaturated α-alkoxy-ß-diketones, which they achieved *via* the metalation of diethylphosphono isoxazole with LDA to produce the 3-alkenyl isoxazoles in excellent yields (91-99%), subsequent reduction with hexacarbonylmolybdenum in moist acetonitrile efficiently produced their target α-alkoxy-ß-diketones, again in excellent yields. These α-alkoxy-ß-diketones provide a versatile sython that can be carried readily into future reactions. [94]

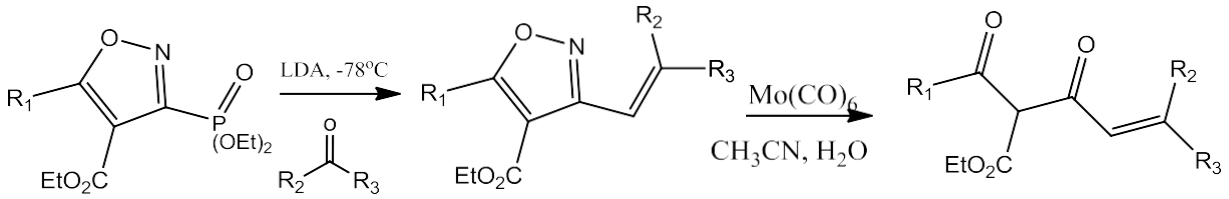

Scheme 1-66 unsaturated α-alkoxy-ß-diketones, which they achieved *via* the metalation of diethylphosphono isoxazole with LDA to produce the 3-alkenyl isoxazoles

Hahnvajanawon et al laterally metalated 3,5-dimethyl isoxazoles and further did a condensation reactions with various aromatic aldehydes sequentially at the C-3 and C-5 positions of the isoxazole to generate curcumin derivatives in good yields (48-80%). The isoxazole ring could be further transformed by using [$Mo(CO)_6$] to generate a β-ketone group via a ring opening of the isoxazole followed by acid hydrolysis (**Scheme 1-67**). [95]

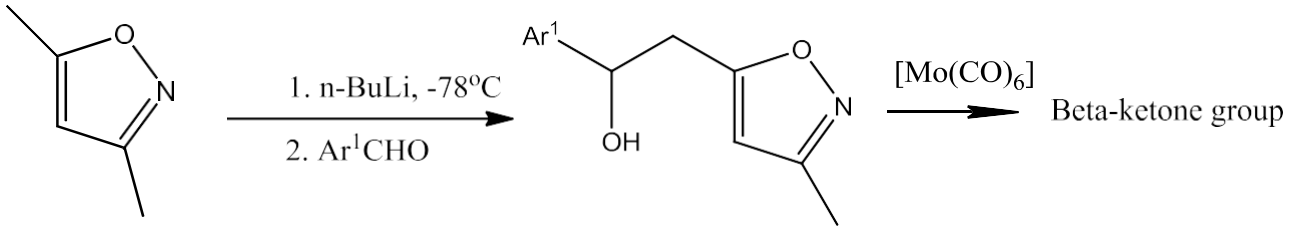

Scheme 1-67 3,5-dimethyl isoxazoles and further did a condensation reactions with various aromaticaldehydes sequentially at the C-3 and C-5 positions of the isoxazole to generate curcumin derivatives

Nitta and Higuchi expanded their previous studies of the reductive ring opening of isoxazoles with hexacarbonylmolybdenum to 5-(2-oxoalkyl) isoxazoles which served as useful precursors to pyridinones (**Scheme 1-68**).[96]

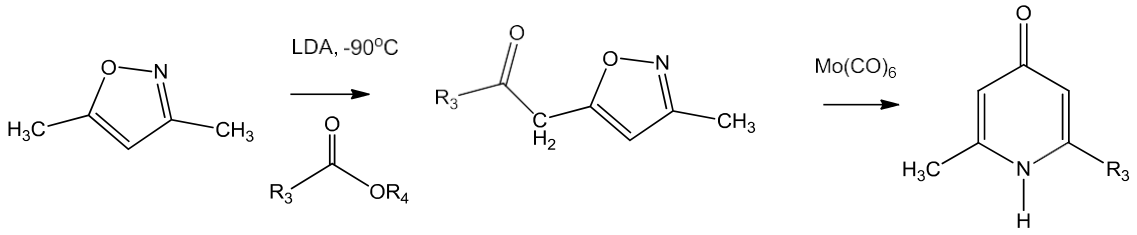

Scheme 1-68 3,5-dimethyl isoxazoles and further did a condensation reactions with various aromatic aldehydes sequentially at the C-3 and C-5 positions of the isoxazole to generate curcumin derivatives

Lateral metalation was employed by Burkhart et al to incorporate lipophilic groups at the C-5 position of putative glutamate neurotransmitter analogs (**Scheme 1-69** and **Scheme 1-70**), which were elaborated using Jacobsen's asymmetric Strecker synthesis). It found the best base for the lateral lithiation was LDA while a variety of electrophiles could be utilized with good yield. This further strengthen the transition step proposed Zhou et al (**Scheme 1-19**) that the reaction proceeds through a stabilizing interaction between the Li and the acetal protecting group leading to the addition of the El at the C-5.The aryl ethyl analogs exhibited selective activity at the System Xc- over the glutamate receptors, with the best example possessing binding affinity comparable to the endogenous substrate.[97,98]

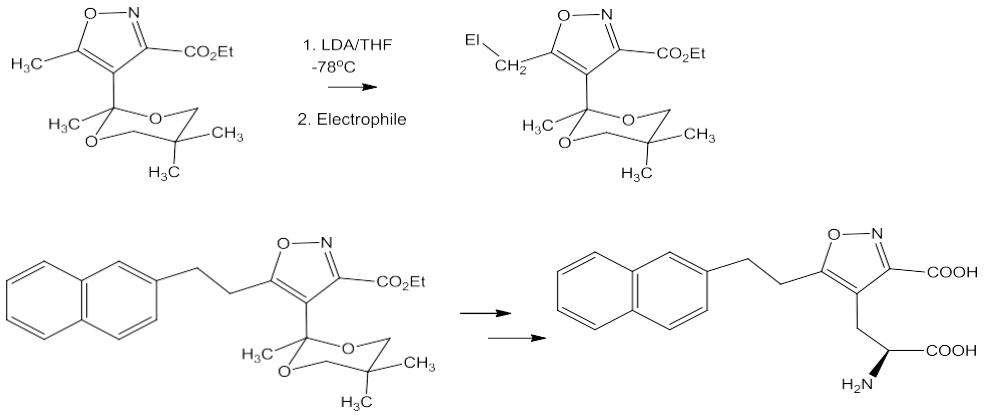

Scheme 1-69 Part 1 of incorporating lipophilic groups at the C-5 position of putative

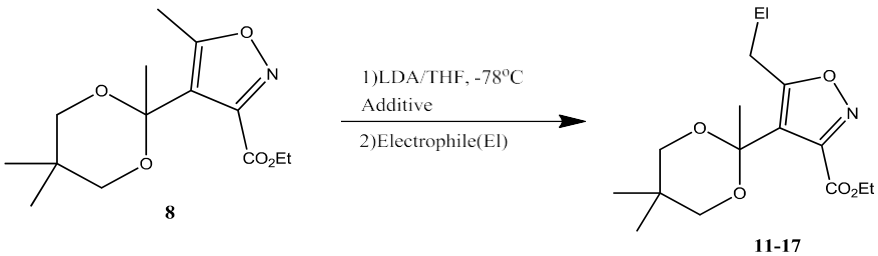

Entry	Electrophile	Product	Yield (%)
1	MeI	**11** (Me)	81
2	BnBr	**12** (Bn)	72
3	Acetone	**13** [C(OH)Me_2]	68
4	TMSCl	**14** ($SiMe_3$)	66
5	Me_3SnCl	**15** ($SnMe_3$)	42
6	MeSSMe	**16** (SMe)	61
7	PhNCO	**17** (CONHPh)	68

Entry	Electrophile	Additive	Product (%)
1	PhCHO	None	**18** (72)
2	PhCHO	6 equiv. LiCl	**18** (95)
3	PhCHO	20% HMPA	**18** (<10)
4	*p*-ClC_6H_4CHO	None	**19** (67)
5	*p*-ClC_6H_4CHO	6 equiv. LiCl	**19** (83)
6	Me_2CHCH_2CHO	6 equiv. LiCl	**20** (79)
7	*trans*-Cinnamaldehyde	6 equiv. LiCl	**21** (82)
8	EtBr	None	**22** (65)
9	EtBr	1.5 equiv. LiCl	**22** (83)
10	EtBr	6 equiv. LiCl	**22** (0)

Scheme 1-70 Part 2 of incorporating lipophilic groups at the C-5 position of putative glutamate neurotransmitter analogs

Early transition metal examples

Calle has reported the synthesis of 3,5-Dimethyl-4-(tributylstannyl)isoxazole (**243**, M = Sn) by lithiation and subsequent quenching with Bu_3SnCl (72 %), which upon cross-coupling with benzoyl chloride afforded **244** (45%).(**Scheme 1-71**)[99] A similar set of examples was reported for 5-iodo-3-(2-pyridinyl)-isoxazole and a comparative study of Sonogashira, Suzuki-Miyarua, Negishi, and Stille protocols gave generally high yields (80–94%).[100]

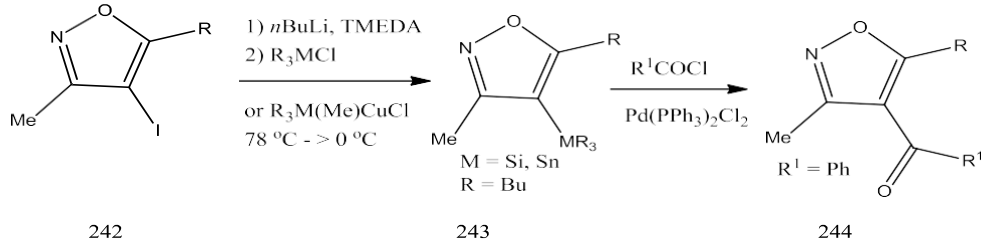

Scheme 1-71 Synthesis of 3,5-Dimethyl-4-(tributylstannyl)isoxazol by lithiation and subsequent quenching with Bu_3SnCl followed by cross coupling with benzoyl chloride

Since the C–Si bond is less polarized than the carbon–metal bonds of other metal organyls, fewer cross-coupling examples with silicon organyls were reported until now. Denmark reported the cycloaddition of aryl and alkyl-substituted alkynyldimethylsilyl ethers with aryl and alkyl nitrile oxides to generate a variety of differently functionalized 3,5-disubstituted 4-silylisoxazoles. A silicon-based cross-coupling reaction with aryl iodides creates a point for further diversification to afford 3,4,5-trisubstituted isoxazoles. The starting material **258** was prepared by a [3+2]cycloaddition from **257**, in which the compound bearing the silicon group in the 4-position was predominantly formed and was accompanied by considerable amounts of the 5-isomer. Compounds **258** were cross-coupled with iodobenzenes to give the cross-coupling products **259** in 55–69% yield (**Scheme 1-72**).[101]

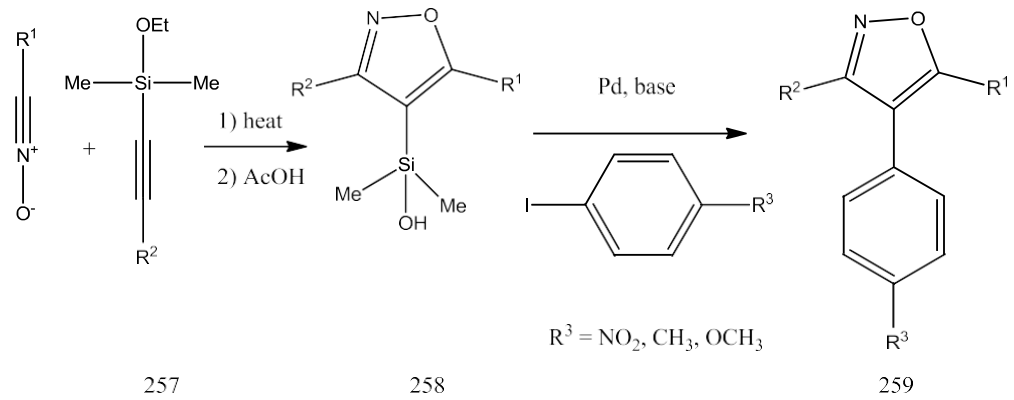

Scheme 1-72 cycloaddition of aryl and alkyl-substituted alkynyldimethylsilyl ethers with aryl and alkyl nitrile oxides to generate a variety of differently functionalized 3,5-disubstituted 4-silylisoxazoles

Organozinc halides, which are prepared either by direct zinc insertion or halogen-magnesium exchange and subsequent transmetalation with $ZnCl_2$, react smoothly with commercially available trichloroacetyl isocyanate to give, after hydrolysis, the corresponding primary amides. This method is compatible with a variety of functional groups such as an ester or a cyano group.

Also heterocyclic-, alkenyl, and acetylenic zinc reagents are converted to the corresponding primary amides under these conditions (**Scheme 1-73**).[102]

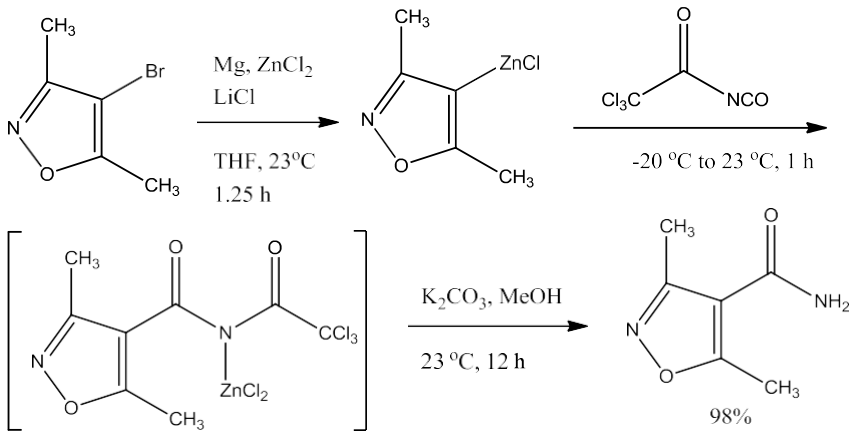

Scheme 1-73 Zinc catalyzed prepartion of primary amide substituted isoxazoles

Stenzel et al used lateral metalation with lower-order cuprate reagents lithium thienylcyanocuprate (Li[ThCuCN]) to allow for easier access to conjugated addition to α,β-unsaturated carbonyls with substitution occurring regio-selectively at the C-4 of the isoxazole. This occurred with good yields and under sterically prohibitive conditions. If samarium was used via Sm(HMDS) was used then the reaction conditions could give access to carbonyl addition.(**Scheme 1-74**) [103]

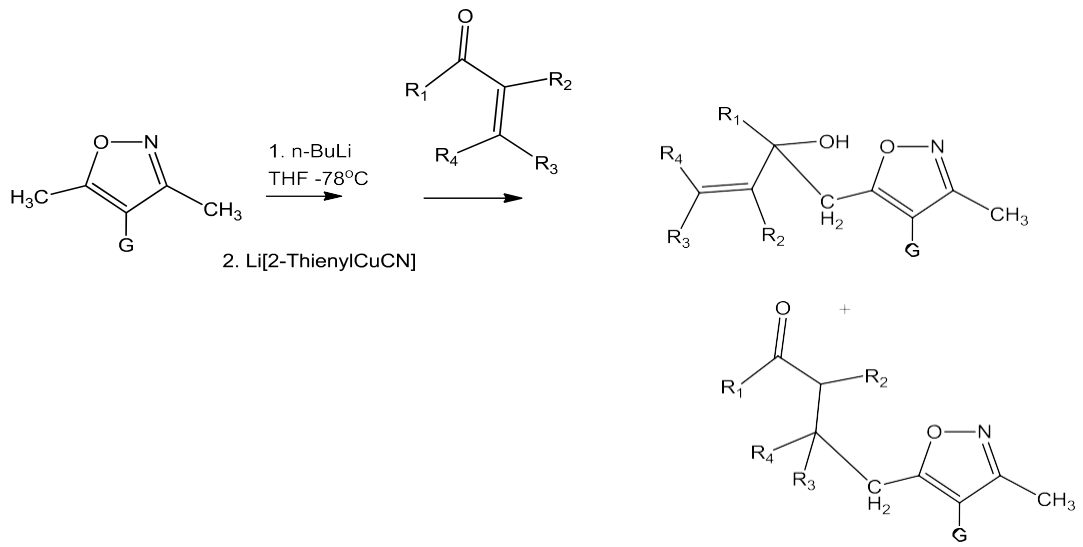

Scheme 1-74 lateral metalation with lower-order cuprate reagents lithium thienylcyanocuprate (Li[ThCuCN]) to allow for easier access to conjugated addition to α,β-unsaturated carbonyls with substitution occurring regio-selectively at the C-4 of the isoxazole

Pd and Rh examples

Kumar introduced boronic acid in the 4-position of **232** by a lithiation strategy; however, no isolated yields were reported. The crude boronic acids **233** were used successfully in Suzuki–Miyaura reactions under standard conditions for the synthesis of cyclooxygenase-2 (COX-2) inhibitors and some isomers in moderate to good yields (**234**: 30–75%)(**Scheme 1-75**). [104]

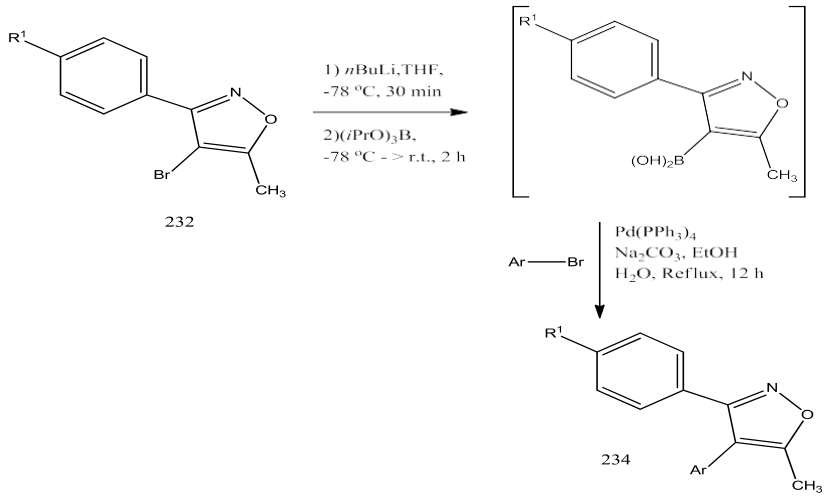

Scheme 1-75 synthesis of cyclooxygenase-2 (COX-2) inhibitors

Zhang et al expands on Kumar and Kapur's study of Rh and Pd catalyzed C-H alkenylation of 3,5-diarylisoxazole to help further understand rate determining step, clarify the steps that determine the regioselectivity, why a they hydroarylation product was not obtained in the Rh catalyzed reaction, and further understand the regioselectivity that is required of the role of co-catalysts in the production of varied products. To further understand the mechanism by which these systems proceeded they used density function theory (DFT). They further supported that Rh preferred the N-directed C7-H alkenylation due to the stronger interaction energy that the nitrogen provided. The overall rate limiting step for the reaction is insertion of the olefin. The palladium catalyst, on the hand, was depend on the co-catalysts that was present. When Ag_2CO_3 was used a switch in regioselectivity to C4-H alkenylation of the isoxazole ring was observed. This occurred due to the strong structural distortion in the competing C7-olenfin transition state resulting in a decrease in N-directed C7-H alkenylation. However this is not the rate determining step but rather a β-hydride elimination. For $Cu(OTf)_2$ the N-directed C-H alkenylation was preferred due to the strong coordination of the N to the Cu center in the Pd-Cu-cat.(**Reaction A**) The mechanism associated with the Cu and Ag helped to understand and design relevant

heterometallic catalysts.(**Reaction B**) For the cationic Rh-cat and Pd-Cu-cat can strongly coordinate with the isoxazole nitrogen directing to the C7-H for functionalization.(**Reaction C**). The stronger structural distortion in the C4-H activation overcomes the coordination with the isoxazole nitrogen in the Pd-Ag-cat resulting in more C4-H olefination. (**Scheme 1-76**)[105]

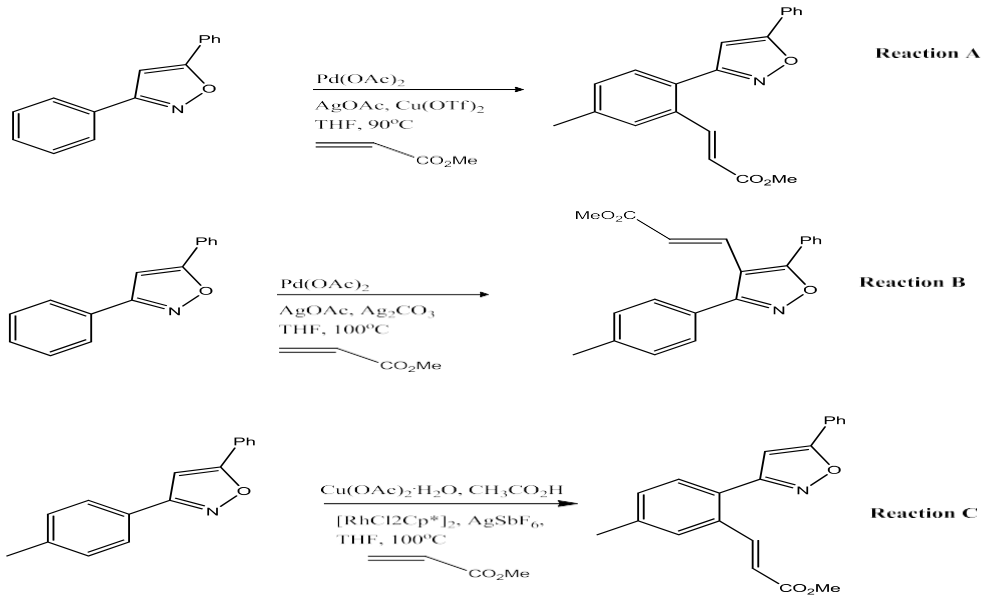

Scheme 1-76 Rh and Pd catalyzed C-H alkenylation of 3,5-diarylisoxazole

Player developed an efficient and versatile method for stereoselective synthesis of asymmetric diarylmethylidenyl indolinones by a palladium-catalyzed tandem Heck-carbocyclization/Suzuki coupling sequence. Factors influencing yield and selectivity, namely catalyst, coordinating ligand, and solvent, were optimized. Subjecting 3,5-dimethylisoxazole-4-boronic acid, copper(I) thiophene-2-carboxylate (CuTC) with Pd(PPh3)4, THF:DMF; 4:1 they obtained *E:Z*; 12:1 selectivity. (**Scheme 1-77**)[106]

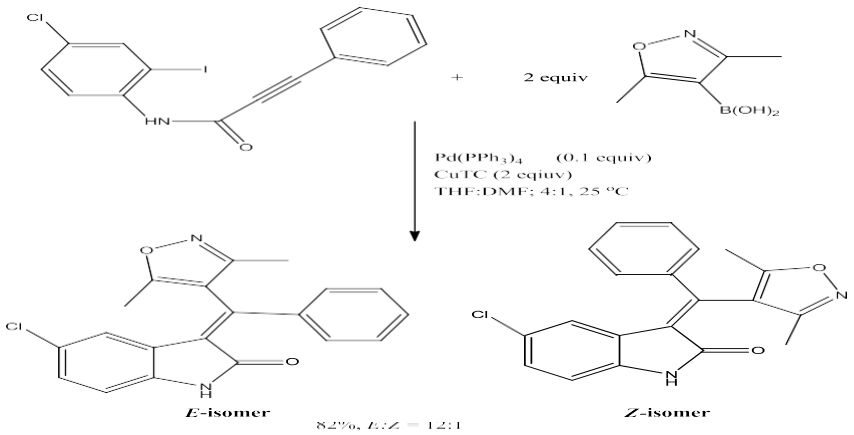

Scheme 1-77 stereoselective synthesis of asymmetric diarylmethylidenyl indolinones by a palladium-catalyzed tandem Heck-carbocyclization/Suzuki coupling sequence

A regioselective, simple and versatile copper(I)-catalyzed procedure for preparation of a series of liquid crystals based on unsymmetrical 3,5-disubstituted isoxazole was developed. Using different substituted chloro oximes and phenyl acetylenes, 1,3-dipolar cycloaddition reaction was carried out. A second series containing the isoxazole ring and a triple bond in the rigid core was also synthesized. From the 3-(4-bromophenyl)-5-(4-(decyloxy)phenyl)isoxazole, new liquid-crystalline compounds were prepared by Sonogashira cross-coupling.(**Scheme 1-78**)[107]

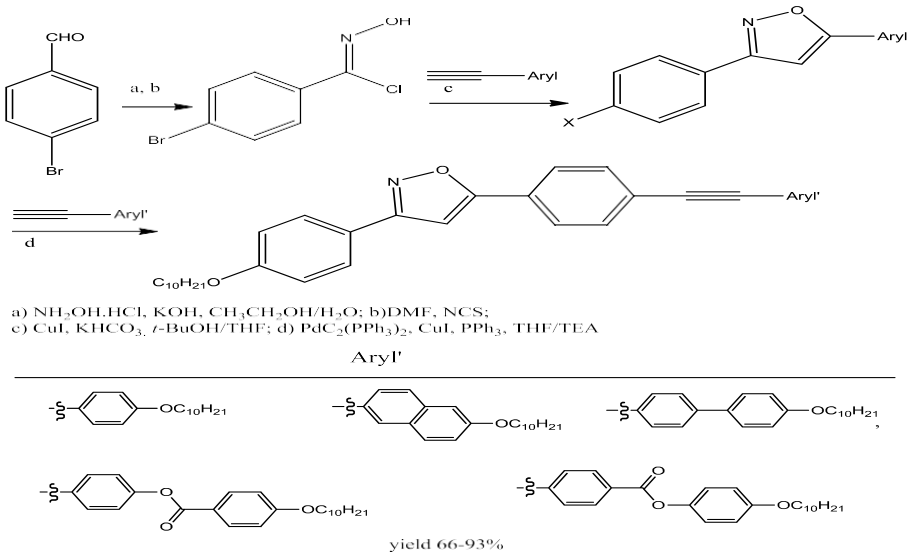

Scheme 1-78 copper(I)-catalyzed series of liquid crystals via unsymmetrical 3,5-disubstituted isoxazole

Yang et al expanded on sonogashira cross-coupling reactions of 3,5-disubstituted-4-iodoisoxazoles with terminal alkynes, which affords 3,5-disubstituted-4-alkynylisoxazole. They found that groups at the C3 and C5 of the isoxazole with C3 having the greatest influence due in large part to steric hindrance versus an electronic effect (Scheme 1-79).[108]

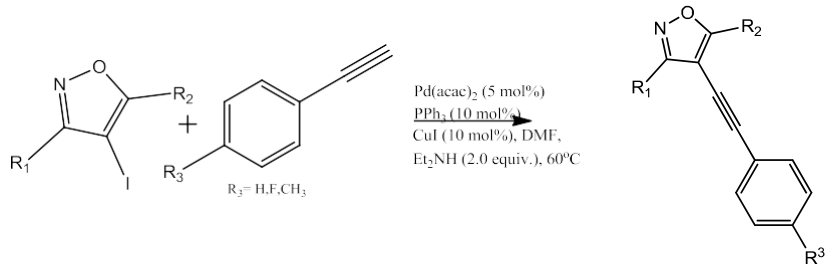

Scheme 1-79 3,5-disubstituted-4-alkynylisoxazole

Sn examples:

Labadie et al used bimetallic palladium-catalyzed coupling reactions in the formation of 4-aryl-3,5-dimethylisoxazole from 3,5-dimethyl-4-iodo isoxazole[109] (**Scheme 1-80**)

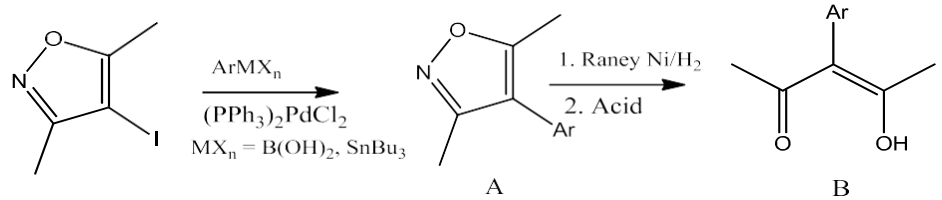

Scheme 1-80 bimetallic palladium-catalyzed coupling reactions in the formation of 4-aryl-3,5-dimethylisoxazole from 3,5-dimethyl-4-iodo isoxazole

Kromann et al reported a palladium catalyzed coupling reaction affording 4-aryl and 4-heteroaryl substituted 3-alkoyisoxazole compounds. (**Scheme 1-81**)[110]

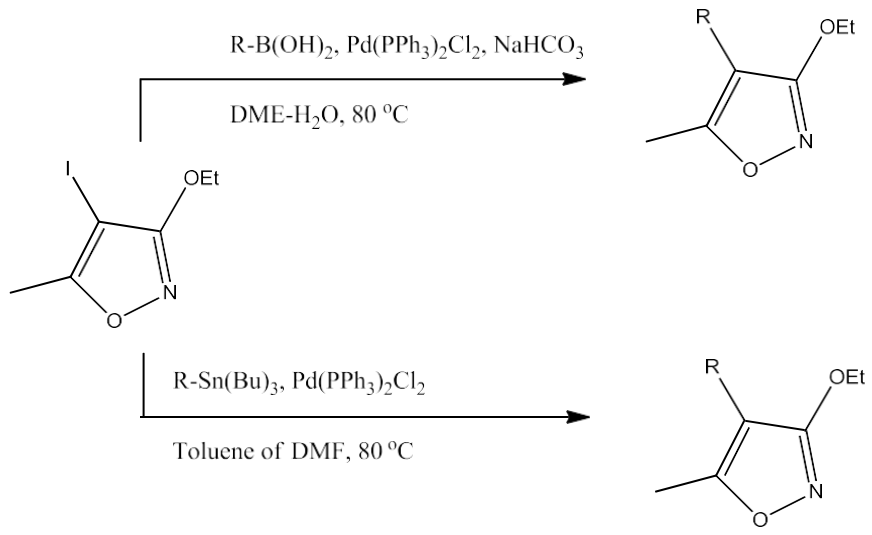

Scheme 1-81 palladium catalyzed coupling reaction affording 4-aryl and 4-heteroaryl substituted 3-alkoyisoxazole compounds

They additionally reported a cross-coupling of isoxazole halides **251** with various stannanes or other organometallic compounds. 4-Bromo and 4-iodoisoxazoles were successfully used in Sonogashira (to **253**), Heck (to **254**), Negishi (to **256**), Stille, and Suzuki–Miyaura reactions (to **252**). [110] As predicted the iodo reagents gave better results (**Scheme 1-82**)1,3-dipolar cycloaddition of bis(tributylstannyl)acetylene (**235**) with nitrile oxides formed (Tributylstannyl)isoxazole **237**.[110]

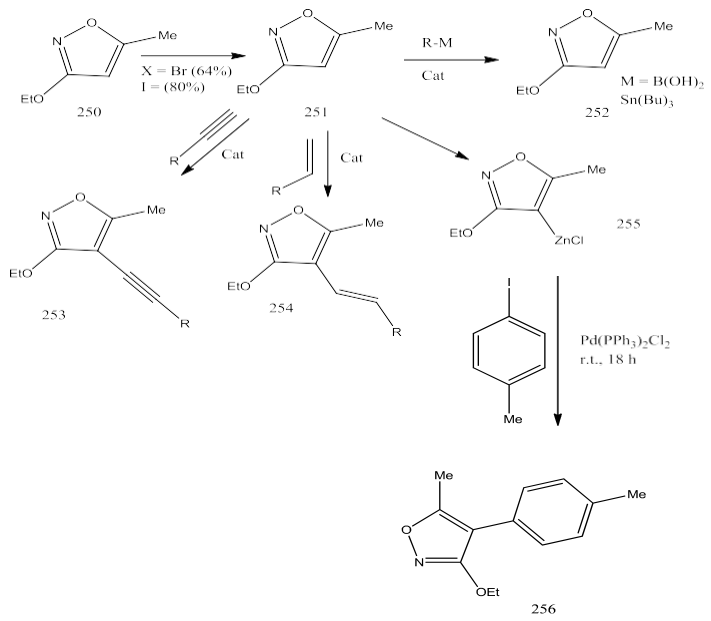

Scheme 1-82cross-coupling of isoxazole halides with various stannanes or other organometallic compound

A mixture of 4- and 5-(tributylstannyl)isoxazole (**246** and **247**) was obtained by cyclization of tributyl(ethynyl)stannane and various substituted chlorooximes **245**. Subsequent cross-coupling with triflate **248** gave novel antibacterial agents **249** (52–93%) (**Scheme 1-83**)[111]

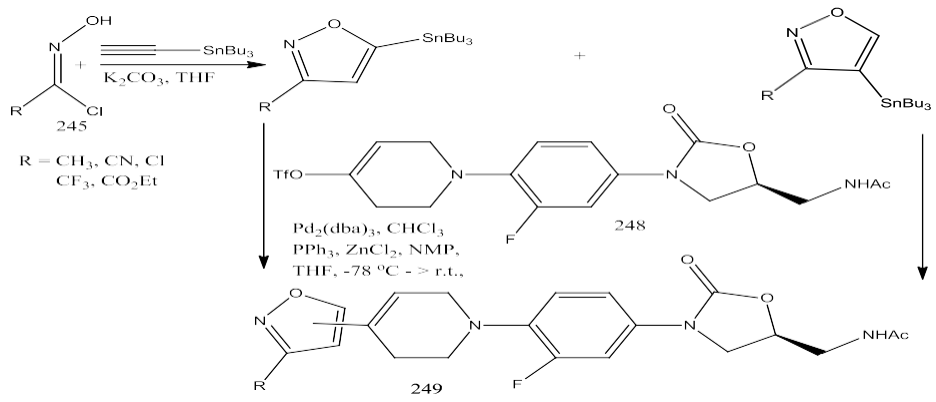

Scheme 1-83 4- and 5-(tributylstannyl)isoxazole via cyclization of tributyl(ethynyl)stannane and various substituted chlorooximes

Treatment of tributyl(3,3,3-trifluoro-1-propynyl)stannane **1** with acetonitrile oxide afforded the corresponding trifluoromethylated tributylstannyisoxazole (**6**) as an inseparable mixture of regioisomers in 77% combined yield. The cross-coupling reaction of **6** with 4-iodoacetophenone was also examined under various conditions. Either of the isomers (**6a** and **6b**) underwent arylation giving the corresponding aryl(trifluoromethyl)isoxazole (**7**) with essentially the same regioisomeric ratio in 90% yield under the optimum conditions (**Scheme 1-84**). Regioisomers of arylated isoxazole could be cleanly separated to each other. These coupling reactions required Cu(I) salt as a co-catalyst, and the use of Cu(I) thiophene-2-carboxylate (CuTC) under these conditions offered advantage over CuI.[112]

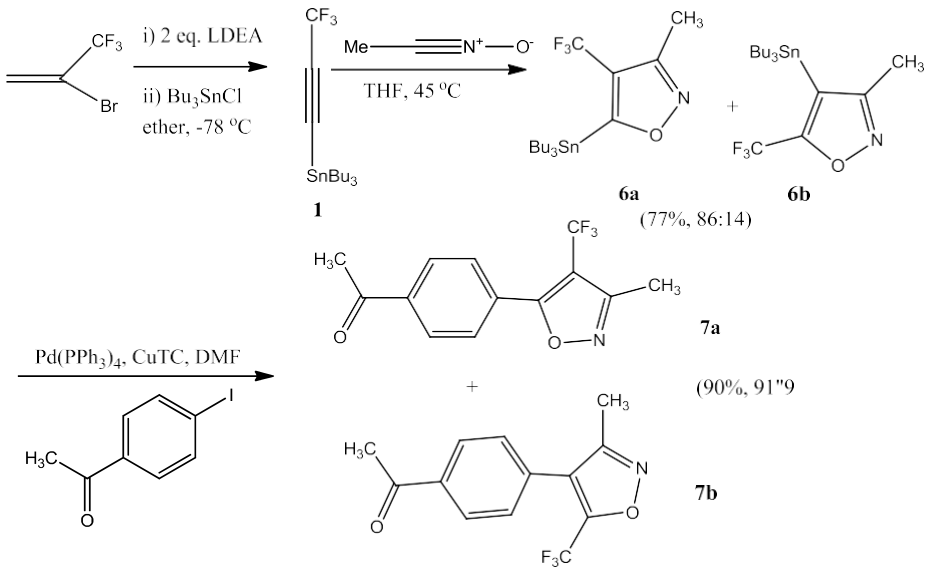

Scheme 1-84 Generation of trifluoromethylated tributylstannyisoxazole followed by palladation

Sakamoto and Uchiyama looked at the formation of 4-aryl-3-methylisoxazole from 4-(tributylstannyl)-3-methylisoxazole. To initially obtain the 4,5-distannane (**236)** addition at the C-4 and C-5 positions of the isoxazole occurs first. Then **236** is further transformed to the 4-

stannyl compound **237** by basic hydrolysis and subsequently used in the Stille reaction with benzoyl chloride (85%) or aryl halides (58–74%) (**Scheme 1-85**). [113, 114]

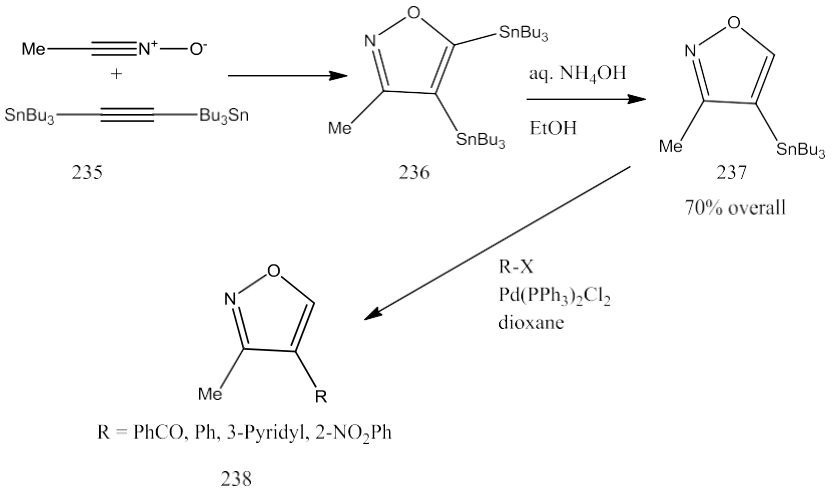

Scheme 1-85 4-aryl-3-methylisoxazole from 4-(tributylstannyl)-3-methylisoxazole

Alternatively, 4-(trialkylstannyl)isoxazoles **240** were prepared by a Grignard reaction from 3,5-dimethyl-4-iodoisoxazole (**239**). The subsequent cross-coupling with dibromoanthraquinone and -anthracene to **241** proceeded in moderate yields (30–47%) (**Scheme 1-86**). [115]

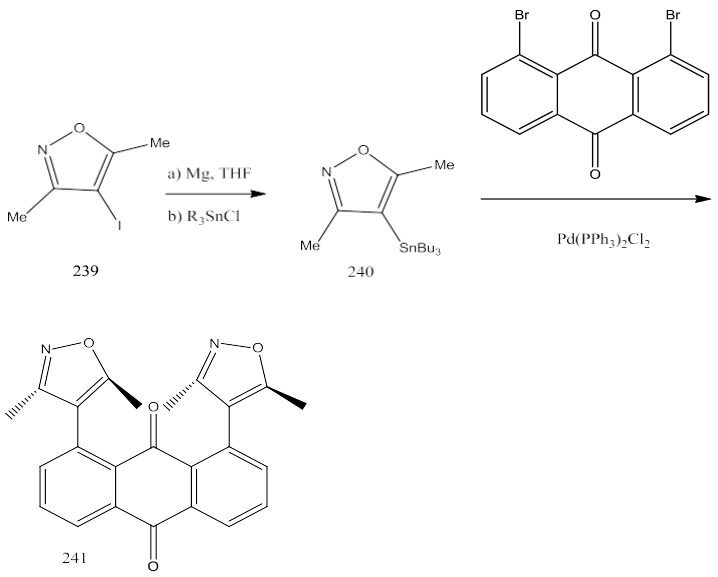

Scheme 1-86 4-(trialkylstannyl)isoxazoles synthesized via Grignard reaction from 3,5-dimethyl-4-iodoisoxazole followed by cross coupling

Conclusion

The isoxazole is an important synthetic intermediate in organic synthesis. In this review, we discussed the various applications of lateral metalation of isoxazoles and its utility in synthetic development of pharmaceuticals and access to new routes to previously difficult to access chemical scaffolds. Illustrated additionally was the variety of metals and co-catalysts that could be used to vary the synthetic method to accommodate a number of reaction conditions and functional groups. This synthetic versatility is crucial for stream lining the development of small molecules and exploring new targets and applications. We will take these ideas and principles and apply them to our small molecule isoxazole 3,4-d pyridazinones and further expand upon our synthetic library of compound that were found to be active at mGluRs.

References

(1) Clark,R.D.;Jahangir, A. *Lateral Lithiation Reations Promoted by Heteroaromatic Substitutents*; 1995; Vol. 47.

(2) Choong, I.C., Ellman, J. A. Annul Reports in Medicinal Chemistry. **1996**, 309–318.

(3) Kubinyi,Hugo, M. G. *Chemogenomics in Drug Discovery*; Kubinyi, H., Müller, G., Eds.; Methods and Principles in Medicinal Chemistry; Wiley, 2004.

(4) Natale, N. R.; Mirzaei, Y. R. The Lateral Metalation of Isoxazoles. A Review. *Org. Prep. Proced. Int.* **1993**, *25* (5), 515–556 DOI: 10.1080/00304949309457997.

(5) Nivina, A.; Yuet, K. P.; Hsu, J.; Khosla, C. Evolution and Diversity of Assembly-Line Polyketide Synthases Focus Review. **2019** DOI: 10.1021/acs.chemrev.9b00525.

(6) Pinho e Melo, T. Recent Advances on the Synthesis and Reactivity of Isoxazoles. *Current Organic Chemistry*. 2005, pp 925–958.

(7) Ch. Camoutsis, S. N.; Camoutsis, C.; Nikolaropoulos, S. *Steroidal Isoxazoles, Isoxazolines, and Isoxazolines*; HeteroCorporation, 1997; Vol. 35, p 731.

(8) Hu, F.; Szostak, M. Recent Developments in the Synthesis and Reactivity of Isoxazoles: Metal Catalysis and Beyond. *Advanced Synthesis and Catalysis*. Wiley-VCH Verlag August 24, 2015, pp 2583–2614.

(9) Zhang, H. Z.; Zhao, Z. L.; Zhou, C. H. Recent Advance in Oxazole-Based Medicinal Chemistry. *European Journal of Medicinal Chemistry*. Elsevier Masson SAS January 20, 2018, pp 444–492.

(10) Badenock, J. C. Metalation Reactions of Isoxazoles and Benzisoxazoles. In *Top Heterocycl Chem*; Springer, Berlin, Heidelberg, 2012; Vol. 29, pp 261–305.

(11) Walunj, Y.; Mhaske, P.; Kulkarni, P. Application, Reactivity and Synthesis of Isoxazole Derivatives. *Mini. Rev. Org. Chem.* **2020**, *17*, 1–23 DOI: 10.2174/1570193x17999200511131621.

(12) Ali, W.; Prakash, G.; Maiti, D. Recent Development in Transition Metal-Catalysed C-H Olefination. *Chem. Sci.* **2021**, *12* (8), 2735–2759 DOI: 10.1039/d0sc05555g.

(13) Roger, J.; Gottumukkala, A. L.; Doucet, H. Palladium-Catalyzed C3 or C4 Direct Arylation of Heteroaromatic Compounds with Aryl Halides by C-H Bond Activation. *ChemCatChem* **2010**, *2* (1), 20–40 DOI: 10.1002/cctc.200900074.

(14) Röthlisberger, D.; Khersonsky, O.; Wollacott, A. M.; Jiang, L.; DeChancie, J.; Betker, J.; Gallaher, J. L.; Althoff, E. A.; Zanghellini, A.; Dym, O.; Albeck, S.; Houk, K. N.; Tawfik, D. S.; Baker, D. Kemp Elimination Catalysts by Computational Enzyme Design. *Nature* **2008**, *453* (7192), 190–195 DOI: 10.1038/nature06879.

(15) Khersonsky, O.; Röthlisberger, D.; Dym, O.; Albeck, S.; Jackson, C. J.; Baker, D.; Tawfik, D. S. Evolutionary Optimization of Computationally Designed Enzymes: Kemp Eliminases of the Ke07 Series. *J. Mol. Biol.* **2010**, *396* (4), 1025–1042 DOI: 10.1016/j.jmb.2009.12.031.

(16) Munsey, M. S.; Natale, N. R. The Coordination Chemistry of Isoxazoles. *Coord. Chem. Rev.* **1991**, *109* (2), 251–281 DOI: 10.1016/0010-8545(91)80019-A.

(17) Duncan, N. S. Molecular Modeling Assisted Design and Synthesis of Unsymmetrical Anthracene Isoxazole Small Molecule Anti-Tumor Agents. *ProQuest Diss. Theses* **2015**, 208.

(18) Devoto, G.; Ponticelli, G.; Preti, C. Complexes of Cobalt(II), Nickel(II) and Copper(II) with 3,5-Dimethylisoxazole as Ligand. *J. Inorg. Nucl. Chem.* **1975**, *37* (7–8), 1635–1639

DOI: 10.1016/0022-1902(75)80289-2.
(19) Burton, A. G.; Forsythe, P. P.; Johnson, C. D.; Katritzky, A. R. The Kinetics and Mechanism of the Electrophilic Substitution of Heteroaromatic Compounds. Part XXVII. The Nitration and Hydrogen Exchange of 1,3,5-Trimethylpyrazole, 3,5-Dimethylisoxazole, and 3,5-Dimethylisothiazole. *J. Chem. Soc. B Phys. Org.* **1971**, No. 0, 2365 DOI: 10.1039/j29710002365.
(20) KobayashiTomoshige; NittaMakoto. Synthesis and Properties of the [n](2,5)Pyridinophane Ring System. *http://dx.doi.org/10.1246/bcsj.58.3099* **2006**, *58* (11), 3099–3103 DOI: 10.1246/BCSJ.58.3099.
(21) Natale, N. R. Selective Reduction of Isoxazoles with Samarium Diiodide. *Tetrahedron Lett.* **1982**, *23* (48), 5009–5012 DOI: 10.1016/S0040-4039(00)85559-8.
(22) Prashanthi, Y.; Kiranmai, K.; Subhashini, N. J. P.; Shivaraj. Synthesis, Potentiometric and Antimicrobial Studies on Metal Complexes of Isoxazole Schiff Bases. *Spectrochim. Acta - Part A Mol. Biomol. Spectrosc.* **2008**, *70* (1), 30–35 DOI: 10.1016/j.saa.2007.07.028.
(23) Pitteri, B.; Marangoni, G.; Cattalini, L. Reactivity of Neutral Nitrogen Donors in Planar D8 Metal Complexes. Part 2. The System [2,6-Bis(Methylsulfanyl-Methyl)Pyridine]Chloroplatinum(II) with Pyridines and Amines in Methanol. Effect of Basicity, π-Acceptor Capacity and Steric Hindrance. *J. Chem. Soc. Dalt. Trans.* **1994**, No. 24, 3539–3543 DOI: 10.1039/DT9940003539.
(24) Chen, Z.; Wu, Y.; Gu, D.; Gan, F. Nickel(II) and Copper(II) Complexes Containing 2-(2-(5-Substitued Isoxazol-3-Yl)Hydrazono)-5,5-Dimethylcyclohexane-1,3-Dione Ligands: Synthesis, Spectral and Thermal Characterizations. *Dye. Pigment.* **2008**, *76* (3), 624–631 DOI: 10.1016/j.dyepig.2006.11.009.
(25) Chen, Z.; Wu, Y.; Gu, D.; Gan, F. Spectroscopic, and Thermal Studies of Some New Binuclear Transition Metal(II) Complexes with Hydrazone Ligands Containing Acetoacetanilide and Isoxazole. *Spectrochim. Acta - Part A Mol. Biomol. Spectrosc.* **2007**, *68* (3), 918–926 DOI: 10.1016/j.saa.2007.01.006.
(26) Chen, Z.; Wu, Y.; He, C.; Wang, B.; Gu, D.; Gan, F. Insights into the Physical Basis of Metal(II) Hydrazone Complexes with Isoxazole and Barbituric Acid Moieties for Recordable Blu-Ray Media. *Synth. Met.* **2010**, *160* (23–24), 2581–2586 DOI: 10.1016/j.synthmet.2010.10.008.
(27) Feng, Z.; Yu, S.; Shang, Y. Novel Pyridine-Bis(Ferrocene-Isoxazole) Ligand: Synthesis and Application to Palladium-Catalyzed Sonogashira Cross-Coupling Reactions under Copper- and Phosphine-Free Conditions. *Appl. Organomet. Chem.* **2008**, *22* (10), 577–582 DOI: 10.1002/aoc.1445.
(28) La Cour, A.; Findeisen, M.; Hazell, A.; Hazell, R.; Zdobinsky, G. Metal(II) N 2 S 2 Schiff-Base Complexes Incorporating Pyrazole or Isoxazole (M = Ni, Cu or Zn). Spin States, Racemization Kinetics and Electrochemistry †. *J. Chem. Soc., Dalt. Trans* **1997**, *10*, 56–72.
(29) Birch, A. J. Biosynthesis of Polyketides and Related Compounds Published by : American Association for the Advancement of Science Stable URL : Http://Www.Jstor.Org/Stable/1720493 REFERENCES Linked References Are Available on JSTOR for This Article : Biosynthesis of Po. *Science (80-.).* **1967**, *156* (3772), 202–206.
(30) Tanaka, T.; Miyazaki, M.; Iijima, I. Acylation of 5-Isoxazolylalkyl Carbanions: Synthesis of Bis- and Tris-Isoxazole Compounds. *J. Chem. Soc. Chem. Commun.* **1973**, No. 7, 233a

DOI: 10.1039/c3973000233a.
(31) Gilbreath, S. G.; Harris, C. M.; Harris, T. M. Biomimetic Syntheses of Pretetramides. 1. Synthesis of Pretetramide by Tandem Extension of a Polyketide Chain. *J. Am. Chem. Soc.* **1988**, *110* (18), 6172–6179 DOI: 10.1021/ja00226a036.
(32) Khosla, C. Structures and Mechanisms of Polyketide Synthases. *J. Org. Chem.* **2009**, *74* (17), 6416–6420 DOI: 10.1021/jo9012089.
(33) Bode, J. W.; Hachisu, Y.; Matsuura, T.; Suzuki, K. Facile Construction and Divergent Transformation of Polycyclic Isoxazoles: Direct Access to Polyketide Architectures. *Org. Lett.* **2003**, *5* (4), 391–394 DOI: 10.1021/ol027283f.
(34) Krogsgaard-Larsen, P.; Nielsen, E.; Curtis, D. R. Ibotenic Acid Analogues. Synthesis and Biological and in Vitro Activity of Conformationally Restricted Agonists at Central Excitatory Amino Acid Receptors. *J. Med. Chem.* **1984**, *27* (5), 585–591 DOI: 10.1021/jm00371a005.
(35) Vogensen, S. B.; Clausen, R. P.; Greenwood, J. R.; Johansen, T. N.; Pickering, D. S.; Nielsen, B.; Ebert, B.; Krogsgaard-Larsen, P. Convergent Synthesis and Pharmacology of Substituted Tetrazolyl-2-Amino-3- (3-Hydroxy-5-Methyl-4-Isoxazolyl)Propionic Acid Analogues. *J. Med. Chem.* **2005**, *48* (9), 3438–3442 DOI: 10.1021/jm050014l.
(36) Ceccherelli, P.; Curini, M.; Marcotullio, M. C.; Rosati, O.; Wenkert, E. Metal-Catalyzed, Intramolecular Reactions of α-Diazo Ketones with Isoxazoles. *J. Org. Chem.* **1994**, *59* (10), 2882–2884 DOI: 10.1021/jo00089a037.
(37) Drummond, J.; Johnson, G.; Nickell, D. G.; Ortwine, D. F.; Bruns, R. F.; Welbaum, B. Evaluation and Synthesis of Aminohydroxyisoxazoles and Pyrazoles as Potential Glycine Agonists. *J. Med. Chem.* **1989**, *32* (9), 2116–2128 DOI: 10.1021/jm00129a016.
(38) Brubaker, J. D.; Myers, A. G. A Practical, Enantioselective Synthetic Route to a Key Precursor to the Tetracycline Antibiotics. *Org. Lett.* **2007**, *9* (18), 3523–3525 DOI: 10.1021/ol071377d.
(39) Alzeer, J.; Nock, N.; Wassner, G.; Masciadri, R. MOM-Protected 3-Hydroxy-5-Phenyl-Isoxazole: Regioselective Preparation and Synthetic Application. *Tetrahedron Lett.* **1996**, *37* (38), 6857–6860 DOI: 10.1016/0040-4039(96)01547-X.
(40) Campana, C. F.; Mirzaei, J.; Koerner, C.; Gates, C.; Natale, N. R. 3-(1,3-Diphenylpropan-2-Yl)-4-Methyl-6-Phenylisoxazolo[3,4-d] Pyridazin-7(6H)-One. *Acta Crystallogr. Sect. E Struct. Reports Online* **2013**, *69* (11) DOI: 10.1107/S160053681302802X.
(41) Hulubei, V.; Meikrantz, S. B.; Quincy, D. A.; Houle, T.; McKenna, J. I.; Rogers, M. E.; Steiger, S.; Natale, N. R. 4-Isoxazolyl-1,4-Dihydropyridines Exhibit Binding at the Multidrug-Resistance Transporter. *Bioorganic Med. Chem.* **2012**, *20* (22), 6613–6620 DOI: 10.1016/j.bmc.2012.09.022.
(42) Patel, S. A.; Rajale, T.; O'Brien, E.; Burkhart, D. J.; Nelson, J. K.; Twamley, B.; Blumenfeld, A.; Szabon-Watola, M. I.; Gerdes, J. M.; Bridges, R. J.; Natale, N. R. Isoxazole Analogues Bind the System Xc- Transporter: Structure-Activity Relationship and Pharmacophore Model. *Bioorganic Med. Chem.* **2010**, *18* (1), 202–213 DOI: 10.1016/j.bmc.2009.11.001.
(43) Li, C.; Twamley, B.; Natale, N. R. Preparation and Crystal Structures of Two 3-anthracenyl Isoxazolyl Sulfonamides. *J. Heterocycl. Chem.* **2008**, *45* (1), 259–264 DOI: 10.1002/jhet.5570450132.
(44) Han, X.; Li, C.; Rider, K. C.; Blumenfeld, A.; Twamley, B.; Natale, N. R. The Isoxazole as a Linchpin for Molecules That Target Folded DNA Conformations: Selective Lateral

Lithiation and Palladation. *Tetrahedron Lett.* **2002**, *43* (43), 7673–7677 DOI: 10.1016/S0040-4039(02)01845-2.

(45) Mosher, M. D.; Natale, N. R. Nucleophilic Aromatic Substitution with the Anion of 3,5-disubstituted Isoxazole-4-carboxylic Acids. *Journal of Heterocyclic Chemistry*. 1995, pp 1385–1387.

(46) Zhou,Peiwen; Natale, N. R. Lateral Lithiation of Ethyl 4-Acetyl-5-Methyl-3-Isoxazolyl Carboxylate with 5,5-Dimethyl-l,3-Dioxanyi as a Directing Group. *Tetrahedron Lett.* **1998**, *39*, 8249–8252.

(47) Nelson, J.; Twamley, B.; Natale, N. R. Ethyl 5-(5-Oxo-2,3-Dihydro-5H-Oxazolo[2,3-a]-Isoindol-9b-Ylmethyl)-4-(2,5, 5-Trimethyl-1,3-Dioxan-2-Yl)Isoxazole-3-Carboxylate: The Product of a Novel Synthetic Method. *Acta Crystallogr. Sect. E Struct. Reports Online* **2004**, *60* (12), 2255–2257 DOI: 10.1107/S1600536804027655.

(48) Natale, N. R.; Rogers, M. E.; Staples, R.; Triggle, D. J.; Rutledge, A. Lipophilic 4-Isoxazolyl-1,4-Dihydropyridines: Synthesis and Structure- Activity Relationships. *J. Med. Chem.* **1999**, *42* (16), 3087–3093 DOI: 10.1021/jm980439q.

(49) Di Nunno, L.; Scilimati, A.; Vitale, P. Regioselective Synthesis and Side-Chain Metallation and Elaboration of 3-Aryl-5-Alkylisoxazoles. *Tetrahedron* **2002**, *58* (13), 2659–2665 DOI: 10.1016/S0040-4020(02)00125-4.

(50) Alguacil, R.; Fariña, F.; Martin, M. V.; Paredes, M. C. 6-Ethylsulfonyl-3-Phenylfuro[3,4-d]Isoxazole-4(6H)-One: A Useful Synthon for Preparation of Heteroanthracyclinone Analogues. *Tetrahedron Lett.* **1995**, *36* (37), 6773–6776 DOI: 10.1016/00404-0399(50)1338-I.

(51) Carmen Paredes, M.; Alguacil, R.; Victoria Martín, M. Polycyclic Hydroxyquinones. Part 31. Regioselective Reactions of 6-Ethylsulfonyl-3-Phenylfuro[3,4-d]Isoxazol-4(6H)-One Anion with Quinone Monoketals. Application to the Preparation of Heteroanthracyclinone Analogues. *Heterocycles* **2000**, *53* (5), 1029 DOI: 10.3987/COM-99-8836.

(52) Diana, G. D.; Volkots, D. L.; Nitz, T. J.; Bailey, T. R.; Long, M. A.; Vescio, N.; Aldous, S.; Pevear, D. C.; Dutko, F. J. Oxadiazoles as Ester Bioisosteric Replacements in Compounds Related to Disoxaril. Antirhinovirus Activity. *J. Med. Chem.* **1994**, *37* (15), 2421–2436 DOI: 10.1021/jm00041a022.

(53) Diana, G. D.; Cutcliffe, D.; Volkots, D. L.; Mallamo, J. P.; Bailey, T. R.; Vescio, N.; Oglesby, R. C.; Nitz, T. J.; Wetzel, J.; Giranda, V.; Pevear, D. C.; Dutko, F. J. Antipicornavirus Activity of Tetrazole Analogues Related to Disoxaril. *J. Med. Chem.* **1993**, *36* (22), 3240–3250 DOI: 10.1021/jm00074a004.

(54) Nelson, J. K.; Burns, C. T.; Smith, M. P.; Twamley, B.; Natale, N. R. R. Synthetic Utility of Epoxides for Chiral Functionalization of Isoxazoles. *Tetrahedron Lett.* **2008**, *49* (19), 3078–3082 DOI: 10.1016/j.tetlet.2008.03.059.

(55) Domínguez, E.; Ibeas, E.; Martínez De Marigorta, E.; Palacios, J. K.; Sanmartín, R. A Convenient One-Pot Preparative Method for 4,5-Diarylisoxazoles Involving Amine Exchange Reactions. **1996**.

(56) Jackowski, O.; Lecourt, T.; Micouin, L. Direct Synthesis of Polysubstituted Aluminoisoxazoles and Pyrazoles by a Metalative Cyclization. *Org. Lett.* **2011**, *13* (20), 5664–5667 DOI: 10.1021/ol202389u.

(57) Kraus, J. M.; Lmj Verlinde, C.; Karimi, M.; Lepesheva, G. I.; Gelb, M. H.; Buckner, F. S. Rational Modification of a Candidate Cancer Drug for Use Against Chagas Disease. DOI: 10.1021/jm801313t.

(58) Singh, V.; Saxena, R.; Batra, S. Simple and Efficient Synthesis of Substituted 2-Pyrrolidinones, 2-Pyrrolones, and Pyrrolidines from Enaminones of Baylis-Hillman Derivatives of 3-Isoxazolecarbaldehydes §, ‡. **2005** DOI: 10.1021/jo048411b.
(59) Li, L.; Tan, T. De; Zhang, Y. Q.; Liu, X.; Ye, L. W. Recent Advances in Transition-Metal-Catalyzed Reactions of Alkynes with Isoxazoles. *Org. Biomol. Chem.* **2017**, *15* (40), 8483–8492 DOI: 10.1039/c7ob01895a.
(60) Hansen, T. V.; Wu, P.; Fokin, V. V. One-Pot Copper(I)-Catalyzed Synthesis of 3,5-Disubstituted Isoxazoles. *J. Org. Chem.* **2005**, *70* (19), 7761–7764 DOI: 10.1021/jo050163b.
(61) Ueda, M.; Sugita, S.; Sato, A.; Miyoshi, T.; Miyata, O. Copper-Catalyzed Synthesis of Trisubstituted Isoxazoles via a Cascade Cyclization-Migration Process. *J. Org. Chem.* **2012**, *77* (20), 9344–9351 DOI: 10.1021/jo301358h.
(62) Himo, F.; Lovell, T.; Hilgraf, R.; Rostovtsev, V. V.; Noodleman, L.; Sharpless, K. B.; Fokin, V. V. Copper(I)-Catalyzed Synthesis of Azoles. DFT Study Predicts Unprecedented Reactivity and Intermediates. *J. Am. Chem. Soc.* **2005**, *127* (1), 210–216 DOI: 10.1021/ja0471525.
(63) Nelson, J. K.; Twamley, B.; Villalobos, T. J.; Natale, N. R. The Catalytic Asymmetric Addition of Alkyl- and Aryl-Zinc Reagents to an Isoxazole Aldehyde. *Tetrahedron Lett.* **2008**, *49* (41), 5957–5960 DOI: 10.1016/j.tetlet.2008.07.169.
(64) Alberico, D.; Scott, M. E.; Lautens, M. Aryl-Aryl Bond Formation by Transition-Metal-Catalyzed Direct Arylation. *Chem. Rev.* **2007**, *107* (1), 174–238 DOI: 10.1021/cr0509760.
(65) Nakamura, N.; Tajima, Y.; Sakai, K. Direct Phenylation of Isoxazoles Using Palladium Catalysts. Synthesis of 4-Phenylmuscimol. *Heterocycles*. 1982, p 235.
(66) Basolo, L.; Beccalli, E. M.; Borsini, E.; Broggini, G.; Pellegrino, S. N,N-Disubstituted Propargylamines as Tools in the Sequential 1,3-Dipolar Cycloaddition/Arylation Processes to the Formation of Polyheterocyclic Systems. *Tetrahedron* **2008**, *64* (35), 8182–8187 DOI: 10.1016/j.tet.2008.06.042.
(67) Chiong, H. A.; Daugulis, O. Palladium-Catalyzed Arylation of Electron-Rich Heterocycles with Aryl Chlorides. *Org. Lett.* **2007**, *9* (8), 1449–1451 DOI: 10.1021/ol0702324.
(68) Sahoo, S.; Pal, S. Rapid Access to Benzimidazo[1,2- a]Quinoline-Fused Isoxazoles via Pd(II)-Catalyzed Intramolecular Cross Dehydrogenative Coupling: Synthetic Versatility and Photophysical Studies . *J. Org. Chem.* **2021**, *86* (5), 4081–4097 DOI: 10.1021/acs.joc.0c02926.
(69) Galenko, E. E.; Novikov, M. S.; Shakirova, F. M.; Shakirova, J. R.; Kornyakov, I. V.; Bodunov, V. A.; Khlebnikov, A. F. Isoxazole Strategy for the Synthesis of 2,2′-Bipyridine Ligands: Symmetrical and Unsymmetrical 6,6′-Binicotinates, 2,2′-Bipyridine-5-Carboxylates, and Their Metal Complexes. *J. Org. Chem.* **2019**, *84* (6), 3524–3536 DOI: 10.1021/acs.joc.9b00115.
(70) Shen, W.-B.; Xiao, X.-Y.; Sun, Q.; Zhou, B.; Zhu, X.-Q.; Yan, J.-Z.; Lu, X.; Ye, L.-W. Highly Site Selective Formal [5+2] and [4+2] Annulations of Isoxazoles with Heterosubstituted Alkynes by Platinum Catalysis: Rapid Access to Functionalized 1,3-Oxazepines and 2,5-Dihydropyridines. *Angew. Chemie* **2017**, *129* (2), 620–624 DOI: 10.1002/ange.201610042.
(71) Frølund, B.; Jensen, L. S.; Storustovu, S. I.; Stensbøl, T. B.; Ebert, B.; Kehler, J.; Krogsgaard-Larsen, P.; Liljefors, T. 4-Aryl-5-(4-Piperidyl)-3-Isoxazolol GABAA

Antagonists: Synthesis, Pharmacology, and Structure-Activity Relationships. *J. Med. Chem.* **2007**, *50* (8), 1988–1992 DOI: 10.1021/jm070038n.
(72) Banerjee, A.; Bera, A.; Santra, S. K.; Guin, S.; Patel, B. K. Palladium-Catalysed Regioselective Aroylation and Acetoxylation of 3,5-Diarylisoxazole via Ortho C-H Functionalisations. *RSC Adv.* **2014**, *4* (17), 8558–8566 DOI: 10.1039/c3ra45403g.
(73) Fall, Y.; Reynaud, C.; Doucet, H.; Santelli, M. Ligand-Free-Palladium-Catalyzed Direct 4-Arylation of Isoxazoles Using Aryl Bromides. *European J. Org. Chem.* **2009**, No. 24, 4041–4050 DOI: 10.1002/ejoc.200900309.
(74) Mokhtar, H. H.; Laidaoui, N.; El Abed, D.; Soulé, J. F.; Doucet, H. Palladium-Catalysed Direct Arylation of Heteroarenes Using 1-(Bromophenyl)-1,2,3-Triazoles as Aryl Source. *Catal. Commun.* **2017**, *92*, 124–127 DOI: 10.1016/j.catcom.2016.12.030.
(75) Piller, F. M.; Metzger, A.; Schade, M. A.; Haag, B. A.; Gavryushin, A.; Knochel, P. Preparation of Polyfunctional Arylmagnesium, Arylzinc, and Benzylic Zinc Reagents by Using Magnesium in the Presence of LiCl. *Chem. - A Eur. J.* **2009**, *15* (29), 7192–7202 DOI: 10.1002/chem.200900575.
(76) Arai, M. A.; Kuraishi, M.; Arai, T.; Sasai, H. A New Asymmetric Wacker-Type Cyclization and Tandem Cyclization Promoted by Pd(II)-Spiro Bis(Isoxazoline) Catalyst. **2001** DOI: 10.1021/ja005920w.
(77) Sasai, H.; Wakita, K.; A. Arai, M.; Kato, T.; Shinohara, T. Spiro Bis(Isoxazole) as a New Chiral Ligand. *Heterocycles* **2004**, *62* (1), 831 DOI: 10.3987/COM-03-S(P)60.
(78) Koranne, P. S.; Tsujihara, T.; Arai, M. A.; Bajracharya, G. B.; Suzuki, T.; Onitsuka, K.; Sasai, H. Design and Synthesis of Chiral Hybrid Spiro (Isoxazole-Isoxazoline) Ligands. *Tetrahedron Asymmetry* **2007**, *18* (8), 919–923 DOI: 10.1016/j.tetasy.2007.04.010.
(79) McDaniel, S. W.; Keyari, C. M.; Rider, K. C.; Natale, N. R.; Diaz, P. Suzuki–Miyaura Cross-Coupling of Benzylic Bromides under Microwave Conditions. *Tetrahedron Lett.* **2011**, *52* (43), 5656–5658 DOI: 10.1016/j.tetlet.2011.08.096.
(80) Davies, M. W.; Wybrow, R. A. J.; Johnson, C. N.; Harrity, J. P. A. Communication A Regioselective Cycloaddition Route to Isoxazoleboronic Esters †. *Chem. Commun* **2001**, 1558–1559 DOI: 10.1039/b103319k.
(81) Moore, J. E.; Goodenough, K. M.; Spinks, D.; Harrity, J. P. Synthesis of 3-Haloisoxazole Boronic Esters: Novel Heterocyclic Synthetic Intermediates Containing Independently Variable Functionality. *Synlett* **2002**, No. 12, 2071–2073 DOI: 10.1055/s-2002-35595.
(82) Waldo, J. P.; Larock, R. C. The Synthesis of Highly Substituted Isoxazoles by Electrophilic Cyclization: An Efficient Synthesis of Valdecoxib. *J. Org. Chem.* **2007**, *72* (25), 9643–9647 DOI: 10.1021/jo701942e.
(83) Okitsu, T.; Sato, K.; Potewar, T. M.; Wada, A. Iodocyclization of Hydroxylamine Derivatives Based on the Control of Oxidative Aromatization Leading to 2,5-Dihydroisoxazoles and Isoxazoles. *J. Org. Chem.* **2011**, *76* (9), 3438–3449 DOI: 10.1021/jo200407b.
(84) Organ, M. G.; Çalimsiz, S.; Sayah, M.; Hoi, K. H.; Lough, A. J. Pd-PEPPSI-IPent: An Active, Sterically Demanding Cross-Coupling Catalystand Its Application in the Synthesis of Tetra-Ortho-Substituted Biaryls. *Angew. Chemie - Int. Ed.* **2009**, *48* (13), 2383–2387 DOI: 10.1002/anie.200805661.
(85) Rajanarendar, E.; Mohan, G.; Kalyan Rao, E.; Srinivas, M. Palladium-Catalyzed Suzuki-Miyaura Cross-Coupling Reaction of Organoboronic Acids with N-Protected 4-Iodophenyl Alanine Linked Isoxazoles. *Chinese Chem. Lett.* **2009**, *20* (1), 1–4 DOI:

10.1016/j.cclet.2008.10.022.
(86) Crossley, J. A.; Browne, D. L. An Alkynyliodide Cycloaddition Strategy for the Construction of Iodoisoxazoles. *J. Org. Chem.* **2010**, *75* (15), 5414–5416 DOI: 10.1021/jo1011174.
(87) Chu, J. H.; Chen, C. C.; Wu, M. J. Palladium-Catalyzed Arylation and Alkylation of 3,5-Diphenylisoxazole with Boronic Acids via C-H Activation. *Organometallics* **2008**, *27* (20), 5173–5176 DOI: 10.1021/om800606c.
(88) Gao, H.; Sun, M.; Zhang, H.; Bian, M.; Wu, M.; Zhu, G.; Zhou, Z.; Yi, W. Stereoselective β-F Elimination Enabled Redox-Neutral [4 + 1] Annulation via Rh(III)-Catalyzed C-H Activation: Access to Z-Monofluoroalkenyl Dihydrobenzo[d]Isoxazole Framework. *Org. Lett.* **2019**, *21* (13), 5229–5233 DOI: 10.1021/acs.orglett.9b01831.
(89) Padwa, A.; Dean, D. C.; Osterhout, M. H.; Precedo, L.; Semones, M. A. Synthesis of Functionalized Azomethine Ylides. **1994**, No. 24, 5347–5357.
(90) Kumar, P.; Kapur, M. Catalyst Control in Positional-Selective C-H Alkenylation of Isoxazoles and a Ruthenium-Mediated Assembly of Trisubstituted Pyrroles. *Org. Lett.* **2019**, *21* (7), 2134–2138 DOI: 10.1021/acs.orglett.9b00446.
(91) Asao, N.; Sato, K.; Yamamoto, Y. AuBr3-Catalyzed Cyclization of o-(Alkynyl)Nitrobenzenes. Efficient Synthesis of Isatogens and Anthranils. *Tetrahedron Lett.* **2003**, *44* (30), 5675–5677 DOI: 10.1016/S0040-4039(03)01357-1.
(92) Ogunlana, A. A.; Bao, X. Mechanistic Insights into the Gold(i)-Catalyzed Annulation of Propiolates with Isoxazoles: A DFT Study. *Chem. Commun.* **2019**, *55* (74), 11127–11130 DOI: 10.1039/c9cc05162g.
(93) Sahani, R. L.; Liu, R. S. Development of Gold-Catalyzed [4+1] and [2+2+1]/[4+2] Annulations between Propiolate Derivatives and Isoxazoles. *Angew. Chemie - Int. Ed.* **2017**, *56* (4), 1026–1030 DOI: 10.1002/anie.201610665.
(94) Jones, R. C. F.; Bhalay, G.; Carter, P. A. An Isoxazole Route to Unsaturated α-Alkoxycarbonyl-β-Diketones. *J. Chem. Soc. Perkin Trans. 1* **1993**, No. 15, 1715–1716 DOI: 10.1039/p19930001715.
(95) Hahnvajanawong, V.; Thaima, T.; Tearavarich, R.; Theramongkol, P. Reductive Ring Opening of 3,5-Bis(2-Arylethenyl)Isoxazoles with Molybdenum Hexacarbonyl: A Novel Route to Symmetrical and Unsymmetrical Curcumin Derivatives. *Orient. J. Chem.* **2016**, *32* (1), 127–135 DOI: 10.13005/ojc/320113.
(96) Nitta, M.; Higuchi, T. Mo(CO)6-Induced N-O Bond Cleavage of Isoxazoles. A Convenient Route to Pyridin-4(1H)-Ones. *Heterocycles* **1994**, *38* (4), 853–857 DOI: 10.3987/COM-93-6654.
(97) Burkhart, D. J.; McKenzie, A. R.; Nelson, J. K.; Myers, K. I.; Zhao, X.; Magnusson, K. R.; Natale, N. R. Catalytic Asymmetric Synthesis of Glutamate Analogues. *Org. Lett.* **2004**, *6* (8), 1285–1288 DOI: 10.1021/ol049619m.
(98) Burkhart, D. J.; Zhou, P.; Blumenfeld, A.; Twamley, B.; Natale, N. R. An Improved Procedure for the Lateral Lithiation of Ethyl 4-Acetyl-5-Methyl-3-Isoxazolyl Carboxylate. *Tetrahedron* **2001**, *57* (38), 8039–8046 DOI: 10.1016/S0040-4020(01)00781-5.
(99) Calle, M.; Cuadrado, P.; González-Nogal, A. M.; Valero, R. Synthesis and Reactions of Silylated and Stannylated 1,2-Azoles. *Synthesis (Stuttg).* **2001**, *2001* (13), 1949–1958 DOI: 10.1055/s-2001-17699.
(100) Ku, Y.-Y.; Grieme, T.; Sharma, P.; Pu, Y.-M.; Raje, P.; Morton, H.; King, S. Kokai Tokkyo Koho JP 79 14,968. (j) Chem. Abstr. 1980, 92, 41920. (K). *F. J.; Schleyerbach,*

R. Ger. Offen. Patents **1998**, *162* (3), 4185–4187 DOI: 10.1021/ol0168162.
(101) Denmark, S. E.; Kallemeyn, J. M. Synthesis of 3,4,5-Trisubstituted Isoxazoles via Sequential [3 + 2] Cycloaddition/Silicon-Based Cross-Coupling Reactions. *J. Org. Chem.* **2005**, *70* (7), 2839–2842 DOI: 10.1021/jo047755z.
(102) Schade, M. A.; Manolikakes, G.; Knochel, P. Preparation of Primary Amides from Functionalized Organozinc Halides. *Org. Lett.* **2010**, *12* (16), 3648–3650 DOI: 10.1021/ol101469f.
(103) Stenzel, J. R.; Natale, N. R. Regiospecific Control of Additions of 4-Substituted 3,5-Dimethylisoxazoles to α,β Unsaturated Carbonyls. *Synthesis (Stuttg).* **1997**, No. 9, 1041–1044 DOI: 10.1055/s-1997-1315.
(104) Dileep Kumar, J. S.; Ho, M. K. M.; Leung, J. M.; Toyokuni, T. Convenient Approach to 3,4-Diarylisoxazoles Based on the Suzuki Cross-Coupling Reaction. *Adv. Synth. Catal.* **2002**, *344* (10), 1146–1151 DOI: 10.1002/1615-4169(200212)344:10<1146::AID-ADSC1146>3.0.CO;2-1.
(105) Zhang, J.; Han, L.; Bi, S.; Liu, T. Distinct Roles of Ag(I) and Cu(II) as Cocatalysts in Achieving Positional-Selective C-H Alkenylation of Isoxazoles: A Theoretical Investigation. *J. Org. Chem.* **2020**, *85* (13), 8387–8396 DOI: 10.1021/acs.joc.0c00721.
(106) Cheung, W. S.; Patch, R. J.; Player, M. R. A Tandem Heck-Carbocyclization/Suzuki-Coupling Approach to the Stereoselective Syntheses of Asymmetric 3,3-(Diarylmethylene)Indolinones. *J. Org. Chem.* **2005**, *70* (9), 3741–3744 DOI: 10.1021/jo050016d.
(107) Vieira, A. A.; Bryk, F. R.; Conte, G.; Bortoluzzi, A. J.; Gallardo, H. 1,3-Dipolar Cycloaddition Reaction Applied to Synthesis of New Unsymmetric Liquid Crystal Compounds-Based Isoxazole. *Tetrahedron Lett.* **2009**, *50* (8), 905–908 DOI: 10.1016/j.tetlet.2008.12.021.
(108) Yang, W.; Yao, Y.; Yang, X.; Deng, Y.; Lin, Q.; Yang, D. Synthesis of C4-Alkynylisoxazoles: Via a Pd-Catalyzed Sonogashira Cross-Coupling Reaction. *RSC Adv.* **2019**, *9* (16), 8894–8904 DOI: 10.1039/c9ra00577c.
(109) Labadie, S. S. 3-Aryl-2.4-Pentanediones from 3,5-Dimethyl-4-Iodoisoxazoles: An Application of a Palladium-Catalyzed Cross-Coupling Reaction. *Synth. Commun.* **1994**, *24* (5), 709–719 DOI: 10.1080/00397919408012650.
(110) Kromann, H.; Sløk, F. A.; Johansen, T. N.; Krogsgaard-Larsen, P. A Convenient Synthesis of 4-Substituted 3-Ethoxy-5-Methylisoxazoles by Palladium-Catalyzed Coupling Reactions. *Tetrahedron* **2001**, *57* (11), 2195–2201 DOI: 10.1016/S0040-4020(01)00052-7.
(111) Lee, J. S.; Cho, Y. S.; Chang, M. H.; Koh, H. Y.; Chung, B. Y.; Pae, A. N. Synthesis and in Vitro Activity of Novel Isoxazolyl Tetrahydropyridinyl Oxazolidinone Antibacterial Agents. *Bioorganic Med. Chem. Lett.* **2003**, *13* (22), 4117–4120 DOI: 10.1016/j.bmcl.2003.08.021.
(112) Hanamoto, T.; Hakoshima, Y.; Egashira, M. Tributyl(3,3,3-Trifluoro-1-Propynyl)Stannane as an Efficient Reagent for the Preparation of Various Trifluoromethylated Heterocyclic Compounds. *Tetrahedron Lett.* **2004**, *45* (41), 7573–7576 DOI: 10.1016/j.tetlet.2004.08.118.
(113) Sakamoto, T.; Kondo, Y.; Uchiyama, D.; Yamanaka, H. Condensed Heteroaromatic Ring Systems. XIX. Synthesis and Reactions of 5-(Tributylstannyl)Isoxazoles. *Tetrahedron* **1991**, *47* (28), 5111–5118 DOI: 10.1016/S0040-4020(01)87123-4.

(114) Uchiyama, Daishi, Yabe, Kameyama, Hiroshi, Sakamoto Takao, Kondo, Yoshinori, and Yamanaka, H. Synthesis and Reactions of 4-Tributylstannyl-3-Methylisoxazole. *Heterocycles* **1996**, *43* (6), 1301 DOI: 10.3987/COM-96-7489.
(115) Del, M.; Benites, R.; Fronczek, F. R.; Hammer, R. P.; Maverick, A. W. A New Binucleating Ligand Based on Anthracene and Its Cofacial Dirhodium(I) and Diiridium(I) Complexes. **1997**.

List of Abbreviations

Ac acetyl
Ad adamantyl
acac acetylacetonate
AIBN azobisisobutyronitrile
aq aqueous
9-BBN 9-borabicyclo[3.3.1]nonane
Bn/Bz benzyl
BINAP 2,2□-bis(diphenylphosphino)-1,1□-binaphthalene
BINOL 1,1□-bi(2-naphthol)
Boc *tert*-butoxycarbamoyl
BOC-ON 2-(*tert*-butoxycarbonyloxyimino)-2-phenylacetonitrile
BOM benzyloxymethyl
(b)rsm (based on) recovered starting material
BQ benzoquinone
CAN cerium(IV) ammonium nitrate
CBS Corey-Bakshi-Shibata
Cbz carboxybenzyl
CBz benzyloxycarbonyl
*c*Hex cyclohexyl
CMD concerted metalation/deprotonation
cod 1,4-cyclooctadiene
coe cyclooctene
Cp cyclopentadienyl
Cp* pentamethylcyclopentadienyl
CSA camphorsulfonic acid
CuTC Cu(I) thiophene-2-carboxylate
Cy cyclohexyl
DABCO 1,4-diazabicyclo[2.2.2]octane
DAST (diethylamino)sulfur trifluoride
Dba *trans,trans*-dibenzylideneacetone
DBAD di-*tert*-butyl azodicarboxylate
DBU 1,8-diazabicyclo[5.4.0]undec-7-ene
DCB 2,4-dichlorobenzoyl
DCC dicyclohexyl carbodiimide
DCE 1,2-dichloroethane
DDQ 2,3-dichloro-5,6-dicyano-1,4-benzoquinone
DEAD diethyl azodicarboxylate
DET diethyl tartrate
DFT density functional theory
(DHDQ) 2PYR hydroquinidine-2,5-diphenyl-4,6-pyrimidinediyl diether
DIAD diisopropyl azodicarboxylate
DIBALH diisobutylaluminum hydride
DIPT diisopropyl tartrate
DMA N,N'-dimethylacetamide
DMB 3,4-dimethoxybenzyl
DMAD dimethyl acetylenedicarboxylate
DMAP 4-(*N*,*N*-dimethylamino)pyridine
DMDO dimethyldioxirane
DME 1,2-dimethoxyethane
DMEDA N,N'-dimethylethylenediamine
DMF N,N'-dimethylformamide
DMSO dimethyl sulfoxide
DMP 3,4-dimethoxyphenyl
DMS dimethyl sulfide
dr diastereomeric ratio
DPPA diphenyl phosphorazidate
dppb 1,4-bis(diphenylphosphanyl)butane
dppf 1,1'-bis(diphenylphosphanyl)ferrocene
dppm bis(diphenylphosphanyl)methane
DMPU 1,3-dimethyl-3,4,5,6 tetrahydro-2(1*H*)-pyrimidone
dtbpy di-tert-butyl-2,2'-bipyridine
ee enantiomeric excess
EE 1-ethoxyethyl
HOBt 1-hydroxy benzotriazole
(HA)SPO (heteroatom-substituted) secondary phosphine oxide
HMDS hexamethyldisilazane
HMPA hexamethylphosphoramide
HMPT hexamethylphosphoric triamide
HWE Horner-Wadsworth-Emmons
*i*Bu isobutyl
*i*pc isopinocampheyl
i-Pr isopropyl
KHMDS potassium hexamethyldisilazide
KIE kinetic isotope effect

KTB potassium *tert*-butoxide
L ligand
LDA Lithium diisopropylamide
LiHMDS lithium hexamethyldisilazide
LiTMP lithium 2,2,5,5-tetramethylpiperidide
LiTMP lithium 2,2,6,6-tetramethylpiperidine
LM Lateral metalation
LTB lithium *tert*-butoxide
MCPBA *m*-chloroperoxybenzoic acid
Mes mesityl
MeS 2,4,6-trimethylphenyl
MOM methoxymethyl ether
Ms methanesulfonyl
MS molecular sieves
MW microwave irradiation
NaHMDS sodium hexamethyldisilylamide
NHC N-heterocyclic carbine
NIS *N*-iodosuccinimide
NMO *N*-methylmorpholine-*N*-oxide
NMP 1-methyl-2-pyrrolidinone
Np 2-naphthyl
OTf trifluoromethanesulfonate
PAH polycyclic aromatic hydrocarbon
PBQ p-benzoquinone
PCC pyridinium chlorochromate
PDC pyridinium dichromate
PhBox 2,2□-isopropylidene-bis(4-phenyl-2-oxazoline)
PhPyBox 2,2□-(2,6-pyridinediyl)-bis(4-phenyl-2-oxazoline)
PIDA phenyliodonium diacetate
Piv 2,2-dimethylpropanoyl (pivaloyl)
PMB 4-methoxybenzyl
PNB 4-nitrobenzyl
$P(nBu)(ad)_2$ *n*-butyl-di-1-adamantyl phosphine
PPTS pyridinium *p*-toluenesulfonate
PTSA 4-toluenesulfonic acid
Py pyridine
Xp (4*S*)-benzyl-2-oxazolidinone
SEAr electrophilic aromatic substitution
SPRIX spirocyclic bis(isoxazoline) ligand
*t*Bu tert-butyl
TEMPO 2,2',6,6'-tetramethylpiperidine-1-oxyl
Tf trifluoromethanesulfonyl
TFA trifluoroacetic acid
TBAB (tetrabutylammoniumbromide)
TBAC (tetrabutylammoniumchloride)
TBAF tetrabutylammonium fluoride
TBAI tetrabutylammonium iodide
TBSOTf *tert*-butyldimethylsilyl triflate
TBDMS *tert*-butyldimethylsilyl
TBDPS *tert*-butyldiphenylsilyl
TBHP *tert*-butyl hydroperoxide
TBS *tert*-butyldimethylsilyl
TC thiophene-2-carboxylate
TCE 2,2,2-trichloroethyl
TEMPO 2,2,6,6-tetramethyl-1-piperidinyl-oxy free radical
TES triethylsilyl
Tf trifluoromethansulfonyl
TFA trifluoroacetic acid
TFAA trifluoroacetic anhydride
THF tetrahydrofuran
THP tetrahydropyranyl
TIPPSeBr 2,4,6-triisopropylphenylselenyl bromide
TIPS triisopropylsilyl
TMEDA N,N,N',N'-tetramethylethylenediamine
TMS trimethylsilyl
Tol-BINAP 2,2□-bis(di-*p*-tolyl-phosphino)-1,1□-binaphthalene
TON turnover number
Tr triphenylmethyl
Tris 2,4,6-triisopropylbenzenesulfonyl
TROC trichloroethoxycarbonyl
Ts 4-toluenesulfonyl
TsO *para*-toluenesulfonate

This paper was published in Bioorganic and Medicinal Chemistry
Gates, Christina; Backos, Donald S.; Reigan, Philip; Kang, Hye Jin; Koerner, Chris; Mirzaei, Joseph; Natale, Nicholas. R., Isoxazolo[3,4-d]Pyridazinones Positively Modulate the Metabotropic Glutamate Subtypes 2 and 4. *Bioorganic Med. Chem.* **2018**, *26* (17), 4797–4803 DOI: 10.1016/j.bmc.2018.08.012.

Chapter 2 Isoxazolo[3,4-d]pyridazinones positively modulate themetabotropicglutamate subtypes 2 and 4

Introduction

The G-protein coupled receptors (GPCRs) are important targets for drug design,[1,2] with about 30% of currently marketed drugs targeting these receptors.[3,4] Within the GPCR family of receptors are the meta- botropic glutamate receptors (mGluRs), which are activated by the neurotransmitter glutamate and are of interest as targets for the treatment of variety of CNS and non-CNS disorders.[5] The mGluR family is divided into three subgroups, which are further divided into eight subtypes, each having the conserved venus flytrap domain (VFD) and seven transmembrane domain (7TM).

The VFD, which is a large bilobed extracellular domain, represents the orthosteric site for this family of GPCRs,[6–8] while the 7TM, common to all GPCRs, is the site for allosteric binding. The orthosteric site is modulated by chloride ions, and is an important area to explore as a potential target for small molecules.[9,10] Due to the high degree of conservation at the VFD throughout the mGluR subgroups, selective targeting at this site is difficult.[1] Incontrast, the allosteric site is less conserved allowing for the potential for greater selectivity within the subgroups. Finding small molecules that not only bind to one of the subgroups is important, but even more so is finding molecules that bind selectively within a subgroup. Many small molecules have been found to bind to mGluR's allosteric site, eliciting a positive or negative effect, also known as positive allosteric modulators (PAM) or negative allosteric modulators (NAM).[1,5,10] Within these groups, there are compounds that may activate the receptor without the endogenous ligand being present, ago-PAM, potentiallyleading to toxicity.[11] Taking this all into consideration, small molecules that target the allosteric site of various mGluRs have been found to selectively help to treat different disease state. PAM activation at $mGluR_4$ is one such target in the treatment of Parkinson's disease.[5,10] When activated, $mGluR_4$ helps to

ease the symptoms of Parkinson's disease in animal models and may even slow progress of the disease.[12,13] (representative lead compounds are shown in **Figure. 2-1**) Positive allosteric modulators of $mGluR_4$ have also been found to have activity against brain tumors.[14,15] Activation of $mGluR_2$ has been implicated in the treatment of anxiety and schizophrenia. This type of selective activation allows for fewer off- target side effects.[1] We were intrigued by the similarity of the aniline moiety of isoxazolo[3,4-d]pyridazinones ([3,4-d] compounds) to VU0155041, and postulated that the isoxazole group could represent a useful bioisostere for the carboxylate group. Data provided by the Psychoactive Drug Screening Program (PDSP) reported herein indicate that the [3,4-d] compounds possess selective functional activity at mGluR 4 and 2. To help further understand the selectivity and activity, computer generated homology models of the receptors were used to develop a structure- based approach as a working hypothesis.

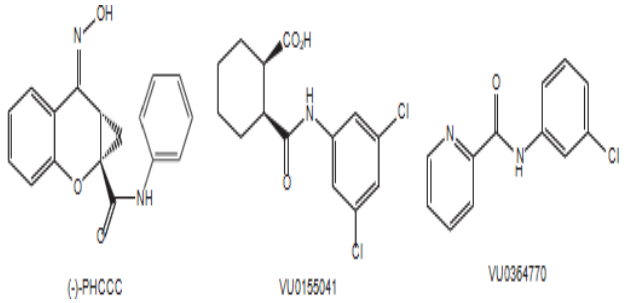

Figure 2-1: Representative allosteric modulators of mGluR, with activity against in vitro modelof Parkinson's disease[1,12,13]

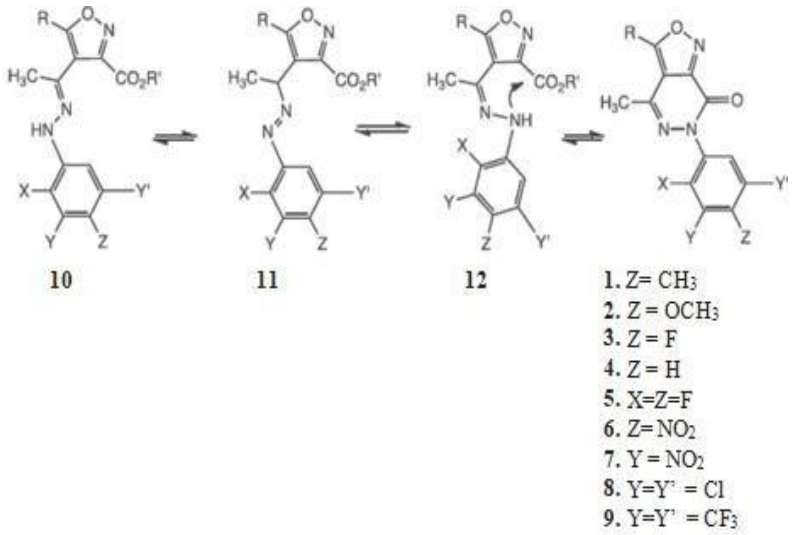

Figure 2-2: Structures of isoxazolo [3,4-d] pyridazinones used in the present study, the PDSP reference numbers is given in parentheses, substitutents not otherwise specified areH

Chemistry

The [3,4-d]s scaffold, as exemplified by the first practical synthesis reported by Renzi and Dal Piaz,[16] has been found to both possess interesting biological activity,[17] and serve as a useful and versatile pre- cursor in medicinal chemistry synthesis.[18] Most recently the isoxazolo [3,4-d] pyridazinone scaffold has served as an entry into the preparation of a newclass of orally active antinociceptive agents.[19] The synthesis of the isoxazolo[3,4-d] pyridazinones (1–9, **Figure 2-2**) used for this study were carried out by the condensation of 4-acetyl-3-carbox-yethyl-5-methyl isoxazole with the corresponding hydrazine to produce *E*-hydrazones 10, and ring closure was performed by continued heating according to the procedure of Dal Piaz.[16–19] This likely proceeds by tautomerization to the diazene 11,which allows for *Z*-12 which can further ring close to 1–9. Full characterization has been previously described.[2]

Assays PDSP primary functional one-dose protocol

For Gi-coupled targets the inhibition of forskolin-stimulated cAMP accumulation was assayed for glutamate $mGluR_2$, $mGluR_4$, and $mGluR_8$. This assay measured the cAMP formation for receptors which are negatively coupled to adenylyl cyclase.[21] Activity of these receptors is determined by measurements of their ability to decrease forskolin- inducedelevated cAMP formation. All assays were performed in the presence or absences of agonists relevant for the different mGluRs and in concentrations equivalent to their EC_{50} values. The following were the EC_{50} concentrations: $mGluR_2$ at1µM glutamate 0.5 µM at $mGluR_4$, and 1 µM 4-aminophosphonobutyrate (AP4) for $mGluR_8$. For the primary assays, a single concentration of the ligand to be tested is used, usually 10 µM unless otherwise agreed upon, and secondary assays are dose-response assays. Testing for antagonism is performed in the presence of EC_{50} concentration of agonist. In the primary assays, compounds are tested in duplicate via two separate experiments performed on different cell passages. Each contains points for the determination of basal activity, maximal agonist stimulation, agonist EC_{50} concentrations and the IC_{50} concentrations of a known antagonistas a comparative positive control and activity calculations. Reported results are calculated for agonists as the percent of maximal activity and antagonists as the percent inhibition of receptor activity. Compounds found to be active as agonists or antagonists may be tested for potency via the secondary assays. Six-point dose-response curves are performed and duplicated twice on two separate passages of cells, sometimes on a third if the first is outsideof the concentrations of the active range. Each compound has four replications which are averaged, and then either the EC_{50} or the IC_{50} values are calculated by non-linear regression using the 4-parameter logistics equations, and reported along with their receptor and comparison values of EC_{50} or IC_{50} of known agonist or antagonists for comparison. The experimental details of the protocols can be found on the PDSP web site.[2]

Secondary concentration response assays for Gi coupled GPCRS – split luciferase cAMP assays

PDSP protocol uses Promega's GloSensor cAMP construct and Luciferin. For the G_i-coupled mGluRs, in this case $mGluR_2$ and $mGluR_4$, the assay buffer was modified Locke's buffer containing 125 mM NaCl, 31 mM NaGluconate, 5.6 mM KCl, 3.6 mM $NaHCO_3$, 1 mM $MgCl_2$, 1.3 mM $CaCl_2$, 5.6 mM glucose, and 20 mM HEPES, pH 7.4. Thereceptors were expressed in CHO cells that are stably express the Glosensor cAMP biosensor. Present switch to past Agonist activity was accessed by looking at the ability to decrease forskolin-induced elevaion of cAMP. The cells were incubated for 1 h at room temperature in 100 µl of the modified lock buffer and 6% w/v D-Luciferin, which is a substrate for the Glosensor enzyme. After 1 h, the basal relative luminescence units (RLU) were measured 5 times, every two minutes. Next, 1 µM forskolin and 6% w/v D-Luciferin was added with or without mGluR agonists, and the incubation was continued for 16 min. Glutamate was used for the agonist with a concentration of 4 µM for $mGluR_4$ and 3 µM for $mGluR_2$. After incubation the RLUs were measured. For secondary assays which were the concentration-response assays, eight-point concentration-response curves were performed induplicate twice on two separate passages of cells (a third curve may be needed if the first range of concentrations used is outside of the activity range. For antagonists, these curves were evaluated in the presence of EC_{50} concentrations of agonists. The results for each of the compounds from four replicates were averaged and then either the EC_{50} or IC_{50} values and also included the EC_{50} or IC_{50} values of known agonists or antagonists for comparison purposes for each receptor. For allosteric evaluation, the allosteric operational model was used to analyze functional results. Functional assays were carried out in the same way as forSchild plot analysis, where the orthosteric agent concentration-response curve were measured in the absence and presence of increasing concentrations of a potential allosteric modulators. Refer to PDSP protocol page 176-178 for more information on the equation used along with more information about the parameters

considered.[21]

Homology model: general experimental

The mGluRs consist of a venus flytrap domain (VFD) which contains the orthosteric glutamate binding site, and the seven transmembrane (7TM) domain which contains the allosteric site. Homology models were constructed of the orthosteric binding site from thecrystal structure coordinates of rat $mGluR_1$, PDB accession number 1EWK, using Discovery Studio 2017. For the allosteric binding site the crystal coordinates of $mGluR_1$, PDB accession number 4OR2,[25] were used, the calculations were performed usingAutodock Vina for $mGluR_2$ and Discovery Studio for $mGluR_4$.

For Discovery Studio the protein structures were typed with the CHARMm forcefield[26] and energy was minimized with the smart minimizer protocol within Discovery Studio[27] using the Generalized- Born with simple switching implicit solvent model to a root mean squaregradient (RMS) convergence < 0.001 kcal/mol prior to use in the docking studies. Docking was performed using the flexible docking protocol,[28] which allows for flexibility in both theligand and the binding site residues. The amino acid residues within the allosteric site were allowed to attain an optimum conformation using flexible docking, for example in $mGluR_4$eleven residues were selected based on Feng's model of allosteric activation,[32] and with numbering according to Isberg[33]: Leu659$^{3.36}$, Met663$^{3.40}$, Leu 753$^{5.40}$, Leu756$^{5.43}$, Leu757$^{5.44}$, Thr794$^{6.46}$, Trp798$^{6.50}$, Phe801$^{6.53}$, Phe805$^{6.57}$, Leu822$^{7.32}$, and Val826$^{7.36}$. The final ranking of the docked poses was performed via consensus scoring, combining the predicted binding energy with the Jain,[29] PLP2,[30] and Ludi3[31] scoring functions. The best poses for each compound in the training set uses a weighted consensus for each of the several scoring functions compared. More or less as expected, while docking poses could begenerated for both potential binding sites, as typified for control VU155041, the allosteric binding energies were

over 30 kcal/mol better than those obtained for the orthosteric site (*Vide infra*).

Results and discussion

Glutamate is the most abundant neurotransmitter in the human central nervous system. During the neuronal action potential, binding occurs at ionotropic and metabotropic receptors, as well as transpor- ters, and thus the design of ligands that selectively bind is a complicated and challenging endeavor. We had previously observed in a study of the system Xc-glutamate-cystine antiporter, that ring closure of active 3- carboxy-isoxazole-4- hydrazones (10) to the corresponding [3,4-d] analogs were accompanied by marked loss of activity at the transporter.[20] Radioligand binding was studied for $GABA_A$ using the psychoactive ligand muscimol,[22] and at the ionotropic, NMDA(iGluR) receptor using MK-801,[23] and at $mGluR_5$ using the allosteric ligand MPEP,[24] which is displaced by the potent allosteric ligand fenobam. The results are summarized in **Table 2-1**. No hits were detected for $GABA_A$ or NMDA (**Table 2-1**). Two moderate hits for compounds (1) and (8) were observed at $mGluR_5$, shown in **Table 2-1** and **Fig. 2-3**. It is important to note that in neither case was the single digit micromolar affinity at $mGluR_5$ suffi- cient to translate into a functional effect.

The [3,4-d] compounds were first examined in a single dose func- tional assay. Functional data indicated that there were six compounds determined as hits, using the PDSP criteria of 25% modulation, Compounds (3), (5) and (9) at $mGlurR_2$, and Compounds (8), (2) and (1) at $mGluR_4$. All of the single dose functional hits at $mGluR_2$ were compounds which contained fluorine on the N(6) aryl (**Table 2-1**, highlighted).

Structure	$GABA_A$, % displacement (muscimol)	NMDA, nM (MK-801)	$mGluR_5$, nM (MPEP)	$mGluR_2$		$mGluR_4$	
				AGO- %MAX:	ANT- %INH:	AGO- %MAX:	ANT- %INH:
1	-13.4	>10,000	1,883	-12	-37	37	-9
2	-21.5	>10,000	>10,000	20	-55	26	9
3	-6.0	>10,000	>10,000	26	23	-21	3
4	-6.0	>10,000	>10,000	-4	-33	-1	-5
5	-10.0	>10,000	>10,000	35	-48	11	-7
6	-4.7	>10,000	>10,000	19	5	21	-3
7	-15.5	>10,000	>10,000	17	48	24	-10
8	-7.8	>10,000	3,077	-3	11	77	-6
9	-7.2	>10,000	ND	36.56	0	9	11

Table 2 - 1 Functional data for mGluRs, courtesy of the Psychoactive Drug Screening Program (Screen capture from the PDSP web site). The most significant hit was observed for PDSP 21318 (8) at $mGluR_4$. Data for mGluR sub- types 1a, 5 and 8 (for which there were no hits) are found in the Supporting Data. Legend: Green represents 25–49 percent activation and blue represents 50–100 percent activation.

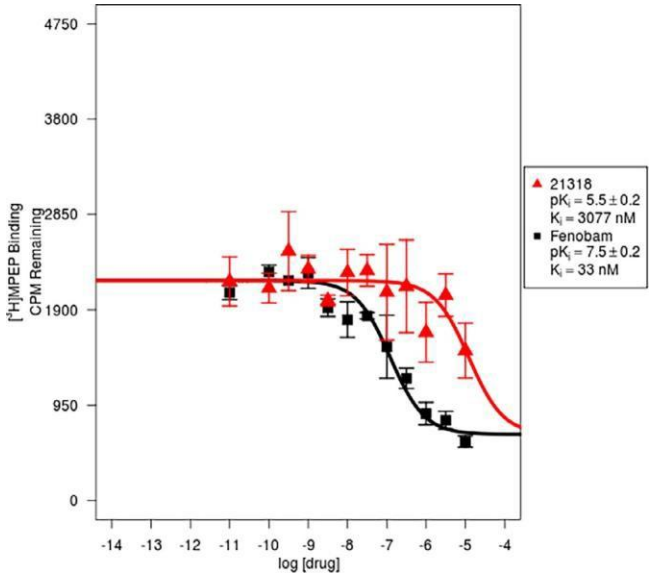

Figure. 2-3. Compound 8 (PDSP 21318) exhibits modest allosteric binding at the $mGluR_5$. It is worthy of note that this modest binding does *not translate into a functional effect.*

The most robust positive modulation of 77% at $mGluR_4$ was ob- served for compound (8), which was reproducible (n = 12) with a narrow standard error (5%) (**Table 2-1**). In light of a similar 3,5-di- chloroaniline functional group in VU015541, we considered that com- pound (8) represents a type of conformational constraint in its inter- action with the receptor.

We then examined a homology model of the $mGluR_4$ in order to develop a workinghypothesis for the observed experimental functional activity. A closer look at experimentalbinding was then undertaken to determine which of the docking models was more realistic.

Homology model: orthosteric site

The orthosteric binding of ligands to the VFD of mGluR has been studied extensively by Kunishima,[6] Tsuchiya,[7] Muto[8] and co-workers. Logical docking poses could be generated for the [3,4-d] series, illu- strated for ligand 8, in **Figure 2-4**. At the orthosteric site Ligand 8 and VU015541 adopt essentially identical poses where the 3,5-dichloro

phenyl moiety of either interacts with Tyr230 (Compare **Figure 2-4B** to the that of VU155041 in the Supporting Data, Table 2-SD-2). However, the binding energy at the allosteric site (*vide infra)* was calculated to be over 30 kcal/mol superior to that of the glutamate binding site. Thus, the computational predicted binding energies provide an explanation forthe lack of observed orthosteric binding. Supplementary data associated with this article can be found, in the online version, at https://doi.org/10.1016/j.bmc.2018.08.012

Orthosteric site secondary binding assay: little or no evidence of binding

Using the PDSP protocol, comparison to both antagonists and ago- nists were examined at the orthosteric site. It was observed that the binding isotherm effect of the [3,4-d] ligands 1–8 was flat, and thus it appeared that little or no indication of orthosteric interaction was obvious at either $mGluR_2$ or $mGluR_4$ (**Figure 2-5**). A similar experimental result was obtained for antagonist activity at the orthosteric site **(Figure 2-SD-11**).

Allosteric binding secondary assay

In the secondary assay, the concentration response curves in some cases were observed

to emerge within experimental error (**Figure 2- 6**), although the magnitude of the response was consistent with the single dose functional data of approximately 10 μM. This effect is modest in comparison to the ligands used as positive controls (**Figure 2- 6**, BINA at $mGluR_2$, and TCN22A at $mGluR_4$, respectively

Homology model: allosteric site

All of the ligands for which single dose functional hits were ob- served at $mGluR_2$, contained fluorine substituents on the N-6 aryl. The computation indicated a possible explanation for selectivity, in which the fluorinated aniline moiety was oriented facing in the extracellular direction within the allosteric vetibule. Among the residues unique to the $mGluR_2$ subtype, Met728 and Met794 have π-alkyl and π-sulfur interactions, respectively, with the fluorine containing electron deficient N-6 aryl (**Figure 2-7**). Thepose with the best Binding Energy calculation at $mGluR_4$ is shown in the **Figure 2 - 8** for (8), a robust computational interaction of−70 kcal/mol. An overview of the allosteric binding of metabotropic glutamate receptors has been provided by Gloriam and co- workers,[34] who identified unique residues as hot spots for selectivity among the different sub-types. An extensive modeling and site directed mutagenesis study of $mGluR_4$ has been reported by Rovira and co-workers.[35] Our modeling results are in reasonable general agreement with these studies in relation to the location of the ligands in the allosteric site (**Figure 2-8A**). Compound 8 occupies the region previously suggested by Rovira for allosteric agonist binding. For the pose with the best binding energy, the carbonyl of the pyridazinone is anchored by a hydrogen bond to Ser760, the dichlorobenzene ring forms a T-shaped pi interaction with Phe 801, and the isoxazole moiety interacts *via* both a

lipophilic interaction with the C-3 methyl of the isoxazole moiety with Leucines 753 and 659, as well as a π interaction with the backbone amide of Leu756 (see LigPlot in **Figure 2-8B**). The latter is unique to $mGluR_4$ and is consistent with the observation of selectivity for this sub-type. The LigPlot summarizes the salient intermolecular drug-receptor interactions (**Figure 2- 8B**). In general the energy difference of the best calculated pose does not differ by a large amount (3–4 kcal/mol) from poses for the same ligand which adopts the opposite orientation, or that has "tumbled" downward in the allosteric cavity (**Figure 2-8C**). A similar result ensemble was observed for VU015541, where the best scores were found for an intermediate position towards the middle of the allosteric site (**Figure 2-8D and Supporting Data**). An overlay of VU0155041 (green), TCN22A[38] (cyan) and two poses for 8 (**Figure 2-8D**), illustrates this point. The highest scoring pose for 8 (grey) occupies the deep allosteric pocket, however a close scoring pose 8 (yellow) co-locates with the two other potent ligands in the middle vestibule. The highest calculated binding energies for the [3,4-d] set were close in value to VU015541, and derivatives substituted with lipophilic groups at the 3-position of the [3,4-d] series gave binding energies calculated to be significantly better and also anchor the ligand in the middle of the allosteric site (**Table 2-SD-2**), whether this hypothesis will give rise to ligands with improved potency which retain selectivity will be tested in future studies.

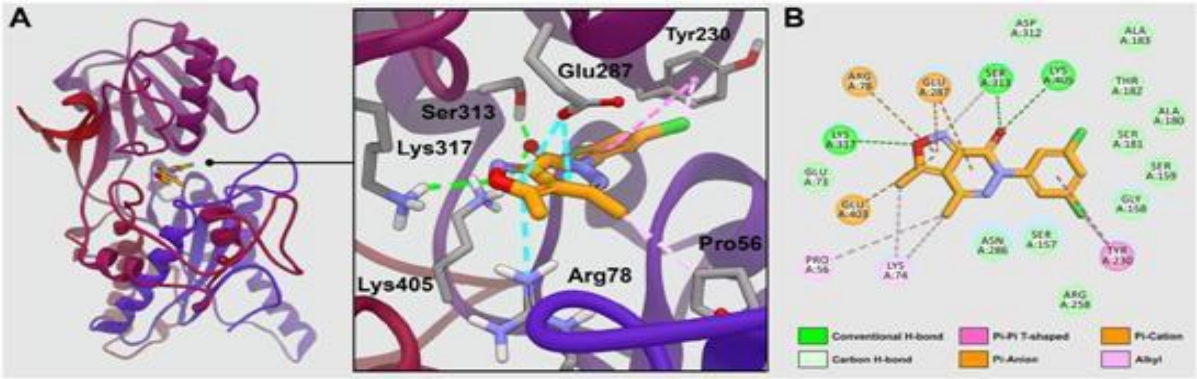

Figure 2-4: Orthosteric docking of [3.4-d] ligand 8 at the complete in the center panel, and a summary of binding interactions.

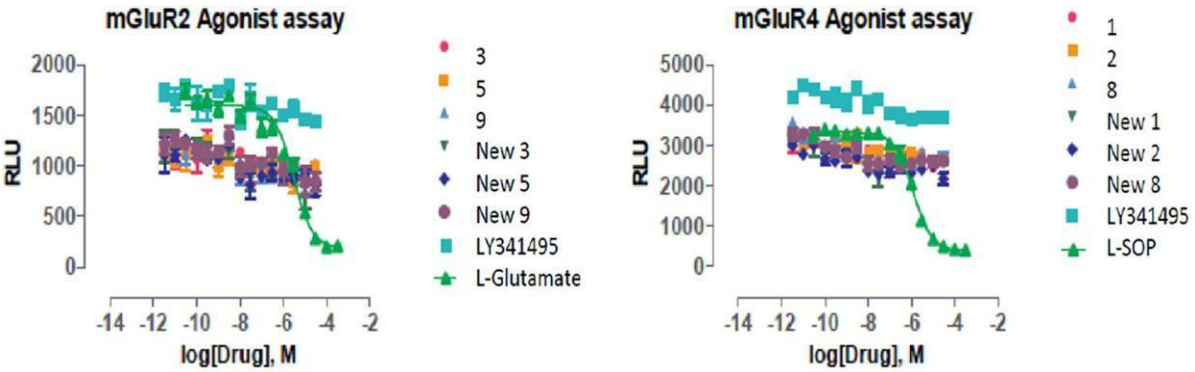

Figure 2-5. Binding isotherms at the orthosteric mGluR sites. Little or no orthosteric binding is evidenced in the agonist assay

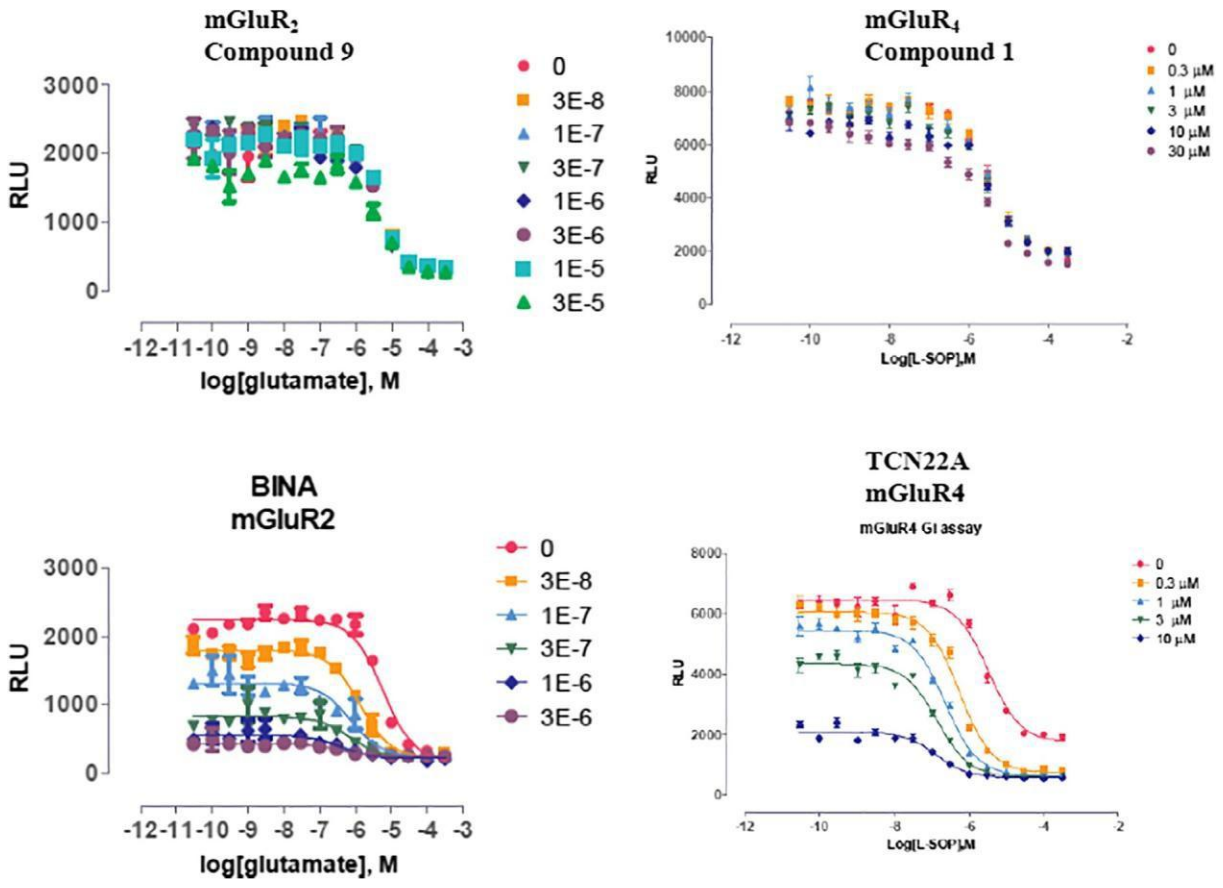

Figure 2-6. Allosteric binding isotherms for [3,4-d]s at $mGluR_2$ and $mGluR_4$, with controls.

Conclusion

Robust and selective positive functional modulation of metabotropic glutamate receptors has been observed for isoxazolo [3,4-d]pyridazinones, suggesting this scaffold as a promising avenue for further development. No significant functional effect was found for mGluR subtypes 1a, 5 or 8; and no activity at $GABA_A$, NMDA, or the System Xc- antiporter was observed. Especially intriguing forour future studies is the tactic of lateral metalation and electrophilic quenching,[36] which can be used to incorporate functional groups to rationally target plausible interactions near the allosteric pocket,[37] as suggested by our current computational working hypothesis. We are actively pursuing this strategy, and will report on our progress in due course.

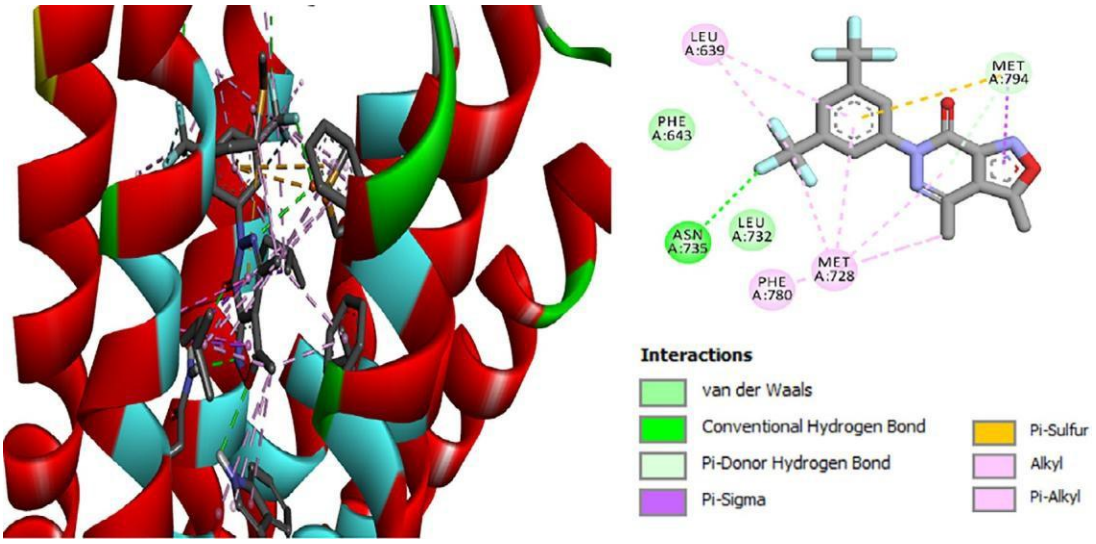

Figure 2 - 7. Possible explanation for selectivity at $mGluR_2$, the electron deficient, fluorine containing ring interacts with the residues unique to this sub-type in the allosteric site, notably Met728 and Met 794.

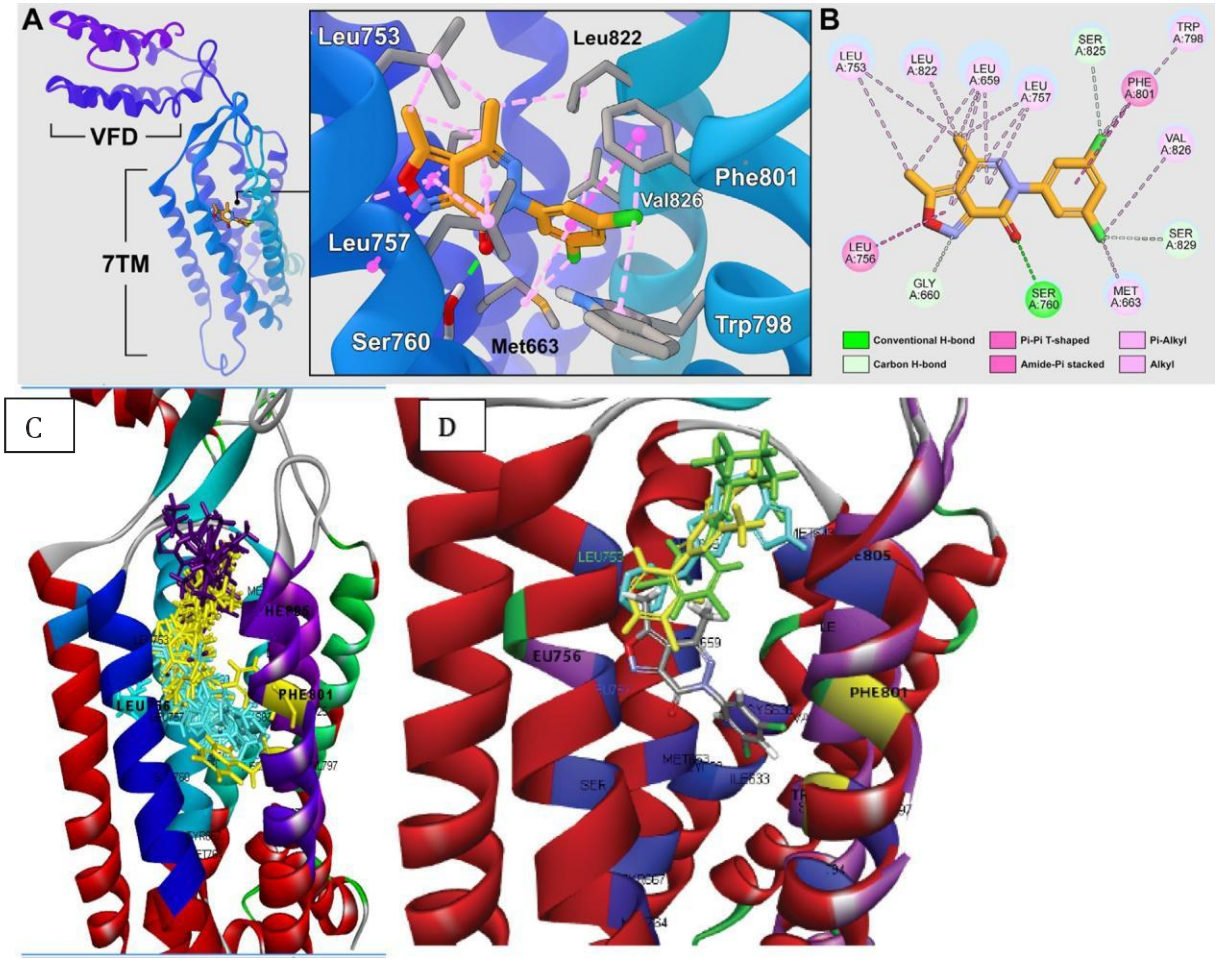

Figure 2-8: Compound 8 (PDSP 21318) binding at the allosteric site of the $mGluR_4$ receptor. A. Homology model of the human $mGluR_4$ receptor, consisting of the Venus Flytrap domain (VFD) and seven transmembrane (7TM) domain containing the allosteric binding site. Inset depicts binding site specific residues and their predicted interactions with 8. B. Schematic representation of the close contacts shown in A. C. Homology model showing the path that the [3,4-d] poses occupy high (magenta) and middle (yellow) vestibule areas, as well as a deep allosteric pocket (cyan). D. Overlay of VU0155041 (green), TCN22A[38] (cyan) and two poses for 8, the highest scoring pose for 8 (grey) and a close scoring pose 8 (yellow), which co-locates with the two other potent ligands in the middle vestibule

Figure 2-SD -1. Orthosteric homology model illustrating [3,4-d] **8** (PDSP 21318) binding at $mGluR_4$, Glutamate binding site in the Venus Flytrap Domain (VFD, orthosteric site), using pdb 1EWK as a template. Note that this utilizedthe intact VFD. *Both compounds dock with the 3,5-dichlorophenylmoiety interacting with Tyr230 of the VFD.*

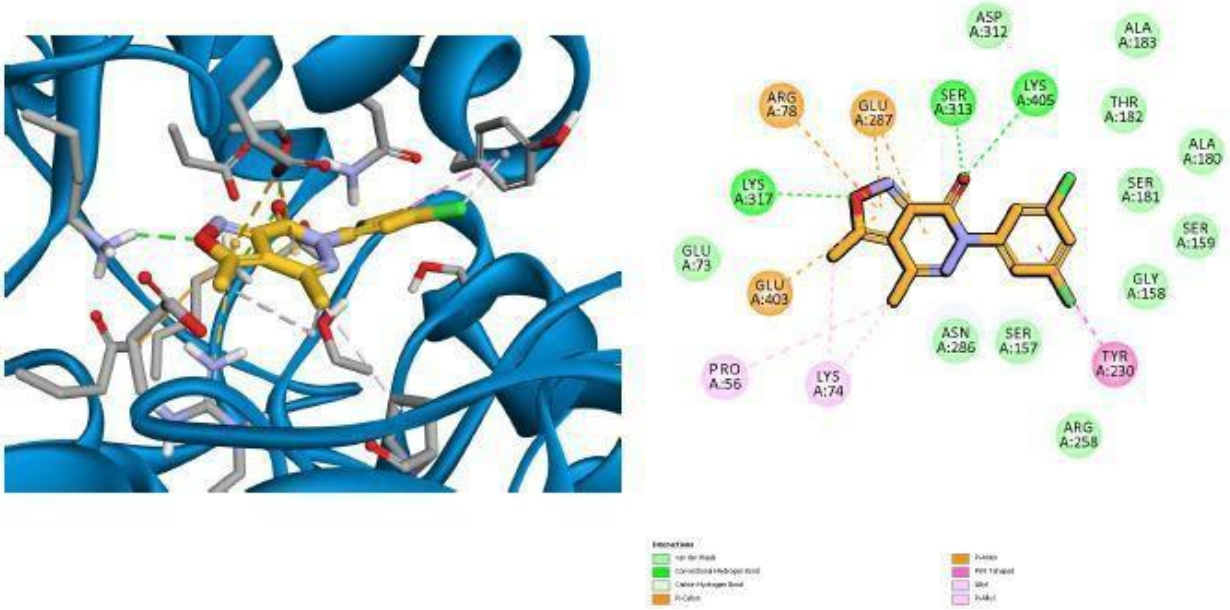

Figure 2-SD-2. VU015541 at the Glutamate binding site in the VFD, orthosteric glutamate site.

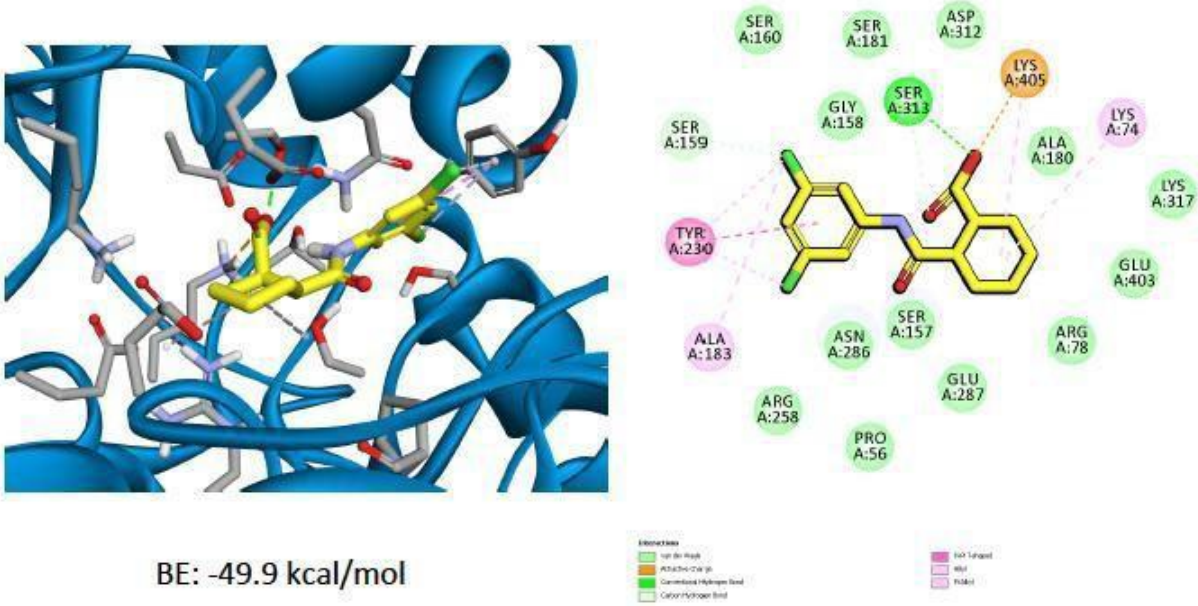

Table 2-SD-1. Discovery Studio Binding Energy Scores for **VU015541** at the allosteric mGluR4 site.

Ligand	Position in allosteric pocket	Binding (kcal/mol)
VU0155041	Deep pocket (bottom)	-52.5
VU0155041	Vestibule 2 (middle)	-83.8
VU0155041	Vestibule 1 (Top)	-73.7

Figure 2-SD-3. Allosteric binding pose with **VU015541**, second best calculated binding energy, at the top ofthe allosteric binding cavity, referred to as Vestibule 1

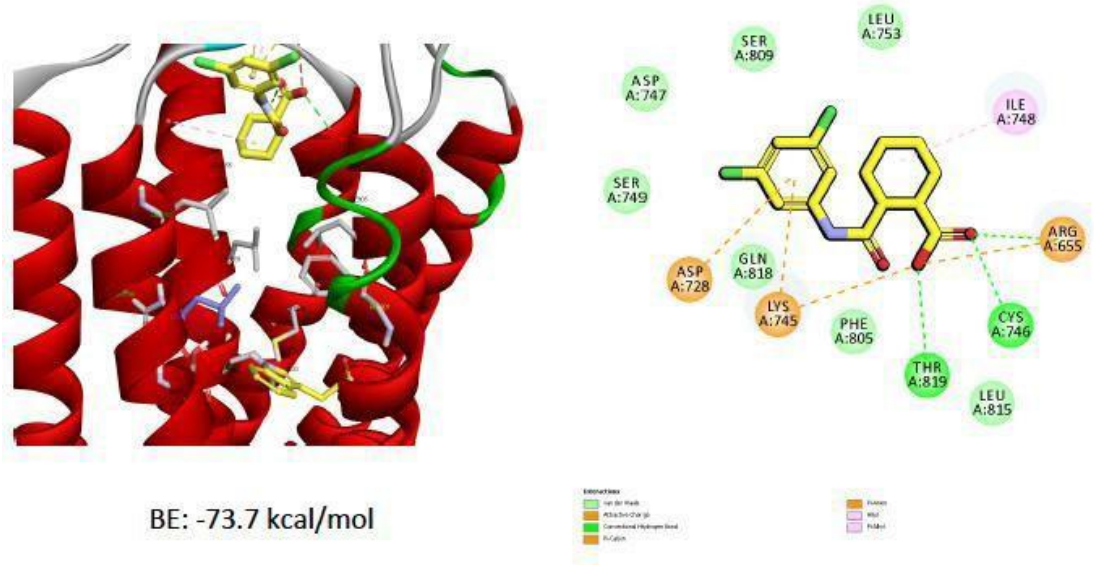

Figure 2-SD-4. Allosteric binding pose with **VU015541**, best calculated binding energy, towards the middleof the allosteric binding cavity, referred to as Vestibule 2.

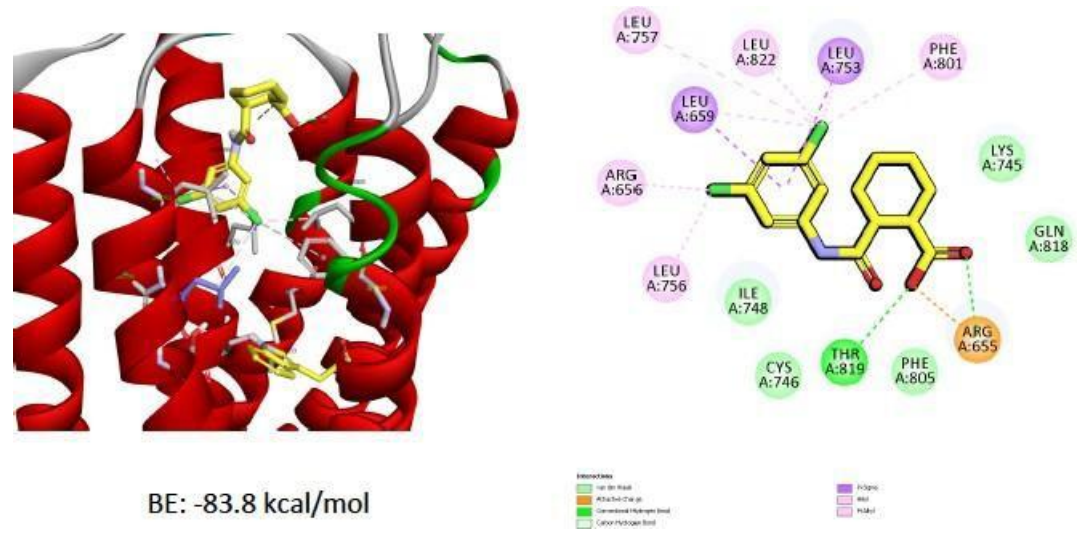

Figure 2-SD-5. Allosteric binding pose of **VU015541**, illustrating binding in the deep pocket.

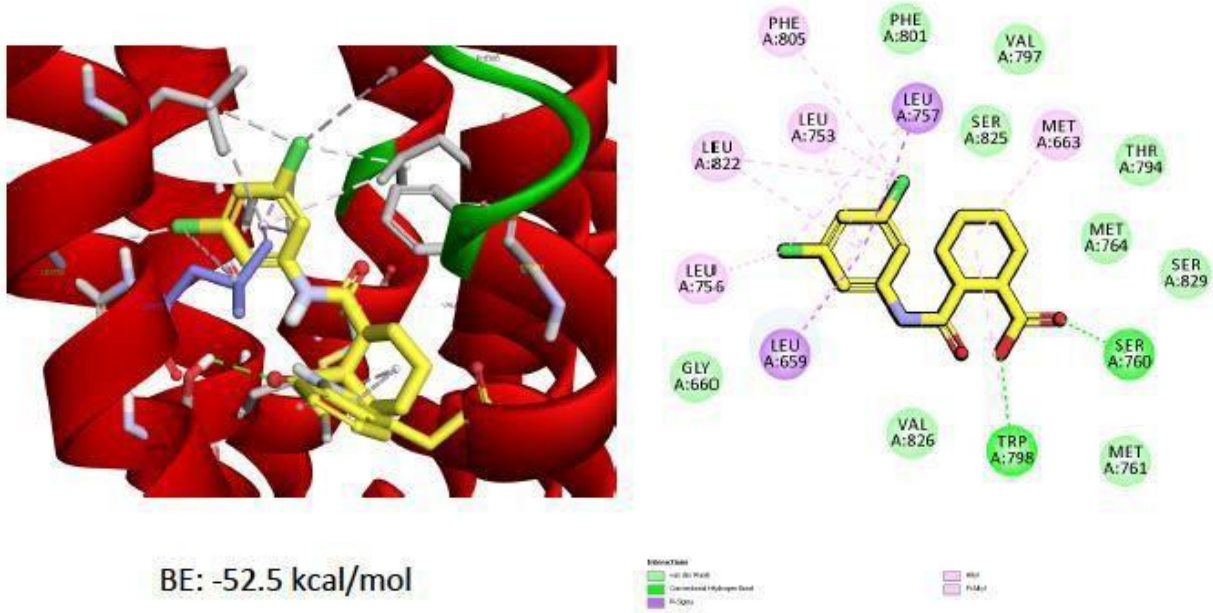

Table 2-SD-2. Discovery Studio binding Energy scores for Compounds **1-9**, and hypothetical [3,4-d]s **10-14** containing lipophilic groups, at the $mGluR_4$ allosteric site. The ligand FITM was the ligand crystallized in the mGluR used for constructing our homology model, pdb accession number 4OR2.

	Ligand	**Binding (kcal/mol)**	**Pose**
*	FITM	-138.878	11
1	Tol	-65.364	15
2	p-OCH_3	-62.2072	6
3	p-F	-56.0582	6
4	H	-83.2094	3
5	2,4 F_2	-61.1928	3
6	p-NO_2	-75.655	8
7	m-NO_2	-73.1841	3
8	3,5 Cl_2	-70.7011	8
9	3,5 CF_3	-76.0328	8
10	4-Ph-Tol	-70.1691	5
11	Mono Bn-Tol	-79.2557	5
12	diBn Tol	-97.1876	4
13	(R) - PhPr Tol	-77.8074	4
14	(S) - PhPr Tol	-85.1114	6

Figure 2-SD-6. Allosteric binding of Ligand **8.**

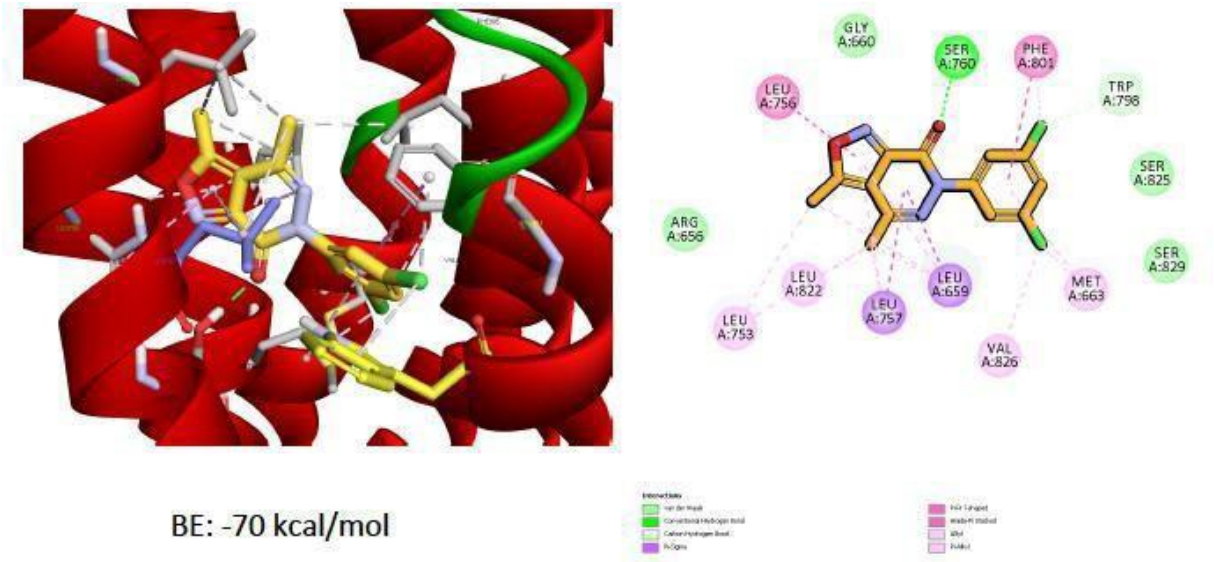

Figure 2-SD-7. Top five binding scores for **13**, illustrating vestibule 1, vestibule 2, and deep pocket binding,analogous to results obtained for VU015541.

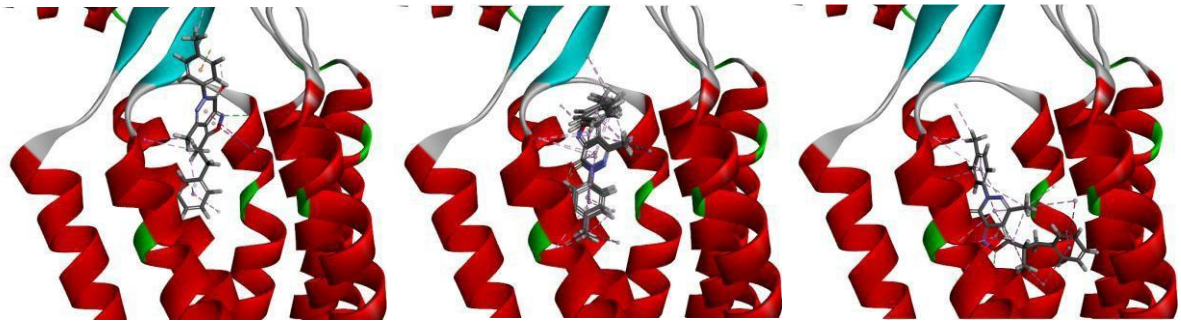

Chart 2-SD-1. Structures for hypothetical [3,4-d]s **10-14** containing lipophilic groups.

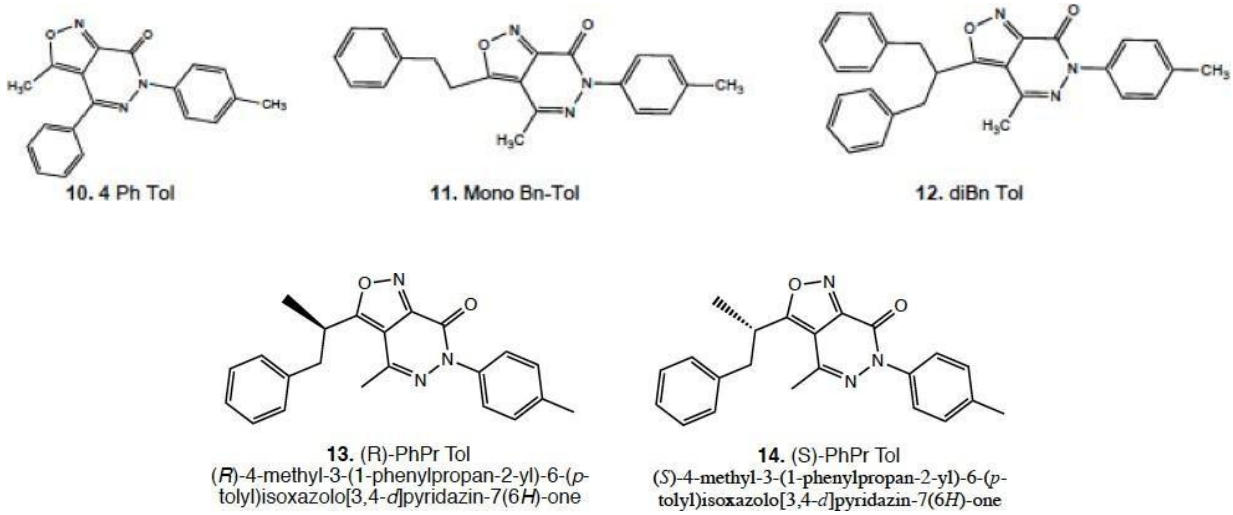

Chart 2-SD-2. Structures of BINA and TCN-22A used in PDSP assay, and FITM (pdb accession number
4OR2).

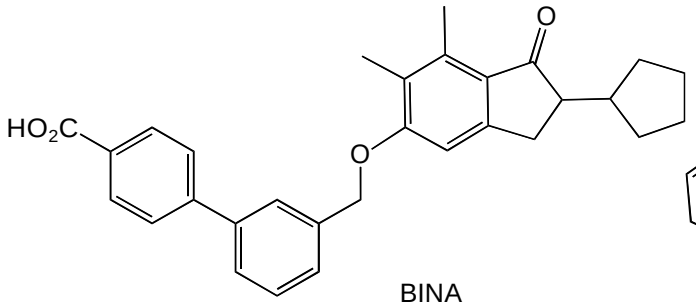

BINA

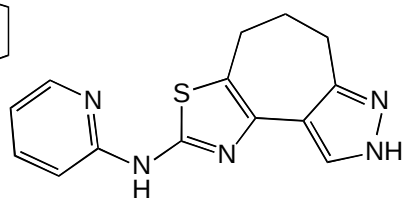

TCN-22A

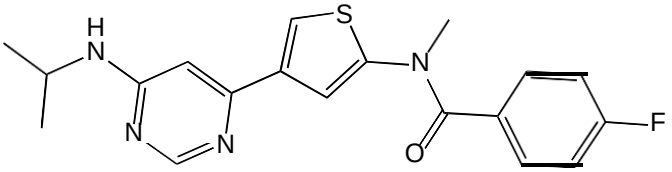

FITM

Table 2-SD-8. Binding interaction computational study of **8** with the allosteric residues of $mGluR_4$, anddegree of conservation among mGluR sub-types.

Residue	Binding interaction	Conserved in mGluRs
Arg 656		all
Leu 659	pyridazinone methyl 3,5 dichloro phenyl ring centroid(Re face), 3,5 dichloro phenyl Chloro	2,3,4,6,7,8
Met 663	Isoxazole ring centroid Isoxazole and pyridazinone methyls	4,7,8
Gly 660	Carboxyl group	all
Ser 760	Isoxazole ring N	4,6,7,8
Leu 753	3,5 dichloro phenyl ring centroid (Si face)	4,6,8
Leu 756	Chloro on 3,5 dichloro phenyl ring pyridazinone methyl	4
Leu 757	Isoxazole ring centroid Pyridazinone ring centroid	all

Table 2-SD-9. Summary of $mGluR_4$ residues determining allosteric shallow or deep pocketbinding.

Shallow allosteric residues of pocket	Deep allosteric residues of pocket
Arg 655 (mutated no activity-Gln)- potential interaction at carboxyl group	Glu 646
Arg 656 (promoted shift more than 10-fold-Ala)	Thr 639
Met 663	Ala638
Ser 664	Ser 664
Thr 639 (mutated more potent-Ile)	Ile 665
Glu 646 (mutated more potent -Ala)	Ser 752
Ser 723	Typ 798
Leu 756 (promoted shift more than 10-fold –Ser or Lys) (signature of shallow pocket binding)	Val826 (signature of deep pocket binding)
Trp798(promoted shift more than 10-fold -Ala)	Val829
Phe801	Phe 801
	Ala 830

R655Q, L756S, and L756K did not affect the deep binding PAMs

Figure 2-SD-10. Complete one dose functional data, including $mGluR_{1a}$ 5 and 8.

CMPD	mGlur2	mGlur4
21311	AGO-%MAX :-12 ANT-%INH: -37	AGO-%MAX :37 ANT-%INH: -9
21312	AGO-%MAX :20 ANT-%INH: -55	AGO-%MAX :26 ANT-%INH: 9
21313	AGO-%MAX :26 ANT-%INH: 23	AGO-%MAX :-21 ANT-%INH: 3
21314	AGO-%MAX :-4 ANT-%INH: -33	AGO-%MAX :-1 ANT-%INH: -5
21315	AGO-%MAX :35 ANT-%INH: -48	AGO-%MAX :11 ANT-%INH: -7
21316	AGO-%MAX :19 ANT-%INH: 5	AGO-%MAX :21 ANT-%INH: -3
21317	AGO-%MAX :-17 ANT-%INH: 48	AGO-%MAX :24 ANT-%INH: -10
21318	AGO-%MAX :-3 ANT-%INH: 11	AGO-%MAX :77 ANT-%INH: -6
21319	AGO-%MAX :36.56 ANT-%INH: 0	AGO-%MAX :9 ANT-%INH: 11

CMPD	mGluR1a	mGlur5
21311	AGO-%MAX :3 ANT-%INH: 17	AGO-%MAX :3 ANT-%INH: 8
21312	AGO-%MAX :5 ANT-%INH: 16	AGO-%MAX :5 ANT-%INH: 5
21313	AGO-%MAX :2 ANT-%INH: 0	AGO-%MAX :14 ANT-%INH: -3
21314	AGO-%MAX :0 ANT-%INH: 22	AGO-%MAX :-2 ANT-%INH: 11
21315	AGO-%MAX :4 ANT-%INH: 15	AGO-%MAX :-6 ANT-%INH: 9
21316	AGO-%MAX :4 ANT-%INH: -3	AGO-%MAX :11 ANT-%INH: -1
21317	AGO-%MAX :6 ANT-%INH: 23	AGO-%MAX :-3 ANT-%INH: 10
21318	AGO-%MAX :4 ANT-%INH: 8	AGO-%MAX :19 ANT-%INH: 10
21319	AGO-%MAX :5 ANT-%INH: -8	AGO-%MAX :4 ANT-%INH: -1

CMPD	mGluR8
21311	AGO-%MAX :22 ANT-%INH: 5
21312	AGO-%MAX :15 ANT-%INH: 9
21313	AGO-%MAX :15 ANT-%INH: 14
21314	AGO-%MAX :13 ANT-%INH: 13
21315	AGO-%MAX :8 ANT-%INH: 15
21316	AGO-%MAX :14 ANT-%INH: 17
21317	AGO-%MAX :7 ANT-%INH: 15
21318	AGO-%MAX :11 ANT-%INH: 12
21319	AGO-%MAX :9 ANT-%INH: 18

Legend:

51-75 Percent Inhibition | 25-49 Percent Activation | 0-50 Percent Inhibition | 50-100 Percent Activation

Figure 2-SD-11 (A). Agonist and antagonist binding isotherms at the Orthosteric Glutamate site.

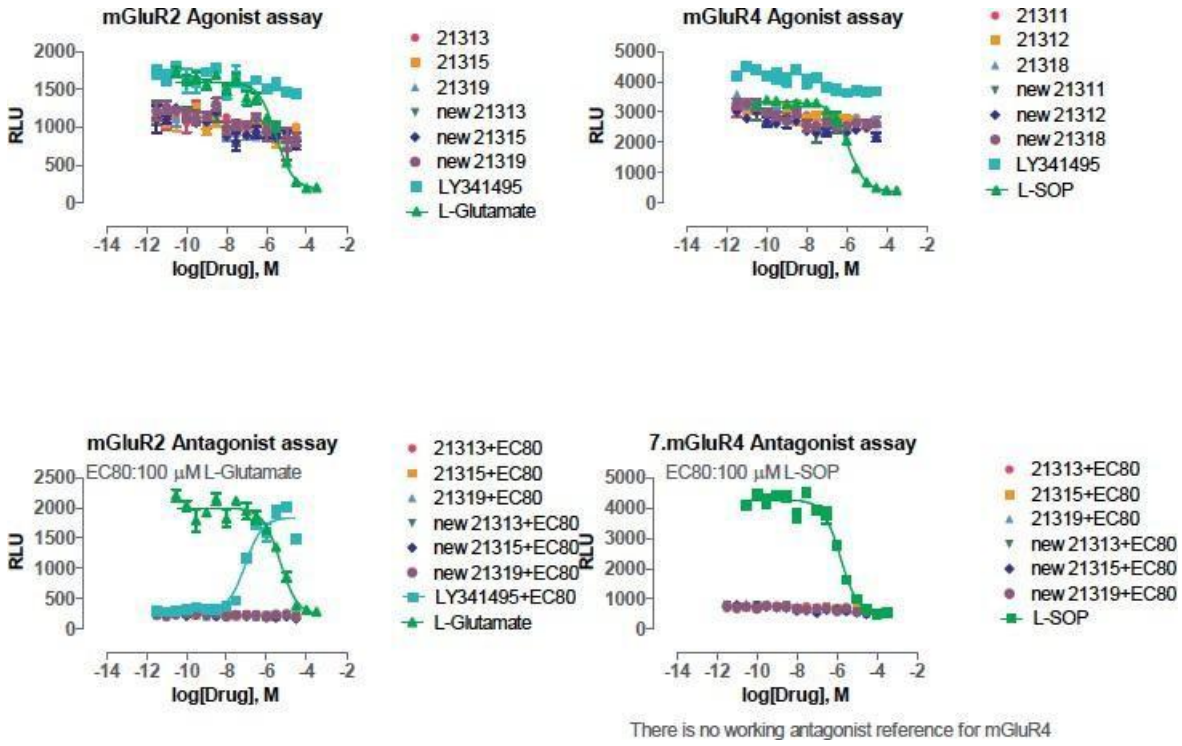

Figure 2-SD-11(B) . Binding isotherms for agonist and antagonist activity at the Allosteric mGluR site.

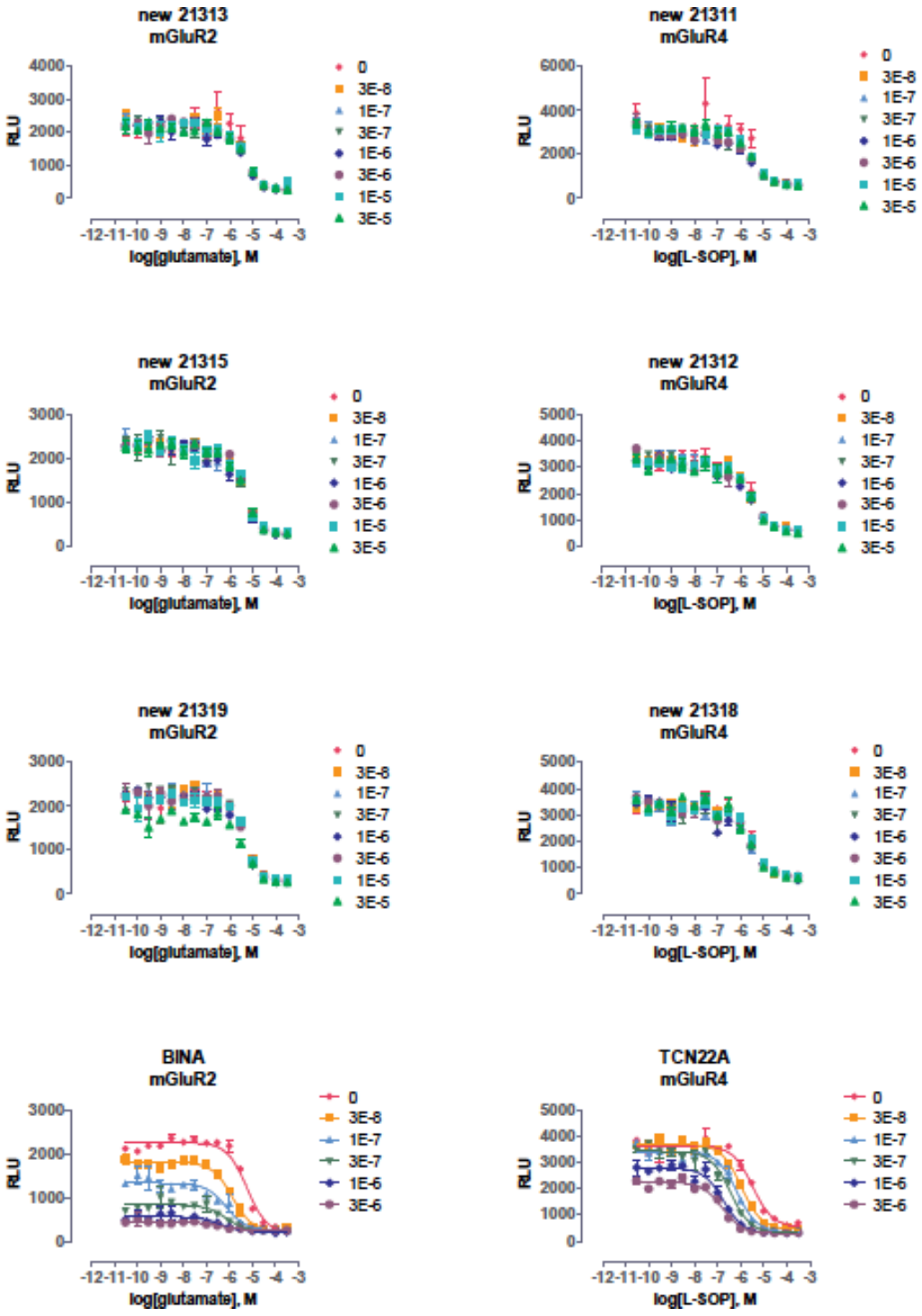

Figure 2-SD-8. Isoxazolo[3,4-d]pyridazinones have no significant interaction (all >10,000 nM) at the NMDA receptor as studied by radioligand binding with MK-801.

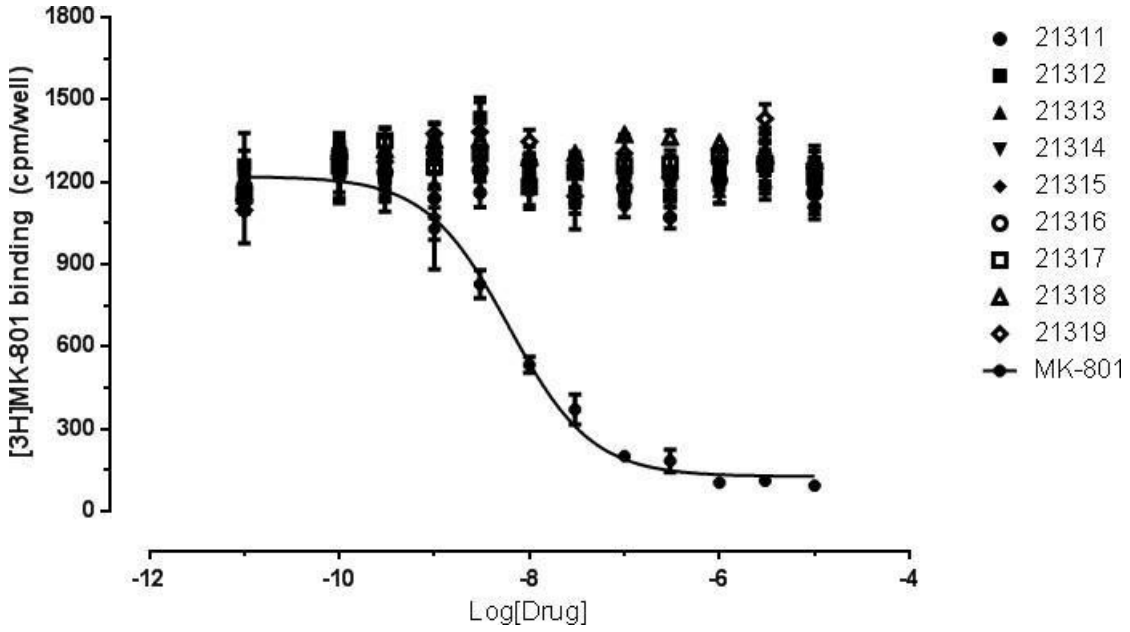

Acknowledgements

Testing data was generously provided by the National Institute of Mental Health's Psychoactive Drug Screening Program, Contract #HHSN-271-2013-00017-C (NIMH PDSP). The NIMH PDSP is Directed by Bryan L. Roth, MD, PhD, at the University of North Carolina at Chapel Hill and Project Officer, Jamie Driscoll, at NIMH, Bethesda MD, USA. The authors thank the Center for Structural and Functional Neuroscience (CSFN) for a pilot grant under NINDS P20 RR015583, the ALSAM foundation Skaggs Scholars Program Grant (NRN, DSB and PR), CBSD CoBRE grant P20GM103546 (NN), and the University of Montana for the award of asmall grant from the University Grants Program. Computational modeling studies were conducted at the University of Colorado Computational Chemistry and Biology Core Facility, which is funded in part by NIH/NCATS UL1 TR001082. We acknowledge Trideep Rajale for technical assistance.

References

(1) Conn, P. J.; Lindsley, C. W.; Meiler, J.; Niswender, C. M. Opportunities and Challenges in the Discovery of Allosteric Modulators of GPCRs for Treating CNS Disorders. *Nat. Rev. Drug Discov.* **2014**, *13* (9), 692–708 DOI: 10.1038/nrd4308.

(2) Gregory, K. J.; Dong, E. N.; Meiler, J.; Conn, P. J. Allosteric Modulation of Metabotropic Glutamate Receptors: Structural Insights and Therapeutic Potential. *Neuropharmacology* **2011**, *60* (1), 66–81 DOI: 10.1016/j.neuropharm.2010.07.007.

(3) Overington, J. P.; Al-Lazikani, B.; Hopkins, A. L. How Many Drug Targets Are There ? PubMed Commons. *Nat. Rev. Drug Discov.* **2006**, *5* (12), 10.

(4) Wood, M. R.; Hopkins, C. R.; Brogan, J. T.; Conn, P. J.; Lindsley, C. W. "Molecular Switches" on MGluR Allosteric Ligands That Modulate Modes of Pharmacology. *Biochemistry* **2011**, *50* (13), 2403–2410 DOI: 10.1021/bi200129s.

(5) Lindsley, C. W.; Emmitte, K. A.; Hopkins, C. R.; Bridges, T. M.; Gregory, K. J.; Niswender, C. M.; Conn, P. J. Practical Strategies and Concepts in GPCR Allosteric Modulator Discovery: Recent Advances with Metabotropic Glutamate Receptors. *Chem. Rev.* **2016**, *116* (11), 6707–6741 DOI: 10.1021/acs.chemrev.5b00656.

(6) Kunishima, N.; Shimada, Y.; Tsuji, Y.; Sato, T.; Yamamoto, M.; Kumasaka, T.; Nakanishi, S.; Jingami, H.; Morikawa, K. Structural Basis of Glutamate Recognition by a Dimeric Metabotropic Glutamate Receptor. *Nature* **2000**, *407* (6807), 971–977 DOI: 10.1038/35039564.

(7) Tsuchiya, D.; Kunishima, N.; Kamiya, N.; Jingami, H.; Morikawa, K. Structural Views of the Ligand-Binding Cores of a Metabotropic Glutamate Receptor Complexed with an Antagonist and Both Glutamate and Gd3+. *Proc. Natl. Acad. Sci. U. S. A.* **2002**, *99* (5), 2660–2665 DOI: 10.1073/pnas.052708599.

(8) Muto, T.; Tsuchiya, D.; Morikawa, K.; Jingami, H. Structures of the Extracellular Regions of the Group II/III Metabotropic Glutamate Receptors. *Proc. Natl. Acad. Sci. U. S. A.* **2007**, *104* (10), 3759–3764 DOI: 10.1073/pnas.0611577104.

(9) Tora, A. S.; Rovira, X.; Dione, I.; Bertrand, H. O.; Brabet, I.; De Koninck, Y.; Doyon, N.; Pin, J. P.; Acher, F.; Goudet, C. Allosteric Modulation of Metabotropic Glutamate Receptors by Chloride Ions. *FASEB J.* **2015**, *29* (10), 4174–4188 DOI: 10.1096/fj.14-269746.

(10) Pin, J. P.; Acher, F. The Metabotropic Glutamate Receptors: Structure, Activation Mechanism and Pharmacology. *Curr. Drug Targets. CNS Neurol. Disord.* **2002**, *1* (3), 297–317 DOI: 10.2174/1568007023339328.

(11) Rook, J. M.; Noetzel, M. J.; Pouliot, W. A.; Bridges, T. M.; Vinson, P. N.; Cho, H. P.; Zhou, Y.; Gogliotti, R. D.; Manka, J. T.; Gregory, K. J.; Stauffer, S. R.; Dudek, F. E.; Xiang, Z.; Niswender, C. M.; Daniels, J. S.; Jones, C. K.; Lindsley, C. W.; Conn, P. J. Unique Signaling Profiles of Positive Allosteric Modulators of Metabotropic Glutamate Receptor Subtype 5 Determine Differences in in Vivo Activity. *Biol. Psychiatry* **2013**, *73* (6), 501–509 DOI: 10.1016/j.biopsych.2012.09.012.

(12) Hopkins, C. R.; Lindsley, C. W.; Niswender, C. M. MGluR4-Positive Allosteric Modulation as Potential Treatment for Parkinson's Disease. *Future Med. Chem.* **2009**, *1* (3), 501–513 DOI: 10.4155/fmc.09.38.

(13) Williams, R.; Zhou, Y.; Niswender, C. M.; Luo, Q.; Conn, P. J.; Lindsley, C. W.; Hopkins, C. R. Re-Exploration of the PHCCC Scaffold: Discovery of Improved Positive Allosteric Modulators of MGluR4. *ACS Chem. Neurosci.* **2010**, *1* (6), 411–419 DOI: 10.1021/cn9000318.

(14) Yu, L. J.; Wall, B. A.; Wangari-Talbot, J.; Chen, S. Metabotropic Glutamate Receptors in Cancer. *Neuropharmacology* **2017**, *115*, 193–202 DOI: 10.1016/J.NEUROPHARM.2016.02.011.

(15) Iacovelli, L.; Arcella, A.; Battaglia, G.; Pazzaglia, S.; Aronica, E.; Spinsanti, P.; Caruso, A.; De Smaele, E.; Saran, A.; Gulino, A.; Onofrio, M. D. '; Giangaspero, F.; Nicoletti, F. Neurobiology of Disease Pharmacological Activation of MGlu4 Metabotropic Glutamate Receptors Inhibits the Growth of Medulloblastomas. **2006** DOI: 10.1523/JNEUROSCI.2285-06.2006.

(16) (a) Renzi G, Dal Piaz V. Studies on some ethyl-4,5-disubstituted isoxazole-3-carboxylates Gazz Chim It. **1965**;95:1478–1491
(b) Renzi G, Pinzauti S. New derivatives of the isoxazolo-(3,4-d)-pyridazin-7-one system [Nuovi derivati del sistema isossazolo-(3,4-d)-piridazin-7-one.]Il Farmaco Ed Sci. **1969**;24:885–892
(c) Dal Piaz V, Pinzauti S, Lacrimini P. J Heterocycl Chem. **1975**;13:409–410
(d) Chimichi S, Ciciani G, Dal Piaz V, et al. Solid state photodimerization reaction of some 3-styrylisoxazolo-[3,4-d]pyridazin-7(6h)-onesHeterocycles. **1986**;24:3467–3471
(d) Dal Piaz V, Graziano A, Haider N, Holzer W. Synthesis and complete 1H, 13C and 15N NMR assignment of substituted isoxazolo[3,4-d]pyridazin-7(6H)-onesMagn Reson Chem.**2005**;43:240–245.

(17) (a)Montesano, F.; Barlocco, D.; Piaz, V. D.; Leonardi, A.; Poggesi, E.; Fanelli, F.; De Benedetti, P. G. Isoxazolo-[3,4-d]-Pyridazin-7-(6H)-Ones and Their Corresponding 4,5-Disubstituted-3-(2H)-Pyridazinone Analogues as New Substrates for A1-Adrenoceptor Selective Antagonists: Synthesis, Modeling, and Binding Studies. Bioorg. Med. Chem. **1998**, 6 (7), 925–935 DOI: 10.1016/S0968-0896(98)00056-X.
(b) Costantino L, Rastelli G, Gamberini M, Giovannoni M, et al. Isoxazolo-[3,4-d]-pyridazin-7-

(6H)-one as a potential substrate for new aldose reductase inhibitors J Med Chem.**1999**;42:1894–1900
(c) Dal Piaz V, Rascon A, Dubra M, et al. Isoxazolo[3,4-d]pyridazinones and analogues as Leishmania mexicana PDE inhibitors Il Farmaco.**2002**;57:89–96
(d) Dal Piaz V, Castellana M, Vergelli C, et al. J Enz Inh Med Chem. **2002**;17:227–233.

(18) (a) Dal Piaz, V.; Ciciani, G.; Chimichi, S. New Functionalized Pyrazoles from Isoxazolopyridazinones. Heterocycles **1985**, 23 (2), 365–369 DOI: 10.3987/R-1985-02-0365.
(b) Dal Piaz V, Ciciani G, et al. J Pharm Sci. **1991**;80:1417–1421
(c) Dal Piaz V, Giovannoni M, Ciciani G, et al. 4,5-Functionalized 6-phenyl-3(2H)-pyridazinones: synthesis and evaluation of antinociceptive activity, Eur J Med Chem. **1996**;31:65–70
(c) Dal Piaz V, Giovannoni M, Castellana M, et al. Novel heterocyclic-fused pyridazinones as potent and selective phosphodiesterase IV inhibitors,J Med Chem.**1997**;40:1417–1421
(d) Barlocco D, Cignarella G, Dal Piaz V, et al Phenylpiperazinylalkylamino substituted pyridazinones as potent α1 adrenoceptor antagonists,J Med Chem. 2001;44:2403–2410
(e) Paola M, Giovannoni M, Dal Piaz V, et al. J Med Chem. **2001**;44:4292–4295
(f) Dal Piaz V, Vergelli C, Giovannoni M, et al. 4-Amino-3(2H)-pyridazinones bearing arylpiperazinylalkyl groups and related compounds: Synthesis and antinociceptive activity, Il Farmaco. **2003**;58:1063–1078
(g) Giovannoni M, Vergelli C, Biancalani C, et al. Novel Pyrazolopyrimidopyridazinones with Potent and Selective Phosphodiesterase 5 (PDE5) Inhibitory Activity as Potential Agents for Treatment of Erectile Dysfunction,J Med Chem. **2006**;49:5363–5371
(h) Giovannoni M, Cesari N, Vergelli C, et al. 4-Amino-5-substituted-3(2H)-pyridazinones as Orally Active Antinociceptive Agents: Synthesis and Studies on the Mechanism of Action,J Med Chem. **2007**;50:3945–3953.

(19) Biancalani, C.; Giovannoni, M. P.; Pieretti, S.; Cesari, N.; Graziano, A.; Vergelli, C.; Cilibrizzi, A.; Di Gianuario, A.; Colucci, M.; Mangano, G.; Garrone, B.; Polenzani, L.; Dal Piaz, V. Further Studies on Arylpiperazinyl Alkyl Pyridazinones: Discovery of an Exceptionally Potent, Orally Active, Antinociceptive Agent in Thermally Induced Pain. J. Med. Chem. **2009**, 52 (23), 7397–7409 DOI: 10.1021/JM900458R/SUPPL_FILE/JM900458R_SI_001.PDF.

(20) Patel, S. A.; Rajale, T.; O'Brien, E.; Burkhart, D. J.; Nelson, J. K.; Twamley, B.; Blumenfeld, A.; Szabon-Watola, M. I.; Gerdes, J. M.; Bridges, R. J.; Natale, N. R. Isoxazole Analogues Bind the System Xc- Transporter: Structure–Activity Relationship and Pharmacophore Model. Bioorg. Med. Chem. **2010**, 18 (1), 202–213 DOI: 10.1016/J.BMC.2009.11.001.

(21) (a) Jacoby E, Bouhelal R, Gerspacher M, Seuwen K. ChemMedChem. 2006;1:760–782.
(b) Shi Q, Savage J, Hufeisen S, et al. J Pharmacol Exp Ther. 2003;305:131–42. (c) The primary assay is found in the PDSP protocol book for **2013**, pp. 162–166. < https://pdspdb.unc.edu/pdspWeb/content/PDSP %20Protocols%20II%202013-03-28.pdf > ; The secondary assay is found in the PDSP protocol book for **2018**. < https://pdspdb.unc.edu/pdspWeb/content/UNC- CH%20Protocol%20Book.pdf > ; Accessed 10.08.18.

(22) Nadler, L. S.; Raetzman, L. T.; Dunkle, K. L.; Mueller, N.; Siegel, R. E. GABAA Receptor Subunit Expression and Assembly in Cultured Rat Cerebellar Granule Neurons. Dev. Brain Res. **1996**, 97 (2), 216–225 DOI: 10.1016/S0165-3806(96)00143-5.

(23) Chiu, J.; Brien, J. F.; Wu, P.; Eubanks, J. H.; Zhang, L.; Reynolds, J. N. Chronic Ethanol Exposure Alters MK-801 Binding Sites in the Cerebral Cortex of the Near-Term Fetal Guinea Pig. Alcohol **1999**, 17 (3), 215–221 DOI: 10.1016/S0741-8329(98)00050-0.

(24) Kozikowski, A. P.; Tuckmantel, W.; Reynolds, I. J.; Wroblewski, J. T. Synthesis and Bioactivity of a New Class of Rigid Glutamate Analogs. Modulators of the N-Methyl-D-Aspartate Receptor. J. Med. Chem. **2002**, 33 (6), 1561–1571 DOI: 10.1021/JM00168A007.

(25) Wu, H.; Wang, C.; Gregory, K. J.; Han, G. W.; Cho, H. P.; Xia, Y.; Niswender, C. M.; Katritch, V.; Meiler, J.; Cherezov, V.; Conn, P. J.; Stevens, R. C. Structure of a Class C GPCR Metabotropic Glutamate Receptor 1 Bound to an Allosteric Modulator. Science (80-.). **2014**, 344 (6179), 58–64 DOI: 10.1126/SCIENCE.1249489/SUPPL_FILE/WU.SM.PDF.

(26) Brooks, B. R.; Brooks, C. L.; Mackerell, A. D.; Nilsson, L.; Petrella, R. J.; Roux, B.; Won, Y.; Archontis, G.; Bartels, C.; Boresch, S.; Caflisch, A.; Caves, L.; Cui, Q.; Dinner, A. R.; Feig, M.; Fischer, S.; Gao, J.; Hodoscek, M.; Im, W.; Kuczera, K.; Lazaridis, T.; Ma, J.; Ovchinnikov, V.; Paci, E.; Pastor, R. W.; Post, C. B.; Pu, J. Z.; Schaefer, M.; Tidor, B.; Venable, R. M.; Woodcock, H. L.; Wu, X.; Yang, W.; York, D. M.; Karplus, M. CHARMM: The Biomolecular Simulation Program. J. Comput. Chem. **2009**, 30 (10), 1545–1614 DOI: 10.1002/jcc.21287.

(27) Onufriev A, Case D, Bashford D. Effective Born radii in the generalized Born approximation: The importance of being perfect, J Comput Chem. **2002**;23:1297–1304.

(28) Koska, J.; Spassov, V. Z.; Maynard, A. J.; Yan, L.; Austin, N.; Flook, P. K.; Venkatachalam, C. M. Fully Automated Molecular Mechanics Based Induced Fit Protein−Ligand Docking Method. J. Chem. Inf. Model. **2008**, 48 (10), 1965–1973 DOI: 10.1021/CI800081S.

(29) Jain A., Scoring noncovalent protein-ligand interactions: A continuous differentiable function tuned to compute binding affinities, J Comput Aided Mol Des. **1996**;10:427–440.

(30) Gehlhaar D, Bouzida D, Rejto P. Rational drug design: novel methodology and practical applications. Washington, DC: American Chemical Society; **1999**.

(31) Bohm H., On the use of LUDI to search the Fine Chemicals Directory for ligands of proteins of known three-dimensional structure, J Comput Aided Mol Des. **1994**;8:623–632.

(32) Feng, Z.; Ma, S.; Hu, G.; Xie, X. Q. Allosteric Binding Site and Activation Mechanism of Class C G-Protein Coupled Receptors: Metabotropic Glutamate Receptor Family. AAPS J. **2015**, 17 (3), 737–753 DOI: 10.1208/S12248-015-9742-8/FIGURES/8.

(33) Isberg, V.; De Graaf, C.; Bortolato, A.; Cherezov, V.; Katritch, V.; Marshall, F. H.; Mordalski, S.; Pin, J. P.; Stevens, R. C.; Vriend, G.; Gloriam, D. E. Generic GPCR Residue Numbers – Aligning Topology Maps While Minding the Gaps. Trends Pharmacol. Sci. **2015**, 36 (1), 22–31 DOI: 10.1016/J.TIPS.2014.11.001.

(34) Harpsøe, K.; Isberg, V.; Tehan, B. G.; Weiss, D.; Arsova, A.; Marshall, F. H.; Bräuner-Osborne, H.; Gloriam, D. E. Selective Negative Allosteric Modulation Of Metabotropic Glutamate Receptors – A Structural Perspective of Ligands and Mutants. Sci. Reports **2015** 51 2015, 5 (1), 1–11 DOI: 10.1038/srep13869.

(35) Rovira, X.; Malhaire, F.; Scholler, P.; Rodrigo, J.; Gonzalez-Bulnes, P.; Llebaria, A.; Pin, J.-P. P.; Giraldo, J.; Goudet, C. Overlapping Binding Sites Drive Allosteric Agonism and Positive Cooperativity in Type 4 Metabotropic Glutamate Receptors. FASEB J. **2015**, 29 (1), 116–130 DOI: 10.1096/fj.14-257287.

(36) Natale, N. R.; Mirzaei, Y. R. The Lateral Metalation of Isoxazoles. A Review. Org. Prep. Proced. Int. **1993**, 25 (5), 515–556 DOI: 10.1080/00304949309457997.

(37) Campana, C. F.; Mirzaei, J.; Koerner, C.; Gates, C.; Natale, N. R. 3-(1,3-Diphenylpropan-2-Yl)-4-Methyl-6-Phenylisoxazolo[3,4-d] Pyridazin-7(6H)-One. Acta Crystallogr. Sect. E Struct. Reports Online **2013**, 69 (11) DOI: 10.1107/S160053681302802X

(38) Hong, S. P.; Liu, K. G.; Ma, G.; Sabio, M.; Uberti, M. A.; Bacolod, M. D.; Peterson, J.; Zou, Z. Z.; Robichaud, A. J.; Doller, D. Tricyclic Thiazolopyrazole Derivatives as Metabotropic Glutamate Receptor 4 Positive Allosteric Modulators. J. Med. Chem. **2011**, 54 (14), 5070–5081 DOI: 10.1021/JM200290Z/SUPPL_FILE/JM200290Z_SI_001.PDF.

This paper was published in Acta Crystallographica Section E[1]

Campana, C. F.; Mirzaei, J.; Koerner, C.; Gates, C.; Natale, N. R. 3-(1,3-Diphenylpropan-2-Yl)-4-Methyl-6-Phenylisoxazolo[3,4-d] Pyridazin-7(6H)-One. *Acta Crystallogr. Sect. E Struct. Reports Online* **2013**, *69* (11) DOI: 10.1107/S160053681302802X.

Chapter 3: Crystal Structure of 3-(1,3-Diphenylpropan-2-Yl)-4-Methyl-6-Phenylisoxazolo[3,4-d] Pyridazin-7(6H)-One

Introduction

In the title compound, $C_{27}H_{23}N_3O_2$, the geminal benzyl groups branching out from the methine adjacent to the isoxazole group are both *syn*-oriented to the methyl group of the pyridazinone moiety, as reflected by C—C distances of 3.812 (2) and 4.369 (2) Å between the methyl carbon and the nearest ring carbon of each benzyl group. This kind of conformation is retained in $CDCl_3$ solution, as evidenced by distinct phenyl-shielding effects on the ^{1}H NMR signals of themethyl H atoms. The isoxazolo[3,4-*d*]pyridazin ring system is virtually planar (r.m.s. deviation from planarity = 0.031 Å), but the N-bonded phenyl group is inclined to the former by an ring–ring angle of 55.05 (3) . In the crystal, the T-shaped molecules are arranged in an interlocked fashion, forming rod-like assemblies along [101]. The molecules are held together by unremarkable weak C—H$^{\cdots}$N, C—H$^{\cdots}$O and C—H.. π interactions (C—O,N,C > 3.4 A), while significant π–π-stacking interactions are absent.

Related literature

For chemistry of isoxazolo[3,4-*d*]pyridazinone preparation, see: Renzi & Dal Piaz (1965)[12]. For deprotonation with sodium alkoxides, see: Dal Piaz *et al.* (1975)[4]; Chimichi *et al.* (1986)[2]. For the rearrangement of the isoxazolo[3,4-*d*]pyridazinone ring system to pyrazole, see: Dal Piaz *et al.* (1985)[3]. For isoxazole lateral metalation, see: Natale & Niou (1984)[10]; Natale *et al.* (1985)[8]; Niou & Natale (1986)[11]; Schlicksupp & Natale (1987). For recent applications of lateral metalation and electrophilic quenching of isoxazoles to targets of biological interest, see: Nakamura *et al.* (2010)[7]; Hulubei *et al.* (2012)[5]. For a review of the lateral metalation and electrophilic quenching of isoxazoles, see: Natale & Mirzaei (1993)[9].

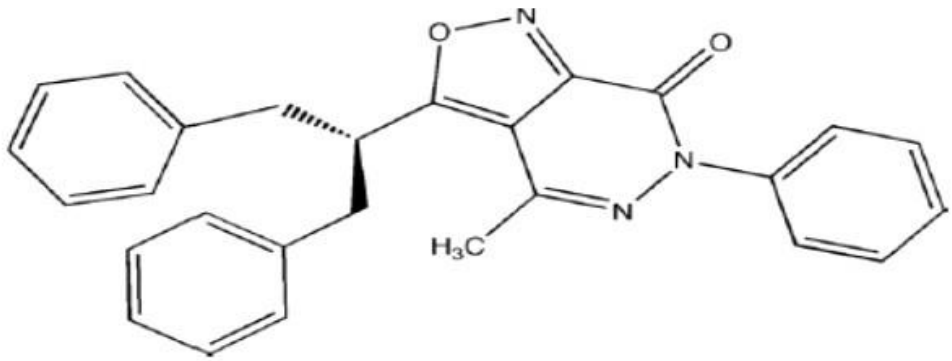

Experimental

Crystal data

$C_{27}H_{23}N_3O_2$
$M_r = 421.48$
Triclinic, $P\overline{1}$
$a = 7.5163$ (4) Å
$b = 9.6774$ (5) Å
$c = 15.9053$ (8) Å
$\alpha = 86.798$ (1)°
$\beta = 83.512$ (1)°
$\gamma = 69.385$ (1)°
$V = 1075.75$ (10) Å^3
$Z = 2$
Cu $K\alpha$ radiation
$\mu = 0.66$ mm^{-1}
$T = 100$ K
0.40 × 0.22 × 0.19 mm

Data collection

Bruker D8 Venture PHOTON 100 CMOS diffractometer
Absorption correction: numerical (*SADABS*; Bruker, 2012)
$T_{min} = 0.80$, $T_{max} = 0.89$
12012 measured reflections
3714 independent reflections
3597 reflections with $I > 2\sigma(I)$
$R_{int} = 0.017$

Refinement

$R[F^2 > 2\sigma(F^2)] = 0.032$
$wR(F^2) = 0.078$
$S = 1.03$
3714 reflections
313 parameters
86 restraints
Only H-atom displacement parameters refined
$\Delta\rho_{max} = 0.22$ e Å^{-3}
$\Delta\rho_{min} = -0.14$ e Å^{-3}

Table 1
Hydrogen-bond geometry (Å, °).

D—H···A	D—H	H···A	D···A	D—H···A
C26—H26···O1^{i}	0.95	2.61	3.4159 (13)	143
C24—H24···N1^{ii}	0.95	2.73	3.5407 (15)	143
C11—H11···C18^{iii}	0.95	2.78	3.6182 (15)	148

Symmetry codes: (i) $-x, -y+1, -z+1$; (ii) $-x+1, -y+1, -z+1$; (iii) $-x, -y+1, -z+2$.

Data collection

SMART (Bruker, 2012); cell refinement: SAINT (Bruker, 2012)[1]; data reduction: SAINT; program(s) used to solve structure: SHELXS97 (Sheldrick, 2008)[14]; program(s) used to refine structure: SHELXL97 (Sheldrick, 2008)[14]; molecular graphics: Mercury (Macrae et al., 2008);software used to prepare material for publication: publCIF (Westrip, 2010)[15].

Comment

The title compound (**Figure 3-1**) was prepared by lateral metalation with lithium hexamethyldisilazide and electrophilic quenching with benzyl bromide (Natale & Mirzaei, 1993)[9], under thermodynamic conditions (Niou & Natale, 1986; Schlicksupp & Natale, 1987)[11,13], during which a facile second deprotonation and quenching leads to double incorporation (Natale*et al.*, 1985, Natale & Niou, 1984)[8,10]. Mono-alkylation and recovered starting material account forsufficient material balance to rule out substantial rearrangement under these conditions. The present study unambiguously establishes the regiochemistry of double alkylation. Previous reports on analogous deprotonation with sodium alkoxides (Dal Piaz, *et al.*, 1975; Chimichi, *et al.*, 1986)[2,4], reported rearrangement to pyrazoles with longer reaction times (Dal Piaz *et al.*, 1985)[3]. The lateral metalation and electrophilic quenching of isoxazoles continues to lead to candidates with promising biological activity (Nakamura, *et al.*, 2010; Hulubei *et al.*, 2012)[5,7] and is the subject of active investigation, to be reported in due course. The conformation observed inthe solid state (**Figure 3-1**) would be expected to result in magnetic anisotropy if maintained in solution, and this is indeed observed, as the ^{1}H NMR resonance of the C(4) methyl is observed at δ 2.55 in the starting material, δ 2.21 in the monoalkylated product, and δ 1.86 in the title compound. Furtherchemistry and pharmacology studies based upon this reaction are underway and will be reported in due course.

Experimental

Starting material, 3-methyl-4-methyl-6-phenylisoxazolo[3,4-d]pyridazin-7(6H)-one (**Figure 3-2**) was prepared according to Renzi and Dal Piaz (1965). To starting material (88 mg, 0.36 mmol) was added freshly distilled tetrahydrofuran (THF, 25 ml), under an argon atmosphere. The temperature was lowered to 195 K, and a solution of lithium hexamethyldisilazide (1 ml, 1.0M in THF, Aldrich, 28% excess) was added dropwise over five minutes. After stirring for 1 h, benzyl bromide was added via syringe (0.1 ml, 0.84 mmol, 14% excess). The reaction was allowed to come to room temperature with stirring overnight, after which time the solvent was removed in vacuo by rotary evaporator, and the residue chromatographed on an 80 x 35 cm silica gel column. Gradient chromatogrpahy was performed beginning with chloro- form-hexane (1:1), and the gradient slowly increased in polarity to ethyl acetate (EtOAc)-hexane-chloroform (1:2:1). The product 3-(1,3-diphenylpropan-2-yl)-4-methyl-6-phenylisoxazolo[3,4-d]pyridazin-7(6H)-one was obtained from the column fraction with Rf 0.6 (SiO2, EtOAc-hexane-chloroform 2:1:1) as a solid (57.1 mg, 38% yield), and was recrystallized by slow evaporation from EtOAc/hexanes to which a small amount of heptane had been added. The resulting crystals were used in the single crystal X-ray study. A clear light yellow prism-like specimen was selected for the X-ray data collection with a Bruker D8 Venture PHOTON 100 CMOS system equipped with a Cu Kα INCOATEC micro-focus source (λ = 1.54178 Å).

3. Refinement

A DELU restraint (Sheldrick, 2008) was used for the U_{ij} of all non-H atoms. Hydrogen atoms were positioned geometrically and refined as riding atoms, with C—H = 0.96–0.99 Å and U_{iso}(H) = 1.5U_{eq}(C) for methyl H atoms, and U_{iso}(H) = 1.2U_{eq}(C) for all other H atoms.

Computing details

Data collection: *SMART* (Bruker, 2012); cell refinement: *SAINT* (Bruker, 2012); data reduction:

SAINT (Bruker, 2012)[1]; program(s) used to solve structure: *SHELXS97* (Sheldrick, 2008)[14]; program(s) used to refine structure: *SHELXL97* (Sheldrick, 2008)[14]; molecular graphics: *Mercury*(Macrae *et al.*, 2008)[6]; software used to prepare material for publication: *publCIF* (Westrip, 2010)[15].

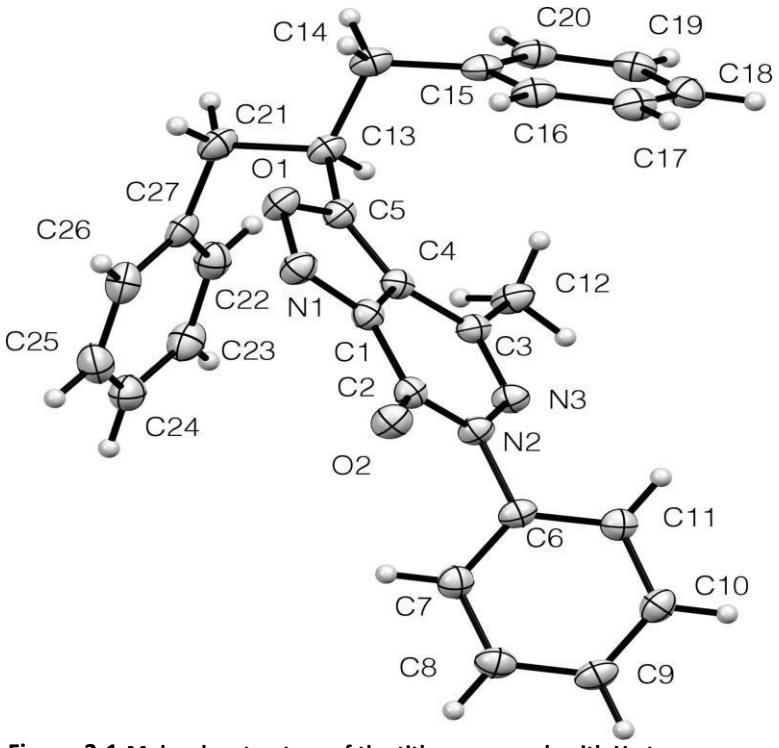

Figure 3-1:Molecular structure of the title compound, with H atoms represented by small spheres of arbitrary radius and displacement ellipsoids at the 50% probability level.

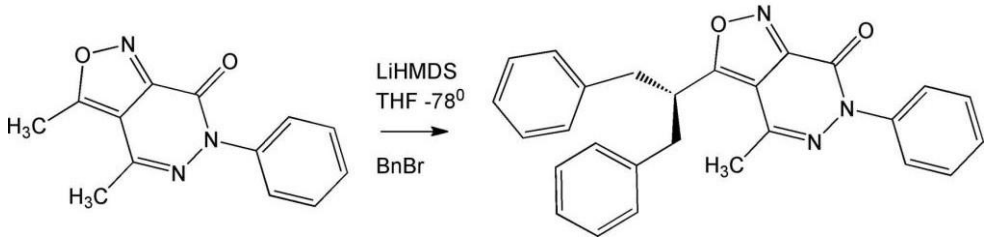

Figure 3- 2: Benzylation of 3-methyl-4-methyl-6-phenylisoxazolo[3,4-d]pyridazin-7(6H)-one as precursor to give the title compound

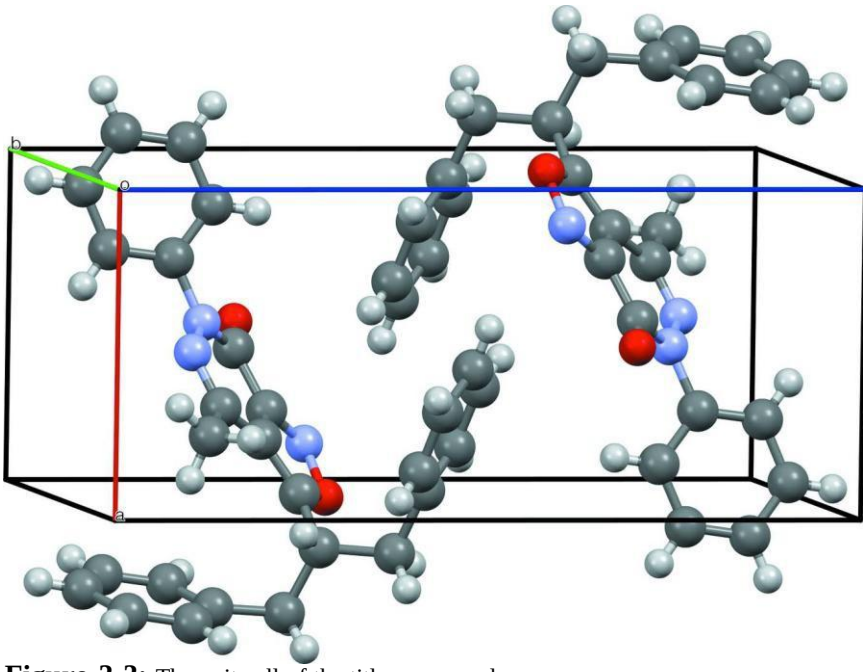

Figure 3-3: The unit cell of the title compound.

3-(1,3-Diphenylpropan-2-yl)-4-methyl-6-phenylisoxazolo[3,4-*d*]pyridazin-7(6*H*)-one

Crystal data

$C_{27}H_{23}N_3O_2$	$Z = 2$
$M_r = 421.48$	$F(000) = 444$
Triclinic, $P\overline{1}$	calculated from global refinement
Hall symbol: -P 1	$D_x = 1.301$ Mg m^{-3}
$a = 7.5163$ (4) Å	Cu $K\alpha$ radiation, $\lambda = 1.54178$ Å
$b = 9.6774$ (5) Å	Cell parameters from 9923 reflections
$c = 15.9053$ (8) Å	$\theta = 2.8$–$68.4°$
$\alpha = 86.798$ (1)°	$\mu = 0.66$ mm^{-1}
$\beta = 83.512$ (1)°	$T = 100$ K
$\gamma = 69.385$ (1)°	Prism, clear light yellow
$V = 1075.75$ (10) Å^3	0.40 × 0.22 × 0.19 mm

Data collection

Bruker D8 Venture PHOTON 100 CMOS diffractometer
Radiation source: Cu Kα
Mirrors monochromator
Detector resolution: 10.4167 pixels mm^{-1}
ω and phi scans
Absorption correction: numerical (*SADABS*; Bruker, 2012)
T_{min} = 0.80, T_{max} = 0.89

12012 measured reflections
3714 independent reflections
3597 reflections with $I > 2\sigma(I)$
R_{int} = 0.017
θ_{max} = 66.6°, θ_{min} = 2.8°
$h = -8 \rightarrow 3$
$k = -11 \rightarrow 11$
$l = -18 \rightarrow 18$

Refinement

Refinement on F^2
Least-squares matrix: full
$R[F^2 > 2\sigma(F^2)]$ = 0.032
$wR(F^2)$ = 0.078
S = 1.03
3714 reflections
313 parameters
86 restraints
0 constraints
Primary atom site location: structure-invariant direct methods

Secondary atom site location: difference Fourier map
Hydrogen site location: inferred from neighbouring sites
Only H-atom displacement parameters refined
$w = 1/[\sigma^2(F_o^2) + (0.0352P)^2 + 0.337P]$ where $P = (F_o^2 + 2F_c^2)/3$
$(\Delta/\sigma)_{max} < 0.001$
$\Delta\rho_{max}$ = 0.22 e Å^{-3}
$\Delta\rho_{min}$ = −0.14 e Å^{-3}

Special details

Geometry. All e.s.d.'s (except the e.s.d. in the dihedral angle between two l.s. planes) are estimated using the full covariance matrix. The cell e.s.d.'s are taken into account individually in the estimation of e.s.d.'s in distances, angles and torsion angles; correlations between e.s.d.'s in cell parameters are only used when they are defined by crystal symmetry. An approximate (isotropic) treatment of cell e.s.d.'s is used for estimating e.s.d.'s involving l.s. planes.

Refinement. Refinement of F^2 against ALL reflections. The weighted R-factor wR and goodness of fit S are based on F^2, conventional R-factors R are based on F, with F set to zero for negative F^2. The threshold expression of $F^2 > \sigma(F^2)$ is used only for calculating R-factors(gt) *etc*. and is not relevant to the choice of reflections for refinement. R-factors based on F^2 are statistically about twice as large as those based on F, and R- factors based on ALL data will be even larger.

Fractional atomic coordinates and isotropic or equivalent isotropic displacement parameters (Å^2)

	x	y	z	U_{iso}*/U_{eq}
O1	0.00502 (11)	0.47448 (8)	0.64153 (5)	0.02756 (18)
N1	0.15001 (13)	0.33590 (10)	0.65000 (6)	0.0270 (2)
C1	0.25346 (14)	0.36020 (11)	0.70485 (6)	0.0222 (2)
C2	0.42780 (15)	0.24940 (11)	0.73381 (6)	0.0226 (2)
O2	0.49243 (11)	0.11970 (8)	0.71482 (5)	0.02828 (18)
N2	0.51293 (12)	0.31237 (9)	0.78613 (5)	0.02217 (19)
N3	0.44085 (12)	0.45480 (9)	0.81882 (5)	0.0235 (2)
C3	0.28457 (14)	0.54911 (11)	0.79389 (6)	0.0224 (2)
C4	0.18507 (14)	0.50724 (11)	0.73305 (6)	0.0217 (2)
C5	0.02762 (15)	0.57547 (12)	0.69057 (6)	0.0232 (2)
C6	0.69832 (14)	0.22965 (11)	0.81342 (7)	0.0224 (2)
C7	0.85159 (15)	0.16976 (11)	0.75336 (7)	0.0260 (2)
H7	0.8334	0.1771	0.6949	0.030 (3)*
C8	1.03243 (15)	0.09880 (12)	0.77969 (7)	0.0278 (2)
H8	1.1385	0.0572	0.739	0.034 (3)*
C9	1.05866 (16)	0.08840 (12)	0.86484 (7)	0.0284 (2)

H9	1.1823	0.0391	0.8826	0.033 (3)*
C10	0.90441 (16)	0.15001 (12)	0.92425 (7)	0.0273 (2)
H10	0.9229	0.1434	0.9827	0.032 (3)*
C11	0.72289 (15)	0.22140 (11)	0.89891 (7)	0.0248 (2)
H11	0.6171	0.264	0.9396	0.025 (3)*
C12	0.21729 (16)	0.69938 (12)	0.83066 (8)	0.0295 (2)
H12A	0.3036	0.7028	0.8717	0.039 (4)*
H12B	0.0879	0.7216	0.8591	0.039 (4)*
H12C	0.2161	0.7725	0.7854	0.043 (4)*
C13	−0.11611 (15)	0.72853 (12)	0.68583 (7)	0.0255 (2)
H13	−0.0688	0.7945	0.7162	0.019 (3)*
C14	−0.31156 (15)	0.73629 (12)	0.73267 (7)	0.0279 (2)
H14A	−0.4109	0.831	0.7186	0.032 (3)*
H14B	−0.3481	0.6549	0.7141	0.029 (3)*
C15	−0.29925 (14)	0.72404 (12)	0.82684 (7)	0.0256 (2)
C16	−0.24282 (15)	0.58718 (12)	0.86891 (7)	0.0280 (2)
H16	−0.222	0.5	0.8387	0.028 (3)*
C17	−0.21682 (16)	0.57717 (13)	0.95421 (7)	0.0306 (3)
H17	−0.1802	0.4835	0.9822	0.038 (4)*
C18	−0.24399 (15)	0.70303 (13)	0.99886 (7)	0.0302 (3)
H18	−0.2237	0.6958	1.0571	0.034 (3)*
C19	−0.30114 (15)	0.83994 (13)	0.95784 (7)	0.0296 (2)
H19	−0.3209	0.9268	0.9882	0.032 (3)*
C20	−0.32932 (15)	0.85002 (12)	0.87290 (7)	0.0278 (2)
H20	−0.3697	0.9442	0.8456	0.034 (3)*
C21	−0.12730 (16)	0.78383 (13)	0.59301 (7)	0.0302 (3)
H21A	−0.1683	0.7183	0.5602	0.029 (3)*
H21B	−0.2235	0.8846	0.5907	0.038 (4)*
C22	0.13242 (17)	0.89367 (13)	0.57720 (7)	0.0308 (3)
H22	0.0532	0.9691	0.6146	0.037 (4)*
C23	0.31273 (18)	0.89326 (13)	0.54685 (7)	0.0336 (3)
H23	0.357	0.9668	0.5641	0.039 (4)*
C24	0.42832 (17)	0.78538 (14)	0.49126 (7)	0.0343 (3)
H24	0.5519	0.7848	0.47	0.039 (4)*
C25	0.36233 (18)	0.67858 (14)	0.46702 (7)	0.0355 (3)
H25	0.4407	0.6048	0.4285	0.046 (4)*
C26	0.18236 (18)	0.67824 (13)	0.49847 (7)	0.0322 (3)
H26	0.1394	0.6036	0.4817	0.036 (3)*
C27	0.06465 (16)	0.78583 (12)	0.55409 (7)	0.0271 (2)

Atomic displacement parameters (Å^2)

	U^{11}	U^{22}	U^{33}	U^{12}	U^{13}	U^{23}
O1	0.0275 (4)	0.0247 (4)	0.0302 (4)	−0.0066 (3)	−0.0104 (3)	0.0004 (3)
N1	0.0273 (5)	0.0231 (5)	0.0295 (5)	−0.0062 (4)	−0.0071 (4)	0.0001 (4)
C1	0.0238 (5)	0.0218 (5)	0.0219 (5)	−0.0093 (4)	−0.0024 (4)	0.0019 (4)
C2	0.0245 (5)	0.0203 (5)	0.0230 (5)	−0.0085 (4)	−0.0019 (4)	0.0013 (4)
O2	0.0309 (4)	0.0197 (4)	0.0334 (4)	−0.0068 (3)	−0.0064 (3)	−0.0008 (3)
N2	0.0219 (4)	0.0175 (4)	0.0257 (4)	−0.0045 (3)	−0.0044 (3)	0.0001 (3)
N3	0.0227 (4)	0.0194 (4)	0.0273 (5)	−0.0057 (3)	−0.0033 (3)	−0.0016 (3)
C3	0.0203 (5)	0.0218 (5)	0.0249 (5)	−0.0074 (4)	−0.0030 (4)	0.0017 (4)
C4	0.0218 (5)	0.0200 (5)	0.0229 (5)	−0.0075 (4)	−0.0013 (4)	0.0021 (4)
C5	0.0232 (5)	0.0241 (5)	0.0236 (5)	−0.0094 (4)	−0.0042 (4)	0.0017 (4)

C6	0.0216 (5)	0.0163 (5)	0.0296 (5)	−0.0063 (4)	−0.0059 (4)	0.0031 (4)
C7	0.0282 (6)	0.0219 (5)	0.0261 (5)	−0.0065 (4)	−0.0039 (4)	0.0013 (4)
C8	0.0244 (5)	0.0222 (5)	0.0336 (6)	−0.0045 (4)	−0.0011 (4)	−0.0012 (4)
C9	0.0241 (5)	0.0215 (5)	0.0383 (6)	−0.0049 (4)	−0.0097 (4)	0.0030 (4)
C10	0.0300 (6)	0.0238 (5)	0.0283 (6)	−0.0083 (4)	−0.0089 (4)	0.0037 (4)
C11	0.0249 (5)	0.0219 (5)	0.0273 (5)	−0.0081 (4)	−0.0027 (4)	0.0013 (4)
C12	0.0243 (5)	0.0244 (6)	0.0389 (6)	−0.0051 (4)	−0.0086 (5)	−0.0052 (5)
C13	0.0237 (5)	0.0230 (5)	0.0295 (6)	−0.0065 (4)	−0.0082 (4)	0.0033 (4)
C14	0.0224 (5)	0.0244 (6)	0.0363 (6)	−0.0064 (4)	−0.0080 (4)	0.0026 (4)
C15	0.0171 (5)	0.0251 (5)	0.0349 (6)	−0.0078 (4)	−0.0035 (4)	0.0023 (4)
C16	0.0235 (5)	0.0232 (5)	0.0387 (6)	−0.0097 (4)	−0.0046 (4)	0.0010 (5)
C17	0.0270 (6)	0.0267 (6)	0.0391 (6)	−0.0116 (4)	−0.0044 (5)	0.0081 (5)
C18	0.0246 (5)	0.0354 (6)	0.0303 (6)	−0.0111 (5)	−0.0002 (4)	0.0022 (5)
C19	0.0230 (5)	0.0274 (6)	0.0365 (6)	−0.0072 (4)	0.0013 (4)	−0.0040 (5)
C20	0.0210 (5)	0.0214 (5)	0.0384 (6)	−0.0050 (4)	−0.0018 (4)	0.0033 (4)
C21	0.0293 (6)	0.0295 (6)	0.0318 (6)	−0.0084 (5)	−0.0124 (5)	0.0076 (5)
C22	0.0362 (6)	0.0266 (6)	0.0277 (6)	−0.0081 (5)	−0.0059 (5)	0.0013 (4)
C23	0.0416 (7)	0.0345 (6)	0.0302 (6)	−0.0188 (5)	−0.0100 (5)	0.0050 (5)
C24	0.0332 (6)	0.0421 (7)	0.0279 (6)	−0.0138 (5)	−0.0056 (5)	0.0075 (5)
C25	0.0425 (7)	0.0348 (7)	0.0256 (6)	−0.0099 (5)	−0.0003 (5)	−0.0002 (5)
C26	0.0437 (7)	0.0307 (6)	0.0251 (5)	−0.0153 (5)	−0.0088 (5)	0.0018 (4)
C27	0.0304 (6)	0.0271 (6)	0.0235 (5)	−0.0081 (4)	−0.0116 (4)	0.0078 (4)

Geometric parameters (Å, º)

O1—C5	1.3506 (13)	C13—H13	1.0
O1—N1	1.4100 (11)	C14—C15	1.5067 (16)
N1—C1	1.3138 (14)	C14—H14A	0.99
C1—C4	1.4122 (14)	C14—H14B	0.99
C1—C2	1.4734 (14)	C15—C20	1.3937 (16)
C2—O2	1.2176 (13)	C15—C16	1.3968 (15)
C2—N2	1.3873 (13)	C16—C17	1.3857 (17)
N2—N3	1.3979 (12)	C16—H16	0.95
N2—C6	1.4434 (13)	C17—C18	1.3851 (17)
N3—C3	1.2961 (13)	C17—H17	0.95
C3—C4	1.4425 (15)	C18—C19	1.3898 (16)
C3—C12	1.4909 (15)	C18—H18	0.95
C4—C5	1.3688 (15)	C19—C20	1.3839 (17)
C5—C13	1.4986 (14)	C19—H19	0.95
C6—C7	1.3851 (15)	C20—H20	0.95
C6—C11	1.3869 (15)	C21—C27	1.5105 (16)
C7—C8	1.3906 (16)	C21—H21A	0.99
C7—H7	0.95	C21—H21B	0.99
C8—C9	1.3835 (16)	C22—C23	1.3850 (17)
C8—H8	0.95	C22—C27	1.3940 (16)
C9—C10	1.3861 (16)	C22—H22	0.95
C9—H9	0.95	C23—C24	1.3847 (18)
C10—C11	1.3895 (15)	C23—H23	0.95
C10—H10	0.95	C24—C25	1.3825 (18)
C11—H11	0.95	C24—H24	0.95

C12—H12A	0.98	C25—C26	1.3893 (18)
C12—H12B	0.98	C25—H25	0.95
C12—H12C	0.98	C26—C27	1.3881 (16)
C13—C21	1.5431 (15)	C26—H26	0.95
C13—C14	1.5492 (15)		

C5—O1—N1	110.86 (8)	C14—C13—H13	107.2
C1—N1—O1	103.37 (8)	C15—C14—C13	109.92 (8)
N1—C1—C4	113.41 (9)	C15—C14—H14A	109.7
N1—C1—C2	124.88 (9)	C13—C14—H14A	109.7
C4—C1—C2	121.68 (9)	C15—C14—H14B	109.7
O2—C2—N2	123.36 (9)	C13—C14—H14B	109.7
O2—C2—C1	125.71 (10)	H14A—C14—H14B	108.2
N2—C2—C1	110.93 (9)	C20—C15—C16	118.33 (10)
C2—N2—N3	127.80 (8)	C20—C15—C14	119.92 (10)
C2—N2—C6	120.74 (8)	C16—C15—C14	121.55 (10)
N3—N2—C6	111.46 (8)	C17—C16—C15	120.73 (10)
C3—N3—N2	119.61 (9)	C17—C16—H16	119.6
N3—C3—C4	120.23 (9)	C15—C16—H16	119.6
N3—C3—C12	116.70 (9)	C18—C17—C16	120.33 (10)
C4—C3—C12	123.07 (9)	C18—C17—H17	119.8
C5—C4—C1	104.21 (9)	C16—C17—H17	119.8
C5—C4—C3	136.51 (10)	C17—C18—C19	119.48 (11)
C1—C4—C3	119.28 (9)	C17—C18—H18	120.3
O1—C5—C4	108.15 (9)	C19—C18—H18	120.3
O1—C5—C13	115.96 (9)	C20—C19—C18	120.14 (11)
C4—C5—C13	135.89 (10)	C20—C19—H19	119.9
C7—C6—C11	121.11 (10)	C18—C19—H19	119.9
C7—C6—N2	119.36 (9)	C19—C20—C15	120.97 (10)
C11—C6—N2	119.33 (9)	C19—C20—H20	119.5
C6—C7—C8	119.17 (10)	C15—C20—H20	119.5
C6—C7—H7	120.4	C27—C21—C13	110.58 (9)
C8—C7—H7	120.4	C27—C21—H21A	109.5
C9—C8—C7	120.33 (10)	C13—C21—H21A	109.5
C9—C8—H8	119.8	C27—C21—H21B	109.5
C7—C8—H8	119.8	C13—C21—H21B	109.5
C8—C9—C10	119.94 (10)	H21A—C21—H21B	108.1
C8—C9—H9	120.0	C23—C22—C27	121.42 (11)
C10—C9—H9	120.0	C23—C22—H22	119.3
C9—C10—C11	120.40 (10)	C27—C22—H22	119.3
C9—C10—H10	119.8	C24—C23—C22	119.85 (11)
C11—C10—H10	119.8	C24—C23—H23	120.1
C6—C11—C10	119.05 (10)	C22—C23—H23	120.1
C6—C11—H11	120.5	C25—C24—C23	119.42 (11)
C10—C11—H11	120.5	C25—C24—H24	120.3
C3—C12—H12A	109.5	C23—C24—H24	120.3
C3—C12—H12B	109.5	C24—C25—C26	120.56 (11)
H12A—C12—H12B	109.5	C24—C25—H25	119.7
C3—C12—H12C	109.5	C26—C25—H25	119.7
H12A—C12—H12C	109.5	C27—C26—C25	120.70 (11)

H12B—C12—H12C	109.5	C27—C26—H26	119.6
C5—C13—C21	110.34 (9)	C25—C26—H26	119.6
C5—C13—C14	110.96 (9)	C26—C27—C22	118.05 (11)
C21—C13—C14	113.70 (9)	C26—C27—C21	121.96 (10)
C5—C13—H13	107.2	C22—C27—C21	119.91 (10)
C21—C13—H13	107.2		
C5—O1—N1—C1	0.42 (11)	C6—C7—C8—C9	−0.07 (16)
O1—N1—C1—C4	−0.08 (11)	C7—C8—C9—C10	−0.54 (16)
O1—N1—C1—C2	−178.31 (9)	C8—C9—C10—C11	0.47 (16)
N1—C1—C2—O2	−4.53 (17)	C7—C6—C11—C10	−0.83 (16)
C4—C1—C2—O2	177.38 (10)	N2—C6—C11—C10	−175.73 (9)
N1—C1—C2—N2	174.91 (10)	C9—C10—C11—C6	0.20 (16)
C4—C1—C2—N2	−3.18 (13)	O1—C5—C13—C21	−53.31 (12)
O2—C2—N2—N3	−172.66 (9)	C4—C5—C13—C21	125.98 (13)
C1—C2—N2—N3	7.88 (14)	O1—C5—C13—C14	73.63 (11)
O2—C2—N2—C6	7.42 (15)	C4—C5—C13—C14	−107.07 (14)
C1—C2—N2—C6	−172.03 (8)	C5—C13—C14—C15	71.49 (11)
C2—N2—N3—C3	−6.84 (15)	C21—C13—C14—C15	−163.44 (9)
C6—N2—N3—C3	173.09 (9)	C13—C14—C15—C20	86.05 (12)
N2—N3—C3—C4	0.28 (14)	C13—C14—C15—C16	−88.63 (12)
N2—N3—C3—C12	−179.32 (9)	C20—C15—C16—C17	−0.22 (15)
N1—C1—C4—C5	−0.26 (12)	C14—C15—C16—C17	174.54 (10)
C2—C1—C4—C5	178.03 (9)	C15—C16—C17—C18	−0.90 (16)
N1—C1—C4—C3	179.63 (9)	C16—C17—C18—C19	1.23 (16)
C2—C1—C4—C3	−2.08 (15)	C17—C18—C19—C20	−0.44 (16)
N3—C3—C4—C5	−176.42 (11)	C18—C19—C20—C15	−0.69 (16)
C12—C3—C4—C5	3.15 (19)	C16—C15—C20—C19	1.01 (15)
N3—C3—C4—C1	3.73 (15)	C14—C15—C20—C19	−173.84 (10)
C12—C3—C4—C1	−176.70 (10)	C5—C13—C21—C27	−59.69 (12)
N1—O1—C5—C4	−0.60 (11)	C14—C13—C21—C27	174.90 (9)
N1—O1—C5—C13	178.88 (8)	C27—C22—C23—C24	1.06 (17)
C1—C4—C5—O1	0.51 (11)	C22—C23—C24—C25	−0.34 (17)
C3—C4—C5—O1	−179.35 (11)	C23—C24—C25—C26	−0.50 (17)
C1—C4—C5—C13	−178.82 (11)	C24—C25—C26—C27	0.65 (17)
C3—C4—C5—C13	1.3 (2)	C25—C26—C27—C22	0.05 (16)
C2—N2—C6—C7	56.43 (13)	C25—C26—C27—C21	−176.67 (10)
N3—N2—C6—C7	−123.50 (10)	C23—C22—C27—C26	−0.90 (16)
C2—N2—C6—C11	−128.58 (10)	C23—C22—C27—C21	175.88 (10)
N3—N2—C6—C11	51.49 (12)	C13—C21—C27—C26	103.38 (12)
C11—C6—C7—C8	0.76 (16)	C13—C21—C27—C22	−73.27 (12)
N2—C6—C7—C8	175.67 (9)		

Hydrogen-bond geometry (Å, º)

D—H···*A*	*D*—H	H···*A*	*D*···*A*	*D*—H···*A*
C26—H26···O1^{i}	0.95	2.61	3.4159 (13)	143
C24—H24···N1^{ii}	0.95	2.73	3.5407 (15)	143
C11—H11···C18^{iii}	0.95	2.78	3.6182 (15)	148

Symmetry codes: (i) −*x*, −*y*+1, −*z*+1; (ii) −*x*+1, −*y*+1, −*z*+1; (iii) −*x*, −*y*+1, −*z*+2

Acknowledgements

NRN, JM, CG and CK thank the National Institutes of Health for grants NINDS P20RR015583 Center for Structural and Functional Neuroscience (CSFN) and P20 RR017670 Center for Environmental Health Sciences (CEHS), We also thankNINDS P30 (NN and JM), and the University of Montana Grant Program (NN).

References

(1) Bruker. No Title. *SMART, SAINT SADABS. Bruker AXS Inc.* **2012**.

(2) Chimichi, S.; Ciciani, G.; Piaz, V. D.; De Sio, F.; Sarti-Fantoni, P.; Torroba, T. Solid State Photodimerization Reaction of Some 3-Styrylisoxazolo-[3,4-d]Pyridazin-7(6h)-Ones. *Heterocycles* **1986**, *24* (12), 3467–3471 DOI: 10.3987/R-1986-12-3467.

(3) Dal Piaz, V., Ciciani, G. and C. New Functionalized Pyrazoles from Isoxazolopyridazinones. *S. Heterocycles* **1985**, *23*, 365–369.

(4) Dal Piaz, V.; Pinzauti, S.; Lacrimini, P. J. Condensation of Some 3-Methylisoxazolo[3,4-d]Pyridazin-7(6H)Ones with Aromatic Aldehydes. *Heterocycl. Chem.* **1975**, *13*, 409–410.

(5) Hulubei, V.; Meikrantz, S. B.; Quincy, D. A.; Houle, T.; McKenna, J. I.; Rogers, M. E.; Steiger, S.; Natale, N. R. 4-Isoxazolyl-1,4-Dihydropyridines Exhibit Binding at the Multidrug-Resistance Transporter. *Bioorganic Med. Chem.* **2012**, *20* (22), 6613–6620 DOI: 10.1016/j.bmc.2012.09.022.

(6) Macrae, C. F.; Bruno, I. J.; Chisholm, J. A.; Edgington, P. R.; McCabe, P.; Pidcock, E.; Rodriguez-Monge, L.; Taylor, R.; Van De Streek, J.; Wood, P. A. Mercury CSD 2.0 – New Features for the Visualization and Investigation of Crystal Structures. *urn:issn:0021-8898* **2008**, *41* (2), 466–470 DOI: 10.1107/S0021889807067908.

(7) Nakamura, M.; Kurihara, H.; Suzuki, G.; Mitsuya, M.; Ohkubo, M.; Ohta, H. Isoxazolopyridone Derivatives as Allosteric Metabotropic Glutamate Receptor 7 Antagonists. *Bioorganic Med. Chem. Lett.* **2010**, *20* (2), 726–729 DOI: 10.1016/j.bmcl.2009.11.070.

(8) Natale, N. R.; McKenna, J. I.; Niou, C. S.; Borth, M.; Hope, H. Metalation of Isoxazolyloxazolines, a Facile Route to Functionally Complex Isoxazoles: Utility, Scope, and Comparison to Dianion Methodology. *J. Org. Chem.* **1985**, *50* (26), 5660–5666 DOI: 10.1021/jo00350a047.

(9) Natale, N. R.; Mirzaei, Y. R. The Lateral Metalation of Isoxazoles. A Review. *Org. Prep. Proced. Int.* **1993**, *25* (5), 515–556 DOI: 10.1080/00304949309457997.

(10) Natale, N. R.; Niou, C. S. A Facile Synthesis of Functionally Complex Isoxazole Derivatives. *Tetrahedron Lett.* **1984**, *25* (36), 3943–3946 DOI: 10.1016/0040-4039(84)80036-2.

(11) R. Natale, N.; Niou, C.-S. Synthesis, Metalation and Electrophilic Quenching of Alkyl-Isoxazole-4-Tertiary Carboxamides. A Critical Comparison of Three Isoxazole Lateral Metalation Methods. *Heterocycles* **1986**, *24* (2), 401 DOI: 10.3987/r-1986-02-0401.

(12) Renzi, G. and Dal Piaz, V. Ricerche Su Alcuni 3-Carbetossi-Isossazoli-4,5-Disostituiti. *Gazz. Chim. It.* **1965**, *95*, 1478–1491.

(13) Schlicksupp, L.; Natale, N. R. Regioselectivity in Lateral Deprotonation of an Isoxazolecarboxamide of (S)-Prolinol. Conformational Correlation by Crystal Structure Solid State Solution 13C NMR. *J. Heterocycl. Chem.* **1987**, *24* (5), 1345–1348 DOI: 10.1002/JHET.5570240522.

(14) Sheldrick, G. M.; IUCr. A Short History of SHELX. *urn:issn:0108-7673* **2007**, *64* (1), 112–122 DOI: 10.1107/S0108767307043930.

(15) Westrip, S. P.; IUCr. PublCIF: Software for Editing, Validating and Formatting Crystallographic Information Files. *urn:issn:0021-8898* **2010**, *43* (4), 920–925 DOI: 10.1107/S0021889810022120.

Ch. 4 The lateral metalation of isoxazolo[3,4-d]pyridazinones and development of a hit-to-lead series of selective positive modulators of metabotropic glutamate receptors

Introduction

The mGluRs are members of the class C of g-protein coupled receptors (GPCR). The mGluRs consist of a venus flytrap domain (VFD) which contains the orthosteric glutamate binding site, and the seven transmembrane (7TM) domain which contain the allosteric site. The mGluRs are located on both post- and pre-synaptic neurons and are involved with signal regulation. Compounds that target mGluRs are important for the treatment of a variety of central nervous system (CNS) disorders, as well as cancer.[1,2,3,4,5] The class is further broken down into 3 subgroups by sequence homology. Subgroup 1 has the excitatory receptors, $mGluR_1$ and $mGluR_5$. Subgroup 2, ($mGluR_{2-3}$) and Subgroup 3 ($mGluR_{4,\ 6-8}$) are inhibitory. [6] Each has therapeutic application associated with them. In particular,$mGluR_2$ is a target for treatment of anxiety and schizophrenia, while activation of $mGluR_4$ helps to ease the symptoms of Parkinson's disease and may even slow progress of the disease. [1,2,7,8] Although there is high sequence homology between the subgroups as well as within, the allosteric sites are less conserved and present a better opportunity to develop novel small molecules to selectively target them. We developed a first series of isoxazolo[3,4-d] pyridazinones (3,4-ds) using synthetic methods by Renzi and Dal Piaz[9–15]. We found that they had selective activity at $mGluR_2$ and $mGluR_4$. We want to further elaborate this series with liphophilic groups and further explore the allosteric site.

Structure active development

Homology model: general experimental

For the allosteric binding site the crystal coordinates of $mGluR_1$, PDB accession number 4OR2,[16] were used, the calculation were performed using Autodock Vina for $mGluR_2$ and Discovery Studio for mGlu For Discovery Studio the protein structures were typed with the CHARMm forcefield[17]

and energy was minimized with the smart minimizer protocol within Discovery Studio[18] using the Generalized-Born with simple switching implicit solvent model to a root mean square gradient (RMS) convergence <0.001 kcal/mol prior to use in the docking studies. Docking was performed using the flexible docking protocol,[19] which allows for flexibility in both the ligand and the binding site residues. The amino acid residues within the allosteric site were allowed to attain anoptimum conformation using flexible docking. For example in $mGluR_4$ eleven residues were selected based on Feng's model of allosteric activation,[19] and with numbering according to Isberg:[33] Leu659$^{3.36}$, Met663$^{3.40}$, Leu 753$^{5.40}$, Leu756$^{5.43}$, Leu757$^{5.44}$, Thr794$^{6.46}$, Trp798$^{6.50}$, Phe801$^{6.53}$, Phe805$^{6.57}$, Leu 822$^{7.32}$, and Val826$^{7.36}$. (**Figure 4-2**)

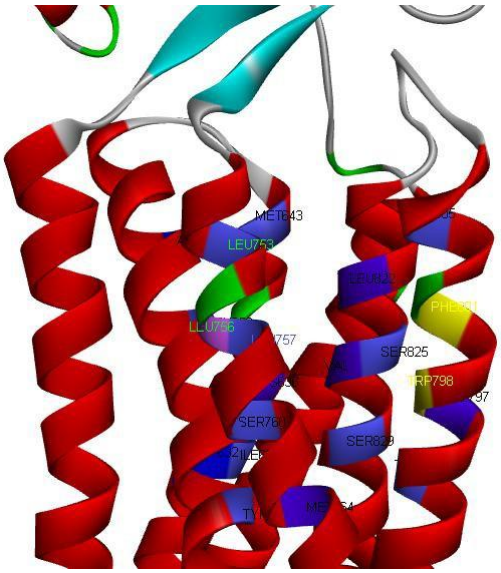

Figure 4-2: **allosteric site of $mGluR_4$ with all allosteric residues highlighted. In yellow is the hinge region made up of Phe 801 and Trp 798 and in light purple is Leu 756 which is unique to $mGluR_4$.**

The final ranking of the docked poses was performed via consensus scoring, combining the predicted binding energy with the Jain,[19] PLP2,[20] and Ludi3[21] scoring functions. The best poses for each compound in the training set uses a weighted consensus for each of the several scoring functions compared.

Homology model: allosteric site

We moved forward with modeling of the second series, based on the most activity from our previous study of the 1st series of 3,4-ds. Using information from the 1st series modeling, in additional to information provided from the literature about unique residues in the allosteric site as well as hot spots for selectivity among the different sub-types. [22,23,24,25.26,27,28, 29, 30,2] Modeling of the known allosteric ligands shown in Figure 4-3 were used as reference, and provided critical understanding of crucial interactions and potential functional groups tolerated.

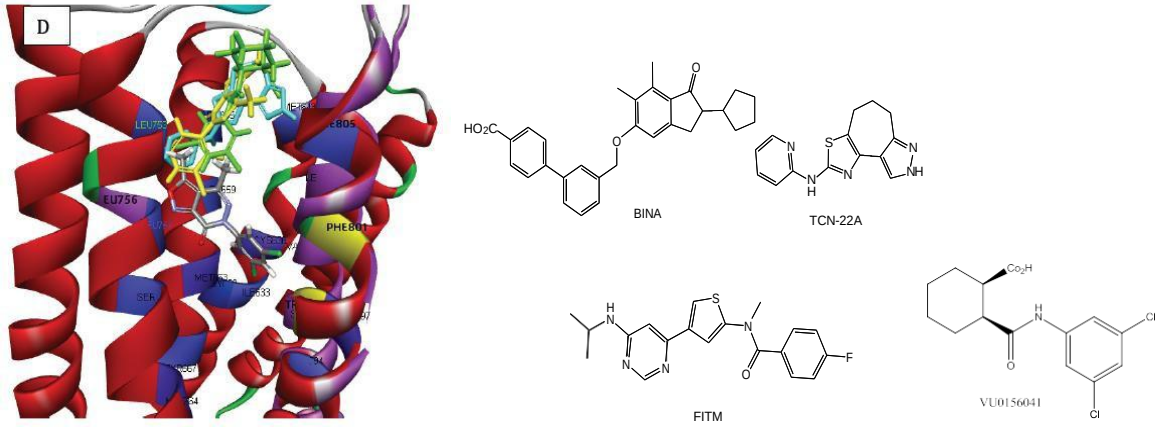

Figure 4-3 **Overlay of VU0155041 (green), TCN22A (cyan)** and the first series highest activity

Predictions using the Discovery Studio platform

With the above information and the observed "tumbling" motion that was observed in the 1st series, modeling was intriguing. (Figure 4-4). For the 3-position substituted analogs are more extending in their conformation and could possibly have room to enter the allosteric site and occupy this area observed in the 1st series.[31]

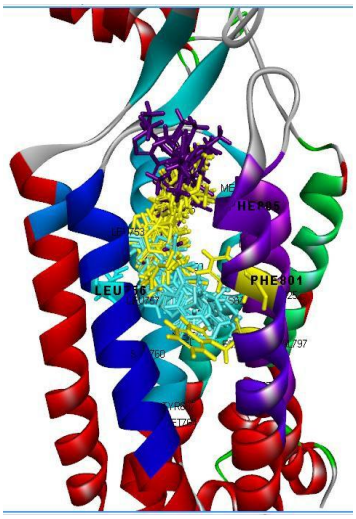

Figure 4-4 All modeling binding poses of [3,4-d] 3,5-Cl_2 overlayed

The second series of compounds with liphophilic groups at the C3 and C4 position on the 3,4-ds modeling results were in general agreement with the literature and reference ligands in relation to overall topology being similar in the allosteric site, but also bearing functional group interacting with the same region to other known mGluR ligands.

Our modeling showed that not only did the 2nd series of molecules follow this same "tumbling" path, as highlighted in the 1st series modeling, but also gained more interactions with the Phe 801 and Trp 498 at the hinge region as well as at Leu 756 (Figure 4-4 and 4-5) in $mGluR_4$ and the Mets in $mGluR_2$. We also observed some interesting interaction with the cysteine linker and the potential that a chiral center could have in providing key interactions. (**Table 4-1**) The binding energy scores overall were better than those from the 1st series. Two notable substitutions were found to have predicted higher binding energies than VU0155041, with disubstitution of benzyl groups, and unsymmetrical substitution which produces a chiral center which has a significant computational eudismic ratio. The highest binding energy was predicted for the dibenzyl substitution. Two notable features are encouraging in this calculation (**1**) the ligand occupies the allosteric middle vestibule position associated with higher potency, and **(2**) an interaction with

the unique Leu756 gives a realistic anticipation for selectivity (**Figure 4-5**).

We selected a training set of ligands accessible by our synthetic methodology for study.

Table 4-1: 2nd series top scoring poses for $mGluR_4$

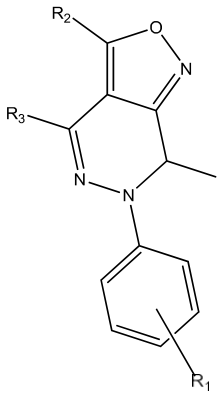

	R_1	R_2	R_3	Binding (kcal/mol)
*	FITM			-138.878
1	3,5 Cl2	Mono-Bn	Me	-42.4299
2	3,5 Cl_2	diBn	Me	-24.6093
3	3,5 Cl_2	1-napthyl	Me	-39.5892
4	Tol	Me	4-Ph	-70.1691
5	Tol	Mono- Bn	Me	-79.2557
6	Tol	diBn	Me	-97.1876
7	Tol	(R) - PhPr	Me	-77.8074
8	Tol	(S) - PhPr	Me	-85.1114
9	3,5-CF_3	Mono-Bn	Me	-38.3177
10	p-OCH_3	Mono-Bn	Me	-39.8292

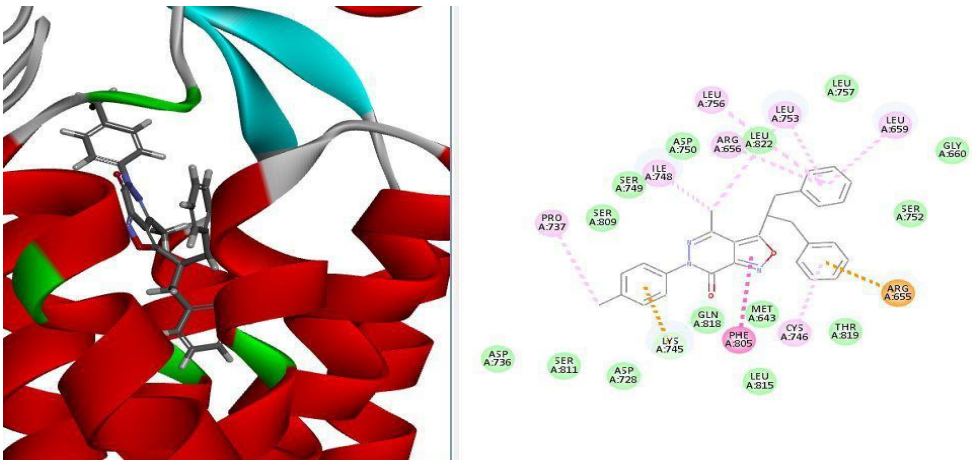

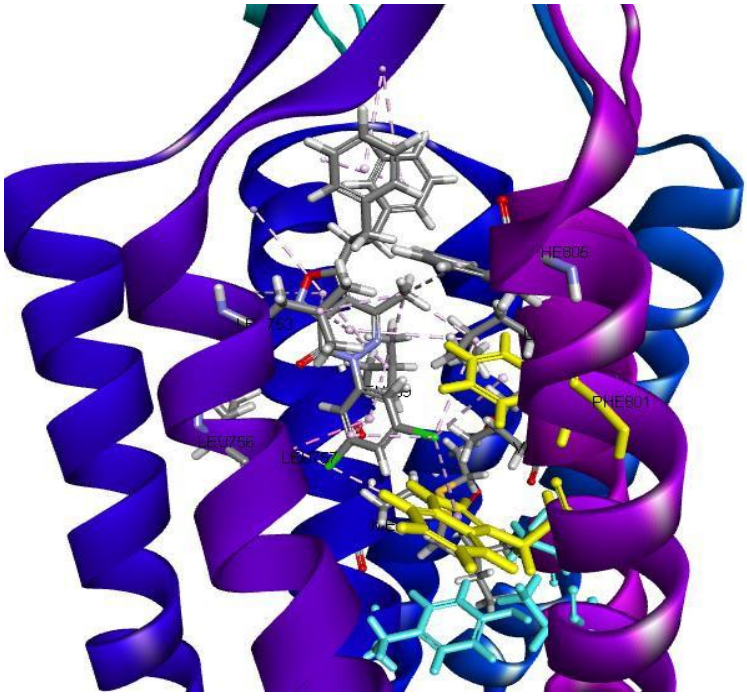

Figure 4-5 **Highest binding energy for the 3,5-Cl_2 Illustrates not only additional potential interactions with the hinge region residues Trp498 and Phe801 and the selective residue Leu756. There are additional interesting interactions as well as an interesting one between the dibn and the cysteine linker.**

Chemistry, Results, and Discussion

The lipohphillic phenyl group was incorporated at the C4 in the [3,4-d] ring via the condensation of 4-phenylacetyl-3-carbox-yethyl-5-methyl isoxazole with the corresponding hydrazine to generate the 3,4-ds. (**Scheme 4-1**) With this substitution the previously observed E to Z converse that was necessary for the 3,4-d ring closure was observed, but more frequently

the reaction would be stopped at the open ring. To try to push the reaction toward ring closure, a strerically hindered non-nucleophillic base was introduced. This helped to improve reaction times but not necessarily yield, and also led to the kemp elimination product being observed.(**Scheme 4-1**)

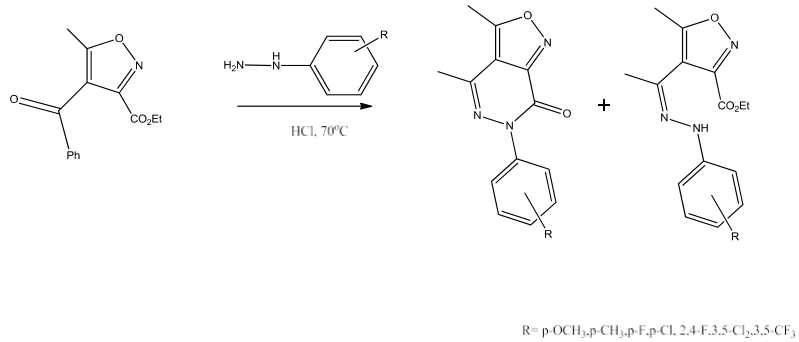

Scheme 4-1 formation of the [3,4-d] from the phenyl isoxazole ester

For the selective addition of functional group at the C3 of the isoxazole, lateral metalation was explored. We are continuing our interest in lateral metalation of isoxazoles.[32,33, 34] This route would provide more direct access to functionalize the C3 of the isoxazole more readily in fewer steps. This was first done by Renzi and Dal Piaz[35], with the first practical syntheses of the isoxazolo[3,4-d] pyridazinones 1, which was found to both possess interesting biological activity,[36,37,38,39] and serve as useful and versatile precursors in medicinal chemistry synthesis[35,40,41,42,43,44,45,46]. An interesting note by earlier reports was that deprotonation of this system occurs with very short reaction times - on the order of 2 minutes - and allowed for isolation of beta hydroxyl adduct 2. Just slightly longer reaction times (5 minutes) gave elimination to the styrl products 3.[14,47](**Scheme 4-2**)

A drawback is that under the strongly basic conditions employed, extended reflux times lead to a rise in the observation of structural rearrangements.[35]

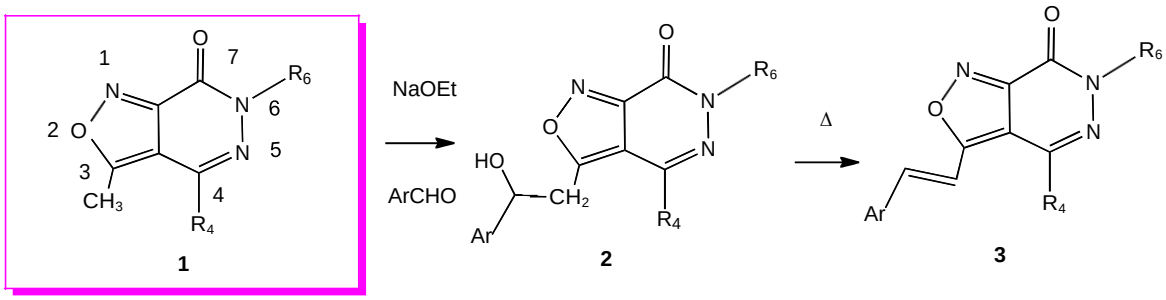

Scheme 4-2. Isoxazolo[3,4-d] pyridazinone numbering, and previous studies by the dal Piaz group.

One such example is the [3,4-d] 3 shown in **Figure 4-2**. When warmed with sodium hydroxide or alkoxide, attack at the 7-carbonyl gave rise to presumed tetrahedral intermediate, (i) which decarboxylates (ii) giving rise to the isoxazolyl-anion **4**, and rapid Kemp elimination proceeds to ring opening.[7] Two pathways for intramolecular ring closure have been described: (1) bond rotation and ring closure on the carbonyl of **6**, followed by ring closure to cyano-pyrazole **7**, or alternatively gong from **2** through ring closure on the nitrile of **5**, which after tautomerization to the keto-pyrazole **8**. In our hands, we observed only 8 for the examples examined. (**Figure 4-6**)

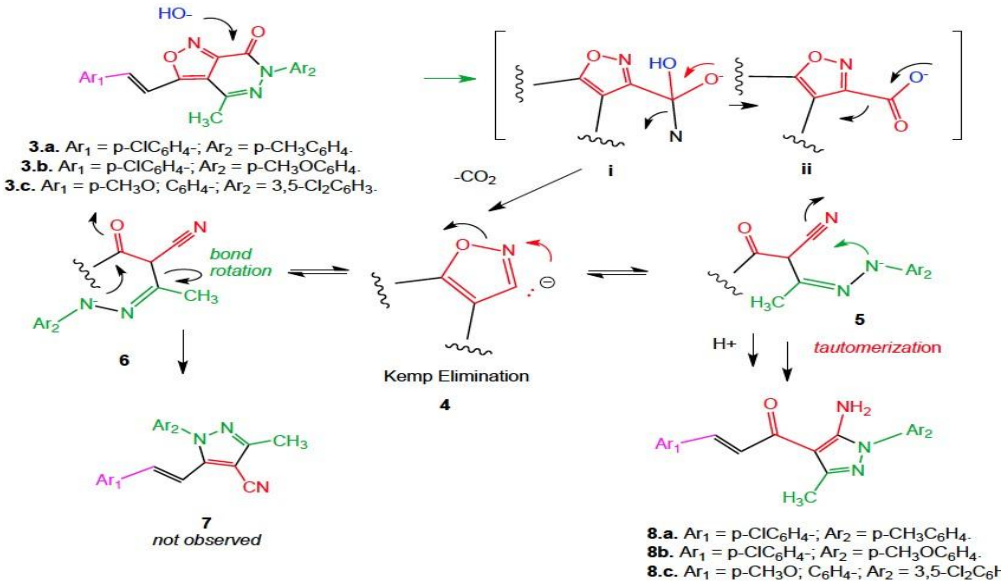

Figure 4-6. Extended reflux in aqueous ethanol produces rearrangement products arising from ring opening of the isoxazole. While two pathways had previously been reported, in our hands only the keto-pyrazole 8 was observed.

For our 3,4-d system we found that LiHMDs or LDA were sufficiently basic enough and sterically hinder enough to produce the desired functionalized products selectively at 3-positionisoxazole from the acetal protected ester using methodology we have previously reported.[48,49] Deprotection of the acetal, followed by reaction with substituted hydrazines produced authentic monosubstituted isoxazolo [3,4-d] pyridazinones. However, the presence of large aromatic groups in the C3 position also remarkably slows the rate of ring closure to the [3,4-d] product. Whereas C4 methyl analogs ring close - with acid catalysis - from the intermediate hydrazone almost completely in a few hours, in contrast, the C3 arylethyl derivatives gave only partial ringclosure after reaction times an order of magnitude longer. (**Scheme 4-3**)

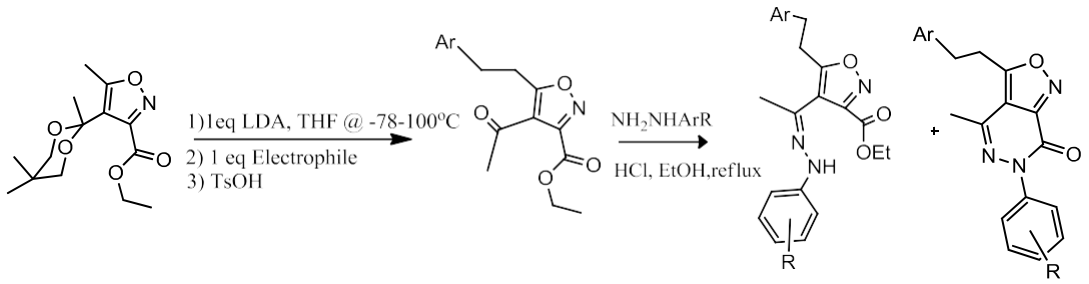

Scheme 4-3. Multi-step synthesis of the mono-benzyl of the [3,4-d]s

Directly laterally metalating the 3,4-ds would provide monosubstituted product in fewer steps as well as avoiding the ring closure issues to finish forming the 3,4-d. This method did present interesting synthteic challenge. Due to the N6-aryl groups being present already, some with halogens, there is the potential for halogen/metal exchange or benzyne formation with strong base (i.e, the 3,5-dichloro, *vide infra*) **Figure 4-7**.

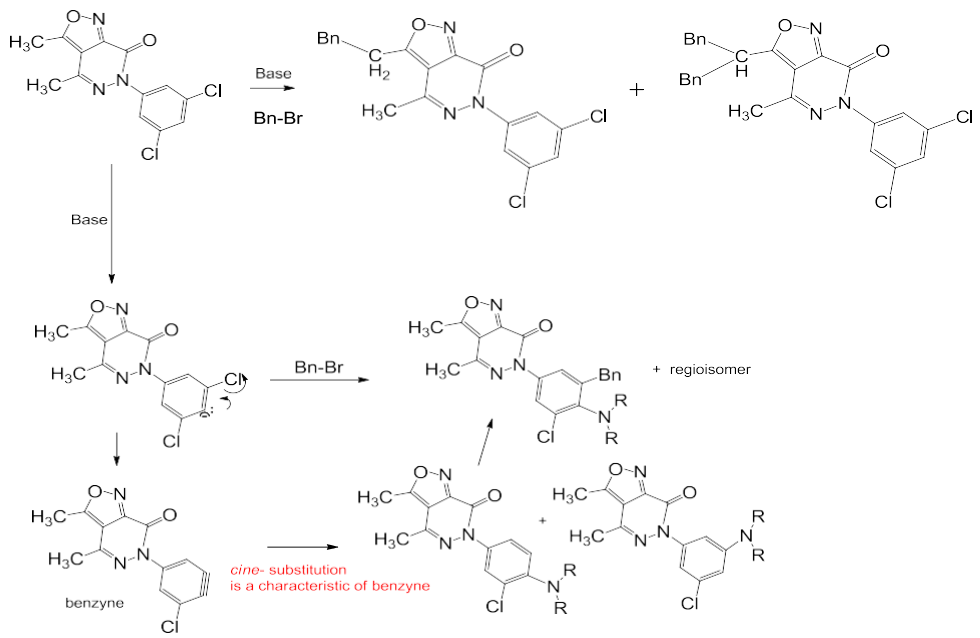

Figure 4-7: **During the lateral metalation reaction of the 3,5-dichloro there is the possibility of anion formation at either the C3 or between the Cls which can lead to a benzyne formation and subsequent addition by the base or the electrophile**

Direct metalation of the 3,4-ds produced both mono- and dialkylated products at the C3 when conducted at -78°C. In contrast, at -20 ^{o}C, monoalkylation predominated. (**Scheme 4-4**) This outcome appears to be complicated as a function of solubility of the lithio-intermediate, which appears to have at best sparing solubility at lower temperatures. This direct metalation was not limited to non-halogenated analogue. The N6-phenyl 3,5-Cl_2 **11** successfully generated both the mono- and dialkylation at the C3 without observing benzyne formation with LiHMDS. For optimum results, the lithium amide base is added slowly dropwise to the [3,4-d], as rapid addition produced a temperature spike leading to considerable decomposition. (**Table 4-2**)

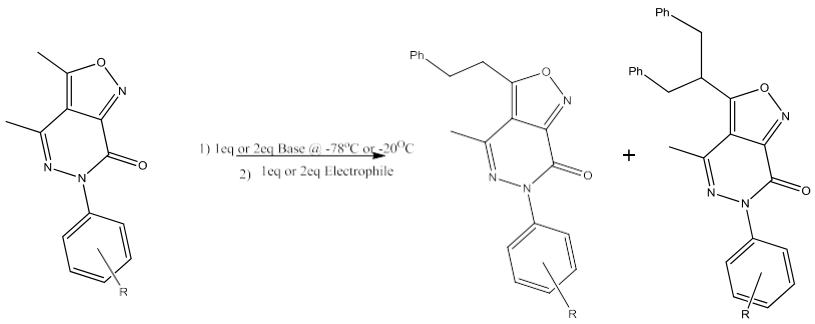

Scheme 4-4- Direct lateral metalation of 3,4-ds

Table 4-2- Experimental conditions and yields for direct lateral metalation of the 3,4-ds.Times noted is the time the base was allowed to react with starting material before introducing the electrophile. All reaction were allowed to come to room temperature with stirring overnight**.**

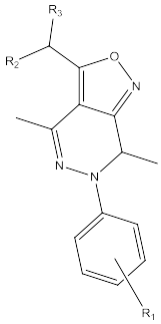

	Base	Temperature (ºC)	time	R_1	Electrophile	Yield R_2/R_3(%)	
						Mono	Double
	LiHMDS	-78	2h	H	BnBr	36	23
	LiHMDS	-40	30m	H	BnBr	trace	
	LiHMDS	-25	30m	H	BnBr	18	22
	2 eq LiHMDS	-78	30m	H	2 eq BnBr	trace	38
	2 eq LiHMDS	-20	1h	H	BnBr		major
5,6	LiHMDS	-20	30m	p-CH3	BnBr	29	
	LiHMDS	-78 to -25	30m	p-CH3	PhCHO	8	
	LDA	0	15m	p-CH3	ClPhCHO	8	
	LiHMDS	-20	30m	p-CH3	ClPhCHO	trace	
10	LiHMDS	-80	30m	p-OCH3	BnBr	27	?
	LiHMDS	-40	30m	p-OCH3	BnBr	18	5
	2 eq LiHMDS	-25	30m	p-OCH3	2 eq BnBr	9	58
9	2 eqLiHMDS	-50	30m	3,5-CF3	2 eq BnBr		12
11	2 eq LiHMDS	-78	30m	3,5-Cl2	2 eq BnBr	5	16
	1 eq LiHMDS	-78	30m	3,5-Cl2	1 eq BnBr	trace	

Although the yields in the table are mixed, it does show that the reaction will proceed and provide mono or double alkylation selectively at the C3. These reactions will need to be further explored and optimized,due to both solubility issues at the low temperature required for the reaction condition to proceed while minimizing decomposition and other side products.

Conclusion

The present report is an illustration of how new chemical synthetic methodology can drive the discovery and exploration of novel biology. With mono-substituted product in hand we can proceed to further expand the series with double substituted analogues at the C3 position. We are actively pursuing the synthesis of ligands for glutamate receptors and transporters and will report on our progress in due course.

Acknowledgement

The authors thank Charles Campana of Bruker for the x-ray crystallography determination. The authors thank David Burkhart, Jared Nelson and Trideep Rajale for the preparation of intermediates in sufficient quantity and purity to serve in the present study, and thank Scott Steiger for scaling up starting materials.

The authors thank the PDSP for biological evaluation. Contract # HHSN-271-2008-00025-C (NIMH PDSP). The NIMH PDSP is Directed by Bryan L. Roth MD, PhD at the University of North Carolina at Chapel Hill and Project Officer Jamie Driscoll at NIMH, Bethesda MD, USA.

NRN thanks the University of Montana an award from the University Research Grant Program, and the NIH for NINDS R15 NS038444 and R21 NS067466. NRN and YRM are grateful for the NINDS P20 RR015583 and P30 NS055022.

General direct lateral metalation conditions:

Argon gas was passed through tubes with indicator Drierite for reactions which required an inert atmosphere. THF was dried over activated sieves then distilled from sodium and benzophenone. NMR spectra were recorded at 400 MHz, unless otherwise specified, in $CDCl_3$ solution and are reported in ppm. The mass spectra were obtained using chemical ionization unless otherwise noted and are reported as m/z (relative intensity). Starting materials for the lateral metalation was prepared via Dal piaz's method for 4-phenyl and 4-methyl 3,4-ds.[47]

All steps were performed under inert atmosphere unless otherwise noted. To pre-dried round bottom cooled under argon the 3,4-d was added. After which dry THF was added in sufficient amount to reach a concentration of 50mM. The reaction was then placed and stirred in a cooling bath at the desired reaction temperature or based on solubility for 5min. Then add 1 or 2 eq of the amine base via syringe dropwise over 5 min. The reaction mixture was then allowed to react for 30min, during which time the solution is usually observed to darken. Then add 1 or 2eq of a 1.7M solution of the electrophile in dry THF that has been cooled to 0^oC or -78^oC (done for 3,5-Cl_2) dropwise slowly. Allow to warm to room temperature, adding saturated ammonium chloride at about -20^oC and allow to finish warming to room temperature. Rotovap down, bring up in dichloromethane(DCM) and wash with water and brine. DCM layer dried over sodium sulfate overnight. Filter and rotovap down and use either PTLC or column to purify with 6:1:1 hexanes, ethylacetate, DCM.

Analytical data for new compounds.

Kemp Rearrangement products, General Experimental: To 25 mL of anhydrous ethanol was added sodium metal (82 mg, 3.5 mol). After reaction to the alkoxide was complete, 1 mmol of

isoxazolo [3,4-d] pyridazinone, followed by aldehyde (in slight excess of 1 mmol) was added in one portion and the reaction heated to reflux overnight. The reaction was cooled, the ethanol concentrated by rotary evaporator, and the residue chromatographed on silica gel, using 4:1:1 hexane-DCM-ethylacetate.

1-p-Tolyl-3-methyl-(4-p-Chlorocinnamyl)-5-amino-pyrazole, 8.a. Ar_1 = p-ClC_6H_4; Ar_2 = p-$CH_3C_6H_4$; $C_{20}H_{19}ClN_3O$ MW 352.8, ESI-MS: m/Z 352.1 (100, M+)); 354.1 (M+2+, 35)

1-p-Anisyl-3- methyl -(4-p-Chlorocinnamyl)-5-amino-pyrazole, 8.b. Ar_1 = p-ClC_6H_4; Ar_2 = p-$CH_3OC_6H_4$; $C_{20}H_{19}ClN_3O_2$ MW 368.8, m/Z 368.1 (100, M+); 370.1 (M+2+, 35)

1-3,5-Dichlorophenyl-3-methyl-(4-p-Methoxycinnamyl)-5-amino-pyrazole, 8.c. Ar_1 = p-$CH_3OC_6H_4$; Ar_2 = 3,5-$Cl_2C_6H_3$; $C_{20}H_{18}Cl_2N_3O_2$ MW: 403.28; ESI-MS 402 (100% rel. I.), 404 (M+2, 65.5); 406 (M+4, 11).

4-methyl-3-phenethyl-6-phenylisoxazolo[3,4-*d*]pyridazin-7(6*H*)-one. ^{1}H NMR (500 MHz, $CDCl_3$): δ 7.57 (d, 1H); 7.46 (t, 2H); 7.32 (t, 1H); 7.30 (t, 2H), 7.28 (t, 1H); 7.12 (d, 2H); 3.47 (t, J = 7.5 Hz, 2H); 3.18 (t, J = 7.5 Hz, 2H), 2.29 (s, 3H). ^{13}C NMR: 172.63, 152.90, 152.39, 140.78, 140.02, 138.85, 128.93, 128.88, 128.37, 127.95, 127.12, 125.81, 112.52, 34.28, 29.63, 19.36. $C_{20}H_{17}N_3O_2$ MW 331.13; ESI-MS m/z 332.0971 (M+H$^+$, 90% rel. I.). HRMS calc'd for $C_{20}H_{18}N_3O_2$ (M+H$^+$): 332.1399, found: 332.1396. -0.9 ppm.

3-(1,3-diphenylpropan-2-yl)-4-methyl-6-phenylisoxazolo[3,4-*d*]pyridazin-7(6*H*)-one. ^{1}H NMR (500 MHz, $CDCl_3$): δ 7.51 (d, 2H); 7.43 (t, 2H); 7.36 (t, 1H); 7.21 (m, 8H); 7.01 (d, 2H); 3.796 (pentet, J = 7.5 Hz, 1H); 3.268 (d, J = 8 Hz, 4H); 1.86 (s, 3H). ^{13}C NMR: 174.49, 152.82, 151.91, 140.61, 139.77, 137.97, 128.78, 128.54, 127.81, 127.06,125.64, 113.37, 45.00, 40.78, 18.92. $C_{27}H_{23}N_3O_2$ MW 421.18; ESI-MS m/z 422.1432 (M+H$^+$, 61% rel. I.). HRMS calc'd for $C_{27}H_{24}N_3O_2$ (M+H$^+$): 422.1869, found: 422.1871. 0.5 ppm.

3-(2-(4-chlorophenyl)-2-hydroxyethyl)-4-methyl-6-(*p*-tolyl)isoxazolo[3,4-*d*]pyridazin-7(6*H*)-one. TLC (SiO_2 4:4:1 hexane-EtOAc-DCM) R_f 0.16. ^{1}H NMR (500 MHz, $CDCl_3$): δ 7.42 (d, J = 8.5 Hz, 2H); 7.259 (m, 4H); 7.08 (d, J=8.5 Hz, 2H); 5.1 (br. m., 1H); 4.04 (dd, J= 7Hz); 3.69 (dd, J = 15, 7Hz, 1H); 3.62 (dd, J= 7, 15 Hz); 2.40 (s, 3H); 2.386 (s, 3H). ^{13}C NMR: IP $C_{21}H_{18}ClN_3O_3$ MW 395.1; ESI-MS m/z 378.0079 (^{35}Cl, M-OH$^+$, 47% rel. I.), 379.9991 (^{37}Cl, M-OH$^+$, 15% rel. I.). HRMS IP

4-methyl-3-phenethyl-6-(p-tolyl)isoxazolo[3,4-*d*]pyridazin-7(6*H*)-one. ^{1}H NMR (400 MHz, $CDCl_3$): δ 7.29 (d, J=8 Hz, 2H); 7.12 (m, 5H); 6.97 (d, J=8Hz, 2H); 3.32 (t, J=8Hz, 2H); 3.03 (t, J=8Hz, 2H); 2.24 (s, 3H); 2.14 (s, 3H). ^{13}C NMR: 172.44, 152.86, 152.35, 139.73, 138.79, 138.23, 137.91, 129.46, 128.88, 128.30, 127.06, 125.58, 112.49, 34.25, 29.58, 21.13, 19.30. $C_{21}H_{19}N_3O_2$ MW 345.39; ESI-MS m/z 346.1176 (M+1$^+$, 100% rel. I.). HRMS: calc'd for $C_{21}H_{20}N_3O_2$ (M+H$^+$): 346.1556, found: 346.1558. 0.6 ppm.

6-(p-methoxyphenyl)-4-methyl-3-phenethyl-isoxazolo[3,4-*d*]pyridazin-7(6*H*)-one. ^{1}H NMR (400 MHz, $CDCl_3$): δ 7.385 (d, J = 8Hz, 2H); 7.16-7.22 (m, 3H); 7.7.65 (d, J+8Hz, d); 6.89 (d, J = 8Hz, 2H); 3.73 (s, 3H); 3.38 (t, J=8Hz, 2H); 3.11 (t, J=8Hz, 2H); 2.20 (s, 3H). ^{13}C NMR: 172.57, 159.03, 152.95, 152.37, 139.80, 138.86, 133.77, 128.91, 127.05,114.13, 55.58, 34.27, 29.62, 19.35. $C_{21}H_{19}N_3O_3$ MW: 361.3. HRMS calc'd for $C_{21}H_{20}N_3O_3$ (M+H$^+$): 362.1505, found: 362.1506. 0.3 ppm.

6-(p-methoxyphenyl)-3-(1,3-diphenylpropan-2-yl)-4-methyl-isoxazolo[3,4-*d*]pyridazin-7(6*H*)-one. ^{1}H NMR (400 MHz, $CDCl_3$): δ 7.41 (d, J=8Hz, 2H); 7.19-7.25 (m, 6H); 7.19 (d, J=8Hz, 4H); 6.94 (d, J=8Hz, 2H); 3.83 (s, 3H); 3.81 (pentet, J = 8Hz, 1H); 3.28 (d, J=8Hz, 4H); 1.85 (s, 3H). ^{13}C NMR: 174.46, 158.96, 152.91, 151.94, 139.62, 138.03, 133.65, 128.82, 128.59, 126.93, 114.06, 113.43, 55.55, 45.01, 40.82, 18.96. $C_{28}H_{25}N_3O_3$ MW: 451.5. HRMS calc'd for $C_{28}H_{26}N_3O_3$ ($M+H^+$): 452.1974, Found: 452.1975. 0.2 ppm.

(*E*)-ethyl 4-(1-(2-(3,5-dichlorophenyl)hydrazono)ethyl)-5-phenethylisoxazole-3-carboxylate. ^{1}H NMR (400 MHz, $CDCl_3$): δ 4.34 (q, J = 8 Hz, 2H); 3.17 (t, 2H); 2.98 (t, 2H); 1.80 (s, 3H); 1.32 (t, J = 8 Hz, 3H). $C_{22}H_{21}Cl_2N_3O_3$ MW: 446.3; ESI-MS m/z 446 ($M+1^+$, 100% rel. I.), 448 ($M+3^+$, 67.4).

6-(3,5-dichlorophenyl)-4-methyl-3-phenethylisoxazolo[3,4-*d*]pyridazin-7(6*H*)-one. ^{1}H NMR (400 MHz, $CDCl_3$): δ 7.515 (d, J = 4 Hz, 2H); 7.18-7.27 (m, 5H); 7.04 (d, 1H); 3.41 (t, 3 J = 8Hz, 2H); 3.12 (t, 3 J = 8Hz, 2H); 2.2 (s, 3H). ^{13}C NMR: 173.01, 152.72; 151.99; 142.12; 140.88; 138.62; 134.81; 128.91; 128.28; 127.15; 124.20; 112.29; 34.20; 29.61; 19.26. $C_{20}H_{15}Cl_2N_3O_2$ MW: 400.26; ESI-MS m/z 400 (M+H, 100%% rel. I.); 402 (M+H+2, 67.7); 404 (M+H+4, 12.2). HRMS Calc'd for $C_{20}H_{16}Cl_2N_3O_2$ 400.0620, Found: 400.0622. 0.5 ppm.

6-(3,5-dichlorophenyl)-4-methyl-3--(1,3-diphenylpropan-2-yl)-isoxazolo[3,4-*d*]pyridazin-7(6*H*)-one.^{1}H NMR (400 MHz, $CDCl_3$): δ 7.532 (d, J = 1.7 Hz, 2H); 7.32 (t, J=1.7(x2),1H); 7.25-7.19 (m, 6H); 7.01-6.99 (d, J = 6.4Hz, 4H); 3.81-3.77 (t, 3 J = 8Hz (x2), 1H); 3.30 (s, 2H); 3.28 (s,2H);1.85(s,3H);1.59(s,1H). ^{13}C NMR: 174.99; 140.68; 137.87; 134.75; 128.84; 128.50; 127.16; 124.11; 45.15; 40.83; 18.88 $C_{27}H_{21}Cl_2N_3O_2$ MW: 490.39; HRMS 489 (M-H, 100%% rel. I.); 491 (M+H). Calc'd for $C_{27}H_{21}Cl_2N_3O_2$ 490.3805, Found: 490.1226.

6-(3,5-dichlorophenyl)-4-methyl-3-(2-(naphthalen-1-yl)ethyl)isoxazolo[3,4-*d*]pyridazin-7(6*H*)-one. ^{1}H NMR (400 MHz, $CDCl_3$): δ 7.96 (d, J = 8 Hz, 1H); 7.90 (d, J = 8 Hz, 1H); 7.79 (d, J = 8 Hz, 1H); 7.37-7.61 (m, H); 7.56 (d, J = 2Hz, 2H); 7.35 (t, 1H); 7.35 (d, J = 2Hz, 1H); 7.21 (d, J = 8 Hz, 1H), 3.675 (dd, 2H): 3.64 (dd, 2H); 2.00 (s, 3H). ^{13}C NMR: δ 172.98, 152.67, 152.0, 142.11, 140.73, 134.83, 134.57, 131.20; 129.26, 127.0, 126.65, 125.57. 124.22, 122.62, 112.46, 31.42, 28.65, 18.92. $C_{24}H_{17}Cl_2N_3O_2$ MW: 450.32; ESI-MS m/z 450 (M+H, 100% rel. I.); 452 (M+H+2, 68.9); 452 (M+H+4, 13.1). HRMS Calc'd for $C_{24}H_{18}Cl_2N_3O_2$ 450.0776, Found: 450.0775. -0.2 ppm.

6-(3,5-dichlorophenyl)-3-methyl-4-phenylisoxazolo[3,4-*d*]pyridazin-7(6*H*)-one. ^{1}H NMR (400 MHz, $CDCl_3$): δ 7. 68 (2H); 7.57 (5H); 7.38 (1H); 5.59 (s, 3H). ^{13}C NMR: δ 208.20,194.33,181.58,170.91,164.94 152.67, 152.0, 142.11, 140.73, 134.83, 134.57, 131.20; 129.26, 127.0, 126.65, 125.57. 124.22, 122.62, 112.46, 31.42, 28.65, 18.92.HRMS Calc'd for $C_{18}H_{11}{}^{35}Cl_2N_3O_2$+H 372.0307, Found: 372.0309. 0.5 ppm.

6-(3,5-bistrifluoromethylphenyl)-4-methyl-3--(1,3-diphenylpropan-2-yl)-isoxazolo[3,4-*d*]pyridazin-7(6*H*)-one.^{1}H NMR (400 MHz, $CDCl_3$): δ 8.13 (s, 2H);7.82(s, 1H); 7.04 (d, 1H); 7.25-7.18 (m, J = 8Hz, 6H); 7.02-7.00 (d, J = 8Hz, 4H); 3.82-3.79 (m,1H); 3.31 (s 2H); 3.29 (s,2H);1.88(s,3H); 1.6 (s,1H). ^{13}C NMR: δ 175.27, 137.82,128.86,128.48,127.17,113.23,45.23.40.86,18.90 ; $C_{29}H_{21}F_6N_3O_2$ MW: 557.49; HRMS m/z 558 (M+H, 100%% rel. I.); 559 (M+H+2); Calc'd for $C_{29}H_{21}F_6N_3O_2$ 557.49, Found: 557.1153

6-(3,5-dichlorophenyl)-3-methyl-4-phenyl-6H,7H-[1,2]oxazolo[3,4-d]pyridazin-7-one. ^{1}H NMR (400 MHz, $CDCl_3$): δ 7.57-7.56 (d, 5H);7.37(t, 1H); 2.58 (s, 3H).^{13}C NMR 170.95;152.59;143.74;142.24;134.92;133.17;130.53;128.96;128.37;127.98;124.33;111.24;13.95 $C_{18}H_{11}Cl_2N_3O_2$ MW: 372.205; HRMS m/z 372.0309 (100%% rel. I.); 374.0289 (M+H+2); Calc'd for $C_{18}H_{11}Cl_2N_3O_2$ 372.20538, Found: 372.0309.

6-(4-methoxyphenyl)-3-methyl-4-phenyl-6H,7H-[1,2]oxazolo[3,4-d]pyridazin-7-one ^{1}H NMR (400 MHz, $CDCl_3$): δ 7.58-7.53 (t, J=8,7H);7.00-6.98(d, J=8,2H); 3.85(s,3H);2.58 (s, 3H).[13] C NMR 170.38; 159.0; 152.82; 152.73; 142.63; 133.77; 130.11; 28.76; 128.40; 127.02; 114.03;111.37;55.52;13.92 $C_{19}H_{15}N_3O_3$ MW: 333.35; HRMS m/z: 333.1113 (100.0%), 334.1147 (20.5%), 335.1181 (2.0%), 334.1084 (1.1%); Calc'd for $C_{19}H_{15}N_3O_3$ 333.3407, Found: 333.1113.

3-methyl-6-(4-methylphenyl)-4-phenyl-6H,7H-[1,2]oxazolo[3,4-d]pyridazin-7-one ^{1}H NMR (400 MHz, $CDCl_3$): δ 7.60-7.58 (m, J=4 ,2H);7.55-7.53(t, J=4,5H); 2.59 (s, 3H);2.40(s,3H).^{13}C NMR 170.58; 152.75; 133.48; 130.30; 128.87; 128.38; 127.68; 115.82; 115.60; 111.40;13.95 $C_{19}H_{15}N_3O_2$ MW: 317.34; HRMS m/z 372.0309 (100%% rel. I.); 374.0289 (M+H+2); Calc'd for $C_{19}H_{15}N_3O_2$ 317.3413, Found: 317.1164.

References

(1) Conn, P. J.; Christopoulos, A.; Lindsley, C. W. Allosteric Modulators of GPCRs: A Novel Approach for the Treatment of CNS Disorders. *Nat. Rev. drug Discov.* 2010, *8* (1), 41–54 DOI: 10.1038/nrd2760.Allosteric.

(2) Conn, P. J.; Lindsley, C. W.; Meiler, J.; Niswender, C. M. Opportunities and Challenges inthe Discovery of Allosteric Modulators of GPCRs for Treating CNS Disorders. *Nat. Rev. Drug Discov.* 2014, *13* (9), 692–708 DOI: 10.1038/nrd4308.

(3) Engers, J. L.; Rodriguez, A. L.; Konkol, L. C.; Morrison, R. D.; Thompson, A. D.; Byers, F. W.; Blobaum, A. L.; Chang, S.; Venable, D. F.; Loch, M. T.; Niswender, C. M.; Daniels, J. S.; Jones, C. K.; Conn, P. J.; Lindsley, C. W.; Emmitte, K. A. Discovery of aSelective and CNS Penetrant Negative Allosteric Modulator of Metabotropic GlutamateReceptor Subtype 3 with Antidepressant and Anxiolytic Activity in Rodents. *J. Med. Chem.* 2015, *58* (18) DOI: 10.1021/acs.jmedchem.5b01005.

(4) Volpi, C.; Fallarino, F.; Mondanelli, G.; Macchiarulo, A.; Grohmann, U. Opportunities and Challenges in Drug Discovery Targeting Metabotropic Glutamate Receptor 4. *Expert Opinion on Drug Discovery*. Taylor and Francis Ltd May 4, 2018, pp 411–423.

(5) Crupi, R.; Impellizzeri, D.; Cuzzocrea, S. Role of Metabotropic Glutamate Receptors in Neurological Disorders. *Frontiers in Molecular Neuroscience*. Frontiers Media S.A. February 12, 2019.

(6) Bai, M. Dimerization of G-Protein-Coupled Receptors: Roles in Signal Transduction. *Cell. Signal.* 2004, *16* (2), 175–186 DOI: 10.1016/S0898-6568(03)00128-1.

(7) De Filippis, B.; Lyon, L.; Taylor, A.; Lane, T.; Burnet, P. W. J.; Harrison, P. J.; Bannerman, D. M. The Role of Group II Metabotropic Glutamate Receptors in Cognition and Anxiety: Comparative Studies in GRM2-/-, GRM3-/- and GRM2/3-/- Knockout Mice. *Neuropharmacology* 2015, *89*, 19–32 DOI: 10.1016/j.neuropharm.2014.08.010.

(8) Niswender, C. M.; Conn, P. J. Metabotropic Glutamate Receptors: Physiology, Pharmacology, and Disease. *Annu Rev Pharmacol Toxicol* 2010, *50* (1), 295–322 DOI: 10.1146/annurev.pharmtox.011008.145533.

(9) Renzi, G. and Dal Piaz, V. Ricerche Su Alcuni 3-Carbetossi-Isossazoli-4,5-Disostituiti. *Gazz. Chim. It.* 1965, *95*, 1478–1491.

(10) Renzi, G. and Pinzauti, S. Nuovi Derivati Del Systema Isossazolo-[3,4-d]Piridazin-7-One. *Farm. Ed. Sci* 1969, *24*, 885–892.

(11) Micetich, R. G.; Chin, C. G. Studies in Isoxazole Chemistry. 111.' The Preparation and Lithiation of 3,5-Disubstituted Isoxazoles. *Can. J. Chem.* 1970, *48*, 1371.

(12) Casey, M. L.; Kemp, D. S.; Paul, K. G.; Cox, D. D. The Physical Organic Chemistry of Benzisoxazoles. I. The Mechanism of the Base-Catalyzed Decomposition of Benzisoxazoles. *J. Org. Chem.* 1973, *38* (13), 2294–2301 DOI: 10.1021/JO00953A006/SUPPL_FILE/JO00953A006_SI_001.PDF.

(13) Sayer, J. M.; Peskin, M.; Jencks, W. P. Imine-Forming Elimination Reactions. I. General Base and Acid Catalysis and Influence of the Nitrogen Substituent on Rates and Equilibriafor Carbinolamine Dehydration. *J. Am. Chem. Soc.* 1973, *95* (13), 4277–4287 DOI: 10.1021/ja00794a600.

(14) Dal Piaz, V.; Pinzauti, S.; Lacrimini, P. J. Condensation of Some 3-Methylisoxazolo[3,4-d]Pyridazin-7(6H)Ones with Aromatic Aldehydes. *Heterocycl. Chem.* 1975, *13*, 409–410.

(15) Piaz, V. D.; Pinzauti, S.; Lacrimini, P. Condensation of Some 3-Methylisoxazolo[3,4-

d]Pyridazin-7(6H)Ones with Aromatic Aldehydes. *J. Heterocycl. Chem.* 1976, *13* (2), 409–410 DOI: 10.1002/JHET.5570130245.

(16) Wu, H.; Wang, C.; Gregory, K. J.; Han, G. W.; Cho, H. P.; Xia, Y.; Niswender, C. M.; Katritch, V.; Meiler, J.; Cherezov, V.; Conn, P. J.; Stevens, R. C. Structure of a Class C GPCR Metabotropic Glutamate Receptor 1 Bound to an Allosteric Modulator. *Science (80-.).* 2014, *344* (6179), 58–64 DOI: 10.1126/science.1249489.

(17) Brooks, B. R.; Brooks, C. L.; Mackerell, A. D.; Nilsson, L.; Petrella, R. J.; Roux, B.; Won,Y.; Archontis, G.; Bartels, C.; Boresch, S.; Caflisch, A.; Caves, L.; Cui, Q.; Dinner, A. R.;Feig, M.; Fischer, S.; Gao, J.; Hodoscek, M.; Im, W.; Kuczera, K.; Lazaridis, T.; Ma, J.; Ovchinnikov, V.; Paci, E.; Pastor, R. W.; Post, C. B.; Pu, J. Z.; Schaefer, M.; Tidor, B.; Venable, R. M.; Woodcock, H. L.; Wu, X.; Yang, W.; York, D. M.; Karplus, M. CHARMM: The Biomolecular Simulation Program. *J. Comput. Chem.* 2009, *30* (10), 1545–1614 DOI: 10.1002/jcc.21287.

(18) Onufriev, A.; Case, D. A.; Bashford, D. Effective Born Radii in the Generalized Born Approximation: The Importance of Being Perfect. *J. Comput. Chem.* 2002, *23* (14), 1297–1304 DOI: 10.1002/jcc.10126.

(19) Koska, J.; Spassov, V. Z.; Maynard, A. J.; Yan, L.; Austin, N.; Flook, P. K.; Venkatachalam, C. M. Fully Automated Molecular Mechanics Based Induced Fit Protein -Ligand Docking Method. *J. Chem. Inf. Model.* 2008, *48* (10), 1965–1973 DOI: 10.1021/ci800081s.

(20) Gehlhaar, D. K.; Bouzida, D.; Rejto, P. A. Reduced Dimensionality in Ligand-Protein Structure Prediction: Covalent Inhibitors of Serine Proteases and Design of Site-Directed Combinatorial Libraries. *ACS Symp. Ser.* 1999, *719*, 292–311 DOI: 10.1021/bk-1999-0719.ch019.

(21) Böhm, H. J. On the Use of LUDI to Search the Fine Chemicals Directory for Ligands of Proteins of Known Three-Dimensional Structure. *J. Comput. Aided. Mol. Des.* 1994, *8* (5), 623–632 DOI: 10.1007/BF00123669.

(22) Amalric, M.; Lopez, S.; Goudet, C.; Fisone, G.; Battaglia, G.; Nicoletti, F.; Pin, J. P.; Acher, F. C. Group III and Subtype 4 Metabotropic Glutamate Receptor Agonists: Discovery and Pathophysiological Applications in Parkinson's Disease. *Neuropharmacology* 2013, *66*, 53–64 DOI: 10.1016/j.neuropharm.2012.05.026.

(23) Leach, K.; Gregory, K. J. Molecular Insights into Allosteric Modulation of Class C G Protein-Coupled Receptors. *Pharmacological Research*. 2017.

(24) Panarese, J. D.; W. Engers, D.; Wu, Y.-J.; J. Bronson, J.; E. Macor, J.; Chun, A.; L. Rodriguez, A.; S. Felts, A.; L. Engers, J.; T. Loch, M.; A. Emmitte, K.; L. Castelhano, A.; J. Kates, M.; A. Nader, M.; K. Jones, C.; L. Blobaum, A.; Jeffrey Conn, P.; M. Niswender, C.; R. Hopkins, C.; W. Lindsley, C. Discovery of VU2957 (Valiglurax): An MGlu4 Positive Allosteric Modulator Evaluated as a Preclinical Candidate for the Treatment of Parkinson's Disease. *ACS Med. Chem. Lett.* 2018, *10* (3), 255–260 DOI: 10.1021/acsmedchemlett.8b00426.

(25) Yang, D.; Zhou, Q.; Labroska, V.; Qin, S.; Darbalaei, S.; Wu, Y.; Yuliantie, E.; Xie, L.; Tao, H.; Cheng, J.; Liu, Q.; Zhao, S.; Shui, W.; Jiang, Y.; Wang, M.-W. G Protein-Coupled Receptors: Structure- and Function-Based Drug Discovery. *Signal Transduct. Target. Ther. 2020 61* 2021, *6* (1), 1–27 DOI: 10.1038/s41392-020-00435-w.

(26) Harpsøe, K.; Boesgaard, M. W.; Munk, C.; Bräuner-Osborne, H.; Gloriam, D. E. Structural Insight to Mutation Effects Uncover a Common Allosteric Site in Class C GPCRs.

Bioinformatics 2017, *33* (8) DOI: 10.1093/bioinformatics/btw784.
(27) Robichaud, A. J.; Engers, D. W.; Lindsley, C. W.; Hopkins, C. R. Recent Progress on the Identification of Metabotropic Glutamate 4 Receptor Ligands and Their Potential Utilityas CNS Therapeutics. *ACS Chem. Neurosci.* 2011, *2* (8), 433–449 DOI: 10.1021/cn200043e.
(28) Lindsley, C. W.; Emmitte, K. A.; Hopkins, C. R.; Bridges, T. M.; Gregory, K. J.; Niswender, C. M.; Conn, P. J. Practical Strategies and Concepts in GPCR Allosteric Modulator Discovery: Recent Advances with Metabotropic Glutamate Receptors. *Chem. Rev.* 2016, *116* (11), 6707–6741 DOI: 10.1021/acs.chemrev.5b00656.
(29) Rovira, X.; Malhaire, F.; Scholler, P.; Rodrigo, J.; Gonzalez-Bulnes, P.; Llebaria, A.; Pin,J.-P. P.; Giraldo, J.; Goudet, C. Overlapping Binding Sites Drive Allosteric Agonism and Positive Cooperativity in Type 4 Metabotropic Glutamate Receptors. *FASEB J.* 2015, *29*(1), 116–130 DOI: 10.1096/fj.14-257287.
(30) Ferreira, L. G.; Lamba, D.; Consiglio, N.; Delle, R.; Dharmendra, I.; Yadav, K.; Kang, S.; Choi, S.; Basith, S.; Cui, M.; Macalino, S. J. Y.; Park, J.; Clavio, N. A. B.; Kang, S.; Choi, S. Exploring G Protein-Coupled Receptors (GPCRs) Ligand Space via Cheminformatics Approaches: Impact on Rational Drug Design. 2018, No. MAR, 128.
(31) Gates, C.; Backos, D. S.; Reigan, P.; Kang, H. J.; Koerner, C.; Mirzaei, J.; Natale, N. R. Isoxazolo[3,4-d]Pyridazinones Positively Modulate the Metabotropic Glutamate Subtypes2 and 4. *Bioorganic Med. Chem.* 2018, *26* (17), 4797–4803 DOI: 10.1016/j.bmc.2018.08.012.
(32) R. Natale, N.; Niou, C.-S. Synthesis, Metalation and Electrophilic Quenching of Alkyl-Isoxazole-4-Tertiary Carboxamides. A Critical Comparison of Three Isoxazole Lateral Metalation Methods. *Heterocycles* 1986, *24* (2), 401 DOI: 10.3987/R-1986-02-0401.
(33) Natale, N. R.; Mirzaei, Y. R. The Lateral Metalation of Isoxazoles. A Review. *Org. Prep. Proced. Int.* 1993, *25* (5), 515–556 DOI: 10.1080/00304949309457997.
(34) Natale, N. R.; McKenna, J. I.; Niou, C. S.; Borth, M.; Hope, H. Metalation of Isoxazolyloxazolines, a Facile Route to Functionally Complex Isoxazoles: Utility, Scope,and Comparison to Dianion Methodology. *J. Org. Chem.* 1985, *50* (26), 5660–5666 DOI: 10.1021/JO00350A047/SUPPL_FILE/JO00350A047_SI_001.PDF.
(35) Dal Piaz, V., Ciciani, G. and C. New Functionalized Pyrazoles from Isoxazolopyridazinones. *S. Heterocycles* 1985, *23*, 365–369.
(36) Montesano, F.; Barlocco, D.; Piaz, V. D.; Leonardi, A.; Poggesi, E.; Fanelli, F.; De Benedetti, P. G. Isoxazolo-[3,4-d]-Pyridazin-7-(6H)-Ones and Their Corresponding 4,5-Disubstituted-3-(2H)-Pyridazinone Analogues as New Substrates for A1-Adrenoceptor Selective Antagonists: Synthesis, Modeling, and Binding Studies. *Bioorg. Med. Chem.* 1998, *6* (7), 925–935 DOI: 10.1016/S0968-0896(98)00056-X.
(37) Costantino, L.; Rastelli, G.; Gamberini, M. C.; Giovannoni, M. P.; Piaz, V. D.; Vianello,P.; Barlocco, D.; L, C.; G, R.; MC, G.; MP, G.; V, D. P.; P, V.; D, B. Isoxazolo-[3,4-d]-Pyridazin-7-(6H)-One as a Potential Substrate for New Aldose Reductase Inhibitors. *J. Med. Chem.* 1999, *42* (11), 1894–1900 DOI: 10.1021/JM981107O.
(38) Dal Piaz, V.; Rascón, A.; Dubra, M. E.; Giovannoni, M. P.; Vergelli, C.; Castellana, M. C. Isoxazolo[3,4-d]Pyridazinones and Analogues as Leishmania Mexicana PDE Inhibitors. *Farm.* 2002, *57* (2), 89–96 DOI: 10.1016/S0014-827X(01)01188-0.
(39) V, D. P.; MC, C.; C, V.; MP, G.; A, G.; V, S.; J, B.; H, R.; JM, P.; Piaz, V. D.; Castellana, M. C.; Vergelli, C.; Giovannoni, M. P.; Gavaldà, A.; Segarra, V.; Beleta, J.; Ryder, H.;

Palacios, J. M. Synthesis and Evaluation of Some Pyrazolo[3,4-d]Pyridazinones and Analogues as PDE 5 Inhibitors Potentially Useful as Peripheral Vasodilator Agents. 2002,*17* (4), 227–233 DOI: 10.1080/1475636021000008494.

(40) Dal Piaz, V.; Giovannoni, M. P.; Ciciani, G.; Barlocco, D.; Giardina, G.; Petrone, G.; Clarke, G. D. 4,5-Functionalized 6-Phenyl-3(2H)-Pyridazinones: Synthesis and Evaluation of Antinociceptive Activity. *Eur. J. Med. Chem.* 1996, *31* (1), 65–70 DOI:10.1016/S0223-5234(96)80008-0.

(41) Barlocco, D.; Cignarella, G.; Dal Piaz, V.; Giovannoni, M. P.; De Benedetti, P. G.; Fanelli,F.; Montesano, F.; Poggesi, E.; Leonardi, A. Phenylpiperazinylalkylamino Substituted Pyridazinones as Potent A1 Adrenoceptor Antagonists. *J. Med. Chem.* 2001, *44* (15), 2403–2410 DOI: 10.1021/jm0009336.

(42) Giovannoni, M. P.; Vergelli, C.; Ghelardini, C.; Galeotti, N.; Bartolini, A.; Dal Piaz, V.[(3-Chlorophenyl)Piperazinylpropyl]Pyridazinones and Analogues as Potent Antinociceptive Agents. *J. Med. Chem.* 2003, *46* (6), 1055–1059 DOI: 10.1021/JM021057U.

(43) Dal Piaz, V.; Vergelli, C.; Giovannoni, M. P.; Scheideler, M. A.; Petrone, G.; Zaratin, P. 4-Amino-3(2H)-Pyridazinones Bearing Arylpiperazinylalkyl Groups and Related Compounds: Synthesis and Antinociceptive Activity. *Farmaco* 2003, *58* (11), 1063–1071 DOI: 10.1016/S0014-827X(03)00162-9.

(44) Giovannoni, M. P.; Vergelli, C.; Biancalani, C.; Cesari, N.; Graziano, A.; Biagini, P.; Gracia, J.; Gavaldà, A.; Dal Piaz, V. Novel Pyrazolopyrimidopyridazinones with Potentand Selective Phosphodiesterase 5 (PDE5) Inhibitory Activity as Potential Agents for Treatment of Erectile Dysfunction. *J. Med. Chem.* 2006, *49* (17), 5363–5371 DOI: 10.1021/jm060265+.

(45) Giovannoni, M. P.; Cesari, N.; Vergelli, C.; Graziano, A.; Biancalani, C.; Biagini, P.; Ghelardini, C.; Vivoli, E.; Dal Piaz, V. 4-Amino-5-Substituted-3(2H)-Pyridazinones asOrally Active Antinociceptive Agents: Synthesis and Studies on the Mechanism of Action. *J. Med. Chem.* 2007, *50* (16), 3945–3953 DOI: 10.1021/JM070161E/SUPPL_FILE/JM070161ESI20070608_091707.PDF.

(46) Biancalani, C.; Giovannoni, M. P.; Pieretti, S.; Cesari, N.; Graziano, A.; Vergelli, C.; Cilibrizzi, A.; Di Gianuario, A.; Colucci, M.; Mangano, G.; Garrone, B.; Polenzani, L.; Dal Piaz, V. Further Studies on Arylpiperazinyl Alkyl Pyridazinones: Discovery of an Exceptionally Potent, Orally Active, Antinociceptive Agent in Thermally Induced Pain. *J.Med. Chem.* 2009, *52* (23), 7397–7409 DOI: 10.1021/JM900458R/SUPPL_FILE/JM900458R_SI_001.PDF.

(47) Chimichi, S.; Ciciani, G.; Piaz, V. D.; De Sio, F.; Sarti-Fantoni, P.; Torroba, T. Solid StatePhotodimerization Reaction of Some 3-Styrylisoxazolo-[3,4-d]Pyridazin-7(6h)-Ones. *Heterocycles* 1986, *24* (12), 3467–3471 DOI: 10.3987/R-1986-12-3467.

(48) Burkhart, D. J.; Zhou, P.; Blumenfeld, A.; Twamley, B.; Natale, N. R. An Improved Procedure for the Lateral Lithiation of Ethyl 4-Acetyl-5-Methyl-3-Isoxazolyl Carboxylate.*Tetrahedron* 2001, *57* (38), 8039–8046 DOI: 10.1016/S0040-4020(01)00781-5.

(49) Zhou,Peiwen; Natale, N. R. Lateral Lithiation of Ethyl 4-Acetyl-5-Methyl-3-IsoxazolylCarboxylate with 5,5-Dimethyl-l,3-Dioxanyi as a Directing Group. *Tetrahedron Lett.* 1998, *39*, 8249–8252.

Ch.5: Future directions: Asymmetric synthesis, Metabolism, and the blood brain barrier

Although there has been progress in our efforts to understand the 3,4-ds potential as selective modulators of mGluRs as shown in the previous chapters,there are many areas that still need to be explored and addressed. A few examples are:(1) homology modeling suggested chiral molecules will have better binding scores to access these asymmetric synthesis condition must be explored,(2) metabolism is key to understanding if any potential toxicities exist and if the they could be metabolized to extensively before reaching their target,(3) developing molecules that are able to cross the blood brain barrier through either synthetic functional group modification or carrier mediated routes.

Asymmetric synthesis:

Asymmetric synthesis is still an area that more thoroughly needs to be explored. The Nobel Prize in Chemistry for 2021 was awarded to Benjamin List and David W.C. MacMillan for their work in asymmetric organocatalysis.[1] Asymmetric molecules could provide a unique interaction and allow for an understanding of how the eudismic ratio would affect the mGluR activity. The difference in enatiomers has been observed for many drugs currently on the market, some such as S-Naproxen needing to be sold as a single enatiomer due to the different activity of its enatiomers[2] and accessibility for activity.[3] Being able to selectively place a chiral center and control R or S configuration is necessary.

We have previously shown that it is possible to lateral metalate selectively and add an achiral center at the C3 position of the isoxazole (by 3,4-d numbering).[4,5] Applying this to the 3,4-ds would be a new direction. Previous work in our group and in the literature showed that

solvent had a large effect on the outcome of the reaction. It has been noted in theliterature about better enantiomeric excess (ee) achieved depending on the solvent.[6,7]

Table 5-1: Previously tried catalysts and solvent used. N.R.= no reaction

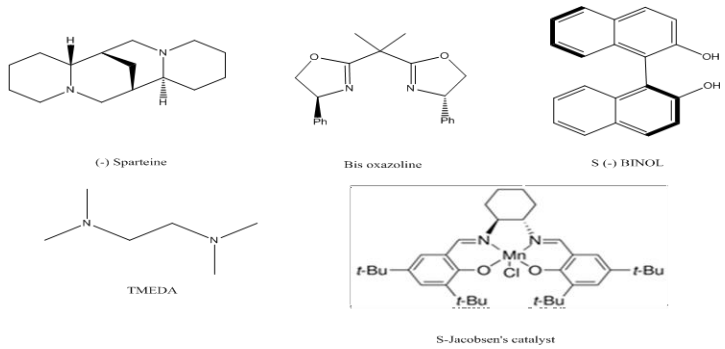

Solvent	Catalyst	Yield(%)	ee(%)
THF	TMEDA	8.1	
THF	LiCl	0	
THF	(R)-4-Phenyl-Bisoxazoline	73	6
Toluene	(R)-4-Phenyl-Bisoxazoline	75	19
THF	(S)-4-Phenyl-Bisoxazoline-Cu Triflate	N.R.	
THF	(S)-4-Phenyl-Bisoxazoline- Cu Triflate +BF_3OEt_2	N.R.	
THF	(S)-Potassium Lanthanide BINOL complex	N.R	
THF	(S)-Jacobsen's catalyst	React w/Cat	
Toluene	(R)-4-Isopropyl-2-Oxazolinyl-Pyridine	4	0
Toluene	(-) Spartiene	< 1	
THF	(-) Spartiene in Ratio 0.8:1 w/base	93%	0
Tol:THF (5:1)	(R)-4-Isopropyl-2-Oxazolinyl-Pyridine	27	0

A good starting point would be to do a more comprehensive investigation of the asymmetric synthesis of the 3,4-ds using THF or toluene. This may help to address some of the previous solubilityissues observed in the lateral metalation step. Along with choosing the solvent a catalyst must be explored that will help us direct to the C3 position as well as control R or S. Previously, we have used several different catalyst in our group with varying success in yield and ee. (**Table 5-1**) We noted that in some cases the more extended catalysts did better for yield but not necessarily ee.

Another promising catalyst that has an extended structure is the 3a, 8aR inda-pybox catalyst that was used with success by Hanhan et al[8] to prepare substituted 3-hydroxy-2-oxindole analogs with controlled stereo-chemistry. They showed that by using this catalyst and various lanthanides they could alter yield and ee as well as incorporate a variety of functional groups. We hypothesize in our 3,4-d system that this catalyst may help to direct the electrophile to the C3 position and this, along with a metal coordination with the isoxazole, will help control R or S formation and provide a good ee. (**Figure 5-1**)

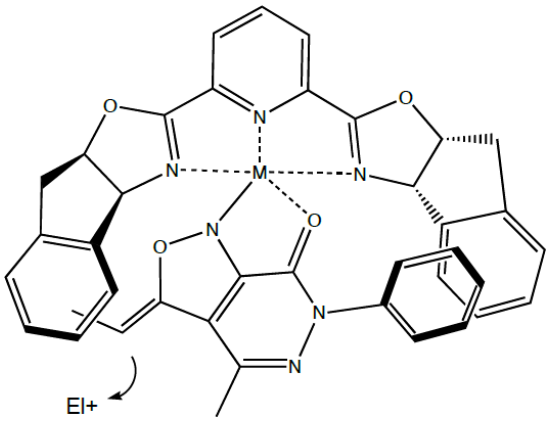

Figure 5-1 – proposed coordination transition state between the 3,4-D,inda-pybox, stabilization of the metal, and the electrophile

As reviewed in chapter one, with lateral metalation different metals can affect how groups add. Using the inda-py catalyst and the synthetic scheme in **Figure 5-2** it is possible to readily exchange out metals and assess their effect on the reaction. As a note chirality can also be introduced in the latera metalation step via aldehyde as an electrophile. We showed this during lateral metalation studies with beta hydroxyl substitutions at the C3 position, but this does not allow for stereochemical control.

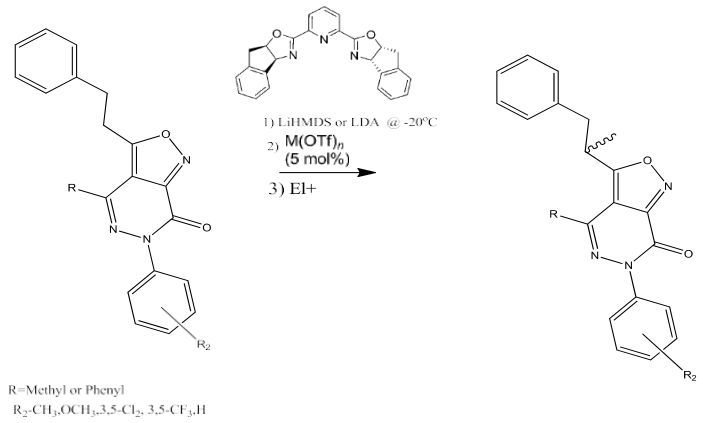

Scheme 5-1: General synthetic scheme for asymmetric synthesis of the 3,4-ds using

Our modeling suggests that a methyl group would allow for a greater potential for the 3,4-d to anchor in the hinge region of mGluRs and interact with the crucial phenylalanine and tryptophan that assist the TM 6 large movement during activation. For both asymmetric and lateral metalation there are other groups that have potential for interacting favorably with other residues in the hinge region, such as groups with hydrogen bonding groups to interact with the salt bridge or water lock that are deeper in the allosteric site that must be disrupted to initiate the TM 6 movement. (**Figure 5-2**)

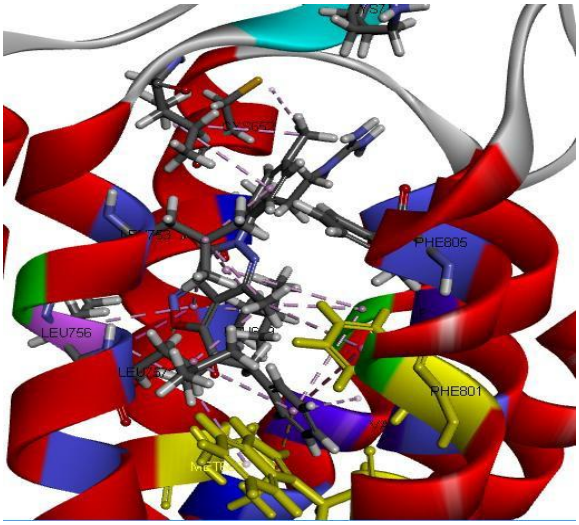

Figure 5-2: chiral 3,4-d modeling illustrating the additional interaction that can be achieved with both the hinge Phen801 and Trp798 as well as providing the interaction with the unique residue Leu756 in mGluR4

Metabolism predictions

In considering novel small molecules in drug development it is important to consider what metabolites will be produced and if they will cause any harm. This can be done *in silico* but ultimately will need to be verified with liver microsomes or another in vitro study and followed by animal studies. Starting with *in silico* allows for quick determination of where a molecule will be metabolized and if any unusual metabolic activities arise that were not previously predict or if there is synthetic variation substitution that can be done to help control metabolism. There are several software programs that can be used to make these predictions. We chose the web software program called Smart Cyp[9] which allows the prediction of major metabolites for user entered molecules for three of themajor CYPs: 3A4/5, 2D6, and 2C9. For all of the 3,4-ds for CYP 3A4 the among the top three were predicted to be the C3 position of the isoxazole or R_3. The last highest scoring would vary depending on the substitution pattern, but frequently it would be the N6, p-OCH_3/CH_3, or one of the branches off the C3 position when substituted with a mono- or di-Bn.(**Figure 5-3**)

For CYP 2D6 and 2C9, the predictions for the top two positions are the same as for CYP 3A4/5 but did predict that the less substituted 3,5-Cl_2 and 3,5-CF_3 of the initial series could be metabolized in the para-position of the N6-aryl, potentially producing a toxic intermediate. However, this was not predicted with the more substituted second series as well as with the chiral molecules.

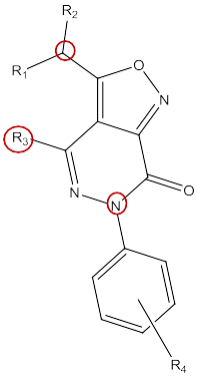

R_1= bn or H
R_2= bn, H, or Me
R_3=Me or Ph
R_4= p-CH_3, p-OCH_3, p-F, p-Cl, 3,5-CF_3,3,5-Cl_2,2,4-F_2

Figure 5-3: General 3,4-scaffold. The top three ranked position for metabolism for 3A4/5 is C3, R_3, and N6.

Blood brain barrier (BBB)–Getting through

Drug molecules must traverse many membranes as well as first and second pass metabolism to get to their targets while maintaining activity and reducing the number of metabolites that could cause toxicity or undesired side effects. Drugs that need to work on receptors in the brain must overcome all of these hurdles as well as additional hurdle of the blood brain barrier (BBB). Drug molecules may not cross or may become hung up in the barrier, or if molecules do get across, they can be metabolized (there are high amounts of CYPs in the BBB) and effluxed by the p-glycoprotein (ABCB1, aka multidrug resistance(MDR)) transporter.[10] There are a number of parameters for small molecules to fit within to try to avoid these issues of reaching their

target in the brain. This initial set of guiding parameters is called Lipenski's rules or the Rule of 5.[11] The Rule of 5 predicts that poor absorption or permeation is more likely when there are more than 5 H-bond donors, 10 H-bond acceptors, the molecular weight is greater than 500, and the calculated Log P (CLog P) is greater than 5. However, Lipinski does acknowledge that the Rule of 5 only holds for compounds that are not substrates for active transporters. These parameters are meant to be guidelines and since publications have both expanded upon and violated these while still producing drugs that reach their respective targets. [12,13] As noted the Rule of 5 is for membranes in general not specifically the BBB, the parameters still apply.

Looking at the 3,4-D series their logPs range from about 3-7, molecular weights are between 250- 500, with 4-5 H-bond acceptors and no donors. Comparing these characterists to the published parameters, logP is the only criterion where the parameters are outside of the range. There are also software programs that can be used to predict BBB permeability with a high degree of accuracy. *In silico* machine learning softwares can be further used to evaluate the BBB permeability molecules.

By using large sets of compounds that are both BBB permeable and BBB non-permeable along with the chemical properties above programs have able to accurately predicted BBB permeability. Creating an accurate prediction of BBB access for CNS drugs has been an ongoing area of research while applying machine learning to gain better insight.[14,15] One such program is lightBBB[16]. This program was able to analyze known drugs to predict which would be able to permeate the BBB with 90% accuracy. When the 3,4-ds are entered into the lightBBB software it was predicted that all of them would be BBB permeable. Up to this point ,we have really only been considering passive transport via diffusion through the BBB. For molecules that are not passively BBB permeable or are substrates for MDR there are couple of different stratagies that could be applied to help them cross the BBB and not be affected by MDR. A MDR an inhibitor

could be introduced and this approach has been successful in treatment of some cancers.[17,18] Also, by using antibodies, other proteins, or making synthetic modification to make a drug molecule into a prodrug that later can be metabolized by CYP or other enzymes could be employed to act as a sort of Trojan horse for BBB transporters to carry the drugs across the BBB.[19,20] This adds a level of complexity due to the need to understand how the modified drug molecule will behave within the body and whether it binds to other receptors compared to the target.

Conclusion

Each new scaffold or modification proposed to be done to a drug molecule or potential drug molecule must undergo an iterative evaluation. This starts with the potential for targeting a specific receptor through modeling, followed by synthesis, testing, and lead optimization, and finally understandin metabolic transformation and receptor targeting and binding. Using both *in silico* simulations and laboratory methods to test and retest these parameters are necessary to provide the most information about the potential of the molecules as a drug candidate.

References

(1) NobelPrize.org. Press release: The Nobel Prize in Chemistry 2021.

(2) Somogyi, A.; Bochner, F.; Foster, D. Inside the Isomers: The Tale of Chiral Switches. *Australian Prescriber*. National Prescribing Service 2004.

(3) Calcaterra, A.; D'acquarica, I. The Market of Chiral Drugs: Chiral Switches versus de Novo Enantiomerically Pure Compounds. *J. Pharm. Biomed. Anal.* **2018**, *147*, 323–340 DOI: 10.1016/j.jpba.2017.07.008.

(4) Burkhart, D. J.; McKenzie, A. R.; Nelson, J. K.; Myers, K. I.; Zhao, X.; Magnusson, K. R.; Natale, N. R. Catalytic Asymmetric Synthesis of Glutamate Analogues. *Org. Lett.* **2004**, *6* (8), 1285–1288 DOI: 10.1021/ol049619m.

(5) Han, X.; Li, C.; Rider, K. C.; Blumenfeld, A.; Twamley, B.; Natale, N. R. The Isoxazole as a Linchpin for Molecules That Target Folded DNA Conformations: Selective Lateral Lithiation and Palladation. *Tetrahedron Lett.* **2002**, *43* (43), 7673–7677 DOI: 10.1016/S0040-4039(02)01845-2.

(6) Wynberg, H.; Greijdanus, B. Solvent Effects in Homogeneous Asymmetric Catalysis. *J. Chem. Soc. Chem. Commun.* **1978**, No. 10, 427–428 DOI: 10.1039/C39780000427.

(7) McLaughlin, C.; Bitai, J.; Barber, L. J.; Slawin, A. M. Z.; Smith, A. D. Catalytic Enantioselective Synthesis of 1,4-Dihydropyridinesviathe Addition of C(1)-Ammonium Enolates to Pyridinium Salts. *Chem. Sci.* **2021**, *12* (36), 12001–12011 DOI: 10.1039/D1SC03860E.

(8) Hanhan, N. V.; Sahin, A. H.; Chang, T. W.; Fettinger, J. C.; Franz, A. K. Catalytic Asymmetric Synthesis of Substituted 3-Hydroxy-2oxindoles. *Angew. Chemie - Int. Ed.* **2010**, *49* (4), 744–747 DOI: 10.1002/anie.200904393.

(9) Rydberg, P.; Gloriam, D. E.; Zaretzki, J.; Breneman, C.; Olsen, L. SMARTCyp: A 2D Method for Prediction of Cytochrome P450-Mediated Drug Metabolism. *ACS Med. Chem. Lett.* **2010**, *1* (3), 96–100 DOI: 10.1021/ml100016x.

(10) Abbott, N. J.; Patabendige, A. A. K.; Dolman, D. E. M.; Yusof, S. R.; Begley, D. J. Structure and Function of the Blood-Brain Barrier. *Neurobiol. Dis.* **2010**, *37* (1), 13–25 DOI: 10.1016/j.nbd.2009.07.030.

(11) Lipinski, C. A.; Lombardo, F.; Dominy, B. W.; Feeney, P. J. Experimental and Computational Approaches to Estimate Solubility and Permeability in Drug Discovery and Development Settings. *Advanced Drug Delivery Reviews*. Elsevier January 15, 1997, pp 3–25.

(12) Meng, F.; Xi, Y.; Huang, J.; Ayers, P. W. A Curated Diverse Molecular Database of Blood-Brain Barrier Permeability with Chemical Descriptors. *Sci. Data* **2021**, *8* (1), 1–11 DOI: 10.1038/s41597-021-01069-5.

(13) Benet, L. Z.; Hosey, C. M.; Ursu, O.; Oprea, T. I. BDDCS, the Rule of 5 and Drugability. *Adv. Drug Deliv. Rev.* **2016**, *101*, 89 DOI: 10.1016/J.ADDR.2016.05.007.

(14) Liu, L.; Zhang, L.; Feng, H.; Li, S.; Liu, M.; Zhao, J.; Liu, H. Prediction of the Blood-Brain Barrier (BBB) Permeability of Chemicals Based on Machine-Learning and Ensemble Methods. *Chem. Res. Toxicol.* **2021**, *34* (6), 1456–1467 DOI: 10.1021/acs.chemrestox.0c00343.

(15) Carpenter, T. S.; Kirshner, D. A.; Lau, E. Y.; Wong, S. E.; Nilmeier, J. P.; Lightstone, F. C. A Method to Predict Blood-Brain Barrier Permeability of Drug-Like Compounds Using Molecular Dynamics Simulations. *Biophys. J.* **2014**, *107* (3), 630–641 DOI: 10.1016/j.bpj.2014.06.024.

(16) Shaker, B.; Yu, M. S.; Song, J. S.; Ahn, S.; Ryu, J. Y.; Oh, K. S.; Na, D. LightBBB: Computational Prediction Model of Blood-Brain-Barrier Penetration Based on LightGBM. *Bioinformatics* **2021**, *37* (8), 1135–1139 DOI: 10.1093/bioinformatics/btaa918.

(17) Lai, J. I.; Tseng, Y. J.; Chen, M. H.; Huang, C. Y. F.; Chang, P. M. H. Clinical Perspective of FDA Approved Drugs With P-Glycoprotein Inhibition Activities for Potential Cancer Therapeutics. *Frontiers in Oncology*. Frontiers Media S.A. November 16, 2020, p 2336.

(18) Liu, R.; Chen, Y.; Liu, G.; Li, C.; Song, Y.; Cao, Z.; Li, W.; Hu, J.; Lu, C.; Liu, Y. PI3K/AKT Pathway as a Key Link Modulates the Multidrug Resistance of Cancers. *Cell Death and Disease*. Nature Publishing Group September 24, 2020, pp 1–12.

(19) Bellettato, C. M.; Scarpa, M. Possible Strategies to Cross the Blood–Brain Barrier. *Ital. J. Pediatr.* **2018**, *44* (Suppl 2), 1DUNNY DOI: 10.1186/S13052-018-0563-0.

(20) Georgieva, J. V.; Hoekstra, D.; Zuhorn, I. S. Smuggling Drugs into the Brain: An Overview of Ligands Targeting Transcytosis for Drug Delivery across the Blood–Brain Barrier. *Pharmaceutics* **2014**, *6* (4), 557–583 DOI: 10.3390/pharmaceutics6040557.